OPTIMISATION OF THE BEARING SURFACE DESIGN OF TOTAL KNEE REPLACEMENTS

by

Shivani Sathasivam

SUBMITTED FOR THE DEGREE OF DOCTOR OF PHILOSOPHY
IN THE UNIVERSITY OF LONDON

DEPT. OF MECHANICAL ENGINEERING,
UNIVERSITY COLLEGE LONDON

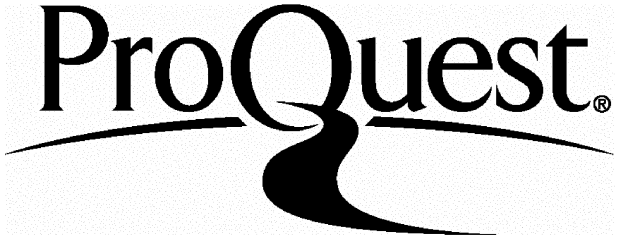

ABSTRACT

A total knee replacement consists of a double-convex, cobalt-chrome layer which resurfaces the femur, and a cobalt-chrome tibial tray with a double-concave polyethylene insert. The longevity of knee replacements is limited, as the polyethylene suffers from fatigue resulting in delamination wear. Previous researchers have analysed the stresses produced in tibial inserts of different designs. However, these studies do not consider the relative displacements and rotations which occur between the prosthetic components during gait. Various designs of knee replacement are currently available and the aim of this study was to investigate the effect of bearing surface geometry on durability.

Rigid body analyses were used to predict the kinematics of different designs of knee replacements during one level walking cycle. The effects of soft tissue restraints were included to compare designs of different conformities, and friction had to be included to obtain realistic motion. These theoretical results were validated by a knee simulating machine. Finite element analyses were carried out at intervals during the walking cycle, to calculate the stresses associated with the orientations of the prosthetic components predicted by the rigid body analyses. Damage functions were formulated which accumulated the fluctuations and average magnitudes of the stresses produced in each element of the tibial inserts. The maximum shear stress damage function to predict subsurface cracking in the polyethylene was equivalent to the strain energy density criterion, used by material scientists to predict crack growth. Using the damage function values, damage maps were generated to indicate the regions of the polyethylene which were most prone to fatigue.

Varying the geometry of the prosthetic bearing surfaces to cover the range of knee replacement designs currently available produced significant differences in the values of the damage functions, suggesting differences in their durabilities. Furthermore the damage functions were used to optimise the prosthetic bearing surface geometries so that the least destructive fatigue mechanisms in the polyethylene would be induced while conserving the laxity of the natural knee.

TABLE OF CONTENTS

LIST OF FIGURES

page

CHAPTER 1

CHAPTER 2

CHAPTER 3

CHAPTER 4

4) LIST OF TABLES

ACKNOWLEDGEMENTS

I thank my supervisor, Prof. P.S. Walker for his guidance and support, and for giving me the opportunity to work at the Centre for Biomedical Engineering in Stanmore.

I am also grateful to Dr. Luger for his help with the cadaveric experiments, Karoline Krohn and Britta Ziimmerman for helping to carry out some of the experiments on the knee simulating machine, Professors Paul and Andriacchi for providing the input cycles for level walking, and Dr.Mike Dewar, Ms.Jessie Smart and Ms. Edith Castle for their interest and encouragement.

This work was funded by the Medical Devices Agency of the Dept. of Health (U.K.) in conjunction with a consortium of manufacturing companies (Biomet, Howmedica, Sulzer, Waldemar-Link and Zimmer), the North-West Thames Regional Health Authority Locally Organised Research Program and the Bristol Myers Squibb/Zimmer Foundation.

Chapter 1

INTRODUCTION

1. INTRODUCTION

1.1 MODERN TOTAL KNEE REPLACEMENT DESIGNS

Total knee replacements are used for the treatment of degenerating joint surfaces, usually caused by arthritis, and for gross knee instability, which may be due to irregular bone geometry or loose ligaments. It is not necessary to reproduce the bearing surfaces of the femur and tibia anatomically when designing the prosthetic components. However, the variety of total knee replacements currently on the market suggests that there is still not a consensus amongst designers on the effects of geometry on the function and longevity of these implants. Even though they are used to treat medical conditions, total knees must be designed and tested in the same manner as engineering components, ensuring that they can withstand the forces exerted on them and that their kinematics replicate the natural joints which they replace.

Total knee replacements are assemblies of four basic components, a cobalt chrome tibial tray, an ultra-high molecular weight polyethylene tibial insert, a cobalt chrome femoral component and a polyethylene patella button. The components are assembled by the surgeon in the operating theatre. A slice of bone is removed from the top of the tibia and a hole is drilled into the trabecular bone. The tibial tray is fitted into the tibia usually with cement, by inserting its central stem into the hole for anchorage, the plateau of the tray replacing the resected bone. The tibial insert is fixed into the tray to act as a bearing surface between the tibial tray and femoral component. Bone cuts are made to the femur so that the femoral component can be fitted, resurfacing not only the part of the bone which interfaces with the tibial insert but also that which comes into contact with the patella. For this purpose a patella groove runs up the anterior face of the femoral component veering laterally, allowing the button which resurfaces the patella to slide up and down in a natural manner. There are different variations of total knee replacement available, depending on the amount of stability required. However, it generally follows that the more stability provided, the more constrained the knee and the more bone removed, both of these being undesirable.

'Condylar' knee replacements (Fig.1) in many forms have been designed since the middle of the ninteenth century. Gunston [1969] is usually credited with the first cemented metal-on-plastic knee replacement. Working in Charneley's department in the 1960s he produced a design consisting of narrow femoral runners embedded in the femoral condyles articulating on two separate plastic tracks embedded in the upper tibia. This design was used in large numbers by the Mayo Clinic group during the 1970s. The results were generally good but there was an increasing incidence of subsidence of the components as well as wear and deformation [Lewallen et al, 1984]. The Mayo group and others went on to develop the Geomedic knee which was very conforming with large contact areas but it was too constrained [Skolnick et al, 1976]. Freeman and Swanson were the first originators of a total knee design which replaced the entire femoral and tibial condylar surfaces [Freeman et al, 1974]. This design was first implanted in 1970. They introduced the roller-in-trough concept and instrumentation which produced rectangular bone cuts. In addition, the femoral and tibial surfaces could rotate and slide at limiting values, so that the forces and moments were not entirely transmitted to the interface between the bone and the prosthesis. The Freeman-Swanson prosthesis was later developed into the Freeman-Samuelson prosthesis which included a metal base-plate for the tibial component.

The first truly anatomical approach was by Seedhom [Seedhom et al, 1974] who replicated the femoral condylar surfaces and produced tibial surfaces which were imprints of the actual femoral-tibial motions. He determined that three sizes of prosthetic knee would suit the needs of 90% of patients [Seedom et al, 1972]. Similarly, Townley [1985] took an anatomical approach, including a patella flange. However, his experience led him to design five sizes because he believed that the wrong size of prosthesis could compromise the stability and range of motion of the joint. In recent years, interchangeability of components, where different sizes of femoral and tibial components can be mated, has also become a feature of knee designs.

The Total Condylar Prosthesis designed by Ranawat, Insall and Walker was first implanted in 1973. It was designed to improve upon the performance of the knees which were in use at the time, by utilising advantageous features of these designs, while introducing the concept of surfaces providing both laxity and

stability [Insall et al, 1979]. In addition, the Total Condylar had an anterior flange for the patella on the femoral component and a central peg on the tibial component to provide fixation which had been lacking in previous knee designs. This design proved to be very successful and is still implanted, though it is reported that the most commonly used condylar knee replacement used today is the Insall-Burstein II posterior stabilised design which requires the cruciates to be removed. Instead, femoral roll-back is guided by a wedge of polyethylene on the tibial insert which engages with a bar across the femoral condyles.

Condylar knee replacements are the most conservative when considering bone removal and also allow the most freedom of movement. Tibial trays and femoral components of many of this type of knee have slots which allow the posterior cruciate ligament to pass through so that it can continue to function after surgery. The geometries of the interfacing surfaces of the femoral component and the polyethylene tibial insert dictate both the magnitude of the stresses generated in the latter and the sliding patterns on its surface during activity cycles. In the natural knee, stability is provided by the ligaments and the joint capsule. On the other hand, the laxity and stability of a condylar knee replacement is balanced by the dishing of the tibial insert and the ligaments and soft tissues that remain, the tibial insert dominating if it is very dished. It is the design of these bearing surfaces which is the focus of this thesis.

It became apparent that the tibial inserts of some condylar knees were suffering from delamination wear [Wright & Bartel, 1986] where severe cracking occurs in the polyethylene leading to rapid disintegration of the bearing surface. In order to reduce the stresses in the polyethylene, the tibial inserts could be designed to be very conforming to the femoral component, however this would not allow relative motion between the femur and tibia, which is necessary for natural gait patterns to be reproduced. This problem had been solved by releasing the tibial insert from the tray to create a mobile bearing which could slide around with only soft tissues and stops built into the tibial tray to restrain its motion (Fig.2).

'Mobile bearing' knees can be even less constrained than condylar knees and also require a relatively small amount of bone removal. The first mobile

bearing knee was the Oxford knee, designed in the early 1970s. It had completely conforming bearing surfaces without clearances [Goodfellow et al, 1987], and its unicompartmental design allowed both cruciate ligaments to be retained. Goodfellow and O'Connor [1978] followed the principle of the four bar linkage mechanism to replicate normal motion with the presence of both cruciates. Evidently, the conforming surfaces produced relatively low contact stresses which has resulted in very low wear rates even after twenty years of implantation. However, due to its complete lack of constraint, there are limitations to the use of this design [O'Connor & Goodfellow, 1996] when the cruciates are absent, especially the anterior cruciate ligament. Buechel and Pappas designed more constrained mobile bearings. In one design, the motion of the plastic inserts is guided in tracks on the metal tibial tray and in another design the plastic insert rotates in the tibial tray. This design, the LCS rotating platform, is the most commonly used mobile bearing design today.

The two types of knees described would not be suitable for cases where the ligaments are in poor condition. 'Superstabilised' knees (Fig.3) are similar to condylar knees except that a rounded post protrudes from the tibial insert and is housed in a cavity in the femoral component. When the knee flexes, the post and the housing work as a cam mechanism. This feature controls the amount that the femoral component rolls back with flexion and its varus-valgus tilting. The Total Condylar II [Walker, 1985] was one of the first knees designed along these lines. Superstabilised knees require more bone removal to accomodate the cam but not as much as that required by 'hinged' knee designs (Fig.4) where a large chunk of bone must be removed to make room for the hinge.

Hinged knees provide the ultimate restraint because the femoral and tibial components are linked together preventing relative motion between the two parts except for flexion/extension. The Attenborough [Attenborough, 1976] was one of the first hinged designs. The femoral component had a stem articulating in a ball socket attached at its centre. Unlike other hinged knees of its time, such as the Walldius and Shiers hinged prostheses, it could internally and externally rotate. Hinges are mainly used for revision cases where bone loss and soft tissue

disturbance from the previous implant have left the knee in disarray and in need of reconstruction.

Total knee replacements are not permanent or fault-free solutions to bone degrading conditions. Each type of knee replacement described has drawbacks. Condylar knees generally fail due to delamination when high stresses are repeatedly exerted on the tibial insert. Mobile bearing knees suffer from abrasion and burnishing due to large contact areas at two interfaces. Superstabilisers can fail by delamination or excess force being applied to the stabilising post. Hinges fail by loosening when the constraint provided by the hinge causes load to be transmitted to the bone. However, the variability between patients, the sparcity of information about knee forces, the problems of recreating the environment in the joint capsule, the changing material properties of sterilised polyethylene with time and the requirement to use only biocompatible materials make improving the durability of knee replacements a difficult task.

1.2 KNEE KINEMATICS

In order to design total knee replacements, the input forces to the natural knee joint and the output motions must be known. The knee is subjected to compression force, anterior-posterior shear, medial-lateral shear, internal-external torque, flexion and varus-valgus moments. The magnitudes of these forces vary considerably with different activities, the functional loads being either the ground reaction force applied to the foot or the inertial load of the leg, the former reaching a maximum of 1.3 times body weight during walking to more than twice body weight during running [Burstein, 1984] and even higher for activities such as squatting. As long as the tibial insert can withstand the stresses imposed without failing, and the combination of the prosthetic components functions naturally, it does not matter how far their designs deviate from the natural bone surface geometries. If however the artificial bearing surfaces do not allow natural motions to occur, the joint becomes overconstrained, forces are transmitted to the junctions between the prostheses and the bones, and loosening occurs. Therefore, the laxity of the natural knee is the initial criterion when deciding on the geometry of the bearing surfaces [Walker et al, 1974, Walker, 1988].

In order to measure the three rotations, and three translations of the natural knee, or to apply them when designing prosthetic components, a coordinate system must be defined relative to which movement occurs. In the literature, flexion is said to occur about an instant centre of rotation in the femur. However, a fixed coordinate system is preferable so that quantities such as total laxity of the joint can be determined. Wismans et al [1980] used Euler's angles to apply flexion, varus/valgus tilt and internal/external rotation to the femur relative to a fixed tibia. Translations were applied subseqently. Grood & Suntay [1983] made a further development by defining a joint coordinate system which was independent of the order in which rotations and translations were imposed.

Cadaveric studies have been carried out to determine the effect of joint load on knee laxity and stability [Markolf et al, 1981]. They showed that the combination of compressive load applied to the joint surfaces, the geometry of the knee joint, tissue compliance and friction between the cartilage surfaces had a stabilizing effect on the natural knee, protecting its ligaments. Joint load is generated by body weight and muscle forces activated by the neuromuscular control sytem. This causes problems when using laxity as a criterion for knee joint design. The forces exerted by the muscles may alter when the brain senses that the artificial knee has a different geometry and friction coefficient compared to the natural knee, changing the stiffness and laxity of the prosthetic knee. In this thesis, it was assumed that the muscle forces for the prosthetic knee were the same as for the natural knee.

Morrison [1968] used a force plate to measure the ground reaction force of subjects with natural knees as they performed activities while being filmed. Markers were used to determine the acclerations of the lower limb segments and a multi-channel electro-myograph recorded the muscle activity. By summing the ground reaction force, gravitational and acceleration effects, the external force system acting on the knee joint was obtained. Surprisingly, hardly any data on gait forces has been published since Morrison, though more recently telemetric methods have been used to measure knee forces directly [Taylor et al, 1997].

La Fortune et al [1992] determined the knee motions of five patients during level-walking by inserting pins into their femurs and tibiae to determine their

three-dimensional relative motions. Knee motions are usually referred to as active or passive, depending on whether the muscles are acting, the muscles having a significant effect. In the literature, references are often made to motions of the tibiofemoral joint. Convention has defined this as relative motion of the tibia with respect to the femur. However, in this thesis, the contact points on the tibial insert were compared for different knee designs [Sathasivam & Walker, 1994], so the relative motion of the femur on the tibia was considered. The natural knee flexes during stance and swing to approximately 20deg and 60deg respectively. Lafortune et al showed that flexion during walking was accompanied by approximately 15mm posterior draw and 5deg internal rotation of the tibia, where the tibia was defined to rotate about its long axis and the origin of the femoral reference frame was located at the deepest point of the intercondylar fossa.

The question is whether force data similar to that calculated by Morrison or La Fortune's displacement data should be input to a prosthetic knee model, in order to determine realistic estimates of the magnitudes of the stresses and positions of the contact areas in the tibial insert. The choice between force and displacement control is a controversial one. In favour of force-control, it could be argued that different knee designs have different laxities due to their variations in conformity. On the other hand, muscle contracture may dominate resulting in unconforming designs moving in a similar way to moderately conforming designs, suggesting that displacement-control would be more appropriate.

Clinical observations support both sides. Andriacchi et al [1982] showed that patients with certain knee replacements showed signs of gait adaptation, that is, their motion patterns were different from normal. A force-controlled model would show gait adaptations for different designs. In this thesis, output motions for the input forces of level walking provided by Andriacchi et al [1995] were determined. The restraining effects of the soft tissues were taken into account in order to compare fairly knees with different conformities between the femoral and tibial components. However, bearing in mind that the anterior cruciate ligament is resected for most condylar replacements, Vergis & Gillquist [1997] showed that subjects with ruptured anterior cruciate ligaments had similar motion patterns to normal subjects when the muscles were active. There was significant difference between the passive motion of the two groups. A displacement-controlled model

would assume that muscle contracture makes the stabilising mechanisms of the knee redundant during active motion.

1.3 WEAR AND STRESSES IN THE POLYETHYLENE

The tibial inserts of total knee replacements suffer from at least three modes of wear, adhesion, abrasion, and fatigue [Fisher & Dowson, 1991]. Adhesion is where asperities on both bearing surfaces cold weld together then break during sliding, resulting in transfer of polyethylene to the femoral component. The transferred polyethylene in turn rubs against the tibial insert producing more wear by abrasion. Abrasion usually occurs when asperities on a hard material plough through a softer material or when loose particles introduced between the bearing surfaces grind as they roll between them. However, the most catastrophic of these mechanisms is fatigue, where subsurface cracks (Fig. 5) propagate and unite, leading to the release of large pieces of polyethylene and eventually the delamination of the tibial insert (Fig.6).

Retrieval studies have shown that in general the more conforming designs suffer less from fatigue failure [Collier et al, 1991]. However, they do suffer from abrasion [Landy & Walker, 1988], especially if the polyethylene surface is very dished and entraps foreign bodies. The patterns of wear are varied, affected by variables other than the geometry of the bearing surfaces. However, Lewis et al [1994] retrieved tibial components of unconforming designs which exhibited severe delamination in the posterior-medial region. Blunn et al [1992] observed that a low conformity design (Marmor) did not delaminate while a design of similar conformity (St. Georg) did. This was probably due to the different manufacturing methods used for the tibial inserts, that of the Marmor being compression moulded rather than machined.

Mobile bearing knees are generally reported to be successful, despite the fact that abrasion of large contact areas between two pairs of interfaces may produce a large quantity of small polyethylene particles. However, the majority of knees implanted today are condylar designs, mainly because they are the traditional solution and they are cheaper. Therefore there is still a need to

determine the design features which make condylar knees more resistant to delamination wear.

Material scientists have tried to predict fatigue failure by using stress-based, strain-based and energy-based criteria. Ellyin [1989] has shown that cracks initiate and propagate when the strain energy density is high. Tests were carried out on specimens which were cyclically loaded in a uniaxial direction. There was a correlation between the total strain energy density and number of cycles to failure. This has led to the formulation of life prediction models using cyclic strain energy density as a criterion for multiaxial fatigue failure. A stress-based approach was applied to formulate damage functions to predict the susceptibility to delamination wear of tibial inserts in this thesis. Bartel [1986] emphasised the importance of the maximum shear stress and maximum principal stress when determining if tibial inserts could withstand static loads. In this thesis a further step was taken to analyse these stresses during fatigue loading. This was achieved by using the damage functions to accumulate the fluctuations and magnitudes of the maximum shear and maximum principal stresses during gait for the entire volume of polyethylene in tibial inserts of different knee designs. Both stresses were required to account for the difference in the compressive and tensile strengths of polyethylene.

Consider a total knee replacement to be simplified to a model of a cobalt chrome sphere loaded onto a flat polyethylene slab. A polyethylene element on the surface in the centre of the contact area, experiences vertical compressive forces due to the loading sphere and horizontal compressive forces from the surrounding bulk of plastic. This element does not suffer from a significant amount of strain. Below the surface, both the horizontal and vertical compressive forces decrease with depth, the former decreasing more rapidly than the latter. Therefore, the strain of the polyethylene is greatest in the subsurface region at a depth where the horizontal compressive forces have almost diminished and the vertical compressive forces are still high, and the difference between them reaches a maximum. For elements in other regions of the polyethylene, which have more complex stress states, the strain is greatest when the difference between the maximum and minimum principal stresses, the maximum shear stress is greatest. Therefore maximum shear stress, an indicator of the regions

where the most subsurface strain occurs, was used as a parameter on which to base a damage function to predict subsurface cracking.

However, it is visible from retrievals, that cracks also emanate from the surface of the polyethylene. These cracks would not be predicted by a damage function based on maximum shear stress. At the surface, around the contact region, the polyethylene is subjected to low minimum principal stresses and relatively high maximum principal stresses. The difference between these two quantities does not peak as high as the difference between the subsurface principal stresses, but the tensile nature of the maximum principal stress in the region around the contact area leaves the polyethylene vulnerable to failure. This is because polyethylene is weaker in tension than in compression. Therefore maximum principal stress was used as a parameter on which to base a second damage function to predict surface cracking.

1.4 KNEE MODELS AND THEIR APPLICATION

It appears that there are two conflicting criteria for designing the bearing surfaces of knees. They should accommodate natural kinematics as well as resist abrasive and delamination wear. Retrieval studies have highlighted the pitfalls of the early designs. However, variables such as thickness of the tibial insert, polyethylene quality, manufacturing methods, sterilisation procedures, surgical accuracy and patient activity levels make it impossible to compare solely the effects of different bearing surface geometries. Meanwhile, new designs are produced every year and it will only be clear if improvements have been made to the bearing surface geometry two decades after they have been implanted. Computer models are useful tools for simplifying complex systems, and also for optimising designs which are defined by variable parameters. Therefore they are ideal for tackling the problem of identifying the knee designs which are likely to suffer from delamination wear and even suggesting new ones.

The earliest models of the knee considered the sagittal plane only, such as the four bar linkage which studied the action of the cruciate ligaments [Zavatsky & O'Connor, 1992]. Two-dimensional models are still used today to examine flexion and anterior-posterior drawer related problems. Wimmer [1995] used a sagittal plane knee model to examine the effects of tractive rolling which produces higher

frictional forces than sliding, and may be the cause of a recently observed striated wear pattern. Wismans [1980], however, developed one of the first three-dimensional knee models which included bone geometry and ligament and capsule restraints. He iteratively solved equilibrium equations to determine the relative positions of the femur and tibia for input forces, and spring elements were used to represent ligament restraints. This was a quasi-static direct dynamics model because it considered the motion of the knee to be a seqence of static positions which varied gradually with time. Andriacchi [1983] and Blankevoort [1991] also created quasi-static knee models. These models increased the understanding of the way the knee worked, in particular, the interaction between the joint surfaces and the ligaments. However, it is not clear what practical applications models such as these have.

The first prosthetic knee models were used to solve the problem of fixation of tibial components to the bone. However, Bartel et al [1986] carried out one of the first studies to analyse the stresses within polyethylene tibial inserts to understand why these components failed. They used a combination of the elasticity solution and finite element analysis with bilinear material properties to show that the thickness of the polyethylene below the dishing should be at least 8mm in order to maintain low stresses, even though surgeons at the time preferred thinner tibial inserts which conserved more bone. More recently, Jin et al [1995] also used the elasticity solution to carry out a parametric analysis to determine the stresses for combinations of femoral and tibial surfaces with different geometries. The results from these studies are useful, but do not help to predict fatigue failure of polyethylene tibial inserts, for which information on the fluctuating nature of the stresses during gait is required.

As finite element analysis became more accessible and cheaper to run, the more sophisticated the models generated. Mottershead et al [1996] carried out finite element analyses of tibial inserts using 20-node bricks and found that the Hertz equations which were originally used to calculate stresses in the knee, and finite element analyses using 8-node bricks, underestimated the stresses. This study used Gaussian point constraints to apply loads. However, the introduction of contact surfaces, which can include the effects of friction, in finite

element packages has meant that analysing the femoral-tibial contact conditions is a relatively simple task.

The current interest in the effects of irradiation on oxidation [Bostrom et al, 1994], and the subsequent increase in the elastic modulus of the polyethylene at the surface has produced more problems to be solved by computer models. Hahn et al [1995] built models of prosthetic knees to determine the effects of varying the elastic modulus of polyethylene to simulate the changes produced by irradation and oxidation. Kurtz et al [1994] examined the stresses in tibial inserts where the elastic modulus was bilinear and varied with depth from the surface to simulate the effects of oxidation. However, he found that the stresses were more sensitive to conformity of the prosthetic components than material properties. In this thesis, the effects of oxidation were not included, only being considered to accelerate wear. Instead the effects of changing the geometry of the contacting surfaces on wear were analysed.

Researchers are beginning to apply cyclic loads to their models instead of static loads and use more realistic material properties for the polyethylene. The elasticity of polyethylene having been modelled as linear, bilinear and non-linear in the past. Ishikawa et al [1996] developed a two-dimensional plane strain model using the constitutive equation for cyclic deformation, to determine the contact behaviour of femoral and elasto-plastic tibial components during gait. Anderson et al [1995] investigated the time-dependent properties of polyethylene when they studied the viscoelastic response of polyethylene in the prosthetic knee, by using finite element analysis. Similarly, Reeves et al [1997] used two-dimensional and axisymmetric finite element models to represent the tibial inserts of unconforming and conforming designs of prosthetic knees undergoing cyclic strain. They assumed that the polyethylene was elastic, visco-plastic. These two-dimensional models are satisfactory for understanding mechanisms such as the effect of cyclic strain on polyethylene with time, but they cannot be used to predict and compare damage such as wear for different knee designs, because they ignore the three-dimensional nature of the geometry and motion of prosthetic knees.

The majority of theoretical analyses carried out on prosthetic knees concern the contact areas and stresses of tibial inserts at different angles of

flexion. Essinger et al [1989] used the total energy minimization principle to find the equilibrium positions of a compressible tibial insert and femoral component which were implanted into a knee model, in order to determine the contact patches produced by different prosthetic designs during flexion. Commercial companies especially, carry out similar experimental analyses to advertise the low stresses produced in their tibial inserts and declare that their designs will not delaminate. However, these studies do not include internal/external rotation and anterior/posterior displacement which vary the contact areas and pressures dramatically. In addition, the extent of these relative motions of the components will vary for different designs. Another aspect that they neglect is that delamination wear is a fatigue mechanism and cannot be predicted by simply analysing a few orientations of the prosthetic components under static load.

A computer model of a prosthetic knee could be set up in which the only variable is the geometry of the bearing surfaces. If the computer model is validated by a physical simulator for existing knee designs, it becomes a simulator in its own right, having the added advantage that it can make predictions for geometries which do not exist. Therefore, it can be utilised further to produce an optimised bearing surface geometry for given design criteria, by analysing the effects of different geometrical parameters. The problem is that for total knee replacements there appear to be two conflicting criteria, unconforming bearing surfaces allow natural knee motions to occur, while conforming bearing surfaces produce low stresses in the polyethylene.

In this thesis rigid body models [Sathasivam & Walker, 1997] were used to indicate the manner in which different bearing surfaces designs would function during gait, finite element analysis was used to determine stress histories during gait for each element of polyethylene which made up each tibial insert, and damage functions were defined to quantify the fluctuating stresses and predict delamination wear. The hypothesis was that the different designs of condylar total knee replacement currently available will have different susceptibilities to delamination wear, and by using damage functions the design of the bearing surfaces can be optimised, so that the knee will function naturally without the tibial insert delaminating.

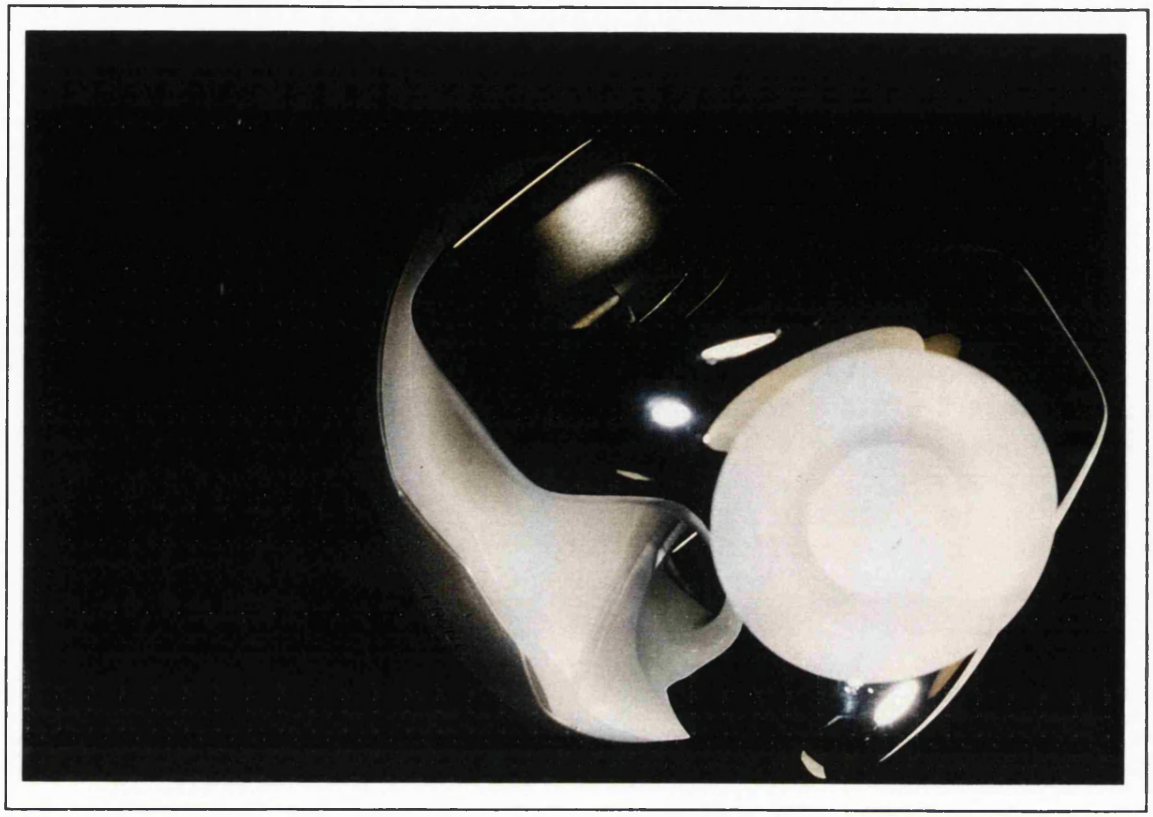

FIG.1 An example of a condylar total knee replacement.

FIG.2 An example of a mobile bearing total knee replacement.

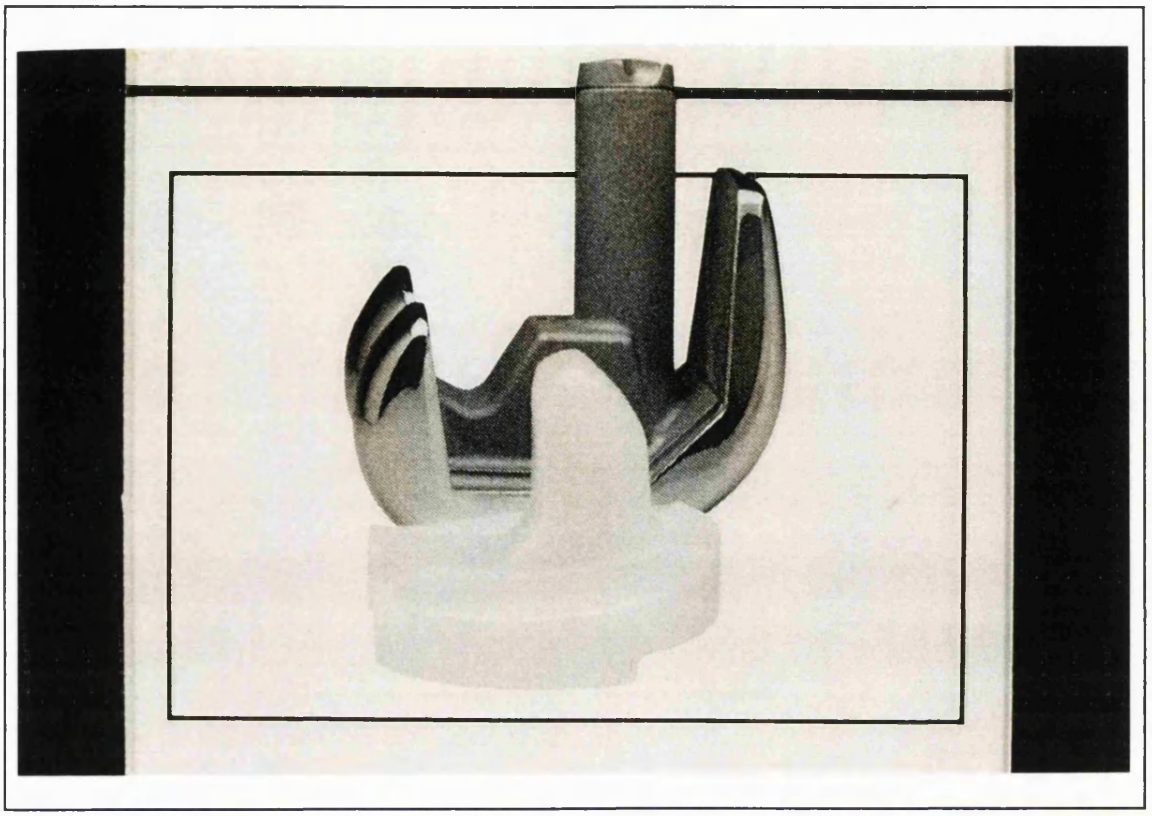

FIG.3 An example of a superstabilised total knee replacement.

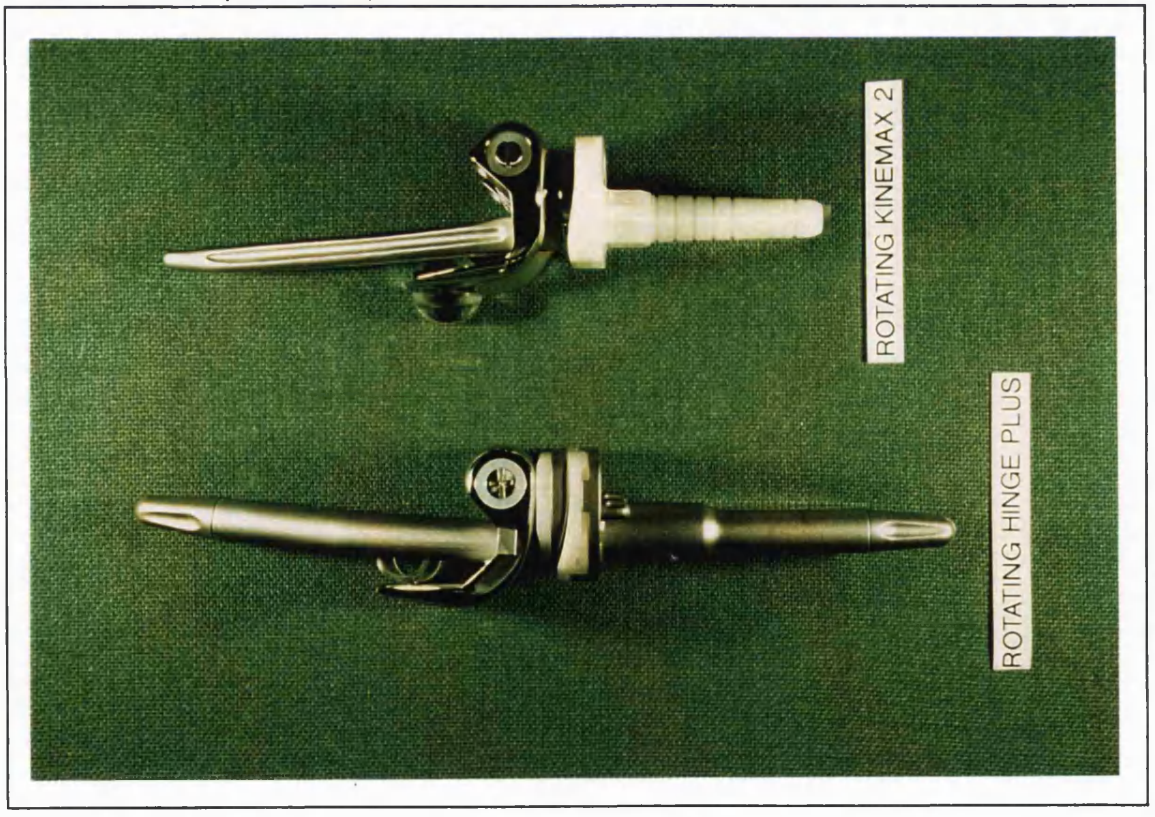

FIG.4 Examples of hinged total knee replacements.

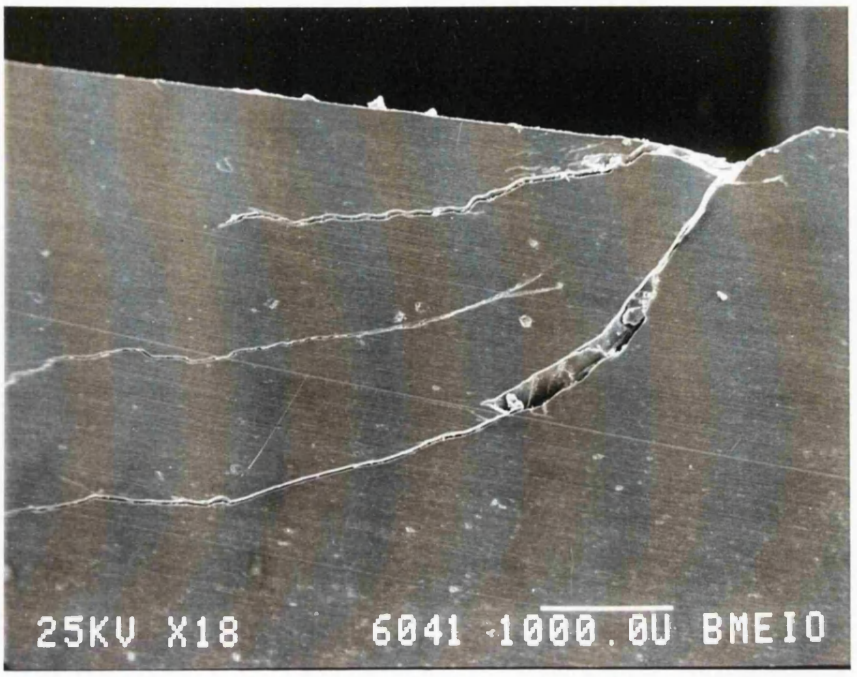

[Blunn et al ,1992]

FIG.5 Subsurface cracking seen by Dr. G.W. Blunn in a thin section from a retrieved tibial insert.

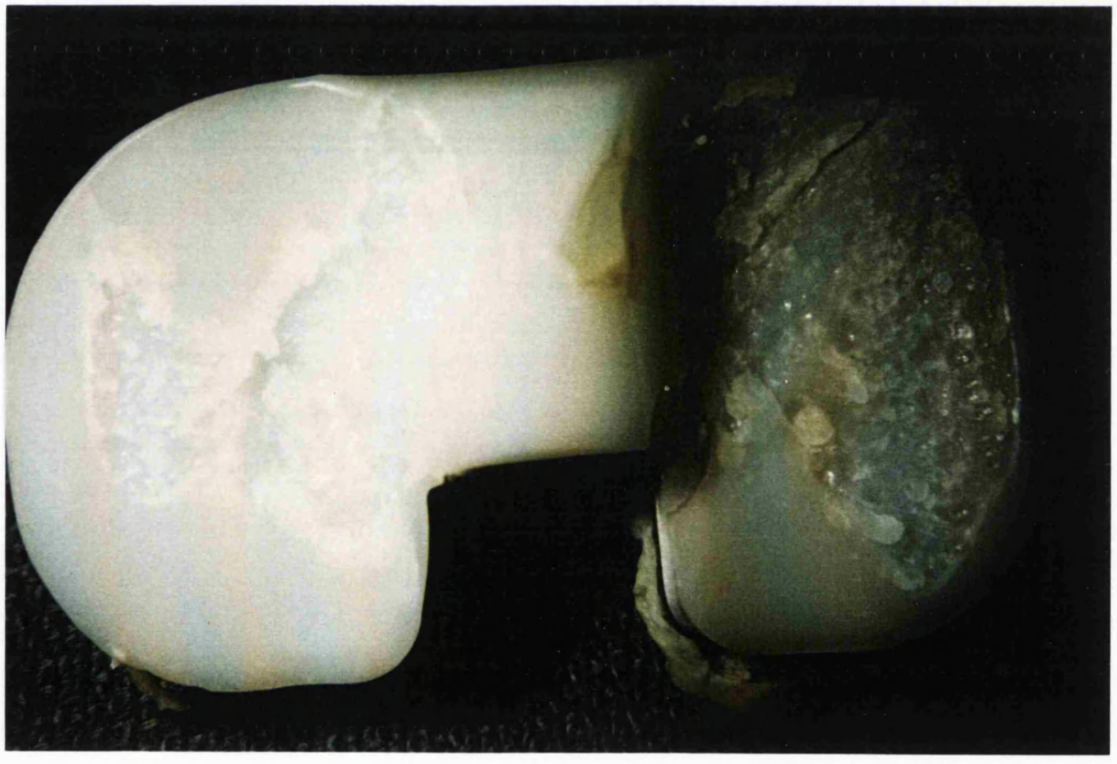

FIG.6 A retrieved delaminated tibial insert.

Chapter 2

A SIMPLIFIED MODEL OF THE TOTAL KNEE REPLACEMENT BEARING SURFACES

2. A SIMPLIFIED MODEL OF THE TOTAL KNEE REPLACEMENT BEARING SURFACES

If the aim is to optimise the design of total knee replacement bearing surfaces, criteria must be set, variable parameters chosen and limits determined for their values. The criteria of wear resistance of the tibial insert and natural function have already been mentioned, and take priority with regards to optimisation, but there are other factors which also have to be considered. For example surgeons prefer components which require less bone resection, and schemes which allow interchangeability where different sizes of femoral and tibial components can be mixed and matched. Criteria such as these decide if the components are implantable, which is important because surgical requirements must be met. If the limits of the values for the parameters are fixed by considering such criteria, then within these limits the parameters can be optimised for wear resistance and natural function. A review of the literature shows that various criteria have been considered important by designers in the past.

Various criteria have been applied to the design of condylar replacement knees, which has led to the manufacture of components which satisfy some of the requirements but with less attention to others. Knees have been designed which exhibit normal or improved patella lever arms, usually by suitably located dishing of the surfaces or by cam mechanisms [Burstein,1984]. Other designs emphasise sufficient laxity for activities of everyday living with progressive restraint to laxities from the neutral position [Thatcher et al.,1987]. El Nahass et al.[1991] measured knee motions in various activities and concluded that a knee prosthesis should allow an internal/external rotation of -12° to +12° and an anterior-posterior displacement of 13mm. Walker et al.[1974] showed theoretically the relationship between the laxities produced by applied forces and moments and the relative curvatures of the femoral and tibial condyles.

However, Bartel et al.[1986] showed that the relative geometry between the femoral and tibial surfaces also affects the contact stresses which are believed to affect the wear and deformation of the plastic. Walker[1988] showed

that the least stresses were experienced with surfaces allowing only fixed axis cylindrical motion, the highest with flat tibial surfaces. However, a study of retrieved specimens by Landy and Walker[1988] concluded that flatter components, although prone to higher stresses, did not necessarily exhibit high wear. Low conformity in the sagittal plane has been included in a number of recent designs to allow for variable positioning and motion patterns, and to allow shear forces to be carried by the posterior cruciate ligament [Andriacchi & Galante,1988]. In an alternative approach where both cruciates are resected, anterior-posterior stability as well as reduced contact stresses are achieved using more conforming surfaces with a posterior contact location [Freeman & Railton, 1988].

In this chapter, a simplified model of the bearing surfaces was parametrised, and different values of the parameters were input to generate bearing surface designs. Some basic analyses were then carried out to show which designs satisfied the criteria of low contact stresses, interchangeability, adequate patella lever arm, maximum stability, and minimal bone resection.

2.1 PARAMETRISATION OF THE BEARING SURFACE GEOMETRY

The bearing surface geometry of total knee replacement components was simplified to pairs of toroidal dishes, one pair convex and the other concave for the femoral and tibial components respectively. The dishes of each component were separated by the condylar bearing spacing in the medial-lateral direction and were defined in perpendicular planes, frontal and sagittal (Fig.1).

The frontal profile of the femoral surface was formed from two equal curves of radius FF, one for each condyle. In the same plane the tibial surface had radii TFI and TFO which mated with the inner and outer surfaces respectively of each femoral condyle. The radii of the two components must be considered in combination because their conformity will affect the stresses. In this analysis a constant femoral frontal radius FF was set and the tibial frontal radii TFI and TFO were varied to examine different conformities. However, it should be noted that for a given clearance between the radii of the mating arcs,

Hertzian theory shows that the conformity will increase along with increased femoral radius. This will be investigated later.

In the sagittal plane, the tibial condylar surface had radius TS. The sagittal condylar profile of the femoral bearing surface was constructed from posterior and distal curves of radii FP and FD. The posterior-distal transition angle (PDTA) was defined as the angle at which the posterior arc ended and the distal arc began, in extension. The axis of flexion was defined to be the centre of the posterior arc of the femoral component in the sagittal plane, therefore the bearing conditions for a femoral component with Xdeg PDTA at 0deg flexion are equivalent to those of a femoral component with 0deg PDTA at Xdeg flexion. If the PDTA is positive, the femoral component bears with its small posterior radius (FP) against the tibial component. If the PDTA is negative, the femoral component begins flexion with the larger distal radius (FD) interfacing with the tibial component, then as the flexion angle becomes greater than the PDTA angle, the posterior radius comes into play.

A simplified model of the bearing surfaces was defined. It consisted of a convex dish within a concave dish. Each dish was defined by three radii, the concave dish was defined by TFI and TFO frontally and by TS sagittally while the convex dish was defined by FF frontally and by FP and FD sagittally. In addition, the convex dish could be rotated in the sagittal plane about the centre of the arc with radius FP. The frontal conformity of the dishes could be varied by changing one value TFO, while the sagittal shape of the convex dish could be changed by simply varying the posterior-distal transition angle (PDTA). The effects of varying these two parameters were analysed.

2.2 DETERMINATION OF CONTACT STRESSES ON THE TIBIAL COMPONENT

2.2.1 METHODS AND MATERIALS

The aim was to determine how contact stress varied for different femoral-tibial conformities. In order to calculate stress, the elastic modulus of ultra-high molecular weight polyethylene had to be determined. Laboratory experiments

were performed to produce contact patches which were similar to those made when knee components are compressed together. Indentors were machined from titanium, one with perpendicular planes of radii 30 and 50mm, representing a femoral condyle in extension, the other with radii 30 and 20mm, a condyle in flexion. Toroidal dishes were machined with minimum thickness 6mm from uniform blocks of ultra-high molecular weight polyethylene, with radii varying from 35 to 200mm. A metal indentor coated with a film of dye was fixed to the loading head of an Instron testing machine. A tibial dish was aligned with the femoral indentor and a compressive force of 1kN was applied in one minute and released immediately. Tests were carried out for each combination of indentor and polyethylene sample and the dimensions of the contact patches were measured.

Applying Hertzian theory, the maximum stress on the polyethylene surface is given by [Roark and Young, 1975] :

$$\max \sigma_c = \frac{1.5\,P}{\pi\, cd} \qquad (1)$$

where P is the total load applied and 2c and 2d are the lengths of the axes of the contact patch. Also,

$$c = \alpha \sqrt[3]{PK\,C_{DE}} \qquad (2) \qquad d = \beta \sqrt[3]{PK\,C_{DE}} \qquad (3)$$

α and β are variables which depend on the geometry of the surfaces making contact. Values were obtained by interpolating results listed in [Roark and Young 1975] for cases where the major and minor axes of the femoral and tibial surfaces are aligned (as in the Instron tests).

The elasticity function is:

$$C_E = \left(\frac{1-\upsilon_F^2}{E_F}\right) + \left(\frac{1-\upsilon_T^2}{E_T}\right) \qquad (4)$$

υ_F and υ_T are the Poisson's ratios of the metal indentor and polyethylene sample respectively.

E_F and E_T are the elastic moduli of the indentor and polyethylene sample.

K_D is a measure of the conformity of the surfaces:

$$K_D = \frac{1.5}{(1/TF)+(1/FF)+(1/TS)+(1/FS)} \qquad (5)$$

where tibial radii are negative, TF=TFI=TFO, FS=FP in flexion and FS=FD in extension

TFI, TFO, FF, TS, FP and FD are defined in Fig.1.

The value of the elastic modulus of polyethylene obtained from these experiments was used to determine a 'full-field' solution of maximum contact stresses (max σ_c) for an entire spectrum of femoral and tibial radii.

2.2.2 RESULTS

The results for the apparent elasticity function of the polyethylene (C_E) plotted against the relative radius of curvature function (K_D) are shown in Fig.2. The apparent elastic modulus of the polyethylene ranged from 400MPa to 600MPa between low and high conformities, for a load of 1kN applied at 1kN/min. The Poisson's ratio of polyethylene was assumed to be 0.4. 600MPa was used for the elastic modulus of polyethylene in subsequent analyses, to represent the worst case as it produced the highest stresses. The elasticity equations were applied again when calculating the maximum contact stresses produced when a femoral component in flexion was paired with a spectrum of tibial components defined by varying sagittal and frontal radii (Fig.3). The lowest stresses occurred when the femoral and tibial radii were similar, in both sagittal and frontal planes (the analysis considered a minimum difference in femoral-tibial radii of 5mm). These very conforming geometries produced stresses which were below the yield strength of polyethylene which is generally quoted as 15-20MPa. However, they covered only a small portion of the spectrum of geometries currently used in

knee replacement design. If the conformity in one plane was reduced, the stresses quickly increased, but then reached an intermediate level where further reduction had little effect. A reduction of conformity in both frontal and sagittal planes led to a rapid increase in contact stresses to high levels.

2.3 INTERCHANGEABILITY BETWEEN SIZES OF THE COMPONENTS

2.3.1 METHODS AND MATERIALS

The main purpose of this analysis was to find the optimum geometry for a tibial component which could accommodate different sizes of femoral components whilst maintaining low stresses. Linear, plane strain, finite element analysis (ANSYS Version 4, educational) was used to model half of the frontal profiles of the knee components. The elasticity equations above could not be used for cases where the contact patches reached the edges of the polyethylene, which can occur when interchanging components of different sizes. The femoral component was modelled as a cylindrical, rigid surface, which is defined in ANSYS as a boundary of nodes beyond which elements cannot penetrate. The tibial insert was deformable, its geometry was based on the simplified model of the bearing surfaces though its width was limited to the half-width of a tibial insert. Gap elements were required at the interface between the femoral and tibial insert if contact was to occur.

The stiffness of these gap elements was determined by applying ANSYS to a rigid, cylindrical indentor loaded onto a large, flat, plastic slab. The slab had elastic modulus 600MPa (determined from the results of the previous experimental study) and Poisson's ratio 0.4. Elasticity theory was considered applicable for this unconforming case. The slab was interfaced against the cylindrical indentor and equal normal forces were applied to the nodes along the base-line of the plastic slab. The analysis was repeated with different normal forces until the reaction forces at the interface summed to 1000N. The analysis was repeated with different stiffnesses for the gap elements until the maximum compressive stress was equal to that predicted by elasticity theory.

This stiffness was used for the analyses of the frontal planes of the tibial inserts. The arrangement of the elements depended on the point of contact, an example is given in Fig 4. In order to determine where the nodes should be concentrated, the contact point was estimated by rigid body analysis. The interface between the rigid, femoral surface and the polyethylene elements was assumed to be frictionless. To check for interchangeability, a standard tibial component with frontal radius 35mm was mated with different sizes of femoral components:

a) which were scaled up and down by 6% where all dimensions varied proportionally.

b) where the radii and width were scaled by 6%, but the bearing spacing was scaled by only 3%.

2.3.2 RESULTS

When a 6% increased femoral component was placed on the standard tibial with 35mm outer radius, contact occurred at the edge of the plastic, making this kind of scaling unfeasible. If the outer tibial radius (TFO) was changed to 40mm, the contact points were within the tibial periphery and the stresses were only elevated by 15%. However, if the bearing spacing of the femoral component was only increased by 3%, the contact points were within the tibial periphery and the stresses were actually reduced by 9%. Fig. 5 compares the Von Mises stresses produced when this scaling method is applied to small, standard and large femoral components mated with a tibial insert which have inner tibial frontal radii of 35mm and outer tibial frontal radii of 40mm.

2.4 CONSIDERATIONS FOR THE SAGITTAL PLANE

2.4.1 METHODS AND MATERIALS

Domed patella components and patella tracks which were located 5mm within the outline of the femoral condylar surface, were added to the sagittal profiles. The tibial sagittal surface was defined to be totally conforming to the femoral

sagittal profile for this part of the study. The anterior-posterior length of the tibial component was 50mm, its posterior edge was located 3mm in front of the posterior of the femoral component in extension and the top of the tibial component was sliced off so that there was a 5mm flat at the anterior. Six femoral profiles were created with PDTA from -15° to 10°, with posterior and distal radii of 20 and 50mm respectively. The reference axis system for the femur and the tibia was based on the transverse axis joining the centres of the 'spherical' posterior femoral condyles with the femur at 0° flexion [Garg and Walker,1990]. The cross (A) marked on Fig.6 shows this axis. The centres of the posterior radial sections of the prosthetic sagittal profiles were located on this cross. Flexed femoral component profiles were positioned so that their lowest points made contact with the deepest points of the tibial dishes. The angle ALPHA described the orientation of the patella ligament and the angle DEL described the orientation of the patella component itself. These angles were iterated using a computer program until the lines of action of the patella ligament, quadriceps and the reaction of the patella on the patella groove crossed at one point, indicating that the patella component was in equilibrium. The patella lever arm was measured in this position as the perpendicular distance from the position of femoral-tibial contact, which is the natural fulcrum point, to the patella ligament, as in the study by Draganich et al [1987].

Also, for each value of PDTA, the heights of the deepest point of the condylar surface to the anterior edge of the tibial dish (HAC) and the gradient of the tangent to the anterior edge of the dish (SAC) were calculated. Finally, the profiles were superimposed on the mid-lateral slice of the 'average knee' to determine how bone resection varied with PDTA at the thickest region of the bone. Bone resection was defined as the perpendicular distance between a 45° slope to the patella track of the prosthesis and a slope at the same angle to the femoral bone. Fitting the femoral component to the femur requires a 45° chamfer at the distal-anterior end and the amount of bone resected depends on the PDTA.

2.4.2 RESULTS

The patella lever arms for the different femoral geometries differed most in early flexion (Fig.7). For PDTA=-15°, the lever arm was 33.6mm, while for PDTA=10° the lever arm was 40.7mm. As flexion increased to 90° the range of values narrowed down to 31.7mm for PDTA=-15° and 33.6mm for PDTA=10°. Hence the main advantage in the femoral components with positive PDTA is increased quadriceps effectiveness in early flexion, rather than at the higher flexion angles.

Another characteristic of positive PDTA was in the increasing anterior height and anterior slope of the tibial surface in the sagittal plane (HAC and SAC, Fig.6). The anterior heights rose steadily with the PDTA angle from 4.9mm for PDTA=-15° to 12.5mm for PDTA=10°. The anterior gradients of the tibial dishes showed a similar increase. This implied the possibility of increased inherent stability for designs with positive PDTA. However, Fig 7 also shows that during 60° flexion and beyond, the patella starts to impinge anteriorly on the tibial insert. This can be solved by reducing the height at the front of the tibial insert which causes a reduction in stability.

As the positive PDTA required a steeper upsweep of the femoral sagittal profile, from distal to anterior, more bone resection would be needed for installation. The profile with PDTA=-15° required only 4.9mm of bone to be resected from the lateral slice, whereas that with PDTA=10° required 12.2mm.

2.5 DISCUSSION

It is generally assumed that the wear and deformation of the plastic increases with contact stress [Rose et al., 1983; Bartel et al, 1986; Rostoker and Galante, 1979] although the evidence from implant retrievals is not entirely clear on this point [Landy and Walker, 1988; Collier et al., 1991]. A complicating factor is that the highly conforming designs (with lower contact stresses) show increased wear due to entrapped particles and areas of deformation due to misalignment.

In order to calculate the contact stresses for a full range of femoral-tibial geometries of toroidal shape, the elasticity equations were used. Elasticity theory, which predicts contact stresses for two elastic bodies when compressed

together, only applies to cases where the bodies are non-conforming and the contact area is small compared with the radii. It also assumes a planar contact area. Finally, stresses calculated using this theory only apply to infinite surfaces [Roark and Young, 1975; Whelan and Little, 1992]. These factors would indicate that standard elasticity theory may be unsuitable for determining the contact stresses (and hence predicting wear properties) of condylar knee replacements. However, for the empirical analysis, the hypothesis was tested that for a fixed thickness of plastic, the apparent elasticity of the component would vary as a function of the conformity of the surfaces. The experiments used to obtain this function involved a dye method, as it produced clearly marked contact patches for all conformities. The dimensions of the contact patches were accurately measured but it was not possible to achieve exact repeatibility, as can be seen from the experimental results (Fig.2), probably due to the viscoelastic nature of the polyethylene. Unfortunately, the variability in the results meant that the hypothesis could not be proved, so the upper bound value for the elastic modulus of ultra-high molecular weight polyethylene was used to make a full-field set of maximum stress calculations (Fig.3). It appeared that contact stress is more sensitive to changes in the tibial geometry when the conformity is high, than when it is not. Therefore once surfaces are in low-moderate conformity, as in the sagittal plane to allow sufficient laxity, slight changes in the tibial geometry in an effort to improve the stresses will have little effect. On the other hand, if the frontal plane is defined to be closely conforming, then varying its geometry will result in a considerable variation in stress.

The lowest stresses occurred when the sagittal and frontal radii of the femoral and tibial surfaces differed by 5mm, the closest conformity considered in this analysis. However, such a geometry would be excessively constrained, allowing much smaller rotations and displacements than those which occur in the normal knee. The stresses were calculated for a femoral condyle with frontal radius 30mm and sagittal radius 20mm. This could represent a femoral component with negative PDTA in flexion, or one with positive PDTA in both flexion or extension. Consequently, the negative PDTA component provides

moderate stresses in extension, but high stresses in flexion. This is because the sagittal profile of the tibial insert must accommodate the large distal radius of the femoral component which makes contact in extension. In contrast, the positive PDTA component, produces moderate stresses throughout the entire range of flexion, as only the small posterior radius makes contact, allowing the tibial insert to be more conforming to the femoral component in its flexed position. Therefore considering stresses alone, positive PDTA seems preferable.

Total knee systems typically include five sizes or more with each component varying about 6% between sizes. The variability of femoral and tibial shapes is such that different sized components may be needed for each component to obtain maximum coverage of the bone surfaces. Such interchangeability of 'one size up or down' was analysed. When a large femoral component is mated with a standard tibial component, the contact patches may reach the periphery of the tibial surface and therefore the elasticity theory is not applicable. Instead, finite element analysis was used, employing a plane strain model in the frontal plane. As might be expected, when proportionate sizing was used for the femoral components, the small size produced higher stresses because of the smaller radii, but for the larger component, the contact points reached the edges of the polyethylene surface, an undesirable situation [Gunsullus and Bartel, 1992]. This effect would be more pronounced for smaller and more conforming frontal radii. Increasing the radii at the sides of the components, on the tibial surface more than the femoral, avoided the problem, but at the expense of higher contact stresses.

It might appear that maintaining a constant bearing spacing across all sizes would allow complete interchangeability. For frontal radii around 30mm, difficulties are encountered at the extremes of size. For the largest size, there is a slight reduction in varus-valgus stability and there is insufficient metal at the sides. For the smallest size, the contact points are too close to the edges of the plastic. The problem of the large size can be addressed by increasing the radii at the outsides of the surfaces. An alternative solution was analysed where the bearing spacing was increased and decreased at half the amount of the overall

component dimensions. It was shown that such a scheme was feasible for one size up and down interchangeability, both for contact stresses and for locations of the contact areas within the periphery of the tibial insert.

The entire form of the femoral sagittal profile could be conveniently altered by varying the PDTA alone, where a negative value implies that the large distal radius is carried round posteriorly, while a positive value implies that the smaller posterior radius is carried round to the anterior. The effect of varying the PDTA on patella lever arm, stability and bone resection was studied. It has been shown that patients with short patella lever arms have compensated gait and problems with stair-climbing [Andriacchi et al.,1982], implying that the longer the patella lever arm, the more advantageous. Using a model where the patella was considered to be subjected to three forces exerted by the quadriceps muscle, patella ligament and the reaction force between the patella groove and the patella [Huberti and Hayes, 1984; Reithmeier and Plitz 1990; Ahmed et al, 1987], it was found that cases with positive PDTA had the longest patella lever arms due the more posterior contact points. However, this is somewhat different from normal, where the contact points move anteriorly in extension [Ahmed & Burke, 1983] leading to femoral roll-back in early flexion [Rovick et al, 1991]. This may well have implications for the action of the hamstrings as well as the quadriceps, both of which are active in late swing and early stance during gait [Inman et al,1981].

When considering stability, complete conformity was assumed in order to make a comparison between the femoral and tibial components for different sagittal geometries, even though in reality the surfaces would be unconforming. The assumption was made, that the steeper the tangent and the greater the height at the anterior of the tibial surface, the greater the horizontal component of the reaction force, and hence the greater the resistance to shear forces. On this basis negative PDTA proved to be the least stable especially in flexion. This was to be expected since tibial surfaces with a large radius at the bottom of the dish more readily allow posterior displacements of the tibial surface relative to the femoral surface. This implies that such surfaces require preservation of the

posterior cruciate ligament, or intercondylar stabilising posts as in some knee designs (eg. Kinemax Stabiliser, Insall-Burstein). On the other hand, surfaces with positive PDTA could conceivably be used without a posterior cruciate or other means (Eg. Freeman-Samuelson). The disadvantage of positive PDTA however was additional distal-anterior bone resection of around five millimetres.

Factors other than those considered in this study are important, such as the behaviour in varus-valgus or medial-lateral loading. However, within the limits of this study, it appeared that the most favourable characteristics occurred for a PDTA around zero to -5 degrees, moderate conformity in the sagittal plane and close frontal conformity. To allow interchangeability, compromises are required in contact stresses, medial-lateral bearing spacing, contact area location on the tibial surface, and general component aesthetics.

This analysis was restricted to a model of the femoral and tibial surfaces represented by toroidal dishes. They were composed of circular arcs in the frontal and sagittal planes, and with sagittal femoral geometry described by a small posterior radius and a larger distal radius, joining at a variable polar angle. This model was satisfactory for the criteria examined here and for determining stresses at different angles of flexion. However, in order to determine femoral-tibial positions after anterior-posterior displacements and internal-external rotations have been imposed, and to predict stresses during gait, complete models of the bearing surfaces of the prosthetic components are required.

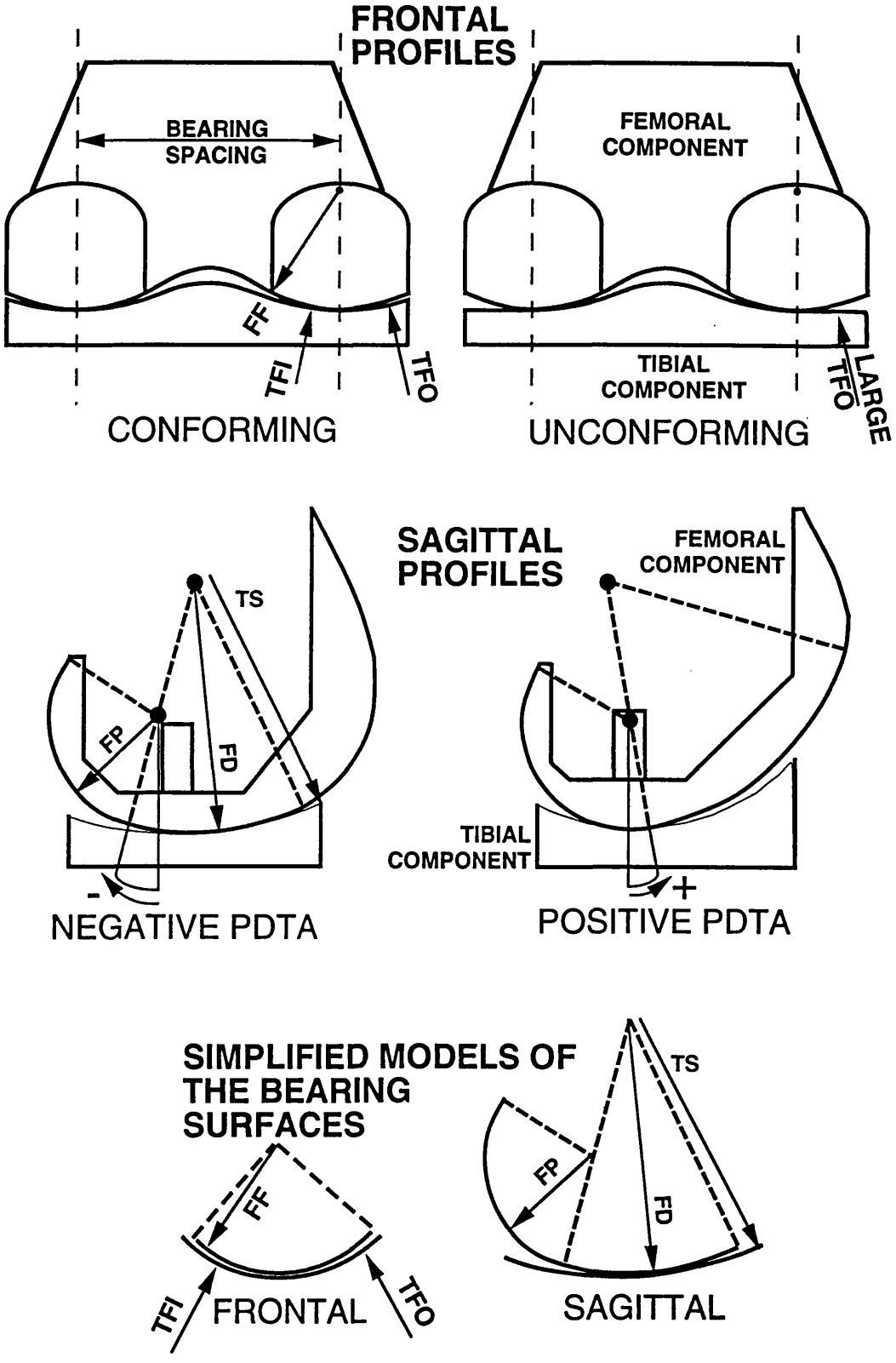

FIG.1 Terminology used to describe the simplified models of the total knee replacement bearing surfaces.

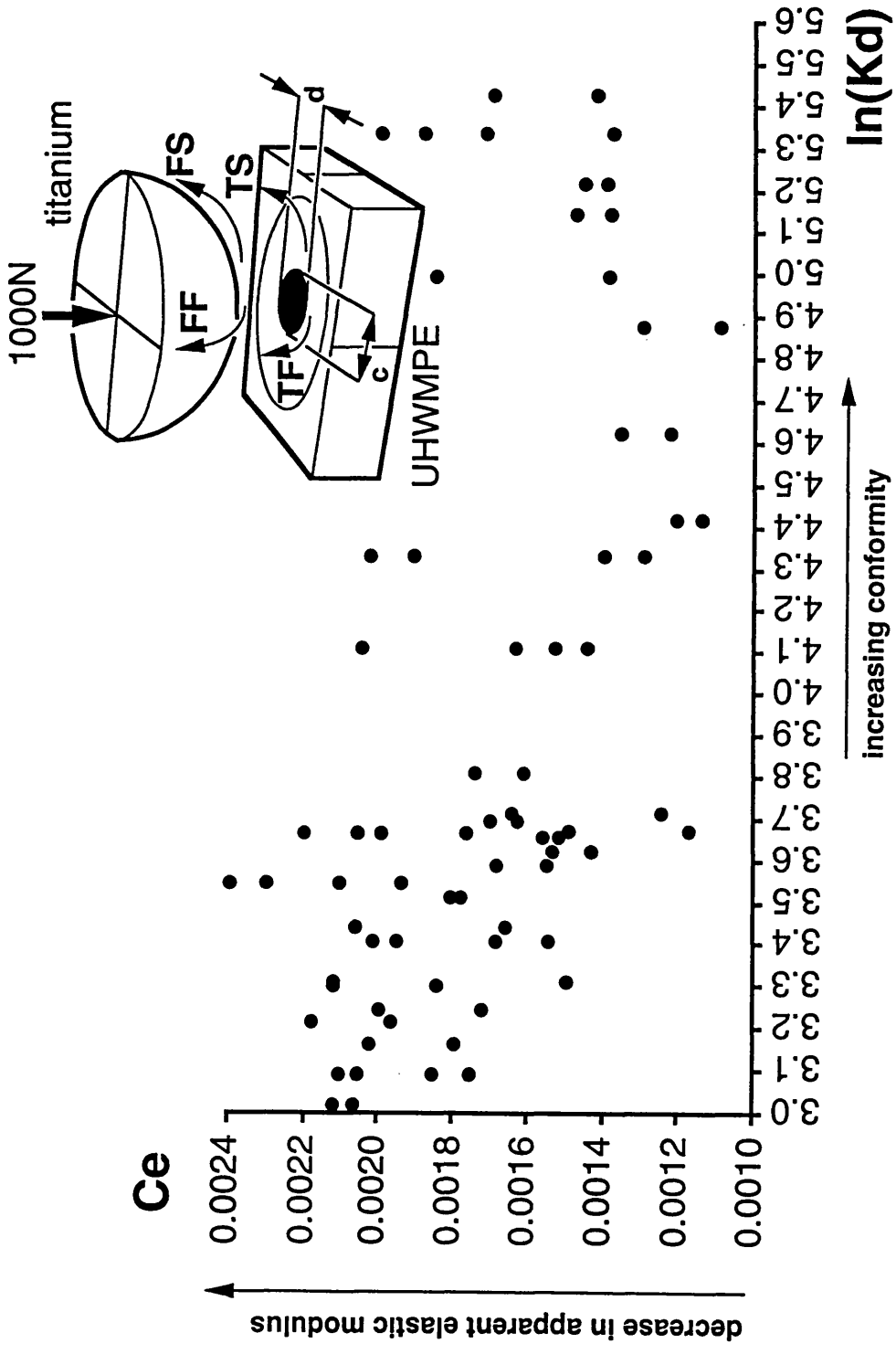

FIG.2 Function C_E (containing the modulus of elasticity of polyethylene) plotted against function Kd (containing relative radii of curvature of the bearing surfaces).

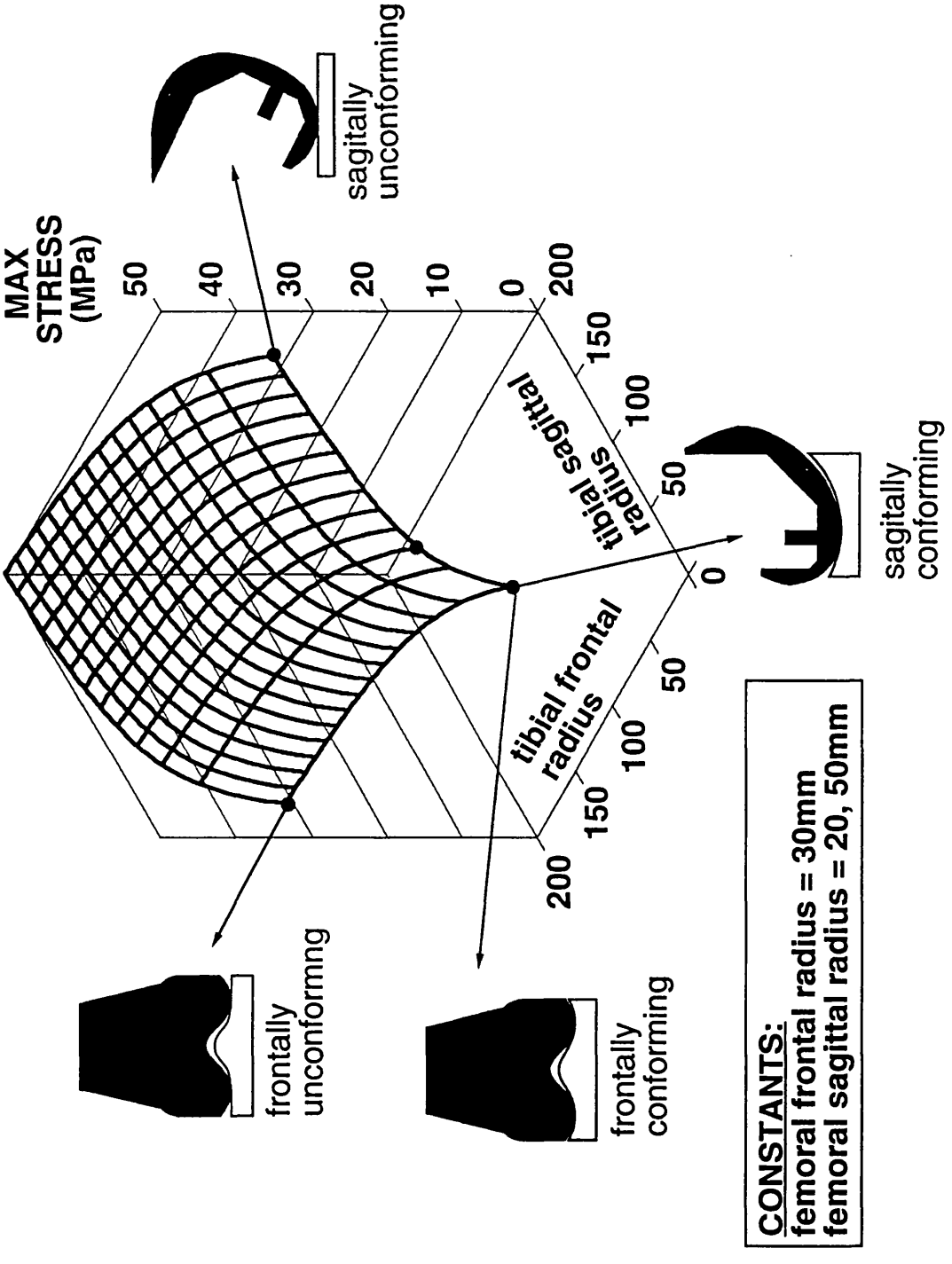

FIG.3 The effect of varying the frontal and sagittal tibial radii on the maximum contact stresses (1000N compression).

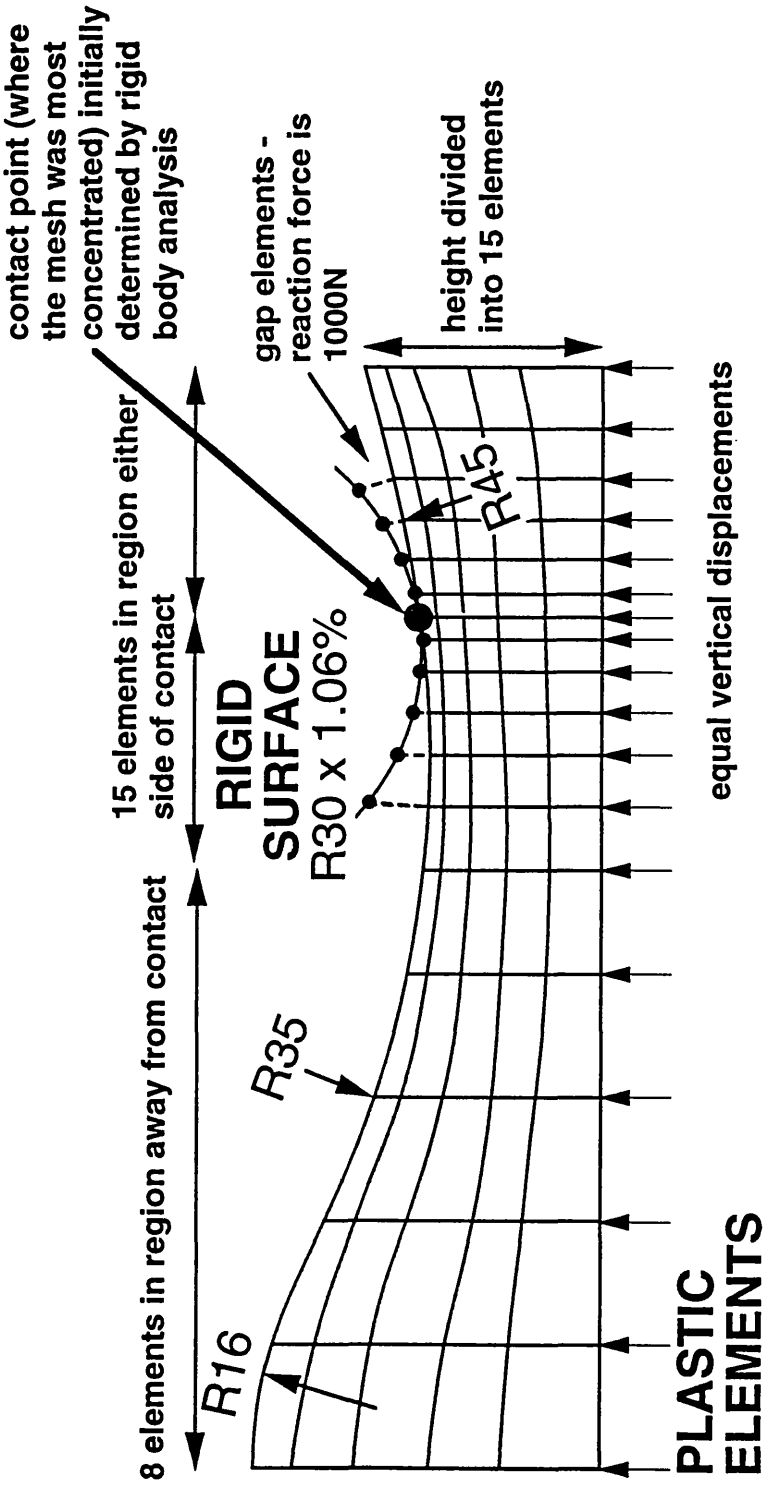

FIG.4 Using FEA to examine interchangeability between sizes. This example shows a case where the outer tibial radius is 45mm and the femoral component is 6% larger than standard. For clarity all the elements are not shown.

FIG.5 Contact stresses in the frontal plane for interchanged components where the outer tibial radius is 40mm. The radii have been scaled by 6% and the bearing spacings by 3%.

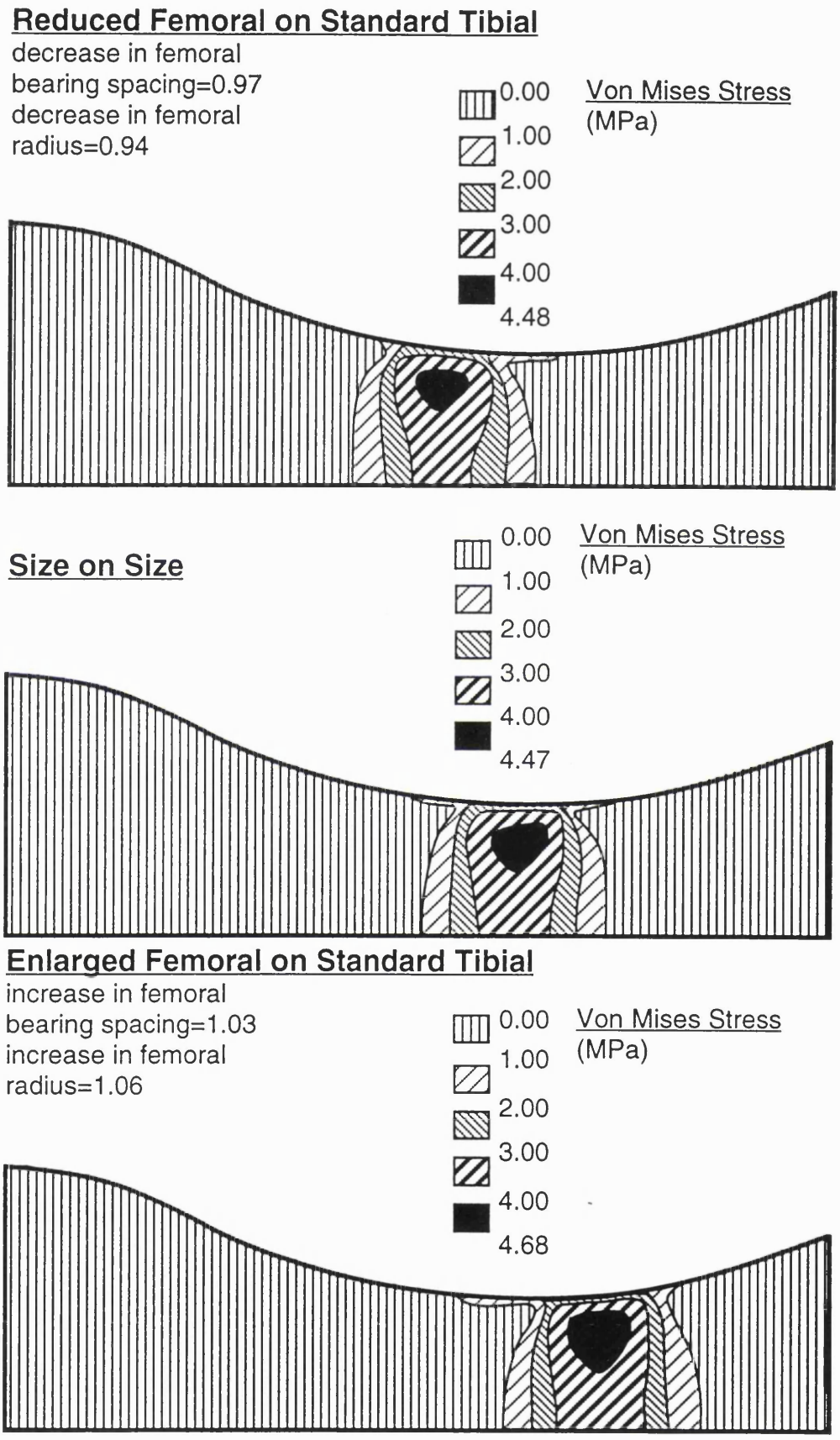

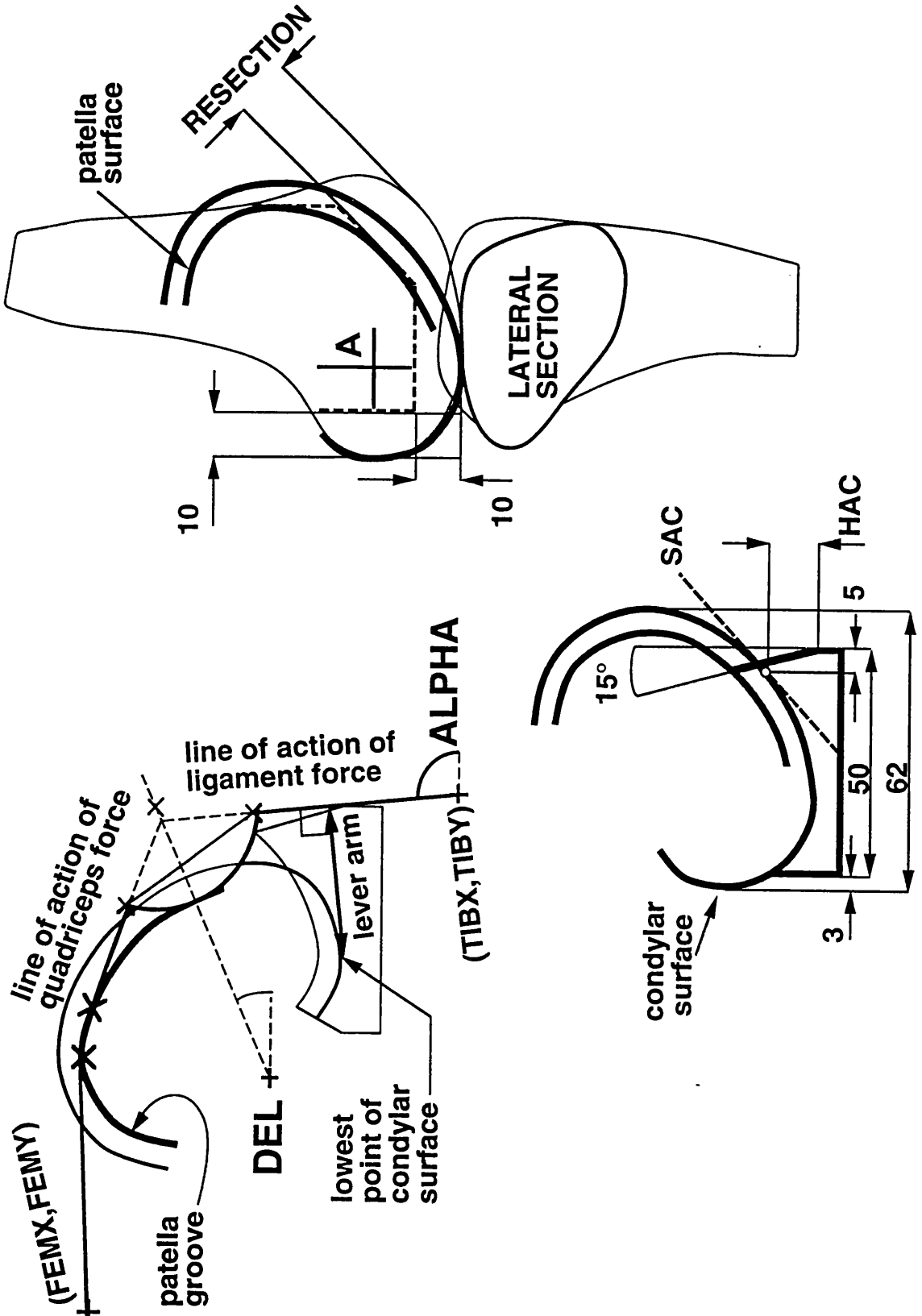

FIG.6 Models used to analyse the sagittal plane. Top left, patella equilibrium positions and lever arms. Bottom left, anterior stability. Right, amount of bone resection on chamfer.

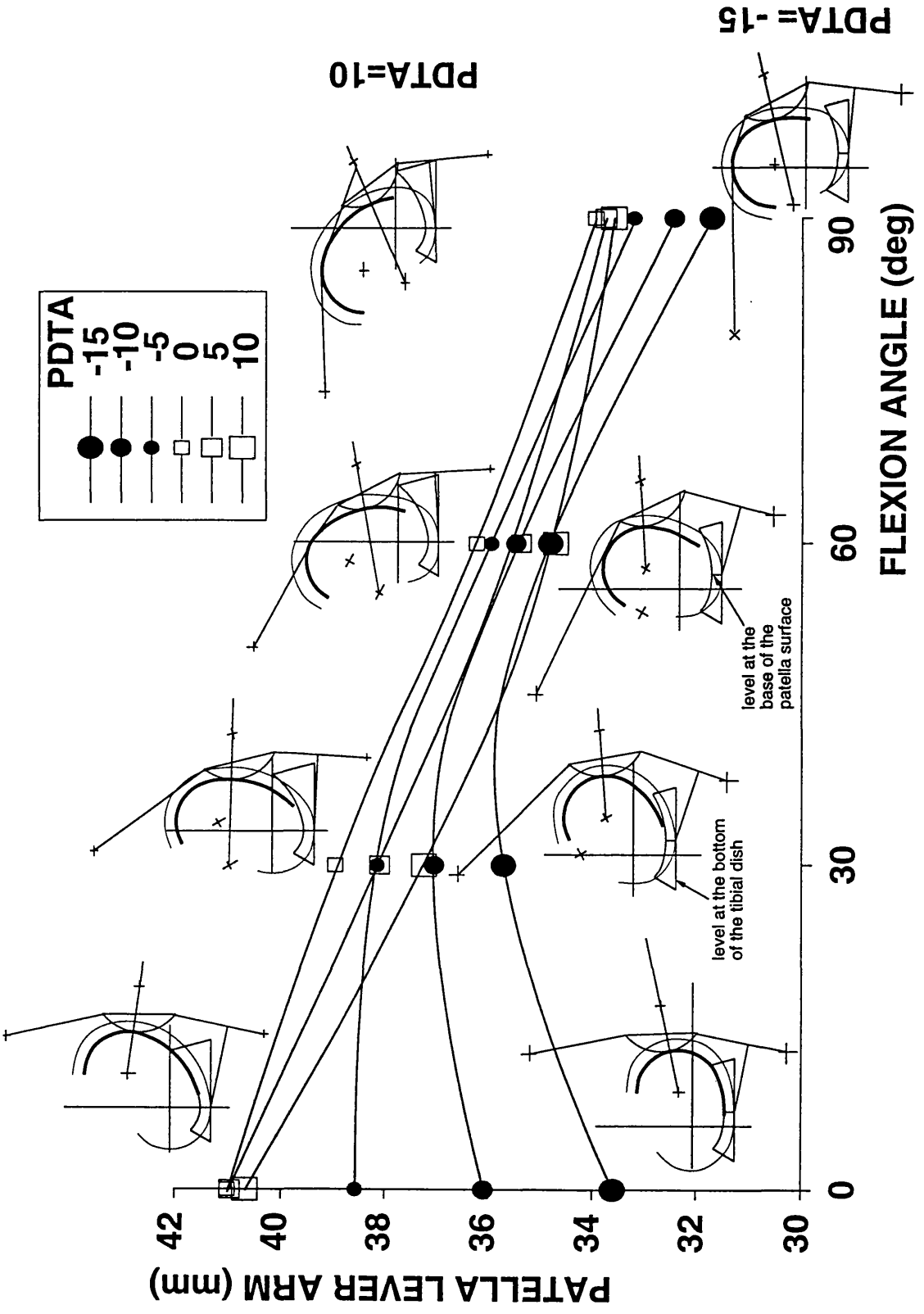

FIG.7 Lever arms of the patella ligament over a range of flexion angles, for femoral components with different posterior-distal transition angles (PDTA).

Chapter 3

GENERATION OF PROSTHETIC MODELS

3. GENERATION OF PROSTHETIC MODELS

Computer-aided drawing software packages exist which can model solid objects in three-dimensions. However, the advantage of writing a computer program which especially catered for total knee replacement components was that the required surfaces could be generated rapidly by inputting a set of parameters, or modifying the parameters of a basic design. The computer program could create simultaneously :

- models for display purposes
- surface meshes for rigid body analyses
- finite element models
- toolpaths for manufacturing prototypes on a CNC machine

Programs for generating points to define the surfaces of knee replacement components have been written [Walker, 1988]. They modelled the surfaces by describing them with a series of points positioned in three-dimensional space, the more points used, the more accurate the surface. The points were generated in an orderly manner to form surface meshes. For example, the femoral component was sliced along its medial-lateral width and points were positioned around each slice starting from the posterior tips of the condyles and finishing at the top edge of the anterior face.

However, these programs were not versatile enough to perform all of the tasks listed above. They could only model symmetric components which meant that it was impossible to generate newer designs which were becoming increasingly assymetric, and they required specific parameters to be input which were not easily found on engineering drawings. In addition, the shapes of the peripheries of the components could not be changed because their variability made parametrisation difficult. Finally, the programs created surfaced rather than solid models, the former being adequate for display purposes but the latter were required for finite element analyses. For these reasons, it was necessary to

review the modelling approach used in the existing surface generation programs in light of the new applications for which they were required.

3.1 THE FEMORAL COMPONENT

The polished outer surface of the femoral component consists of lateral and medial condyle surfaces which bear on their corresponding dishes of the polyethylene tibial component, and an anterior surface which incorporates a shallow groove (which may veer laterally) for the sliding patella. These outer surfaces have associated inner surfaces to interface with the flat faces of the resected femur, which is cut to the correct shape using specially designed instrumentation. Finally, a periphery travels around the component joining the outer and inner surfaces and defining an intercondylar notch, if required, to allow the posterior cruciate ligament to move freely. The metal layer which resurfaces the femur is thin (≈1mm) near the top of the anterior surface as the prosthesis merges with the bone, and is relatively thick (≈9mm) in the region of the condyles where it replaces cut bone. The periphery can be various shapes, symmetrical so that the same components can be used for right and left knees, or asymmetrical to copy the shape of the bone for which there are many representations. The parts of a femoral prosthesis described here are illustrated in Fig.1.

A major requirement was that the parameters defining the models could be easily obtained from conventional engineering drawings. The dimensions shown on these two-dimensional drawings were used as input parameters for a computer program which generated three-dimensional models. In general, engineering drawings define two sagittal (side-view) profiles of the lateral and medial condyles and three or more frontal sections distributed between the tips of the condyles and the top edge of the anterior surface. It is important to note the difference between 'profile' which is an outline cast by a whole object and 'section' which is the shape of a cut surface. A new femoral component generating program was written with the following features:

1) Any amount of curves could be used to define the sagittal profiles.

2) The lateral and medial sagittal profiles were independent of each other. This meant that the femoral component could be assymetric or even anatomical.

3) The component could have any number of frontal sections. These describe how the surface undulates in the medial-lateral direction.

4) Each frontal section could be constructed from different internal and external radii for lateral and medial condyles and they could have different lateral and medial depths for the patella groove region and variable groove slope angles.

5) Any shape of periphery could be input, with or without an intercondylar notch.

6) The patella groove could start at any point, it could have a flat or curved base and veer laterally at the top of the flange if required.

7) The femoral component was constructed from six grids, each with equal numbers of points in each slice. This was important because a solid model could be generated easily if this format was used.

Therefore, for any given conventional engineering drawing of a femoral component :

STAGE 1 - Data was input for the lateral profile. This was defined as a series of any number of tangential arcs. The number of arcs and their radii had to be input, a starting angle for each arc and also a finishing angle for the last. This was called the reference sagittal profile (Fig.2)

STAGE 2 - As well as the reference sagittal profile, there were a variable number of reference frontal sections. Typically, there were four reference frontal sections to describe the following regions (Fig.3):

1) bearing surface

2) base of the patella groove

3) middle of the patella groove

4) top of the patella groove

However, if a more detailed surface was required, an unlimited number of reference frontal sections could be specified. For example, in one particular design, the frontal section through the condyles remained a constant shape but tilted slightly so that the lateral condyle was lower at 45deg flexion, as this encouraged natural rotation about the medial condyle. In order to include this design feature using the computer program it would be necessary to construct an extra reference frontal section including the tilt and position it in the appropriate region of the condyles. Alternatively, some designs favour the lateral side to bulge out anteriorly in order to resist the patella, these designs would require extra reference frontal sections in the anterior region to emphasise the difference between the lateral and medial sides.

The reference frontal sections (Fig.4) were described by the following parameters:

1) separate medial and lateral outer frontal radii

2) separate medial and lateral inner frontal radii

3) separate medial and lateral groove depths

4) separate medial and lateral groove slopes or radii (they could not both be specified if the groove depths were to be maintained. The groove radius was used for the bearing surface, but for the patella groove, the groove slope was considered more important for seating the patella)

5) centres of the frontal radii

6) width of the flat base of the patella groove (used to make the groove veer laterally)

The position of each reference frontal section was defined by an angle from the centre of the reference sagittal arc on which it lay (Fig.3)

STAGE 3 - The reference sagittal profile was split at equal intervals by the computer program, the number of intervals determined by the operator, depending on the refinement of surface mesh (or for a solid model, the density of the elements) required. Points were located at each interval. Spokes were

constructed from the centre of each arc to the points which lay on it. The length of each spoke was used to position the frontal sections, the tip of each spoke representing the peak of the lateral region of its corresponding frontal section.

STAGE 4 - The frontal sections belonging to the spoke points were determined by varying the parameters describing the reference frontal sections linearly between consecutive reference frontal sections. The variation could be non-linear if required, though the information required to accurately model between the frontal sections is not provided in conventional engineering drawings. Thus frontal sections were defined for the entire femoral surface using the reference frontal sections to dictate changes in shape medial-laterally, while the reference sagittal profile was used to orientate and locate them, spreading them from the tips of the condyles to the top edge of the anterior portion so that they formed the outer surface of a femoral component.

STAGE 5 - As the shape of the periphery was variable, it could not easily be expressed in parameters. Therefore, the periphery was input in four parts.

1) the anterior face

2) the base region up to the beginning of the intercondylar notch

3) the base region beyond the intercondylar notch

4) the posterior face

Each part was split into a number of horizontal slices, as many as was required to define the shape (Fig.5). Each slice was specified by the horizontal distances of its two extreme points from the origin and their height from the origin. For the posterior face and the base region beyond the intercondylar notch, four periphery points were input, the extra two points indicated the position of the intercondyar notch. The program positioned points along each of the frontal sections described above by dividing the distance between the periphery points of each section into equal intervals. Thus even though the shape of the periphery was changing, the number of points in each frontal section remained constant, the number again being specified by the operator. When the points of

the outer surface had been calculated, gridlines were passed through them sagittally and frontally to form a mesh.

STAGE 6 - The inner surface which interfaced with the bone cuts, was defined by another set of grid points with the same refinement as the outer surface. That is, for every outer surface point there was a corresponding inner surface point. The inner surface, in general, was defined by five flat planes. The joining points (in the sagittal view) of the planes had to be input to the program, again a variable number of these could be specified. These were defined by a distance and angle from the centre of the reference sagittal arc to which they were adjacent (Fig.6). Points were spread evenly around the flat planes of the inner surface in the sagittal view, and in the frontal view the inner surface points were aligned with their corresponding outer surface points in the horizontal direction.

STAGE 7 - The outer and inner surfaces of the femoral component were created by this stage, shaped according to the desired periphery. Any number of layers of points could be inserted between the inner and outer surface points to define elements inside the surfaced model, thus creating a solid model. This method created elements which were thinner in some regions than in others eg. at the tips of the condyles and at the anterior of the femoral component. Extremely thin elements would usually be detrimental in a finite element analysis, however it was fortunate that the regions which were composed of very thin elements were not likely to be in or near the regions of contact with the tibial insert.

3.2 THE TIBIAL INSERT

The existing program which defined the shape of a tibial component with a series of points also required modifying. The plastic tibial component consists of two dishes which provide bearing surfaces for the femoral condyles. Some designs have an intercondylar notch which is aligned with the intercondylar notch of the femoral component. The shape of the outer periphery of the tibial component is as varied as the periphery of the femoral component, ranging from symmetrical designs with curved edges to anatomical designs which are supposed to represent the shape of the tibial plateau.

The existing tibial component generating program used gridlines and cross-gridlines which were equally spaced to define the component. The curved edges were formed by wrapping the gridlines around the periphery if they travelled beyond it. This produced a very neat surface model because the curved gridlines formed smooth edges (Fig.7a). However, this program could not be used to create a solid model for finite element analysis because the curved gridlines would not form brick-shaped elements. It could not be used for rigid body analyses either because the points on the curved gridlines were unsuitable for determining polynomials for local patches. An alternative method would be to terminate the gridlines once they passed over the edge of the periphery, but then the curved edges would appear to be stepped and finite element analyses where contact occurred at the edges of the tibial component would be inaccurate.

Ideally a solid model of the tibial component would have its rounded corners as well defined as the interior regions, with brick elements which follow the shape of the contoured regions. This was possible if the shape of the tibial component was split into rectangular regions and curved sectors. A new tibial component program was written along these lines (Fig.7b). In the rectangular regions the elements had a regular pattern separated by gridlines which travelled anterior to posterior and medial to lateral. The sectors were split into an outer curved band and an inner rectangular region. The elements followed the curve around the edge of the sector in the outer curved band, but in the inner region they had a regular pattern as for the rectangular regions already mentioned.

The tibial dishes were represented by toroidal surfaces which had :

1) separate medial and lateral outer frontal radii
2) separate medial and lateral inner frontal radii
3) separate medial and lateral anterior sagittal radii
4) separate medial and lateral posterior sagittal radii
5) 4 rounded corners with variable centres and radii

6) variable joining angles between the anterior and posterior sagittal arcs and the medial and lateral frontal arcs

7) variable basic dimensions such condylar spacing (the frontal width between the bases of the dishes), medial-lateral and anterior-posterior lengths

In reality, the underside of the plastic tibial component is machined so that it can clip into the tibial tray. For the purpose of this study, the plastic tibial component was modelled with a flat underside which could be positioned at various depths below the base of the tibial dishes. The underside had corresponding points for every point on the tibial surface and as for the femoral component, any number of layers of points could be inserted between the surface and underside points, to produce internal elements when generating a solid model.

3.3 APPLICATION OF MODELLING PROGRAMS (1) - MANUFACTURE OF CUSTOMISED KNEE REPLACEMENTS

The ability of the prosthetic component modelling programs to design implants given values for set parameters and to generate data-files describing three-dimensional shapes, made it feasible to design and manufacture customised knees replacements. However, the data-files could not be input directly to a computer numeric controlled (CNC) milling machine. Tool correction programs had to be written so that the tool machined around the required shapes without digging into them.

3.3.1 METHODS AND MATERIALS

Computer programs were written to produce CNC toolpaths where the size of the tool was a variable. The tibial inserts were machined, using a ball-nosed tool, from blocks of polyethylene held in a vice. The tool machined parallel lines back and forth (0.2mm apart) in the anterior-posterior direction, the toolpath varying the height of the tool to machine a set of curves which formed the tibial dishes. The computer program was modified to enable manufacture of tibial inserts with superstabilising posts. To cut the post, the program calculated a toolpath which

machined horizontal contours around the post which reduced in height from the top to the bottom of the post.

The femoral components were machined from solid bars of stainless-steel held perpendicular to their central axes in the rotating chuck of a CNC machine. A special toolpath program was written for the outer surface which was machined using the side of the tool. This was done by incrementally rotating the chuck which held the stainless-steel bar. For each angle the program calculated a toolpath which would make the side of the tool closest to the stainless-steel bar machine the furthestmost points which protruded along the medial-lateral width of the component. As the ball-nose of the tool was not being used, the height of the tool did not matter, however the tool had to be positioned low enough so that it was deeper than the central axis of the bar. This was not possible for large components because the tool-holder would collide with the bar. For these cases, the outer surface was machined twice, first with the tool machining in front of the bar and then machining behind it. Any parts which were too low below the central axis to be machined when the tool was in front, would be machined when the tool was behind, as these parts would then be above the central axis.

The computer program also calculated toolpaths for the inner surfaces of the femoral component which interface with the bone cuts. For superstabilised designs, toolpaths for machining a housing for the superstabilising post and a boss to hold a fixation stem were also generated (Fig.8).

3.3.2 RESULTS

Production of at least five completely customised superstabilised knee replacements, which were all implanted into patients (Fig.9), proved that this manufacturing method was feasible. However, machining the femoral component from stainless-steel was a very time consuming process. Efforts were made to speed up the design process by adding a user-friendly interface to the program, which could be used by workshop technicians. This modified program suggested a basic design to the operator and allowed key parameters to be changed.

When these parameters were input, CNC code for the milling machine was automatically produced.

3.3.3 DISCUSSION

If the femoral component was being machined by conventional machining packages which are commercially available, it would probably be machined in two halves using the ball-nosed end of the tool, which happens to be its bluntest part. The method described here where the side of the cutter was used to machine the outer surface of the femoral component was successful, but overall the time taken to manufacture the femoral component out of stainlesss-steel was too long. This meant that these customised knee replacements could not be made on a routine basis. For the tibial components, machining speed was not a problem but the surface finish of the bearing surface was not as smooth as moulded polyethylene inserts which are available on the market. However, despite these factors, the computer program provided an urgently needed solution for patients suffering from extreme cases of deformity or bone loss, who could not be treated with off-the-shelf products. To date their follow-up reports are satisfactory.

3.4 APPLICATION OF MODELLING PROGRAMS (2) - FINITE ELEMENT ANALYSIS OF MOBILE BEARING TIBIAL INSERTS

Tibial inserts of total condylar knees cannot be designed to be completely conforming to their mating femoral components because they must allow relative motion between the two parts if natural function is to be reproduced. On the other hand, in mobile bearing knees, the bearing surface design is not restricted in the same way because relative motion can occur between the tibial insert and the tibial tray instead. The modelling programs were applied again, this time to produce finite element models, to analyse the advantages of a completely conforming femoral-tibial interface in a mobile bearing knee replacement.

3.4.1 METHODS AND MATERIALS

Five knee designs were defined. The femoral components were identical for all of the designs. They had frontal radii of 30mm, posterior sagittal radii of 20mm, distal sagittal radii of 48mm and posterior-distal transition angles of -8deg. The intercondylar grooves had radii of 15mm and the distances between the two condyles were 48mm.

The tibial inserts had varying designs :

	FRO (mm)	**INT** (mm)	**ANT** (mm)	**POST** (mm)
tibial insert 1	30	16→20	48	20
tibial insert 2	31	16→20	49	21
tibial insert 3	33	16→20	51	23
tibial insert 4	36	16	60	40
tibial insert 5	40	16	70	70

where: FRO=frontal radius, INT=intercondylar crest radius,

ANT=anterior sagittal radius, POST=posterior sagittal radius

The tibial insert's intercondylar crest radius was changed to 20mm for Designs 1 to 3 to avoid impingement with the femoral intercondylar groove.

Finite element models were generated for the five different designs. The femoral component bearing surface was modelled with 15740 rigid body elements and was meshed very finely in comparison to the tibial component to minimise errors due to misalignment of the contact nodes. The component was stabilised by a spring with stiffness of 10N/mm. The tibial insert models consisted of 4660 8-noded solid brick elements with an elastic modulus of 600MPa and a Poisson's ratio of 0.4.

To determine an acceptable element size consistent with accuracy, stress data was obtained for a spherical contact between a rigid femoral-like indentor of 20mm radius and a 70mm radius spherical dish of polyethylene, the polyethylene

measuring 32mm on each side. The analytical results were compared with the Hertz solution. Element sizes from 4mm down to 1mm were examined. Convergence of the contact stress values and agreement with the Hertz data were obtained for a 2mm element size, consistent with that determined by Mottershead et al [1996]. Changing the element sizes from 2 to 1mm, increased the maximum contact pressure from 60.40 to 61.62MPa and the maximum shear stress from 33.60 to 35.42MPa. The element sizes for the models in this study were approximately 1.8x1.0x0.7mm.

Five layers of elements were used for the tibial insert, the layers reducing in height approaching the articulating surface to obtain more accurate results. The interfacing surfaces of the femoral component and tibial insert were defined as frictionless contact surfaces and the base nodes of the tibial insert were constrained in the vertical direction to represent the support provided by a metal tibial tray. The tibial inserts of all the designs had thicknesses of 6mm from the base of the dish to the base of the insert, to represent the thinnest thickness currently used. ABAQUS version 5.4 (Hibbitt, Karlsson, and Sorensen, Inc., Pawtucket, RI) finite element analysis was used to compress the prosthetic models together under 2000N compression, to determine the stresses in each element of the polyethylene inserts. Tests were carried out in extension and 60deg flexion.

3.4.2 RESULTS

The greatest values of the maximum shear stress and maximum principal stress were recorded for each tibial insert at each angle of flexion and are plotted in Fig.10. The magnitudes of the stresses reduced with increased conformity, the most conforming design having a maximum shear stress in extension which was approximately one quarter of that of the least conforming design. Increasing the clearance between the bearing surfaces from 1mm to 3mm increased the stresses in extension by one third. However, when the most conforming design was flexed, the maximum shear stress doubled, whereas for the least conforming design there was not a significant difference. The maximum principal stress also

reduced with conformity when the different designs were in extension, while in flexion there was not a significant difference between the designs.

SEE APPENDIX FOR MORE RESULTS

3.4.3 DISCUSSION

Fig. 11 compares the maximum shear stress contours in Design 2 and Design 5 at 60deg flexion under 2000N compression. (ABAQUS plots the Tresca criterion which is twice the maximum shear stress.). It can be seen that for the more conforming interface (Design 2), the magnitudes of the maximum shear stresses were significantly lower. For the less conforming design (Design 5), the maximum shear stress peaked in a stress concentration just below the surface, in the region where subsurface cracking which leads to delamination usually initiates. The stresses for Design 2 were even lower in extension, but these very low stresses were not maintained when flexion was imposed. This is because when the posterior-distal transition angle is negative, the large distal radius makes contact with the tibial insert during extension. The tibial insert must be designed accordingly, with a large radius to accommodate the femoral component. However, during flexion the femoral component bears with its smaller posterior radius, and the unconforming situation which arises between the bearing surfaces produces higher stresses. Designing with a positive posterior-distal transition angle solves this problem, because the femoral component bears with its smaller radius throughout flexion, so the tibial component can also be designed with a small sagittal radius. However, a positive posterior-distal transition angle does have drawbacks, such as excess femoral bone resection, which has already been discussed in the previous chapter.

The simplified model developed in the previous chapter would not have been sufficient to analyse these mobile bearing designs, because the close conformity of two of the designs meant that slight changes in the bearing surface geometry could transfer contact from the tibial dishes to the intercondylar crest. During gait, a similar scenario may occur even for less conforming designs, due to rotation and displacement of the femoral component with respect to the tibial insert. Contact may also occur near the edges of the polyethylene during gait. The simplified model of the tibial dishes, which does not include a periphery

defining the edge of the component, would not give accurate results for such situations because the stresses increase as contact approaches the edge of the tibial insert.

Therefore, complete bearing surfaces have to be modelled if stresses are to be analysed during gait. In this chapter, computer programs were devised for generating complete bearing surfaces, and these programs were applied to create finite element models. The next step was to determine the relative orientations of the prosthetic components during gait so that realistic stresses produced in tibial inserts could be quantified.

THE COMPONENTS OF A FEMORAL KNEE PROSTHESIS

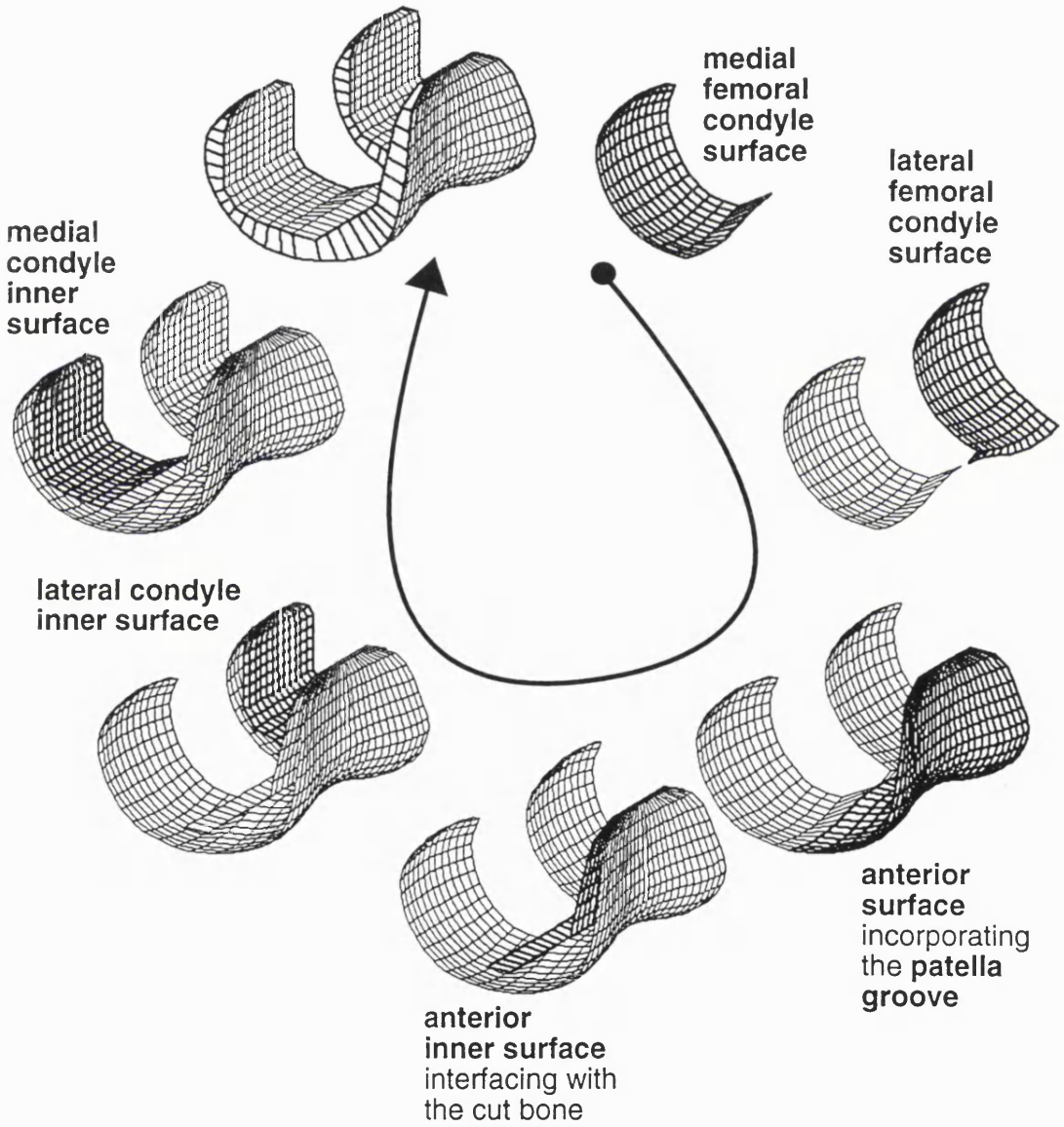

FIG. 1 The different regions which make up the femoral component.

FIG. 2 Typical arcs defining the sagittal profile of the femoral component.

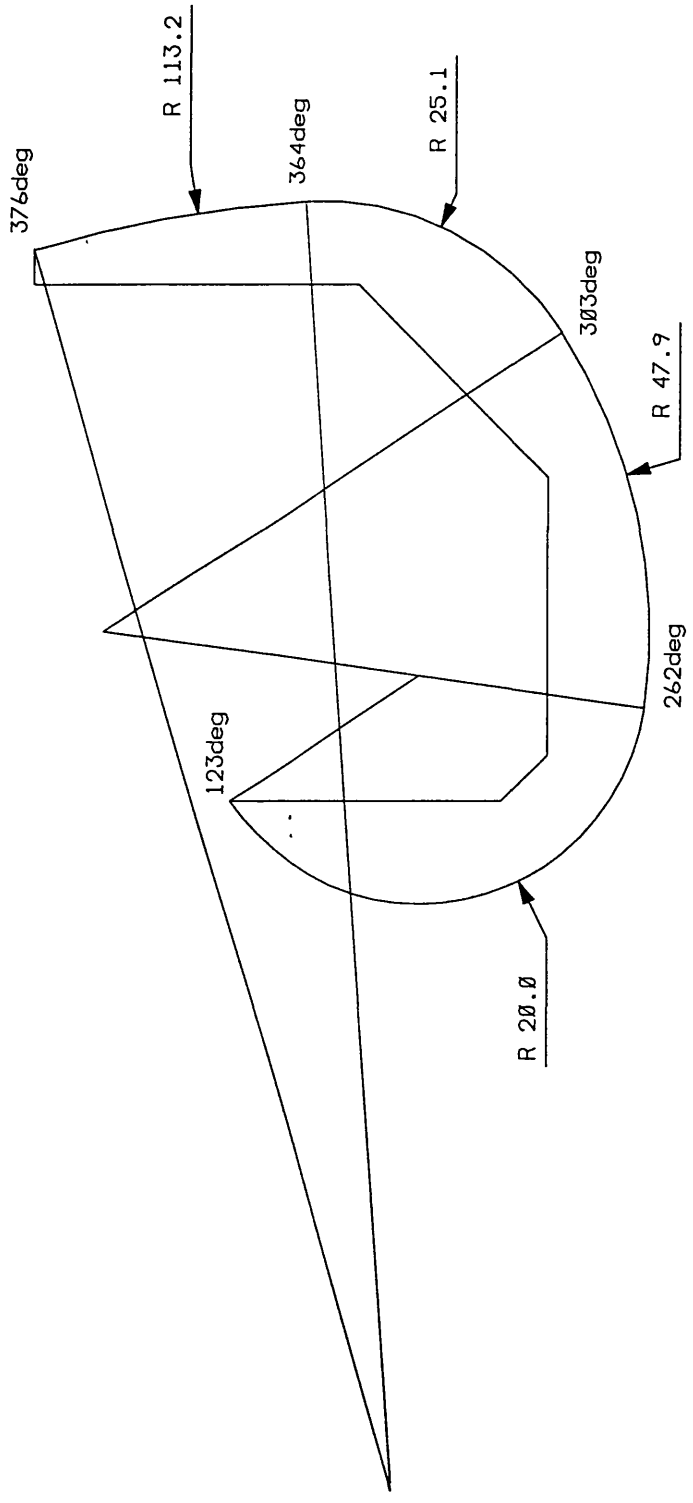

FIG. 3 A typical set of reference frontal sections.

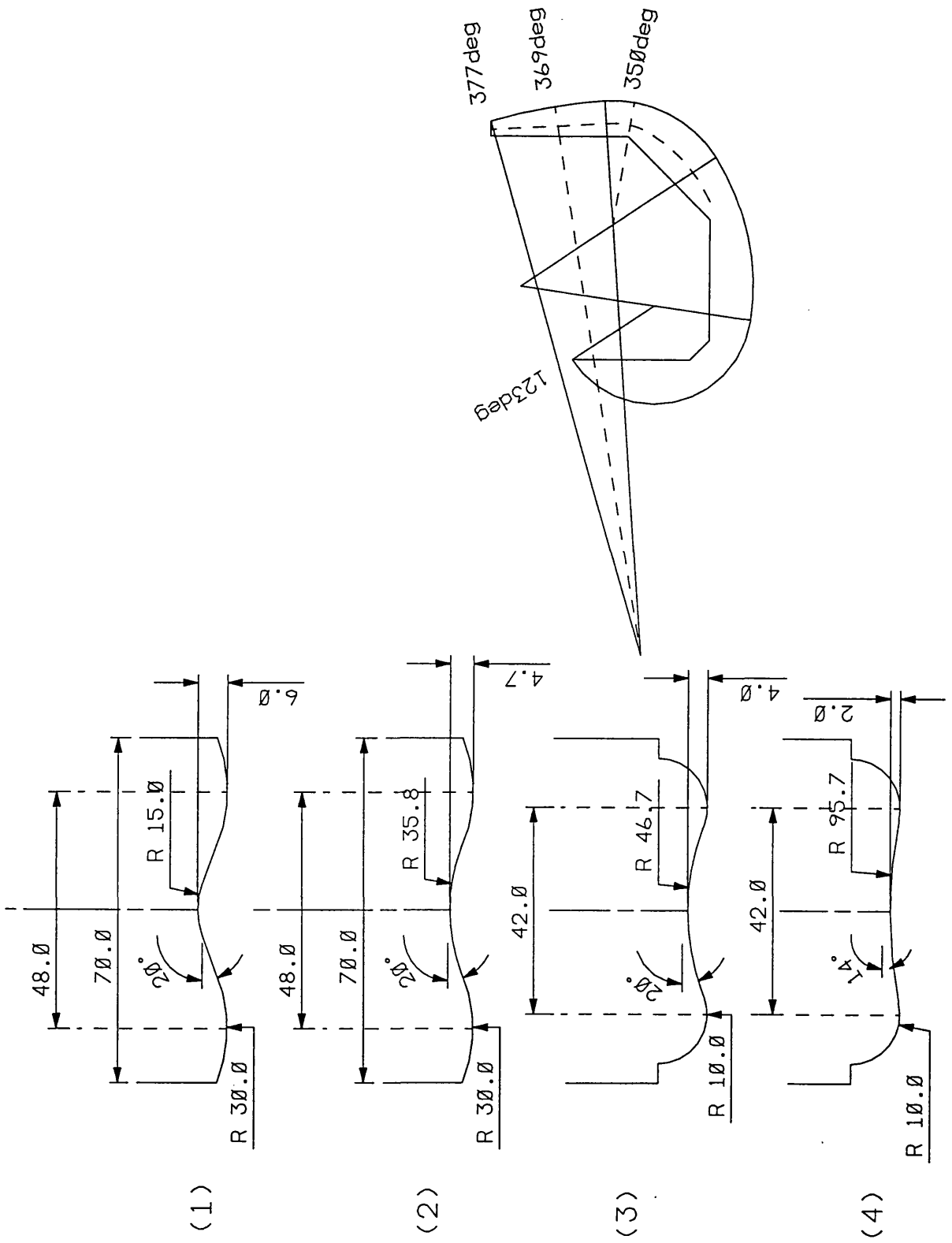

FIG. 4 Variable parameters for a reference frontal section.

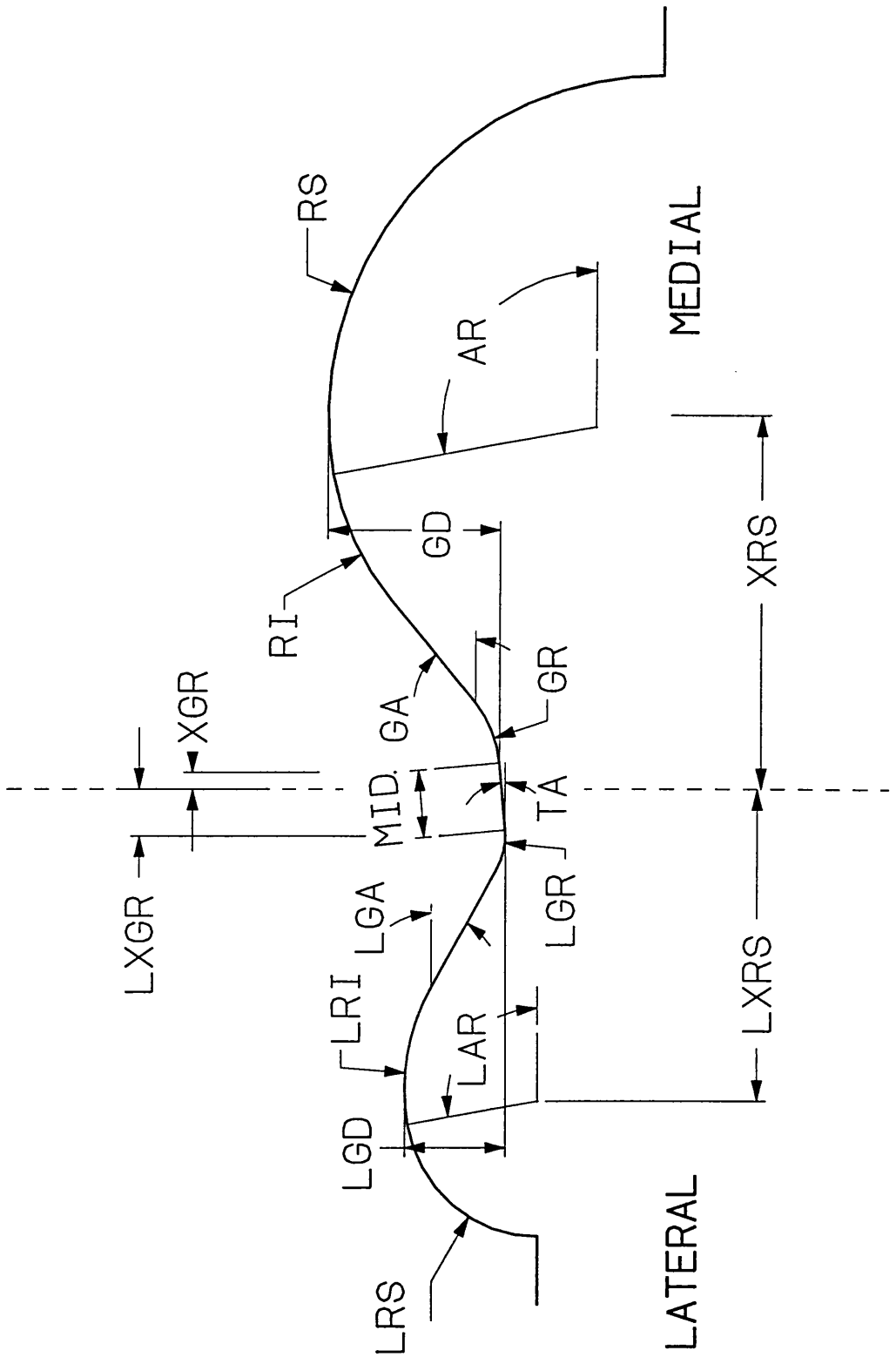

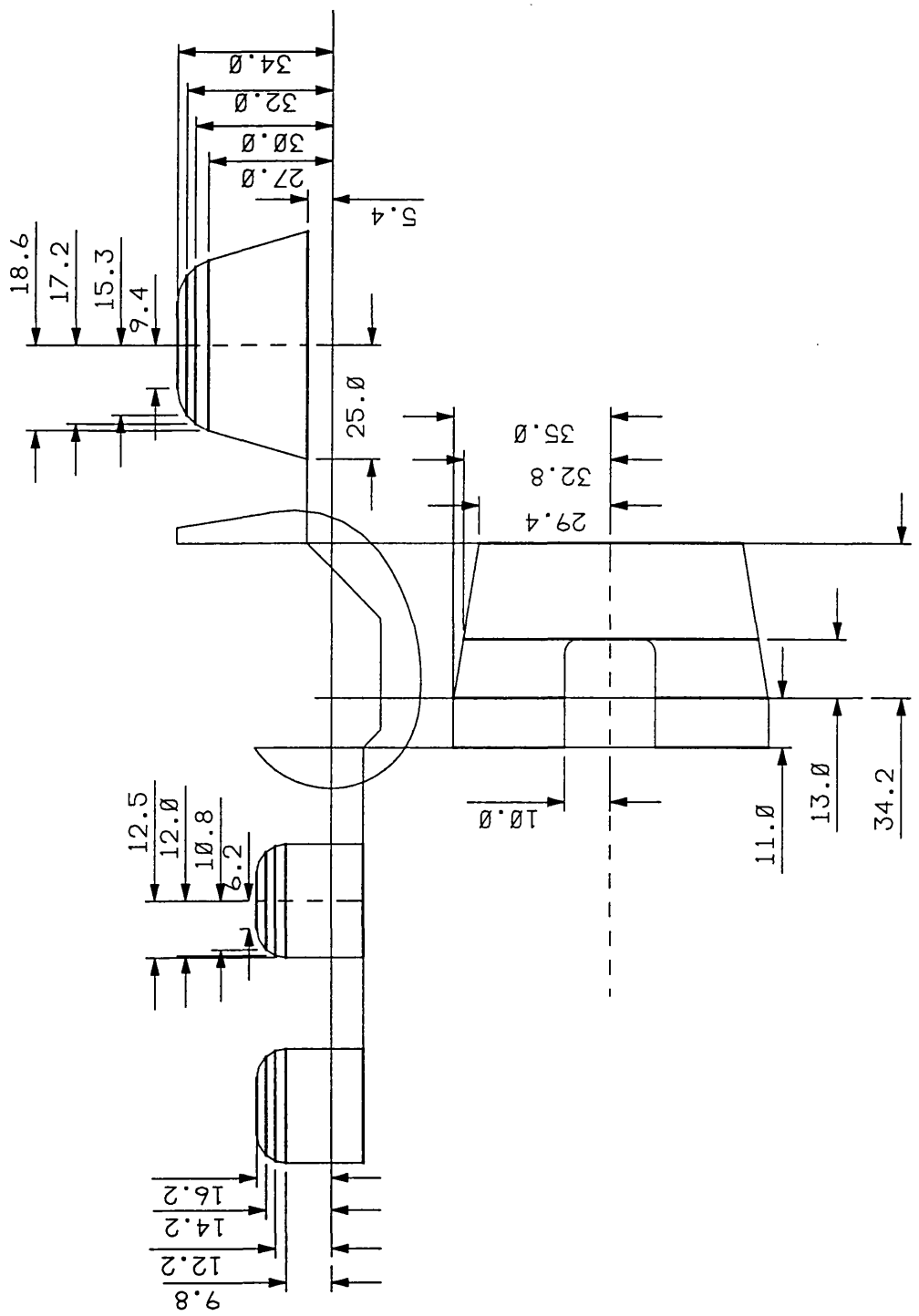

FIG. 5 Defining the periphery of the femoral component.

FIG. 6 Defining the regions of the femoral component which interface with the bone.

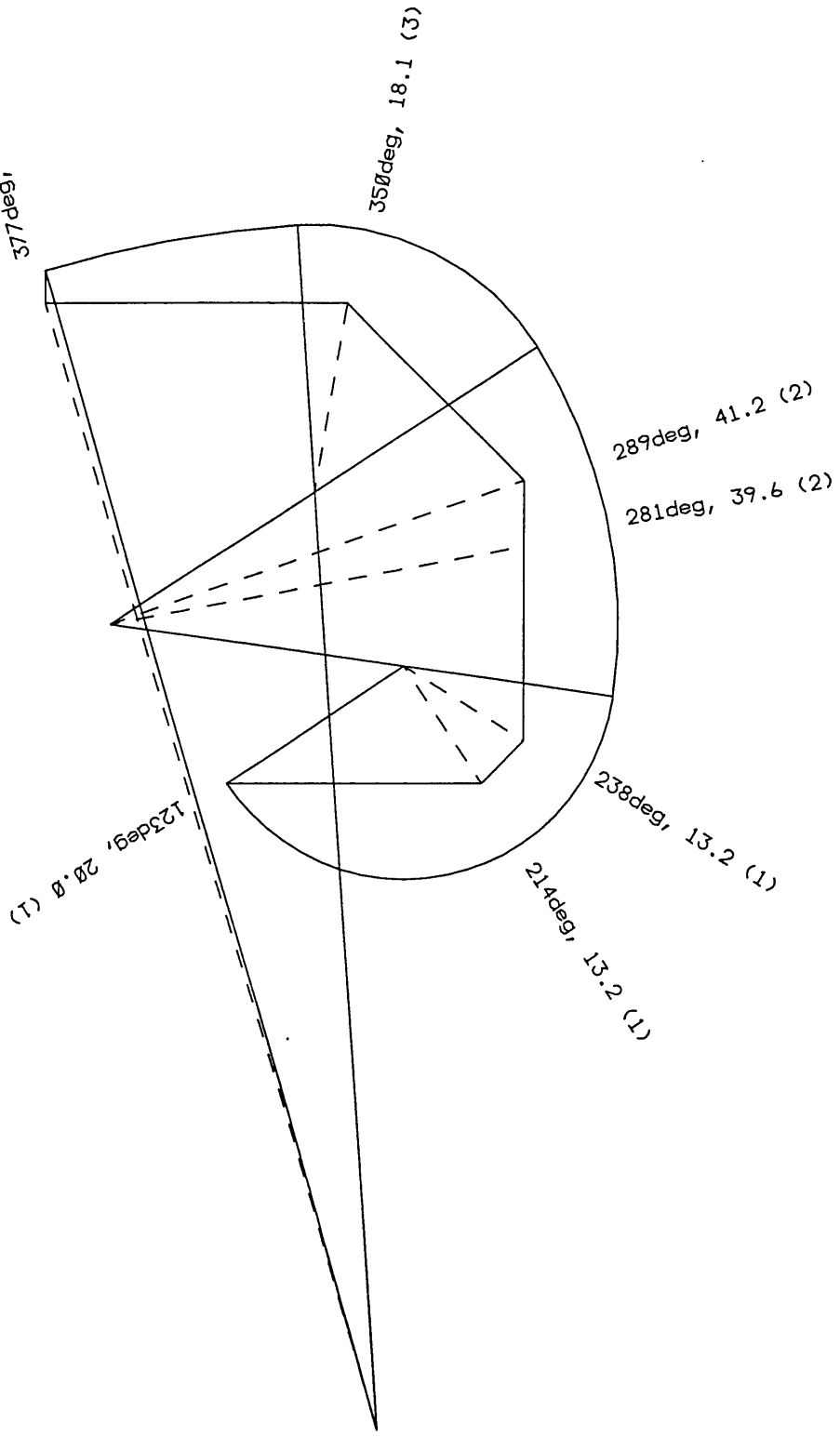

a)

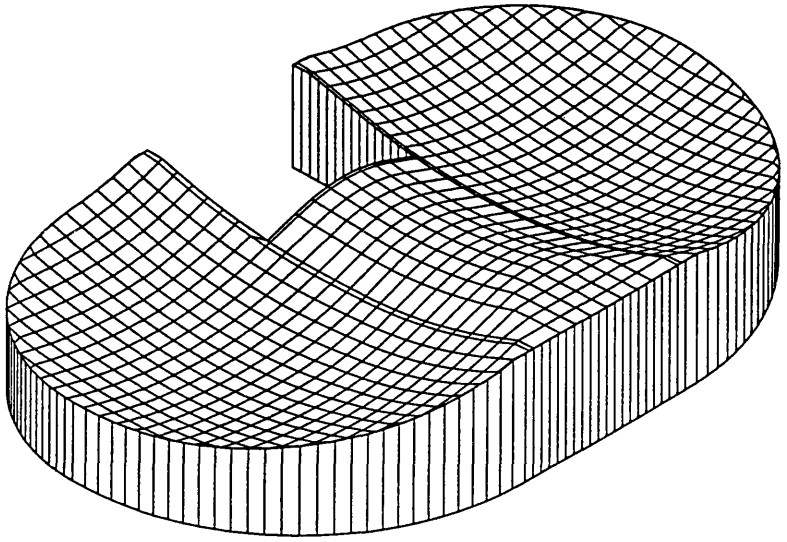

b)

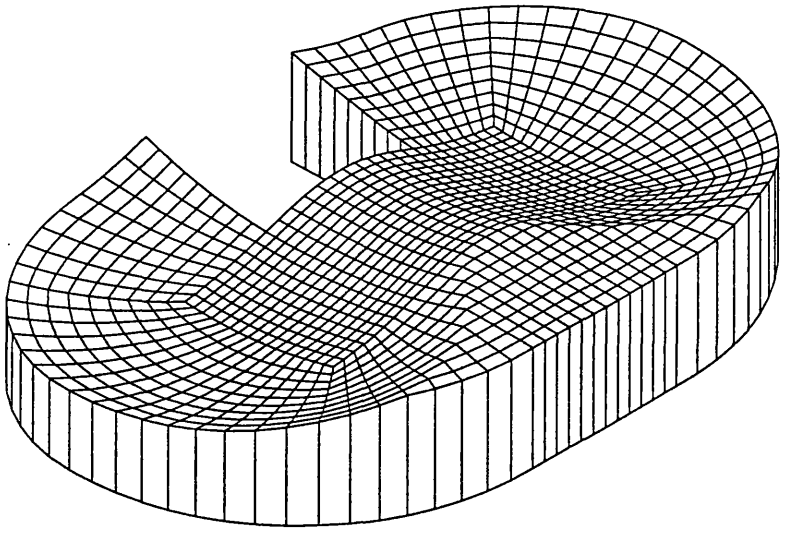

FIG. 7 a) The rigid body model of the tibial component. b) The finite element model of the tibial component.

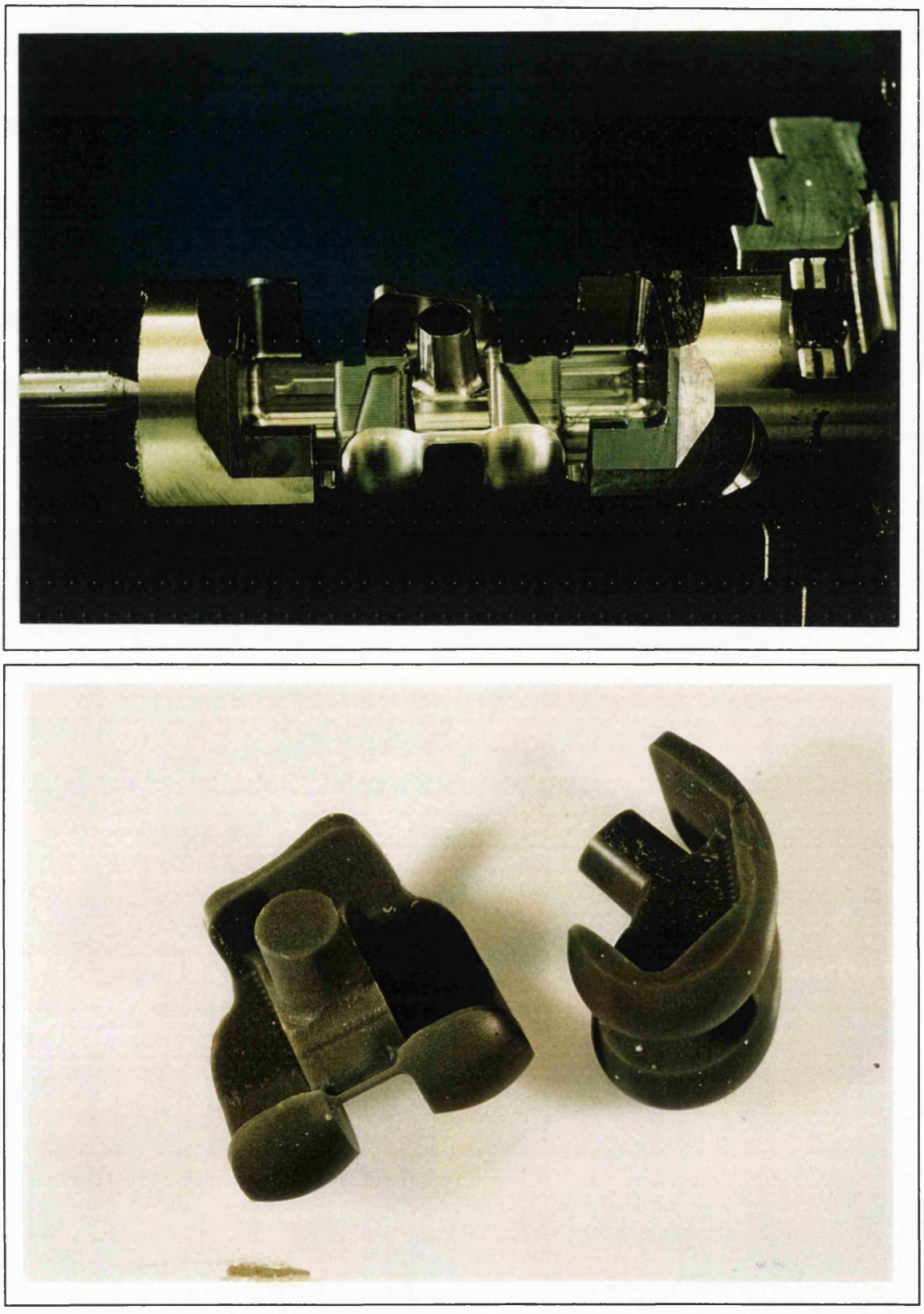

FIG. 8 A superstabilised stainless-steel femoral component and casting waxes manufactured using a CNC machine and computer software developed to generate surface models of the prosthetic components.

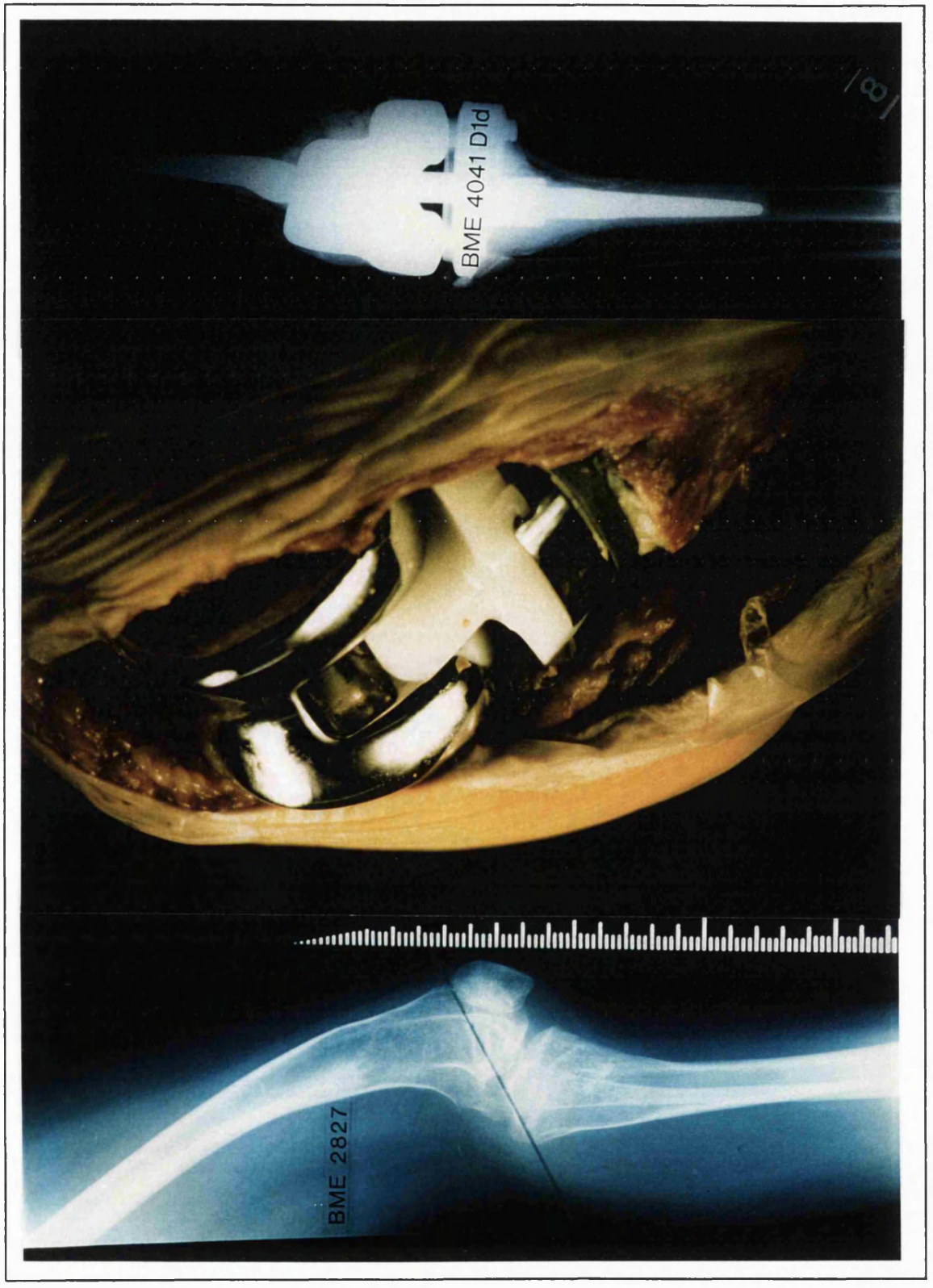

FIG. 9 BOTTOM : A patient who requires a customised knee. MIDDLE : A customised knee being implanted. TOP : A post-operative radiograph.

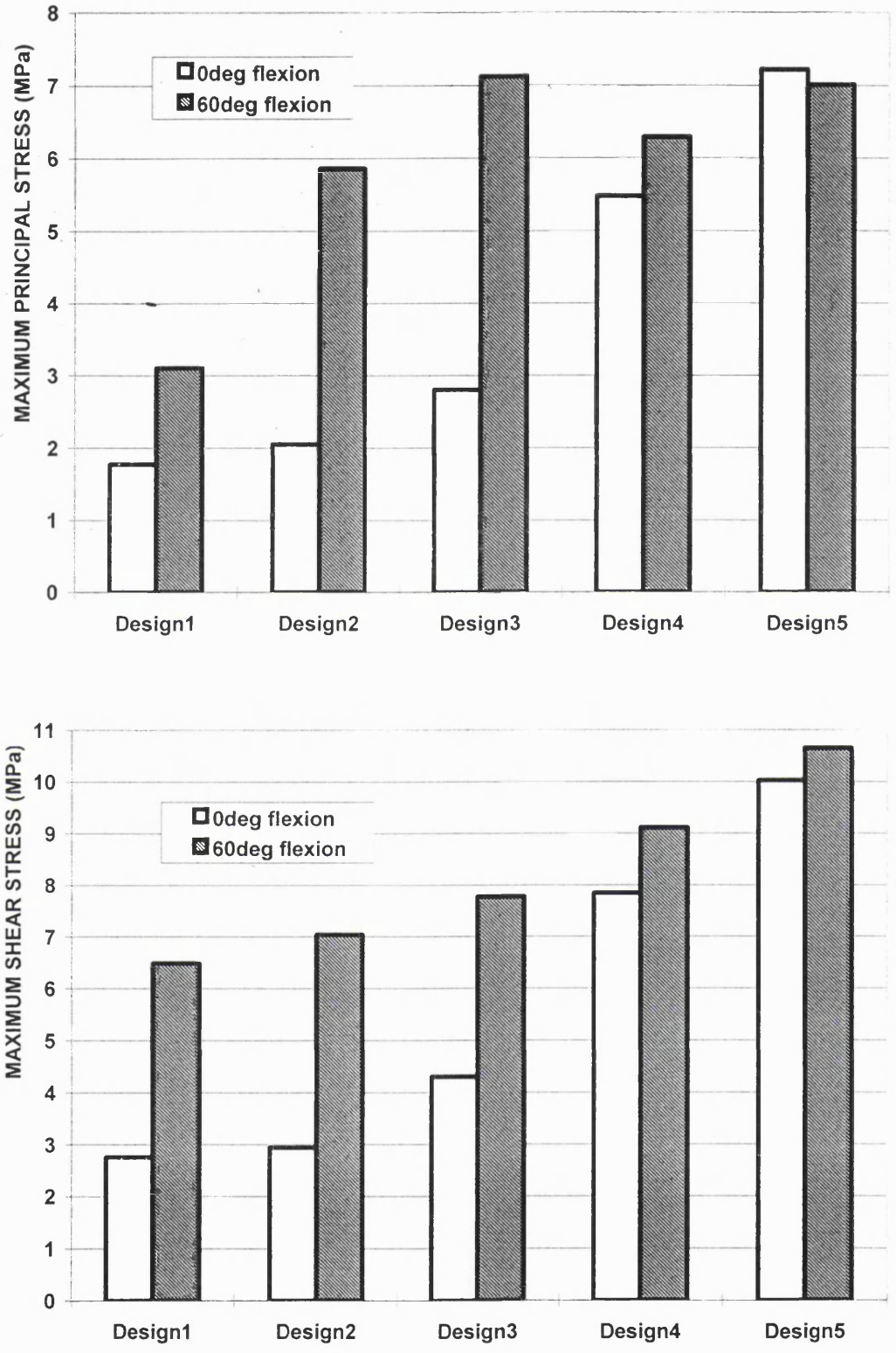

FIG. 10 Graphs comparing the maximum shear and maximum principal stresses in the tibial inserts of five mobile bearing designs with different conformities.

THE KNEES WERE LOADED AT 60DEG FLEXION.
THEY WERE SECTIONED SAGITTALLY IN THE REGION OF CONTACT.
TRESCA CRITERION (TWICE MAX SHEAR) CONTOUR PLOTS WERE MADE

DESIGN 2 ABAQUS

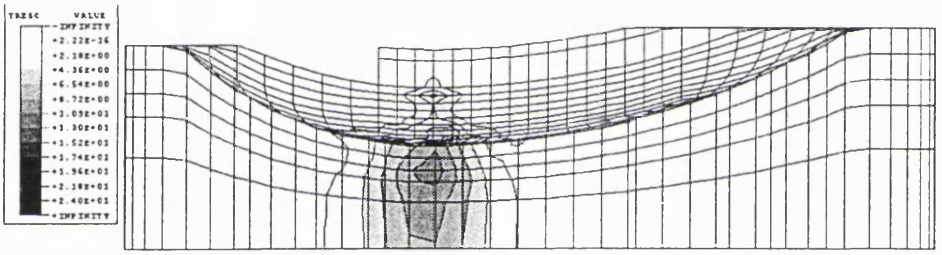

DESIGN 5 ABAQUS

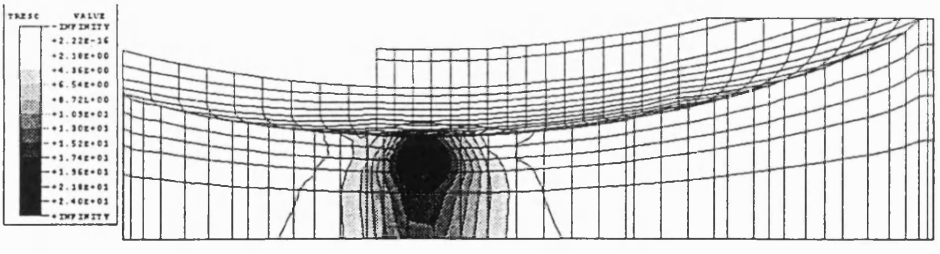

FIG. 11 Maximum shear stress contoured plots for very conforming and unconforming mobile bearing designs.

Chapter 4

USING RIGID BODY ANALYSIS TO DETERMINE PROSTHETIC KNEE KINEMATICS

4. USING RIGID BODY ANALYSIS TO DETERMINE PROSTHETIC KNEE KINEMATICS

4.1 INTRODUCTION

The motion at the femoral-tibial articulation in total knee replacements during function has a number of important implications. The contact point location directly affects the lever arm of the quadriceps, which determines the force which needs to be generated for a given external moment [Otis et al, 1986; Mikosz et al, 1988]. Repetitive sliding of the surfaces under load is likely to lead to an increase in the wear of the polyethlene [Blunn et al, 1991]. In addition, excessive anterior-posterior displacements or internal-external rotations lead to contact locations at the extreme edges of the tibial insert [Sathasivam & Walker, 1994], which can be especially damaging as noted on retrieved specimens [Collier et al, 1991; Blunn et al, 1994]. Inadequate sliding motion on the other hand can impair function by increasing the likelihood of a flexion contracture, reducing range of flexion and internal-external rotation, and over-tensing of the soft tissues [Iversen et al, 1989; Warren et al, 1994].

However, motion at the bearing surfaces is difficult to determine accurately in vivo. Direct measurement on normal subjects has been achieved by attaching pins to the bones themselves [Lafortune et al, 1992], while for total knee replacement, a cine-radiographic method was used to show that variable anterior-posterior translation patterns occurred for different total knee replacement designs when the patients stood up from a squatting position [Gabriel et al, 1996]. Other studies have used external methods to measure prosthetic knee motion under different conditions [Stein et al, 1988; El Nahass et al, 1991; Warren et al, 1994; Walker et al, 1995]. These studies demonstrated that the displacements and rotations were reduced not only by the compressive force, but also by friction. In addition, under functional loads, the displacements could be sufficiently small due to the condylar geometry and friction, that soft tissue restraints would play a minor role for the moderate to high constraint

designs. It is notable that the coefficient of friction in artificial joints is in the range of 0.03 - 0.10 [Fisher & Dowson, 1991] whereas in the natural joint, friction will have less effect on kinematics because the coefficient of friction is only 0.002 - 0.03 [Mow & Soslowsky, 1991].

The effect of the different variables can be determined experimentally or by using a theoretical knee model. Previous models have varied in their complexity, and have included condylar and ligament geometries, soft tissue and bearing surface material properties, and muscle actions [Crowninshield et al, 1976; Andriacchi et al, 1983; Wismans et al, 1980; Blankevoort et al, 1991; Essinger et al, 1989; Garg & Walker, 1990]. The position of the femur on the tibia has been determined by equilibrium methods [Wismans et al, 1980; Blankevoort et al, 1991], by imposing defined motion parameters [Garg & Walker, 1990], by minimum energy [Essinger et al, 1989], and by a stochastic process [Mikosz et al, 1988 & 1993]. None of the above models took friction into account, primarily because their main application was to the normal intact knee where the friction is small.

Delamination wear is a fatigue mechanism which is caused by polyethylene in the tibial insert being repeatedly loaded and unloaded with excessive stresses. To solve the problem of delamination, the characteristics of designs which are likely to make them prone to fatigue failure have to be identified. In order to do this, the locations of the contact patches and the magnitudes of the stresses produced in the tibial inserts of different knee designs when gait loads are applied need to be determined. In this chapter, a new quasi-static model for total knee replacement was developed, which could determine the displacements and rotations of the femoral component relative to the tibial insert and hence the locations of the contact patches on the polyethylene, as a function of condylar geometry, input forces, soft tissue restraints and surface friction. This was achieved by using the programs for modelling the complete bearing surfaces described in the previous chapter, inputting cycles of flexion, compression load, anterior-posterior force and

internal external torque to the models, and calculating their kinematics using a quasi-static rigid body analysis.

4.2 METHODS & MATERIALS

4.2.1 DESCRIPTION OF THE BEARING SURFACES AND AXIS SYSTEMS

The bearing surfaces of condylar replacement knees were defined in terms of geometric parameters. Meshes of any required density, typically spaced at 0.8mm, were then generated to describe the surfaces. A coordinate system was fixed in the tibia (Fig. 1), such that the transverse axis passed through the lowest points on the lateral and medial tibial surfaces, the anterior-posterior axis passed along the centre line of the tibial surface, and the vertical axis was mutually perpendicular. For the femur, the transverse axis passed through the centres of the circular arcs of the posterior femoral condyles. The tibial surface was considered fixed and the femoral surface moved relatively. The applied forces and moments were defined relative to the tibial axis system and applied to the femoral component.

4.2.2 RELATIVE FEMORAL-TIBIAL POSITION & CONTACT POINTS

One contact point for each condyle could be calculated for any orientation of the femoral component relative to the tibial insert. To obtain an initial estimate of the contact points on the lateral and medial sides, the grid points of closest approach on the femoral and tibial surfaces were determined by iteration [Walker, 1988]. Utilising the eight points around each of these grid points and the grid point itself, an equation of the surface was expressed as follows:

$$y = f(x,z) = A + B.x + C.z + D.x^2 + E.z^2 + F.x.z. + G.x^2.z + H.x.z^2 + I.x^2.z^2 \qquad (1)$$

To obtain a more precise solution for the contact points, a search routine was carried out at the required accuracy (0.01mm) starting from the initial grid points and travelling through the local surface patches defined by (1). The unit vector of the contact normal at each contact point P was calculated, designated as ux, uy, uz (Fig.1).

4.2.3 EQUILIBRIUM CONDITIONS

The purpose of the analysis was to determine the path of motion of the femoral component relative to the tibial insert for input cycles of compression load, anterior-posterior force, internal-external torque and flexion (Fig.2) which were changing with time. The path of motion was defined by the successive contact points on the lateral and medial tibial surfaces, but could also be expressed as the rigid body motion of the femoral origin. The movement of the contact points and the movement of the femoral origin would be similar if the conformity of the tibial insert to the femoral component was low, but would differ as conformity increased, the femoral origin moving less compared to the contact points.

The problem was formulated by considering successive increments of the input cycles at discrete time intervals dt. Assuming an equilibrium position at time t, the problem was to determine the new position at time t+dt. The equilibrium equations included the input forces and moments, the reaction forces along the contact point normals, the frictional shear forces, and the forces due to soft tissue restraint. The force equilibrium equations took the following form :

$F_i + FB_i + RL.ul_i + RM.um_i + SL.vl_i + SM.vm_i = 0$ $\quad i = x,y,z$ ....(2, 3, 4)

F = applied force

FB = soft tissue force

RL = normal reaction force on lateral side

ul = unit vector at lateral contact point

RM = normal reaction force on medial side

um = unit vector at medial contact point

SL = frictional shear force at the lateral contact point

vl = unit vector along line joining previous to new contact points on the lateral side

SM = frictional shear force at the medial contact point

vm = unit vector along line joining previous to new contact points on the medial side

(**vl** and **vm** were assumed to be normal to **ul** and **um** respectively with sufficient accuracy).

Similarly, equations were written for the moments about the three axes:

$$\Sigma M(i)=0 \qquad i=x,y,z \qquad (5, 6, 7)$$

4.2.4 CALCULATING THE RESIDUALS

It was assumed that equilibrium would be achieved at time t+dt at a unique position, with specific normal vectors at the two contact points. For a given orientation of the femoral component on the tibial insert, equilibrium was examined as follows. Equation (3) $\Sigma F(y) = 0$ and equation (6) $\Sigma M(z) = 0$ were used to solve for RL and RM. Equation (5) $\Sigma M(x)$ would be satisfied by the applied flexion moment. The values for RL and RM, and the other known values, were substituted into the remaining equations. Except in the equilibrium position, these equations would not be satisfied and hence they were rewritten as :

$$\Sigma F(x)=ex \qquad \Sigma F(z)=ez \qquad \Sigma M(z)=gy \qquad (8, 9, 10)$$

where ex, ez, gy = residual errors in the equations.

An error function was defined as :

$$RES = (|ex| + |ez| + |gy/CS|) \qquad (11)$$

where CS = half the lateral-medial condylar spacing, introduced to make the terms numerically and dimensionally similar. The new equilibrium position would occur for a RES value of zero, but due to the incremental method of obtaining the solution, the problem was to determine the new femoral position with a minimum value of RES.

4.2.5 MOTION OF THE FEMORAL COMPONENT

The orientation of the prosthetic components at the beginning of the rigid body analysis was with the femoral condyles located at the lowest points in the tibial

dishes. In order to move the femoral surface to a new position, a transformation matrix was applied to the femoral points in an ordered sequence of flexion, internal rotation, varus-valgus, anterior-posterior displacement and medial-lateral displacement. For each increment of the input cycles, the femoral component had a choice of any number and combination of 31 motions in increments of 0.2mm for anterior-posterior displacement, 0.05mm for medial-lateral displacement, and 0.5° for rotation. These were :

1) remaining in the same position
2) anterior translation
3) posterior translation
4) clockwise rotation
5) anti-clockwise rotation
6) lateral translation
7) medial translation
8) anterior translation with clockwise rotation
9) anterior translation with anti-clockwise rotation
10) posterior translation with clockwise rotation
11) posterior translation with anti-clockwise rotation
12) clockwise rotation and medial translation
13) anti-clockwise rotation and medial translation
14) clockwise rotation and lateral translation
15) anti-clockwise rotation and lateral translation
16) anterior translation and medial translation
17) anterior translation and lateral translation
18) posterior translation and medial translation
19) posterior translation and lateral translation
20) anterior translation with clockwise rotation and lateral translation
21) anterior translation with anti-clockwise rotation and lateral translation
22) posterior translation with clockwise rotation and lateral translation
23) posterior translation with anti-clockwise rotation and lateral translation
24) anterior translation with clockwise rotation and medial translation

25)anterior translation with anti-clockwise rotation and medial translation
26)posterior translation with clockwise rotation and medial translation
27)posterior translation with anti-clockwise rotation and medial translation
28)spinning clockwise about the medial condyle
29)spinning clockwise about the lateral condyle
30)spinning anticlockwise about the medial condyle
31)spinning anticlockwise about the lateral condyle

These covered all the possible motions of the femoral component except for flexion motion, which was included as an input cycle, and varus-valgus motion. After the contact points had been found for one of the positions above, the heights between the lateral femoral and tibial contact points and the medial femoral and tibial contact points were determined. They were both positive because the femoral axes were positioned 10mm above the tibial axes to make sure that the component surfaces did not overlap. If the heights were different (beyond a specified tolerance) a varus tilt was applied. The contact points were found again and if the heights were still different the component was tilted again. This process was repeated up to three times if necessary.

4.2.6 THE PATH OF REDUCING RESIDUALS

The residual values RES were calculated for each of the 31 possible positions of the femoral component. If all new positions produced residuals greater than for the present position, the present position was considered to represent equilibrium. Otherwise, the position of lowest residual was taken as the new position from which a further set of positions were examined. It was assumed that a femoral position of minimum residual could be found within a field of continuous slope in the vicinity of the present position. The curves for the input flexion, forces and torque were divided into small time increments, and the equilibrium positions were determined successively for each increment. The composite of these positions defined the motion path for that loading sequence. The time intervals for force input were such as to provide successive equilibrium positions close to the previous positions. Numerous test runs were carried out to

determine the appropriate incremental values for achieving local convergence and producing smooth motion paths.

The path of reducing residuals referred to the method of searching through the 31 options of femoral movement until the least residual was found and then searching again from this point until an even lower residual was found. The residuals were calculated by adding the errors produced when equilibrirum was not satisfied. There were two ways that this could be done.

1) The anterior-posterior force and torque residuals could be considered separately. Only if both residuals reduced could the rigid body analysis make its way down the passage of reducing residuals.
2) The anterior-posterior force and torque residuals were summed together to determine if the rigid body analysis could make its way down the passage of reducing residuals.

The latter was chosen because tests showed that the first method would 'stick' before the true solution had been found. However, even when using the latter method, high residuals could be produced even if the rigid body anlysis had found the nearest solution to the true solution. For example, for an anterior-posterior draw test, the increment size for movement at the base of the tibial dish was too large to describe movement at the steep anterior region of the tibial dish, so high residuals occurred as the femoral component moved up the anterior region.

Therefore the sizes of the anterior-posterior displacement, rotation and medial-lateral displacement increments were very important. The values of these increments, ie. 0.2mm for anterior-posterior displacement, 0.5deg for rotation and 0.05mm for medial-lateral displacement were determined by carrying out rigorous tests to find out which combination of incremental values would produce the lowest values of residuals over a gait cycle. If the field of residuals undulated and the sizes of the increments were small, then the rigid body analysis would stop searching for a solution because it had found a dip in the field of residuals. However, it might have found a better solution if it had travelled further on. Alternatively, if the sizes of the increments were too large, then the rigid body

analysis might miss the true solution. In order to avoid both these problems, a rough estimate of the solution was first obtained by carrying out a 'crude search' before searching for the accurate solution.

The crude search involved all the possible combinations of anterior-posterior displacement, medial-lateral displacement, and internal-external rotation. Large increments were used, and large ranges of possible translations and rotations were covered. The difference between finding a solution using the crude mesh and the previous method was that the rigid body analysis did not have to make its way down a long passage of reducing residuals. Once the crude solution had been determined, the rigid body analysis continued as before, using small increments to search for the true solution starting from the crude solution. This method was less sensitive to undulations in the field of residuals.

4.2.7 INCLUDING FRICTIONAL FORCES

"Sliding is defined as the relative linear velocity between two surfaces at their point of contact.....Rolling is defined as the relative angular velocity between two bodies about an axis lying in the tangent plane of the point of contact.....Spin is defined as the relative angular velocity about the common normal of the bodies in contact." [Johnson, 1985, p.3,4]. The friction effects for these three cases had to be determined and included in the rigid body analysis.

Before limiting friction occurs, the opposing frictional forces are greater than the applied forces. In order to be able to use the equilibrium equations during the period when the femoral component was stationary on the tibial insert, the value of the static friction coefficient and the friction directions were iterated until the equilibrium equations were satisfied. This gave the stationary position a slight advantage over the other positions. However, the acceptable residual limit for the stationary position was set to a lower value compared to the other options of motion to make sure that it did not have an unfair advantage.

The same values for static and dynamic coefficients of friction were set, after observing results from laboratory tests (see next chapter), though there was the option to have different values. For sliding between the present and new contact points :

$$SL = \mu.RL \quad (12)$$

$$SM = \mu.RM \quad (13)$$

μ = coefficient of friction, taken to be 0.07 under all conditions.

For zero relative sliding between the femoral and tibial surfaces, which could occur if the shear force did not exceed the limiting friction in a time interval with zero flexion change, or if pure rolling occurred:

$$\mu.RL > SL > -\mu.RL \quad (14)$$

$$\mu.RM > SM > -\mu.RM \quad (15)$$

The speeds of the cycles of flexion, compression load, anterior-posterior force and torque input to the rigid body analysis were irrelevant, however it was important to take into account the relative surface velocities of the femoral and tibial inserts as these would affect the frictional forces. Consider the following cases of rolling and sliding in a simplified two-dimensional model, points 1,2,3,4 on the femoral component make contact with points a,b,c,d on the tibial insert :

(a) A large anterior-posterior force and zero flexion were applied causing one point of the femoral component to slide across the tibial insert (Fig.3a).

(b) Zero anterior-posterior force and a large flexion were applied causing the femoral component to roll on one point of the tibial insert (Fig.3b).

(c) A moderate anterior-posterior force and a small flexion were applied causing the femoral component to slide across the tibial insert while rolling slightly (Fig.3c).

(d) A moderate anterior-posterior force and a large flexion were applied causing the femoral component to roll while sliding across the tibial insert slightly (Fig.3d).

These cases show that when motions caused by flexion and anterior-posterior forces oppose each other, the frictional forces produced change direction depending on their surface velocities.

Friction directions were calculated by comparing the relative motion of the femoral and tibial contact points between times t+dt and time t on the timescale of the input cycles. For the simplified two-dimensional case shown in Fig. 4a, a

positive anterior force makes the femoral component slide from a to b, so a frictional force from b to a is exerted by the tibial component on the femoral component to oppose its motion. However, if a positive flexion is also applied, a frictional force in the direction of 1 to 2 is superimposed. This method of determining the friction direction, applied in three-dimensions, could cope with all cases of rolling and sliding. Spin occurs when one condyle sticks and the other condyle moves. For this case, the friction directions were iterated in the plane of contact and the friction coefficient value was also iterated for the condyle about which spin occurred, this being a similar situation to when the component was stationary.

As the tibial insert remained stationary, the direction of the frictional force exerted by the tibial component on the femoral component (vector b to a) was obtained by comparing the contact points of the current force increment (at time t+dt) with the contact points of the previous one (at time t). However, it was not as simple to find (vector 2 to 1) the direction of the friction force exerted by the femoral component on the tibial component because the former was mobile. Therefore once the femoral contact points were determined, they were temporarily translated and rotated so that they were in the original (reference) orientation of the femoral component at the beginning of the rigid body analysis. When the old and new contact points were all in the reference orientation, the vectors between them could be calculated and input to the friction direction equation.

If the friction direction was zero because the vector from b to a was equal and opposite to the vector from 2 to 1, pure rolling occurred (Fig.4b):"Ideally rolling contact should offer no resistance to motion, but in reality energy is dissipated in various ways which give rise to 'rolling friction' "[Johnson, 1985, p306]. This was found to be true for knee replacements, where tractive forces produced during rolling proved to be more detrimental compared to friction forces produced during sliding [Wimmer & Andriacchi, 1995]. However, pure rolling did not occur in the model described in this chapter because the incremental nature of

the analysis meant that it was unlikely that the two vectors would ever be exactly equal.

A few analyses were carried out in order to examine the effects of including tractive forces. Tolerances of relative motion were set within which pure rolling was allowed to occur, even though the relative displacements of the contact points on the femoral and tibial components were not equal and opposite. Within these tolerances the friction coefficent values were iterated up to the static coefficient of friction and friction directions were iterated in the plane of contact.

4.2.8 SOFT TISSUE RESTRAINTS

In the natural knee, the posterior cruciate ligament restrains the femur as it moves forward relative to the tibia and the anterior cruciate ligament restrains the femur as it moves back. The strength and length of these structures varies between different individuals and data on the material properties of the ligaments is sparse. However, these restraints had to be included in the rigid body analysis if the contact paths of different knee designs were to be compared. If a design of low constraint, where the tibial dishes were not conforming to the femoral condyles, was analysed by the rigid body analysis without providing soft tissue restraints, the femoral component would ride up the shallow sides of the tibial insert and dislocate. However, a highly conforming design would not dislocate because the steep sides of the tibial dishes would limit its motion. Therefore, it would be unfair to compare low and high conformity designs under these conditions.

For the rigid body analysis, the ligament and soft tissue restraints were modelled by pairs of elastomeric bumpers which were positioned at the anterior and posterior of the tibial tray holder, 50mm between each pair. Quadratic stiffness curves of the bumpers were calculated to match the data from a number of studies of anterior-posterior and rotatory stiffnesses of the knee [Fukubayashi et al, 1982; Markolf et al, 1981, Gollehon et al, 1987; Shoemaker et al, 1985, Mills & Hull 1991, Blankevoort et al, 1988]. The anterior bumpers had one third the strength of the posterior bumpers to represent a knee where the anterior cruciate ligament had been resected, for implantation of prostheses, and the

posterior cruciate ligament retained [Fukubayashi et al., 1982]. The stiffness curves for each of the anterior bumpers (one third strength) was given by :

$$Fa=(0.444x^2+2.334x)/2 \quad .....(17)$$

and for each of the posterior (full strength) bumpers :

$$Fp=(3.910x^2+7.960x)/2 \quad .....(18)$$

where Fa and Fp are the forces exerted by the bumpers and x is the compression of the bumper.

This simplified representation of the soft tissue restraints was chosen, for validation purposes, to match the bumper system of a knee simulator which will be discussed in the next chapter. In the knee simulator, the tibial insert rotated and displaced with respect to the femoral component while the latter flexed and was free to tilt in the varus-valgus direction. The tibial insert was housed in a rectangular casing and the bumpers rested against this, uncompressed for the neutral position of the knee, which was with the knee extended and the femoral condyles positioned at the bases of the tibial dishes. When rotation of the tibial insert occurred, one anterior bumper and the diagonally opposite posterior bumper would compress while the remaining two bumpers would detach from the tibial insert casing. Similarly for anterior-posterior displacements of the tibial insert, both anterior or posterior bumpers would be compressed depending on the direction of motion.

This bumper system was represented in the computer model by including the geometry of the casing surrounding the tibial insert, and as it moved the bumpers exerted forces against it depending on how much they were compressed. As relative motions were imposed on the femoral component with respect to the tibial insert in the computer model, for each of the 31 possible motions imposed on the femoral component, the same but reverse motions were applied to an independent model of the tibial insert casing to determine the forces exerted by the bumpers. The direction of these forces were then reversed and applied back to the femoral component to provide the effects of soft tissue

restraints. The validity of such a soft tissue model will be discussed in the next chapter.

4.2.9 APPLICATION OF THE RIGID BODY ANALYSIS

4.2.9.1 TO DETERMINE THE EFFECT OF BEARING SURFACE GEOMETRY

Comparisons were made between the motions of two different knee replacement designs predicted by rigid body analysis, when simple loading patterns were applied. The Kinemax Condylar with the standard tibial insert (CONDYLAR) and the 'hi-stability' insert (LOWSTRESS) of higher constraint were modelled for this purpose. An anterior-posterior force test was carried out, with an oscillating force on the tibia of 300N anteriorly and 300N posteriorly, with a 1500N constant compressive force, at 10 degrees and 60 degrees of flexion. Next, an internal-external torque test was carried out with an oscillating torque of ±10 Nm, again with a compressive force of 1500N and at 10° and 60° of flexion. Full strength bumpers were used at the anterior and posterior of the tibial insert for these tests.

4.2.9.2 TO DETERMINE THE EFFECT OF FRICTION

To predict the effects of varying the coefficient of friction, the computer model was used to determine the anterior-posterior and rotational responses for coefficients of friction of zero, 0.07, and 0.15. This was the range which was considered applicable, including cases where small fragments of acrylic cement become entrapped between the bearing surfaces. For these tests, full strength bumpers were used posteriorly and one third strength bumpers were used anteriorly.

In addition, three tests were run without soft tissue restraints on the LOWSTRESS design to investigate the effects of combining flexion and anterior-posterior force. For all three tests there was a constant compressive load of 1500N, and an oscillating anterior-posterior force of 200N. For the first test, flexion was increased from 35 to 60deg while the anterior-posterior force increased from 0 to 200N, then the flexion was decreased from 60 to 10deg while the anterior-posterior force decreased from 200 to -200N. For the second test,

flexion was decreased from 35 to 10deg while the anterior-posterior force increased from 0 to 200N, then the flexion was increased from 10 to 60deg while the anterior-posterior force decreased from 200 to -200N. For the third test, flexion remained at 35deg while the anterior-posterior force increased and decreased. Similarly, torque tests were carried out while flexion and extension were imposed.

4.2.9.3 TO DETERMINE THE EFFECT OF SOFT TISSUE RETRAINTS

To demonstrate the effect of soft tissue restraint, an analysis was carried out using the CONDYLAR design, with and without the constraint term in the equations, equivalent to running the experiments with and without bumpers. The analysis was extended to consider an additional tibial geometry where the sagittal radius of curvature was 120 mm, considered to be a design of low constraint.

4.2.9.4 APPLYING GAIT INPUT CYCLES

Before applying the gait input cycles, tests were carried out to see if the model could accept input cycles were both the anterior-posterior force and internal-external torque varied. The CONDYLAR design was tested under 1500N compression load, at 60deg flexion without bumpers, and cycles of ±150N anterior-posterior force and ±5Nm torque which increased and decreased in phase were input.

The kinematics were determined for a complete level walking cycle using the LOWSTRESS design and the bumper system representing a knee with its anterior cruciate ligament resected. The four input cycles provided by Prof. J. Paul [J.P. Paul, 1993] are shown in Fig. 5. Another set of input cycles for level-walking was also obtained [Andriacchi et al, 1995] (see next chapter for these cycles), these were input to the LOWSTRESS design to see if the kinematics were different and also to test two aspects of the model. These were the sizes of the increments used when moving the femoral component to find its equilibrium

position, and the inclusion of a tolerance for the relative displacement between the prosthetic components within which pure rolling would be allowed to occur.

Finally, in order to demonstrate the potential of the model for predicting the relative kinematics between different total knee geometries, the contact paths for the stance phase of a level walking cycle provided by Andriacchi were determined for total knee replacements with different frontal plane geometries. Three designs were generated where the only variables were the outer frontal radii of the femoral component and tibial insert, these were 30 on 40mm, 70 on 80mm and 150 on 200mm respectively.

4.3 RESULTS

4.3.1 THE EFFECT OF BEARING SURFACE GEOMETRY

The force-displacement and torque-rotation curves are shown in Fig 6. A stiffening with displacement was observed and there was a period where there was no displacement when the force direction changed. This latter phenomenon, indicated by the flat lines at the top and bottom of the curves, was attributed to the friction, causing the surfaces to 'stick' until there was sufficient force or torque in the opposite direction to cause movement again. The displacements and rotations of the more conforming design (LOWSTRESS) were slightly lower compared to the less conforming design (CONDYLAR).

4.3.2 THE EFFECT OF FRICTION

The model was used to show the significant effects of the value of the friction coefficient (Fig. 7). These tests had full strength bumpers at the posterior of the tibial insert and one third strength bumpers at the anterior to represent a knee with the anterior cruciate ligament resected. There was no hysteresis loop for zero friction. At 60 degrees flexion, the total anterior-posterior displacement was 15mm for $\mu = 0.0$, 10mm for $\mu = 0.07$, and only 3.5mm for $\mu = 0.15$. The equivalent values for rotation were 55° for $\mu = 0.0$, 40° for $\mu = 0.07$, and 22° for $\mu = 0.15$.

Fig. 8 shows the effect of combining flexion with anterior-posterior force, with friction acting. When the flexion was held at a constant angle, the work done against friction was indicated by the area inside the hysteresis loop as for the previous tests. When the femoral component was flexing or extending in opposition to the anterior-posterior force, the friction force limited motion in the same way as when the flexion remained constant, except when the anterior-posterior force and flexion angle changed directions, instead of the femoral component sticking until it overcame static friction, it continued to slide. Therefore, the hysteresis loop was larger due to the extra work done against friction. Conversely when flexion or extension were applied in the same direction as the anterior-posterior force, work was not done against friction because the relative motion of the components was very small. This meant that the hysteresis loop almost approximated a straight line. For a test where the flexion was held at a constant value, such a hysteresis loop would only occur if the coefficient of friction was zero.

Similarly for the torque tests, if flexion and torque were applied at the same time, the friction would limit movement of one femoral condyle while affecting the other condyle less. This was because one condyle would be moving in the opposite direction to the flexion while the other would be moving in the same direction. This was apparent when viewing the contact points produced which showed that contact points for one condyle were not as widespread as for the other.

4.3.3 THE EFFECT OF SOFT TISSUE RESTRAINTS

The effect of the soft tissue restraints is shown in Fig. 9. For the CONDYLAR design, there was only a 20% reduction in the anterior-posterior displacement due to the restraints. However, for a design of low constraint with a sagittal radius of 120 mm, there was a 50% reduction.

4.3.4 KINEMATICS DURING GAIT

Fig. 10 shows the displacements and rotations which occurred for one cycle of the mixed anterior-posterior force and internal-external torque cycles. Even though equal torque was applied in each direction, the superimposed anterior-posterior force had the effect of increasing the rotation significantly when the femoral component moved forwards with the respect to the tibia compared to when it moved back.

Having confirmed that the computer model could accept mixed anterior-posterior force and internal-external torque cycles, level-walking cycles, which in addition had varying compression loads and flexion angles, were input to the LOWSTRESS design. There was an oscillating anterior-posterior displacement of the tibia of 4mm during most of the stance phase (Fig. 11), but in the last part of stance, when the knee was rapidly flexing, there was posterior tibial displacement of 5mm. The internal-external rotation followed a similar pattern, with only a few degrees of rotation in early stance followed by an internal tibial (external femoral) rotation in late stance. The main difference between the output motions for the Paul and Andriacchi cycles was that the femoral component externally rotated once during stance for the former and twice for the latter. The distance between the bumpers had to be changed to 75mm when the Andriacchi cycles were input to prevent excessive rotation.

In order to analyse the effects of including pure rolling, the static coefficient of friction was increased to 0.15. If the relative sliding distance of the femoral component with respect to the tibial insert was within a tolerance of the relative sliding distance between the tibial insert with respect to the femoral component, then pure rolling was allowed to occur. For the rigid body model, this meant that the friction coefficient could be iterated until the nominal static coefficient of friction and the friction direction could be iterated as well, until equilibrium was reached. Tolerances of 10% and 20% were tried and the output kinematics were plotted in Fig. 12. There was not a significant difference in the results.

Fig. 13 shows the different contact paths obtained for the different frontal geometries during level walking. It was observed that the larger the frontal

radius, the more widespread the contact points suggesting that the stability and wear characteristics of the designs would differ, even by altering this single variable. The contact paths are plotted for a right knee.

4.4 DISCUSSION

This data illustrates the importance of including friction forces in a model which includes artificial bearing surfaces from materials such as metal-polyethylene. Under a compressive force of 1500 N, over 100 N of shear force was required to initiate motion, while under torque loading, 2.5 Nm of torque was required. When the shear force or torque was reversed, there was no sliding until the value of the reversed force again reached the level of the frictional resistance. This implies that the motion in a total knee replacement will not be smooth and continuous, in contrast to the situation in a natural knee where the friction is much smaller. The magnitudes of the displacements and rotations were considerably attenuated due to the friction. In activities where the compressive forces reach three times body weight and the shear force and torque imposed by the particular gait pattern are less than the above values, it is possible that sliding motion would not occur at all. If the friction was higher than for metal-on-polyethylene, such as when there were small acrylic particles embedded in the surface, this would be expected to result in a predominance of rolling when the angle of flexion was changing rather than sliding, which could then impose high forces on the ligamentous restraints, or result in jerky motion. The behaviour when flexion-extension was combined with anterior-posterior shear forces indicated that a wide range of rolling and sliding conditions could occur in vivo. Tractive rolling was likely to occur in some circumstances, for which the frictional shear forces would range from zero to the limiting value. This could have an important effect on the wear of the polyethylene [Wimmer & Andriacchi, 1995]

In addition, the data showed that it was essential to include soft tissue restraints, particularly for designs of low constraint. Even with high constraint, if there were loading conditions involving high anterior-posterior forces or torques with low compressive force, soft tissue restraint would be necessary. The

representation of soft tissue restraint in the model was simplified in order to conform with the mechanical arrangement of a simulating machine. The main simplification was that the model for soft tissue restraint was independent of the flexion angle, rather than being stiffer towards zero flexion as occurs in reality. Despite this, it was shown that for joint surfaces with even moderate constraint, the attenuation in the sliding and rotation was small so long as there was a compressive force applied. However, during the swing phase, such constraint would be necessary. The constraint was also shown to be important under weight-bearing conditions for condylar surfaces of low constraint, as illustrated by the example with a 120 mm sagittal radius of the tibial surface.

The rigid body analysis was used to apply the combined effects of flexion, compression load, anterior-posterior force and internal-external torque exerted during gait and predict contact points for different knee designs. The contact points appeared to be more widespread for the designs with larger outer frontal radii and this was believed to have implications for the wear of their tibial inserts. The different fatigue levels of the polyethylene could not be determined from the contact points themselves, additional information on contact areas and stresses was required. However, the contact points were useful for predicting realistic orientations of the prosthetic components with flexion, anterior-posterior displacement and internal-rotation imposed. For a given set of input cycles these orientations will vary for different designs, just as the contact points vary, and this was taken into account when calculating contact areas and stresses in a later chapter.

In conclusion, the computer model could be used to predict the kinematic behaviour of different designs of condylar replacement knees under simple loading conditions as well as under functional loading. The locations of the contact points and the relative amounts of rolling and sliding were influenced by the geometry of the bearing surfaces, the friction at the surfaces and by soft tissue restraint. However, it was recognised that there would be some error due to the rigid body assumption of the model, because the surface geometries would change due to deformation of the polyethylene, while the centres of

pressure of the contact areas might not be coincident with the predicted contact points. Therefore, having developed a computer model of the prosthetic components to predict kinematics and contact points it was necessary for some experiments to be carried out to check the validity of the quasi-static motion and rigid body assumptions.

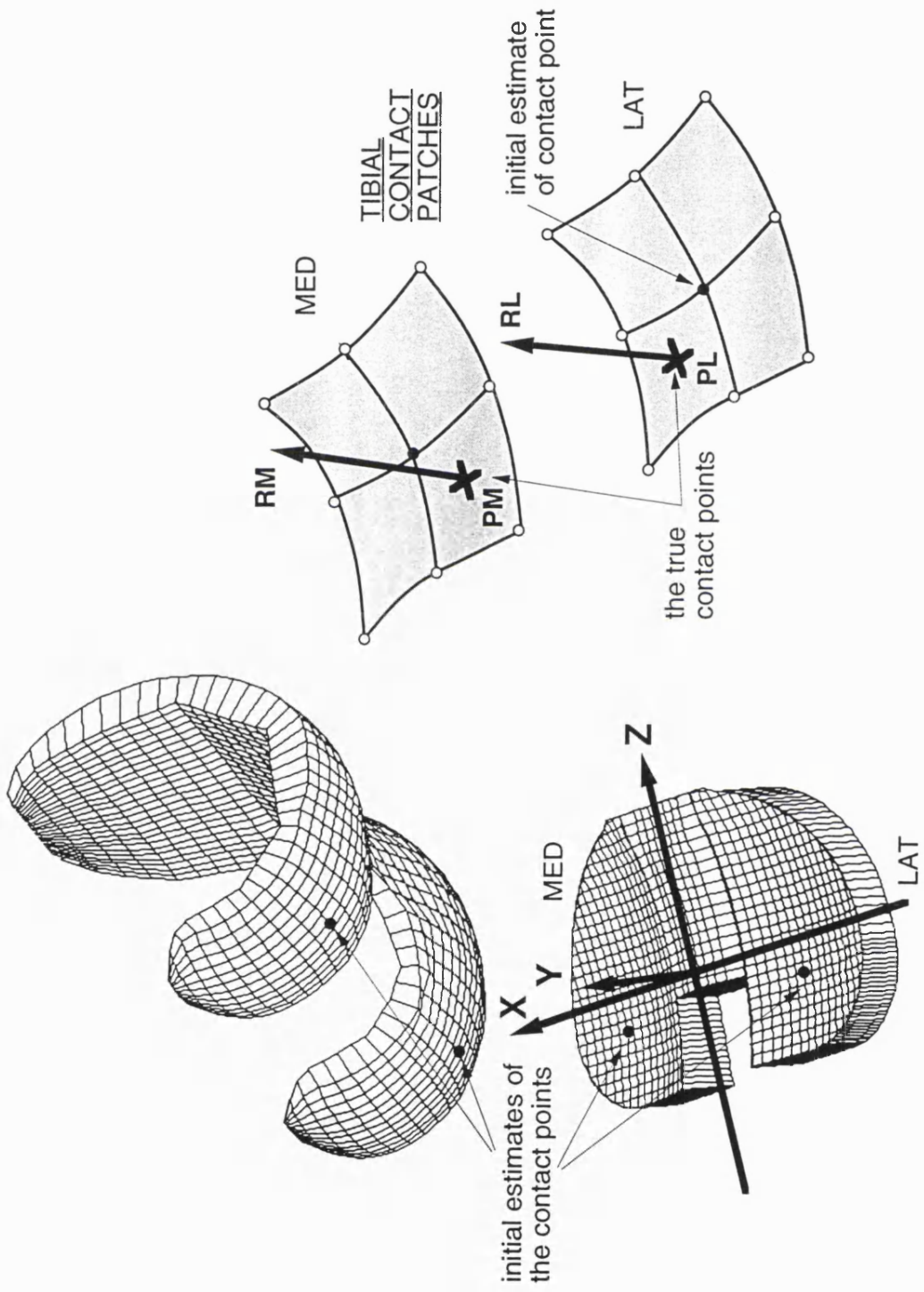

FIG. 1 The component surfaces are described by points on a grid. The surface in the vicinity of a grid point is described by a polynomial. The normal vector is then calculated.

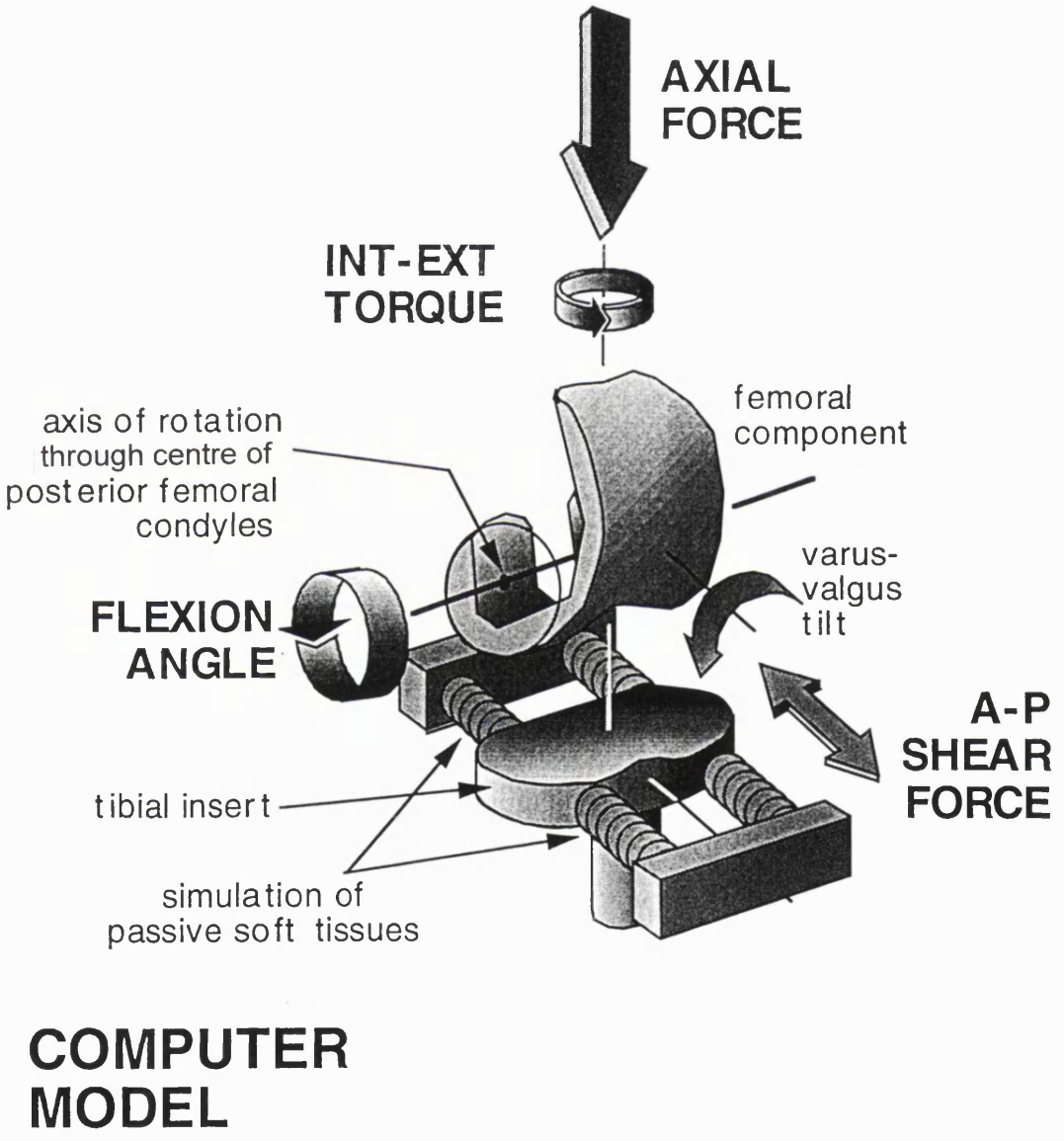

FIG. 2 A schematic diagram of the computer model.

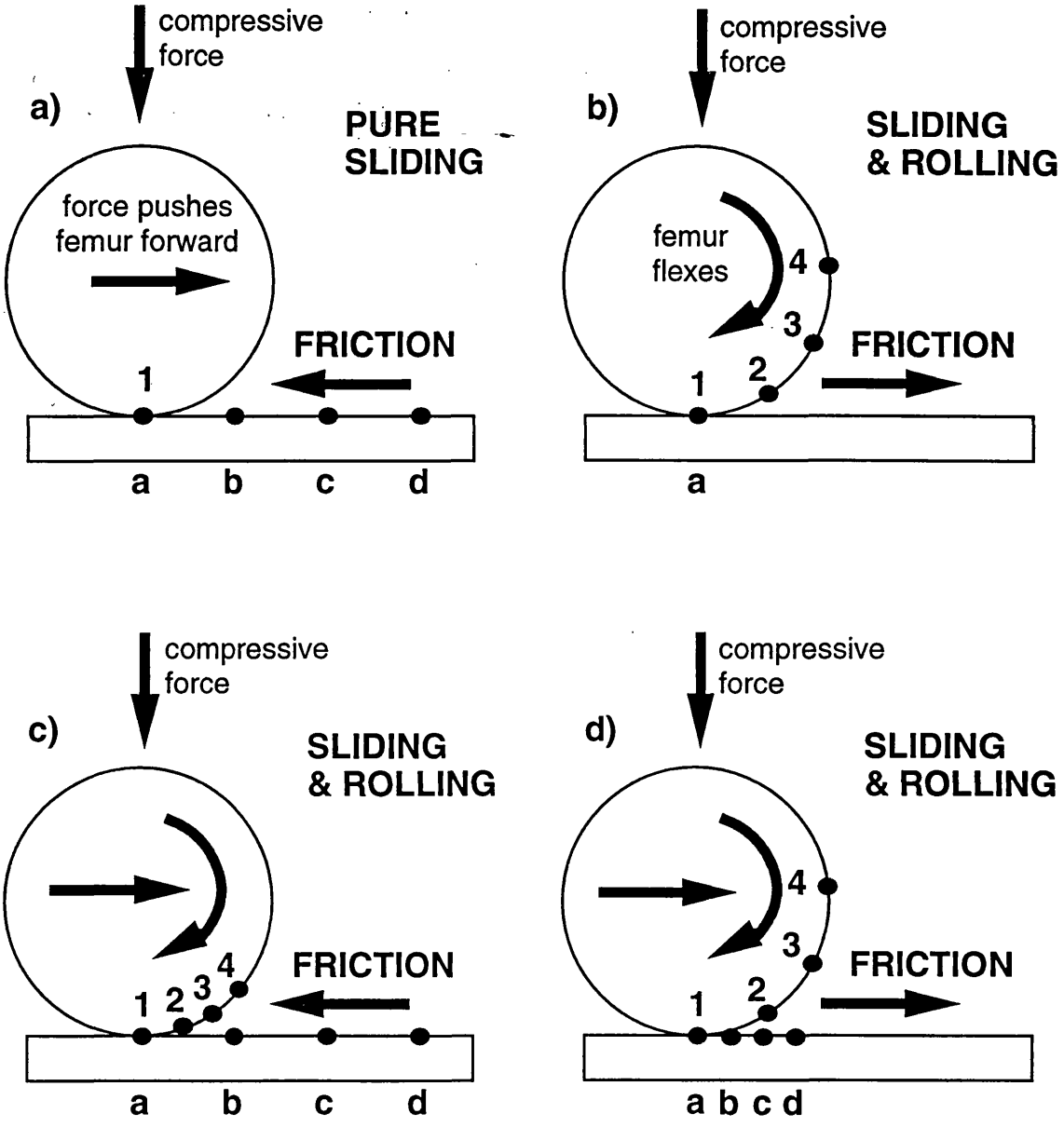

FIG. 3 Including relative surface velocities in the computer model.

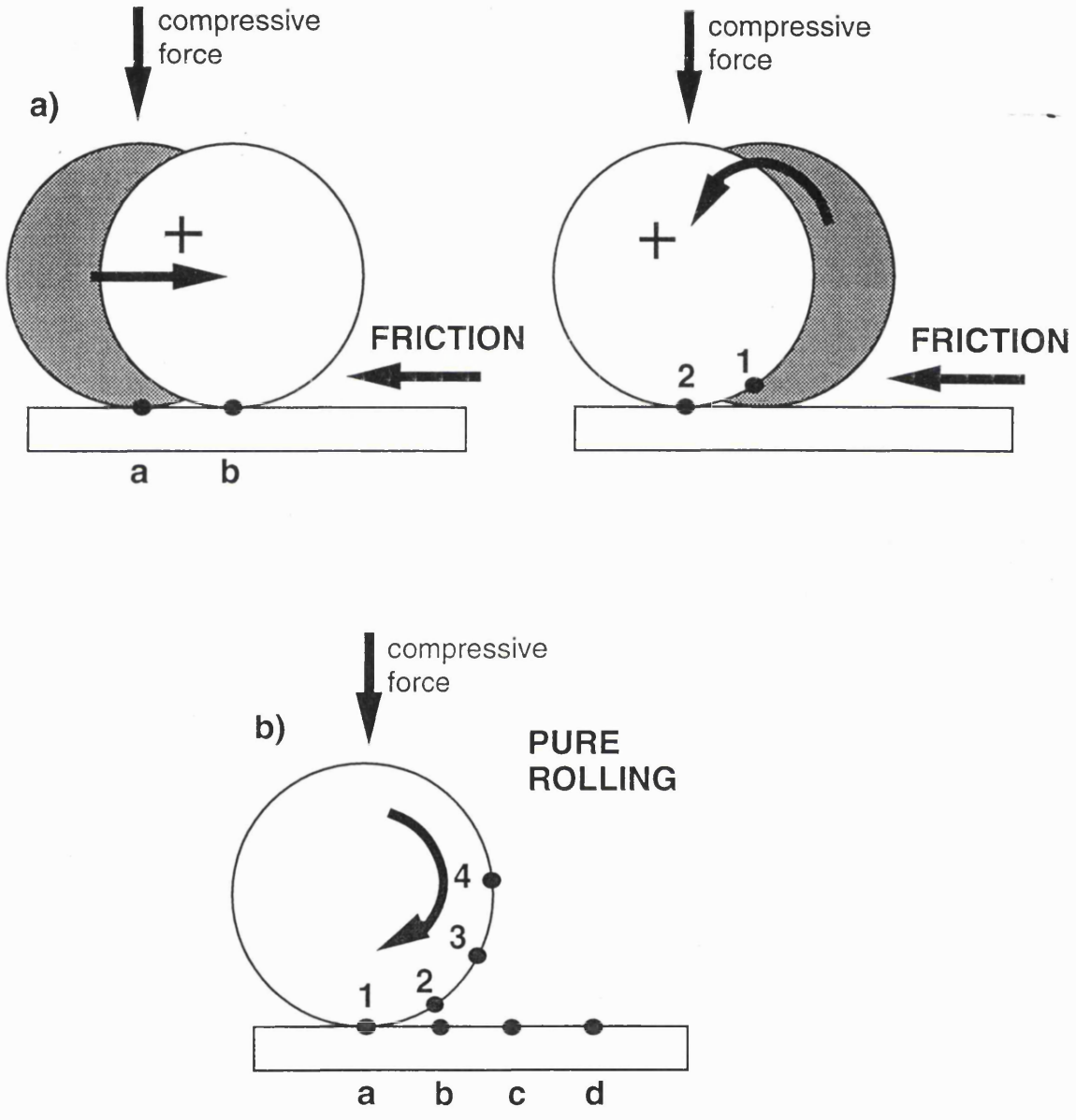

FIG. 4 Determining the friction direction.

Positive torque refers to internal torque applied to the tibia relative to the femur.
Positive anterior-posterior shear force refers to force pushing the tibia forwards relative to the femur.

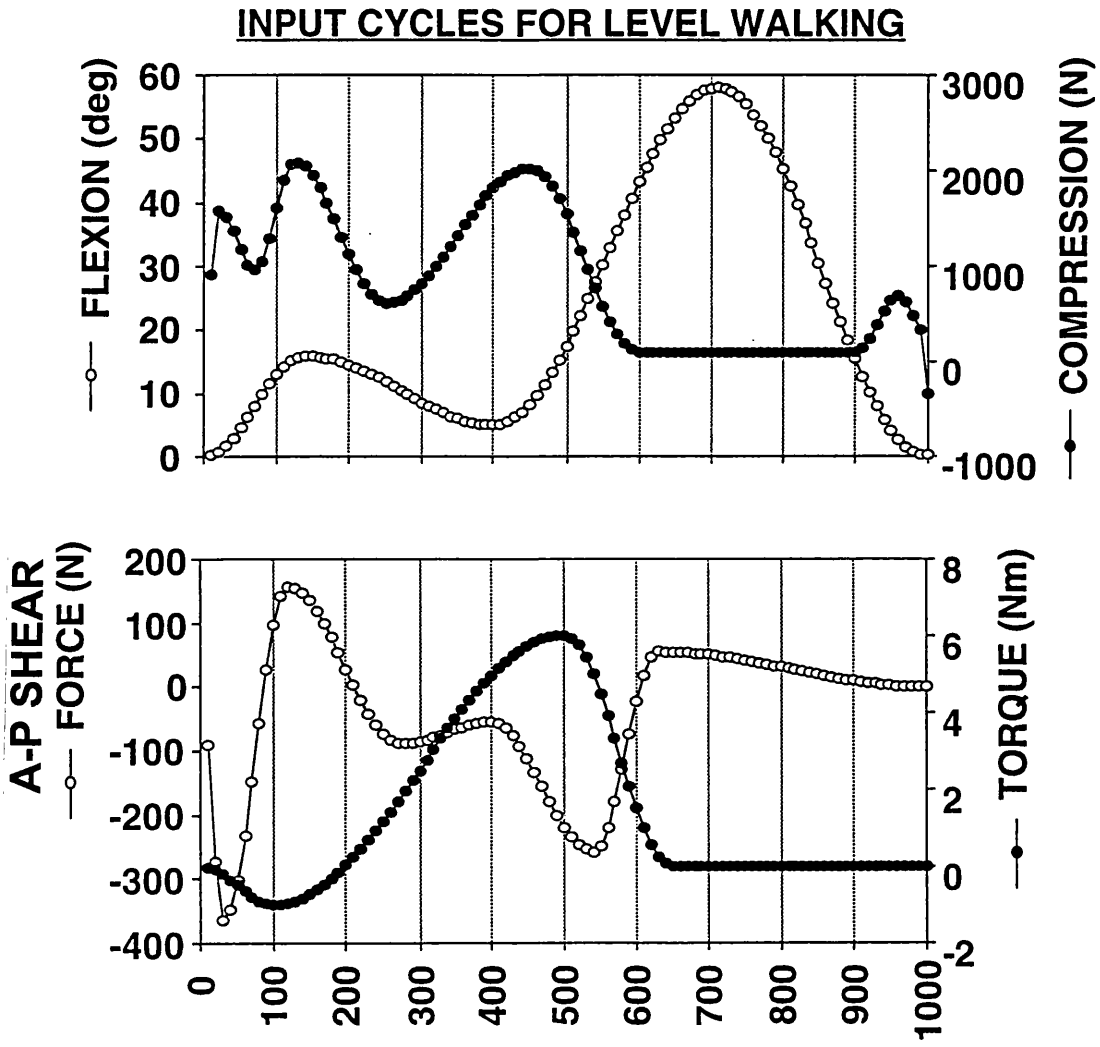

FIG.5 Level walking input cycles for the computer model (provided by J.P.Paul).

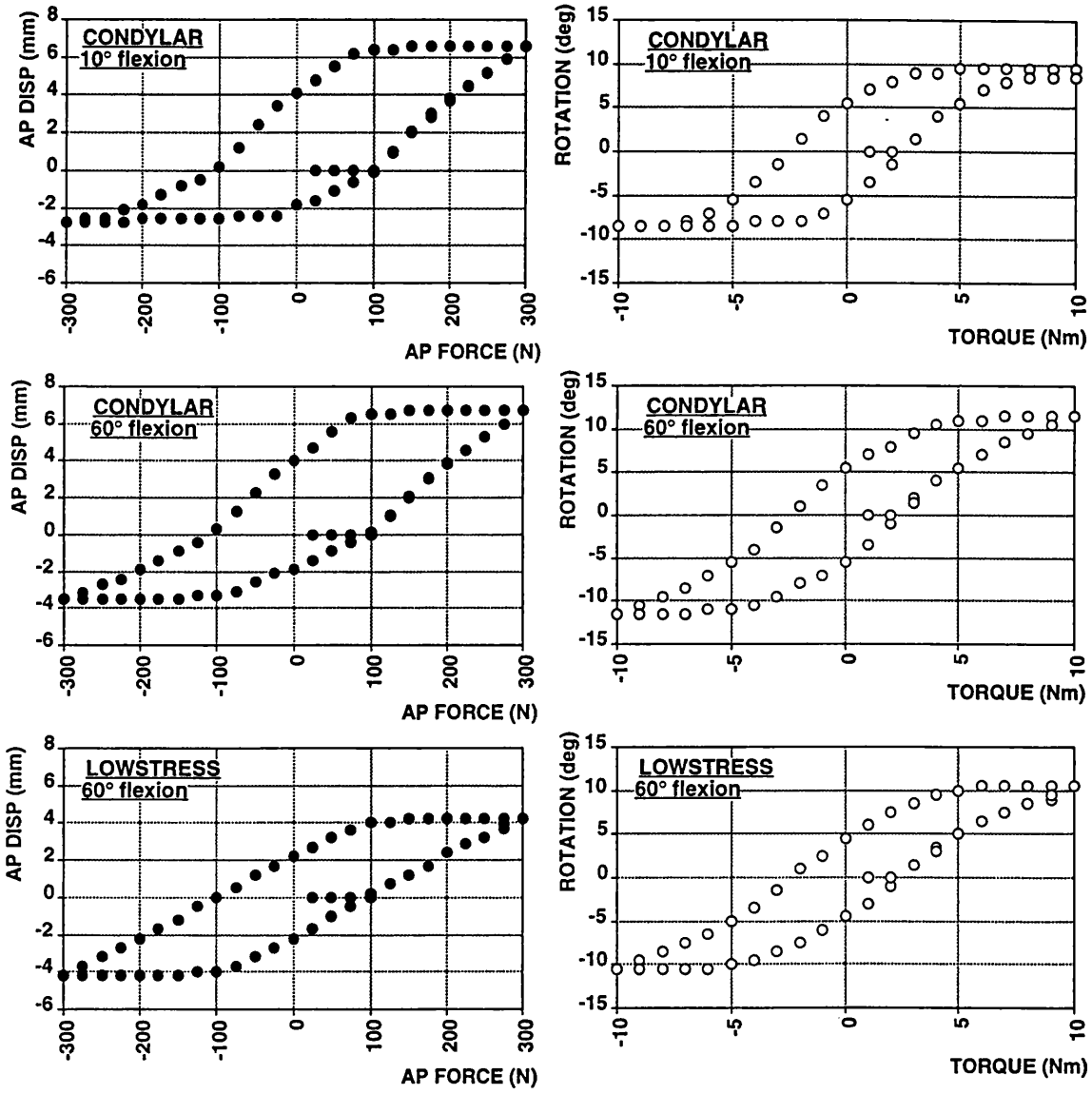

FIG. 6 Force-displacement and torque-rotation curves, computed by the model. Positive displacement indicates anterior movement of the tibial insert. Full strength bumpers were used anteriorly and posteriorly.

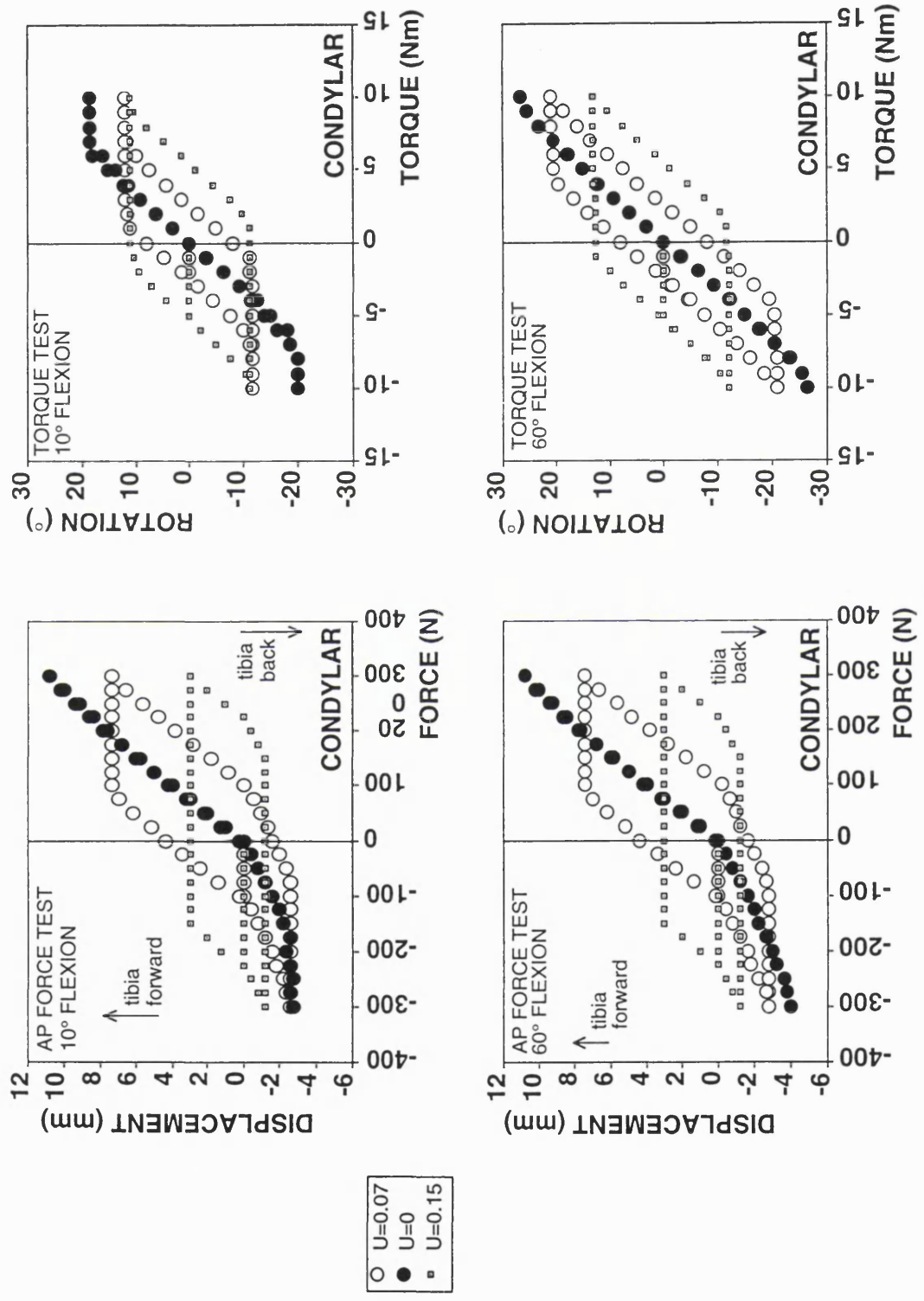

FIG. 7 The effect of friction coefficient on the anterior-posterior displacement (left) and internal-external rotation (right) predicted by the computer model. Full strength bumpers posteriorly, one third strength anteriorly.

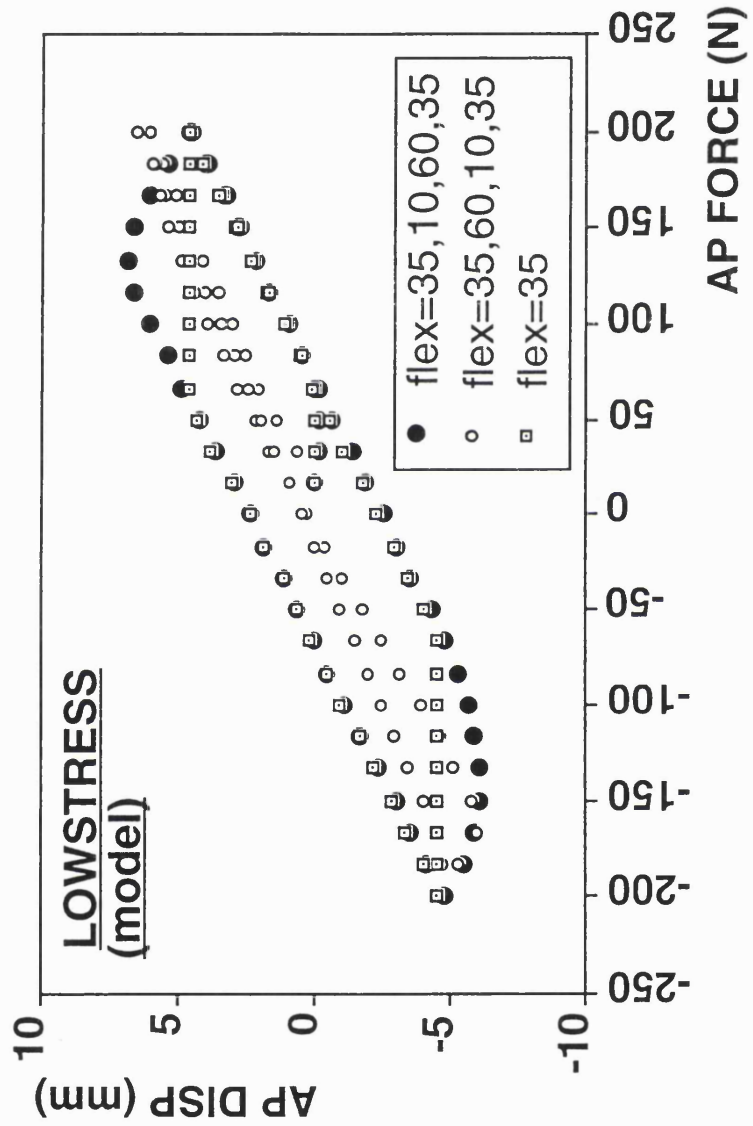

FIG. 8 Curves comparing the effect of combining flexion with anterior-posterior force. The same anterior-posterior force cycle was applied to all three tests, and the direction of the flexion cycle was changed

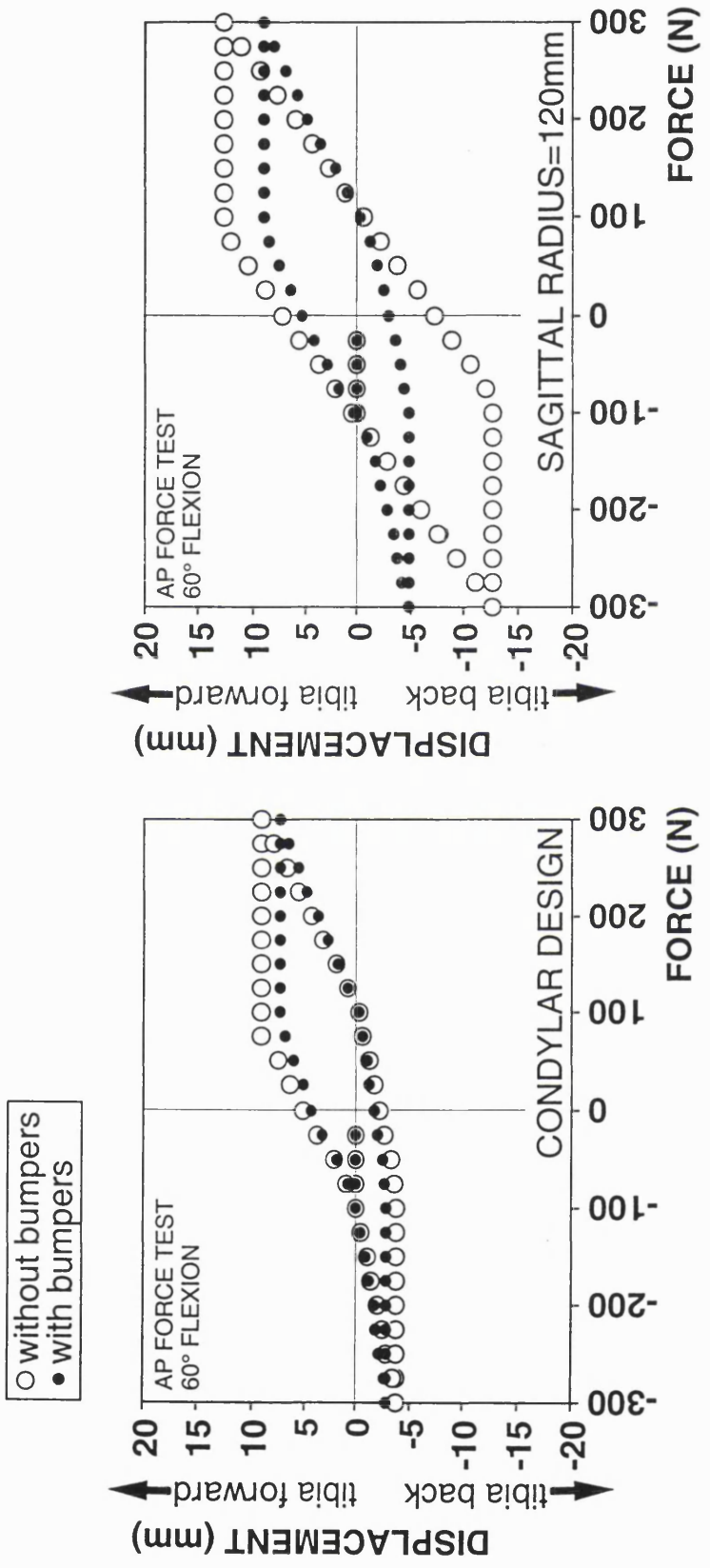

FIG. 9 Effect of soft tissue restraint for a design with sagittal tibial radius 50mm anteriorly, 80mm posteriorly and one with sagittal tibial radius 120mm.

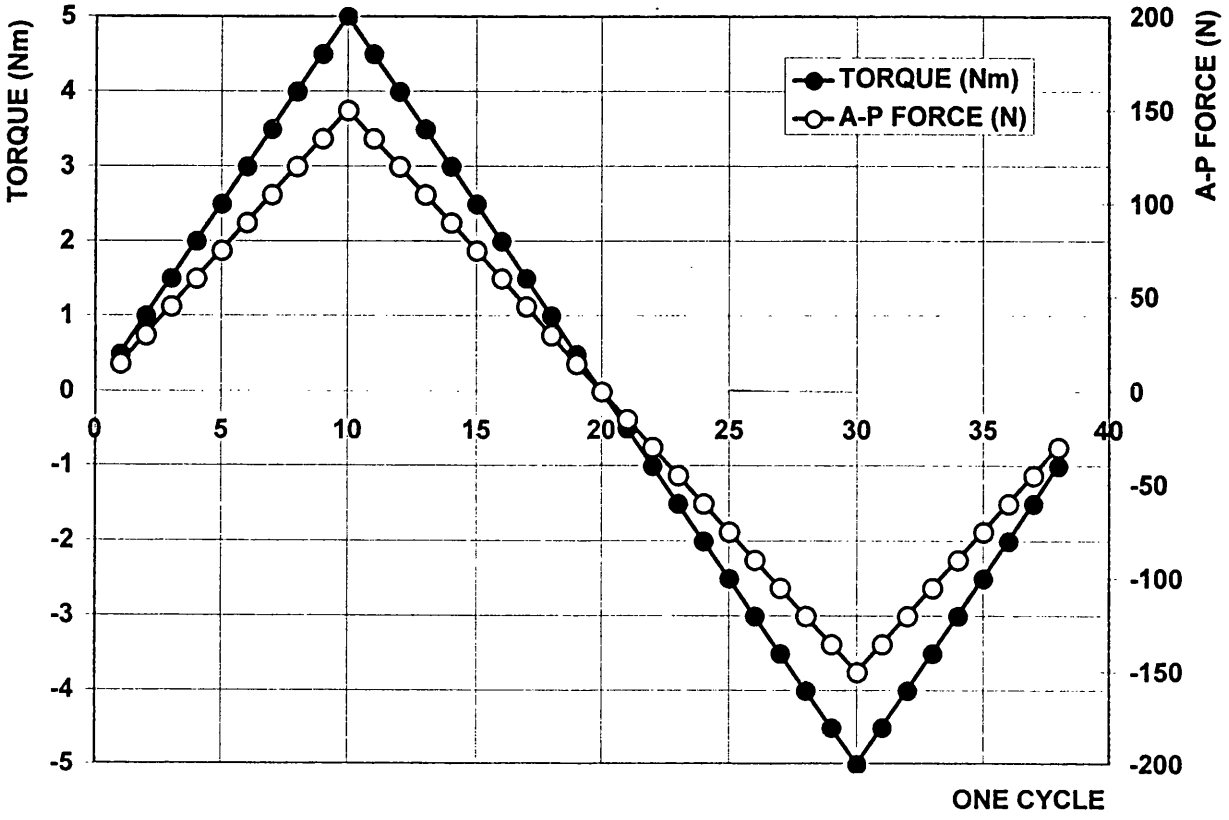

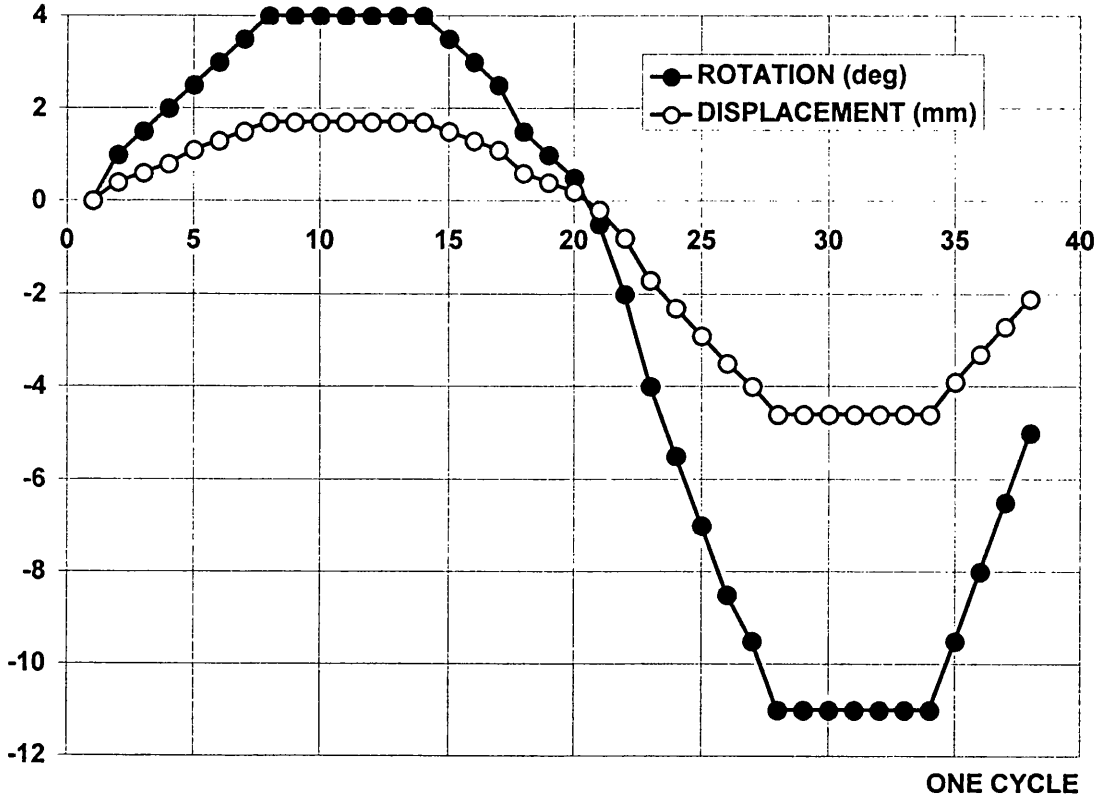

FIG. 10 A combination of anterior-posterior force and internal-external torque cycles were input to the computer model of the CONDYLAR design. The compression load was 1500N and the knee was at 60deg flexion.

Positive rotation refers to internal rotation of the tibia relative to the femur.
Positive displacement refers to the tibia displacing forwards relative to the femur.

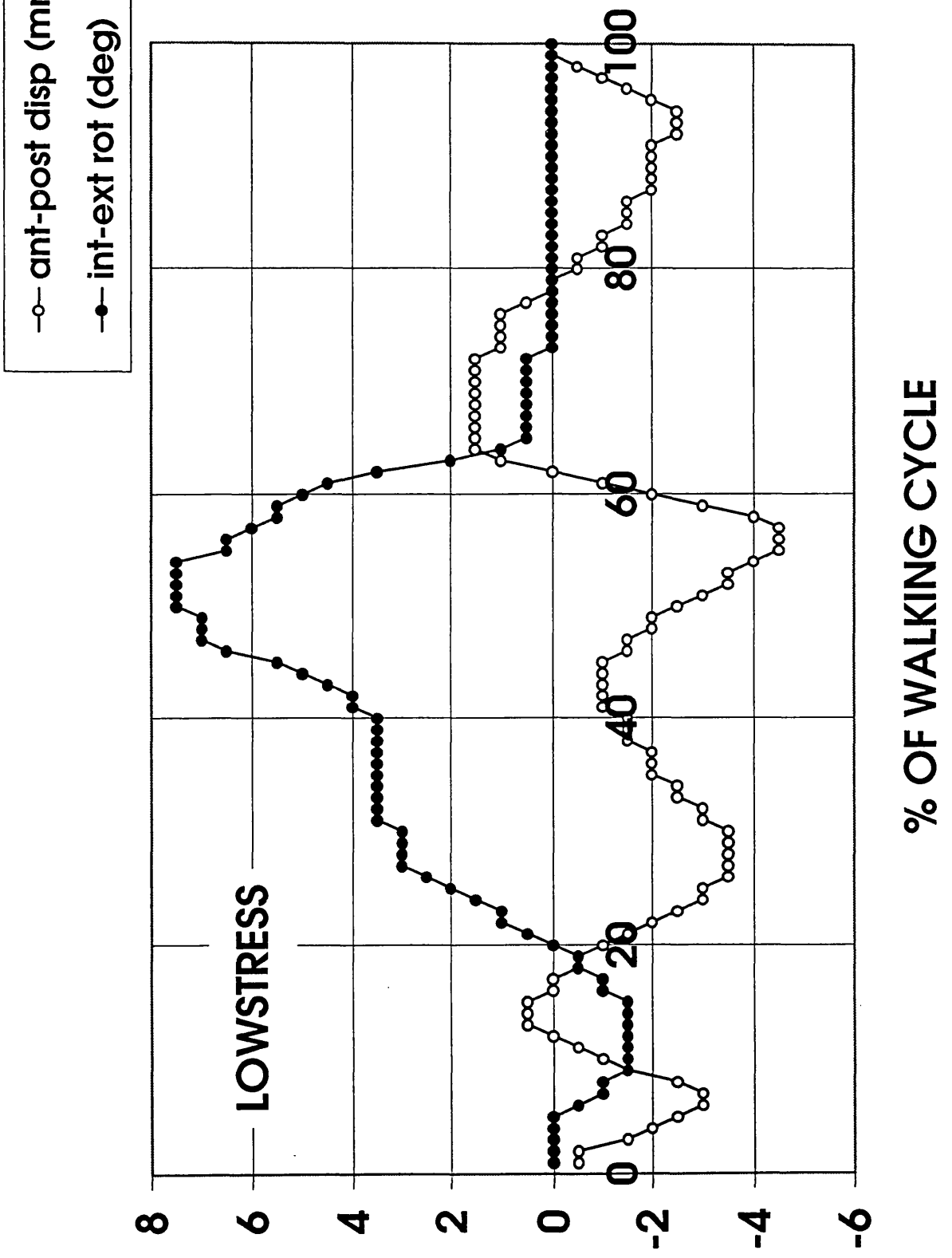

FIG. 11 Displacements and rotations of the tibial insert relative to the femoral component in level walking. Input cycles provided by J.P. Paul.

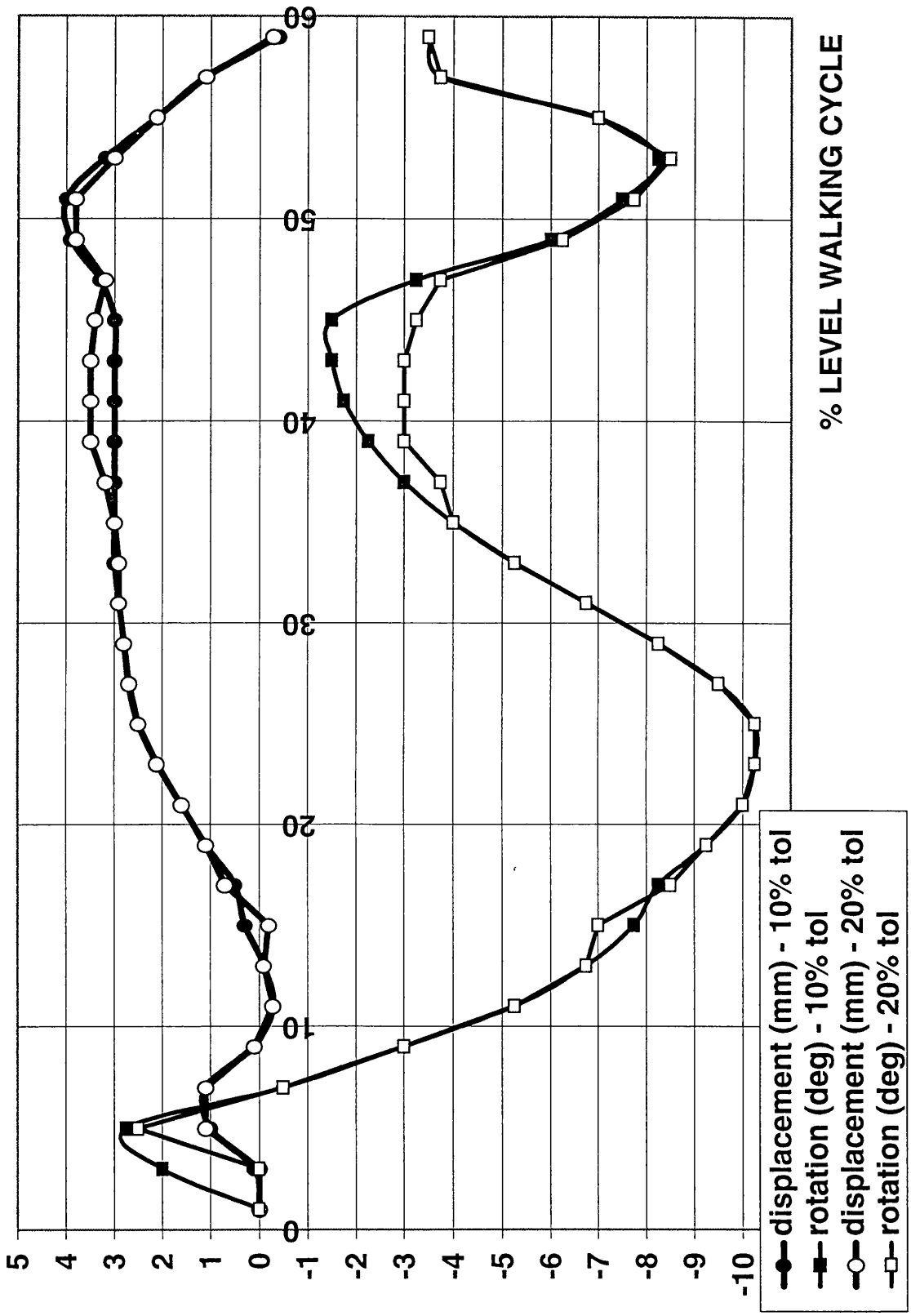

Positive values refer to the femoral component moving forwards and rotating internally with respect to the tibial component.

FIG.12 To include the effects of tractive rolling, different tolerances of relative displacement between the prosthetic components were set, within which pure rolling was allowed to occur.

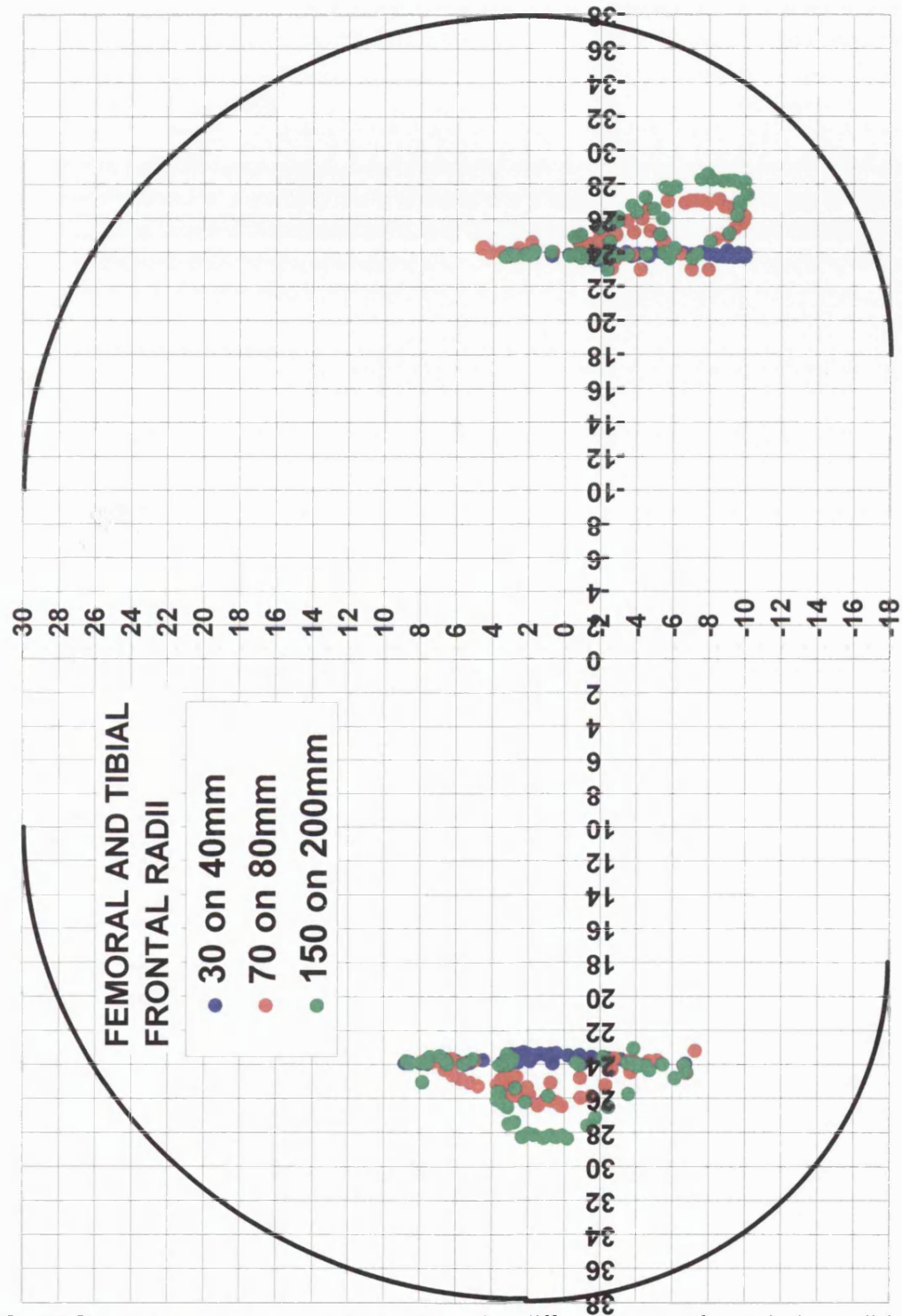

FIG. 13 Predicted contact point locations for different outer frontal plane tibial radii, during the stance phase of a normal gait cycle. The sagittal radii were : femoral distal 48mm, femoral posterior 20mm, tibial 56mm

Chapter 5

VALIDATION OF THE RESULTS PRODUCED BY THE RIGID BODY ANALYSIS

5. VALIDATION OF THE RESULTS PRODUCED BY THE RIGID BODY ANALYSIS

5.1 INTRODUCTION

The condylar surfaces of the intact knee, together with the interposed menisci, are adapted primarily for compressive loading. The externally applied shear forces and torques are controlled by the ligaments and capsule as well as by differential forces in the various muscles around the joint. The frictional forces between the cartilage surfaces are negligible [Mow & Soslowsky, 1991].

However, there is some dishing of the medial tibial plateau, as a result of which a decrease in the laxity when shear forces and torques are applied is to be expected when a compressive force is acting. This was confirmed in early studies when anterior-posterior and rotary laxity reductions of more than 50% were measured when physiological loads were applied [Wang & Walker, 1974; Hsieh & Walker, 1976]. In these tests, motions other than those being applied were constrained, or coupled [Piziali et al, 1977]. However, in unconstrained tests, the reductions in laxity were only in the range of 12-25% [Markolf et al , 1981]. After resection of the anterior cruciate ligament, there was a 2-3 times increase in the anterior drawer but this increase was reduced by around one half when compressive load was applied [Fukubayashi et al, 1982; Shoemaker & Markolf, 1985].

Condylar knee replacements appear to behave in a different way. Typically, both the lateral and medial tibial surfaces are dished and in partial conformity with the metallic femoral condyles. Under relatively low compressive loads, the shear forces and torques which can be sustained by the surfaces themselves are relatively small and below those of functional activities, requiring ligamentous and muscle forces for stability. However, once the compressive forces reach 2 to 3 times bodyweight, the dishing of the surfaces can sustain significant shear forces and torques which can provide self-stabilisation for activities such as level walking [Walker et al, 1995]. The amount of stability

provided is a function of the relative femoral and tibial radii. In addition, the friction between the surfaces adds to the stability. For example, at a compressive force of 2000N, the frictional shear force is 100N, a substantial proportion of the maximum shear forces which have been calculated to be in the range of 100-300N [Morrison, 1969; Morrison, 1970].

Another important aspect is the interaction between the total knee replacement and the joint itself. The lever arm of the quadriceps can change due to the contact points in the prosthetic knee being different from those in the natural knee [Mahoney et al, 1994]. Due to the surgical technique, the sizing and geometry and the variations between different knees, the tensions in the ligaments can vary considerably [Incavo et al, 1994], although this can be modified to some extent by adjustments to ligaments and bone cuts at surgery [Arima et al, 1994; Booth et al, 1994; Ritter et al, 1988]. In the functional situation changes in shear forces and contact points are evidently responsible for gait adaptation patterns which modify the forces acting on the joint [Draganich et al, 1987; Andriacchi et al, 1982; Andriacchi & Mikosz, 1991].

The rigid body model of the prosthetic components developed in the previous chapter, included a bumper system to provide the soft tissue restraints in the knee capsule. This consisted of two pairs of elastomeric bumpers at the anterior and posterior of the tibial insert. The magnitudes of the forces exerted by these bumpers were crucial when determining the difference in kinematics between high and low conformity knee replacement designs. For a high conformity design, the soft tissues would be almost redundant, while for a low conformity design the dishing of the tibial insert would not be adequate to restrain the motion of the knee, and the soft tissues would come into play. The simplification of this model of the soft tissues meant that the forces were generated by impingement of the tibial insert against the bumpers. However, the tibial insert was only allowed to internally/externally rotate and anterior/posterior displace so the assumption was made that flexion of the knee did not affect the bumper forces.

Other assumptions that were made in the rigid body model were that the motion of the knee was quasi-static, the femoral condyles made contact with the tibial dishes at contact points rather than contact areas and inertial effects were negligible. All of these assumptions had to be justified experimentally, which is the purpose of this chapter.

5.2 METHODS AND MATERIALS

5.2.1 THE KNEE SIMULATING MACHINE

A knee simulating machine (Fig.1) was constructed which could apply any wave forms of forces, moments and flexion-extension to a total knee replacement [Walker et al ,1997]. The femoral component was mounted on a shaft, with the centre of curvature of the posterior femoral condyles aligned with the axis of the shaft. Each end of the shaft was constrained to move only in a vertical direction, but allowing varus-valgus. The shaft was flexed and extended by a crank driven from a servo-motor. The vertical compression force was applied to the shaft at each side of the femoral component.

The tibial component was mounted in a chamber fixed to the top of a long beam, which was in a low-friction spherical pivot at the base. This allowed the tibial component unrestricted translation in a horizontal plane (with minimal error) and rotation about a vertical axis. An anterior-posterior shear force and an internal-external torque were applied to the beam by servo-hydraulic cylinders. The applied forces, moments, and flexion angle were controlled by the computer. The anterior-posterior displacement and internal-external rotation were monitored continuously. In order to produce realistic constraints such as are provided by the passive soft tissues, strain-stiffening elastomeric bumpers were interfaced with the front and the back of the tibial housing. Quadratic stiffness curves of the bumpers were calculated to match the data from a number of studies of anterior-posterior and rotatory stiffnesses of the knee [Fukubayashi et al, 1982; Markolf et al, 1981, Gollehon et al, 1987; Shoemaker et al, 1985, Mills & Hull 1991, Blankevoort et al, 1988]. To simulate the absence of a cruciate

ligament, bumpers of one third strength in the appropriate direction were used [Fukubayashi et al., 1982].

5.2.2 TO DETERMINE THE COEFFICIENT OF FRICTION

Pin-on-disk experiments have been carried out to determine the coefficient of friction between cobalt chrome and polyethylene [Lilley, 1994]. However, the coefficient of friction varies with load, surface geometry and temperature. Therefore, a coefficient of friction which was relevant to tests carried out on the knee simulating machine using prosthetic components had to be determined. This was done by using the machine to slowly apply an anterior force of 300N to a tibial insert which was interfaced with a femoral component flexed at 90deg under a compression load of 1500N, with distilled water lubrication. The simulator recorded the output displacement of the tibial insert for input force and thus the shear force at which movement began to occur (when friction was limiting) could be recorded. This test was also carried out under different compression loads and for different conformities to determine the variability of the value of the static friction coefficient. The static coefficient of friction was calculated by dividing the shear force at which motion began to occur by the compression load.

5.2.3 EXPERIMENTAL AND THEORETICAL STUDIES

The knee simulating machine and computer model were constructed so that they would have the same relative motion between the components, though there were differences in the components to which the input cycles were applied. In the knee simulating machine, the femoral component was flexed and was free to tilt in the varus-valgus direction while the tibial insert was subjected to anterior-posterior forces and internal-external rotation. In the computer model the tibial component remained stationery, though in order to calculate the bumper forces, the relative motions of the tibial insert with respect to the femur were considered so that results could be compared with the machine.

Comparisons were made between the theoretical results from the rigid body analysis in the previous chapter and experimental results from the knee simulating machine. As before, the Kinemax Condylar with the standard tibial insert (CONDYLAR) and the 'hi-stability' insert (LOWSTRESS) of higher constraint were used. An anterior-posterior force test was carried out, with an oscillating force on the tibia of 250N anteriorly and 300N posteriorly, with a 1500N constant compressive force, at 10 degrees and 60 degrees of flexion. Next, an internal-external rotation test was carried out with an oscillating torque of ±10 Nm, again with a compressive force of 1500N and at 10° and 60° of flexion. Distilled water was used as a lubricant, this having been found to give similar data to using serum or synovial fluid [Walker et al 1995]. When the bumper system (described in the previous chapter) with full strength bumpers at the posterior and one third full strength bumpers at the anterior was used, representing a knee with the anterior cruciate ligament resected, the knee with lower conformity dislocated when tests were carried out at 60deg flexion. Therefore for these tests, full strength bumpers were used anteriorly and posteriorly.

Two more knee designs were tested in the simulating machine, under the conditions stated above, to observe the effects of using a bumper system which represented a knee with the anterior cruciate ligament resected. These were the NEXGEN and PFC designs, which were both relatively conforming frontally, though the NEXGEN had shallower dishes which increased its laxity. In the sagittal plane the NEXGEN was less conforming compared to the PFC, almost flattening out posteriorly. The bumper system which had full strength bumpers posteriorly and one third strength bumpers anteriorly was applied for one set of tests and removed for a second set.

Three tests were run without bumpers on the LOWSTRESS design to investigate the effects of combining flexion and anterior-posterior force. Data-files were input to the Labview software which controlled the knee simulating machine, so that different combinations of flexion and anterior-posterior force could be applied. For all three tests there was a constant compressive load of

1500N, and an oscillating anterior-posterior force of 200N. For the first test, flexion was increased from 35 to 60deg while the anterior-posterior force increased from 0 to 200N, then the flexion was decreased from 60 to 10deg while the anterior-posterior force decreased from 200 to -200N. For the second test, flexion was decreased from 35 to 10deg while the anterior-posterior force increased from 0 to 200N, then the flexion was increased from 10 to 60deg while the anterior-posterior force decreased from 200 to -200N. For the third test, flexion remained at 35deg while the anterior-posterior force increased and decreased.

Finally, experiments were carried out under the loading conditions simulating that of walking. Varying cycles of flexion, anterior-posterior force, torque and compression load were input to the Labview software. The higher conformity design was used with a bumper system representing a knee with the anterior cruciate ligament resected (Fig. 2). Results were compared with the rigid body model results from the previous chapter.

5.2.4 CADAVERIC TESTS

Six cadaveric knees without degenerative changes were obtained. Pins were placed at the femoral and tibial attachments of the cruciate and collateral ligaments. Anterior-posterior and medial-lateral radiographs were taken with the beam centred on the line through the centres of the lateral and medial condyles and with the knee at 0° of flexion. Transparencies of the medial-lateral profiles of a total knee replacement, sized to the femur, were superimposed on the radiographic film. The profile of the femur was then flexed to 90°, so that the femoral surface was at the 'bottom of the dish' of the tibial surface. The lengths of the ligaments between the femoral and tibial attachments were measured at 0° and 90°.

The knees were stripped of skin, fat and muscles so that the bones and the capsule around the knee remained and then mounted in the knee simulating machine, using the femoral axis as a reference. At each angle of flexion from 0° to 50° in intervals of 10°, an anterior-posterior test and rotary test were

performed. The test consisted of applying a compressive force of 1500N and applying a cyclic shear force of ±350 N, followed by an internal-external torque of ±10Nm. For two of the knees, the tests were carried out for compressive forces of 500, 1000 and 1500N. Force-displacement and torque-rotation curves were recorded [Luger et al, 1997].

5.3 RESULTS

5.3.1 THE COEFFICIENT OF FRICTION

The following tests analysed the variation of the static coefficient of friction with conformity. Distilled water was used as a lubricant :

flex	FS	TS	FF	TF	KD	comp	coeff
60	20	-94	30	-46	29.437	1500	0.08
10	20	-94	30	-46	29.437	1500	0.09
60	20	-50	30	-46	36.063	1500	0.07
60	20	-56	30	-40	37.059	1500	0.07
60	20	-56	30	-40	37.059	1500	0.08
10	20	-56	30	-40	37.059	1500	0.08
10	48	-50	30	-46	120.700	1500	0.11
10	48	-56	30	-40	132.632	1500	0.11

The following tests analysed the variation of the static coefficient of friction with compression load. Distilled water was used as a lubricant :

flex	FS	TS	FF	TF	KD	comp	coeff
60	20	-56	30	-40	37.059	750	0.09
60	20	-56	30	-40	37.059	750	0.09
60	20	-56	30	-40	37.059	1125	0.08
60	20	-56	30	-40	37.059	1125	0.08
60	20	-56	30	-40	37.059	1500	0.09
60	20	-56	30	-40	37.059	1500	0.08

where **flex** is the flexion angle in degrees.

FS is the femoral sagittal radius in contact **TS** is the tibial sagittal radius

FF is the femoral frontal radius in contact **TF** is the tibial frontal radius

KD is a measure of the conformity **comp** is the compression load in N

Simultaneously, identical analyses were carried out with the rigid body analysis and it was found that when static and dynamic coefficient of friction values of 0.07 were used, the experimental and theoretical curves matched. Therefore, even though the static coefficient of friction is usually larger than the dynamic coefficient of friction, and the rigid body model could accept different values for these coefficients, a value of 0.07 was used for both.

5.3.2 EXPERIMENTAL AND THEORETICAL RESULTS

The force-displacement and torque rotation curves are shown for the theory and the experiment in Fig.3. These tests had full strength bumpers at the anterior and posterior of the tibial component. In all cases the shape of the theoretical curves matched the experimental, in particular, the stiffening with displacement and the period where there was no displacement when the force direction changed. The discrepancy at the top of the anterior-posterior curves is due to the maximum force reached by the machine being less than for the model. The results for the NEXGEN and PFC designs are shown in Figs.4 and 5, and clearly show that including the bumpers altered the shapes of the hysteresis loops and their heights.

Fig. 6 shows the effect of combining flexion with anterior-posterior force. The results from the computer model and the knee simulating machine tests followed the same trends. When the tibial insert was moving anteriorly and the femoral component was flexing, the friction produced was minimal because the components were moving together. The flat regions in the hysteresis loop disappeared and the tibial insert began to move in the opposite direction as soon as the cycles reversed direction. However, when the tibial insert moved forward while the femoral component was extending, the motions of the two components opposed each other. When the cycles reversed direction, the tibial insert continued to move in the same direction for a little while driven by friction from the flexing femoral component.

Fig. 7 shows the effect of inputting cycles of ±150N anterior-posterior force and ±5Nm internal-external torque to the CONDYLAR design when 1500N compression load and 60deg flexion were applied, without bumpers present. These results can be compared with those in the previous chapter generated by the rigid body analysis. Experimental and theoretical results for level walking (see previous chapter for the input cycles [J.Paul, 1993]) are shown in Fig.8. The theoretical curves for anterior-posterior displacement and rotation followed the experimental data closely in the stance phase. However, in the swing phase, the theoretical results deviated from the experimental, probably due to the low compression values.

5.3.3 CADAVERIC TESTS

The radiographic study showed that the mean increase in separation of the attachment points of the central fibres of the medial collateral ligament was -12% (reduction) after flexion from 0 to 90deg. For the posterior cruciate ligament, the attachment points of the anterior fibres increased in separation by 44% and the posterior fibres by 5%. For comparison, for flexion of the natural knee under quadriceps control, the equivalent percentage elongations of these ligaments respectively were -8%, 26% and 3% respectively [Rovick et al, 1991]. The total anterior-posterior displacements for a compressive force of 1500N and an anterior-posterior shear force of ±350N were in the range of 5-12mm at 0° flexion (Fig.9). The displacement increased with flexion but decreased with further flexion in some of the knees. The effect of the compressive force was to decrease the displacement primarily by reducing the posterior displacement of the tibia (Fig 10). The reduction in the total anterior-posterior displacement from 500N to 1500N compressive force was most pronounced at 0° flexion (50% reduction) but less pronounced at other flexion angles (24% reduction).

For internal-external rotation, as the compressive force was increased, although there was a change in the shape of the hysteresis loops, the rotational laxity was maintained (Fig.11).

5.4 DISCUSSION

It is important to consider the role of the anterior cruciate ligament in knee stability because this is absent after total knee replacement. In passive flexion-extension, a force in the anterior curciate ligament only occurred close to zero flexion, but a force in the quadriceps greatly increased the ligament force, and even up to 20° flexion, the ligament force was almost 20% that of the quadriceps [Markolf et al, 1990]. However, the increase in force of the anterior cruciate ligament in early flexion due to the quadriceps, could be completely negated by a simultaneous force in the hamstrings [Draganich & Vahey, 1991]. This ligament also experienced forces up to 250N when a 10Nm internal torque was applied, but less than half that in external rotation. When a 925N compressive force was applied, the ligament force reduced by 46% at 20° flexion, but there were only small changes in the ligament force in internal-external rotation. In the posterior cruciate ligament, tensions were generated only after 60° flexion. These forces then increased with flexion, with internal rotation, and with quadriceps force [Wascher et al, 1993]. These findings are consistent with the cruciate ligament length patterns of the anterior and posterior fibres when knee specimens were moved through a complete flexion-extension range under the control of the quadriceps [Rovick et al, 1991].

In knees where the anterior cruciate ligament is ruptured, adaptations of posture occur which reduce the flexing moment on the knee, requiring less force in the quadriceps presumably to avoid excessive shear forces [Berchuck et al, 1990]. Under different loading conditions, such as ascending stairs, the situation was found to be more complex with a greater posterior tibial translation and rotational abnormalities occurring compared to normal knees [Jonsson & Karrholm, 1994]. An additional consideration is the lever arm of the quadriceps [Draganich et al, 1987]. This increased considerably up to 20° flexion but then only slightly even after anterior cruciate ligament excision. However, after posterior cruciate ligament excision, the lever arm reduced considerably after 50° flexion due to the posterior displacement of the tibia caused by the quadriceps. Hence, the displacements and rotations are seen to be highly

dependent upon the presence or absence of the cruciate ligaments, in both light loading and under functional conditions.

The situation with total knee replacement is complex due to the variables of the type of design, which of the cruciates are preserved, and the placement of the components in the joint. In designs where the posterior cruciate ligament is resected, in stair climbing, patients showed a reduced angle of flexion during stance, which was attributed to the inability of the quadriceps to sustain a higher force to counteract the reduced lever arm, caused by an abnormally anterior contact point [Draganich et al, 1987; Andriacchi & Mikosz, 1991]. For a low conformity design where the cruciates were preserved a quadriceps avoidance pattern was noted in level walking, probably to reduce the anterior shear force on the tibia. However in other cases, a quadriceps overuse pattern was measured [Andriacchi & Mikosz, 1991].

In previous studies, the coupling or uncoupling of other degrees of freedom played a major role in explaining the reductions in laxity of the natural knee with compressive force applied. Another factor was the line along which an anterior-posterior force was applied. If this line was perpendicular to the long axis of the tibia, a posteriorly applied force would be strongly resisted by the anterior slope of the upper tibia. The experiments carried out in this study show the relatively modest effect of compressive force on the laxity of the natural knee, the only exception being a high reduction in anterior-posterior displacement at 0° flexion. It was found that despite this effect, the anterior-posterior laxity peaked in the range of 10-30° flexion, but reduced again at higher flexion. This finding is consistent with the data of Arima *et al.* [Arima et al, 1994].

A well recognised surgical problem is to achieve the correct tensioning of the posterior cruciate ligament such that it is neither too tight nor too loose in flexion. However, this is assessed with no compression force across the joint. This problem may be much more acute under compressive loading conditions when the femoral component is constrained to lie close to the bottom of the tibial dish (Fig.12). In this figure, the outlines of the natural knee were those of the

average knee undergoing average motion under quadriceps control [Rovick et al, 1991; Garg & Walker, 1990]. The internal rotation and femoral rollback at 90° flexion can be seen. The prosthetic knee surfaces are of a moderate conformity total knee replacement and were computer generated [Sathasivam & Walker, 1997]. The components were positioned anatomically onto the femur and tibia, and at 0° flexion, the femoral-tibial position is correct in the anterior-posterior direction. However, there is a serious incompatibility of femoral-tibial position at 90° where, the femur is prevented from posterior translation, exposing the posterior cruciate ligament to very high elongation.

This was illustrated in the cadaveric study where there was a 44% increase in the distance between the attachment points of the anterior fibres of the posterior cruciate ligament, compared with an elongation of this ligament of 26% in the natural knee where rollback occurs. The resulting increase in the posterior cruciate force would increase the compressive forces on the polyethylene, and possibly accelerate the onset of delamination. The stiffness characteristics of the natural knee, used to define the shape of the bumpers in the computer model and knee simulating machine, did not include an increased force exerted by the posterior cruciate ligament with flexion, which might explain why dislocation occurred for one of the total knee replacements tested in the knee simulating machine.

When the low conformity tibial insert was subjected to cyclic anterior-posterior forces of 250N anteriorly and 300N posteriorly under 1500N compression load, the femoral component climbed over the posterior edge of the tibial insert. Replacing the one third strength bumpers at the front with full strength bumpers solved the problem, reducing the laxity. For tests carried out at constant flexion, different bumpers systems could be designed to represent the different stiffnesses of the knee during flexion. However, during functional activities the flexion varies. In order to include soft tissue restraints which vary with flexion, realistic representations of the ligaments and other soft tissues could be included in the knee simulating machine and the computer model. Attachment points of the ligaments could be found from cadaveric specimens and springs could be attached between them. However, even then, the question

would still remain as to whether it is correct to input compression load, anterior-posterior force and internal-external torque based on natural knee data to a knee simulating machine testing a prosthetic knee.

By comparing the data from the computer model with that from the knee simulating machine, it was considered that the model provided an accurate representation of the kinematics for a range of surface geometries and input force and motion conditions, the inclusion of friction in the computer model playing a key role. Therefore, the assumptions of quasi-static motion, contact made at points between the prostheses rather than contact areas and negligible inertial effects were satisfactory with regards to predicting kinematics. There were other assumptions which could not be validated because they were made for both the experimental and theoretical tests on the prosthetic components.

It was assumed that the forces and moments of a natural knee could be applied to prosthetic knees of different designs during gait. In addition, it was assumed that the ligament restraints would not be affected by flexion. Results from tests carried out on cadaveric specimens showed that the bumper system which was used in both the computer model and the knee simulating machine was not an accurate representation of the action of the ligaments if flexion was applied. However, these tests also showed that the ligament stiffnesses varied considerably between different knees. It was concluded that the computer model could predict kinematics accurately for a given set of input forces and moments with a given set of ligament restraints. However in order to predict accurate kinematics during gait, more knowledge about the changing muscle forces in the knee and their effect on the ligament forces is required.

FIG.1 TOP : A schematic of the knee simulating machine.
BOTTOM : The knee simulating machine.

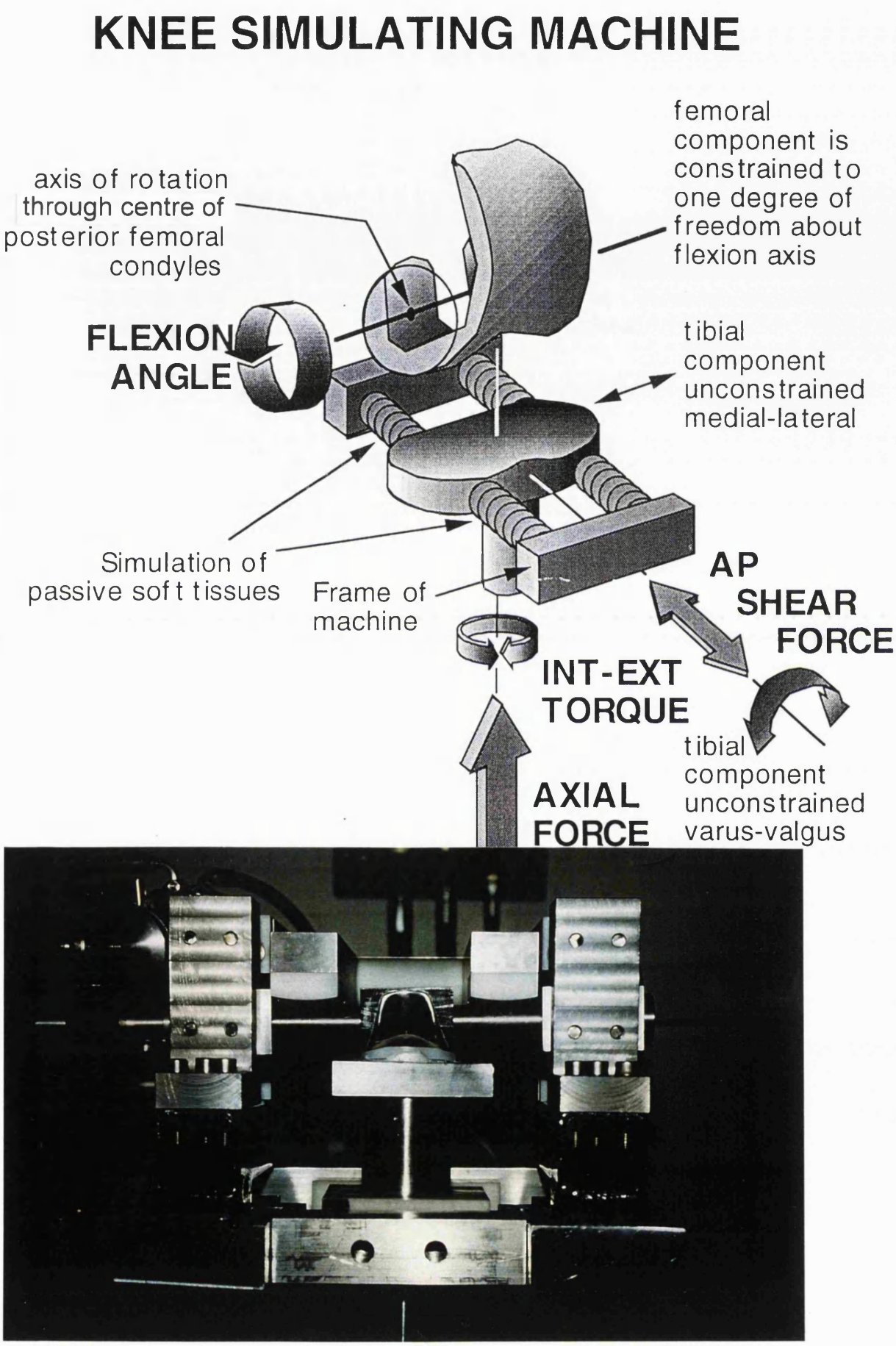

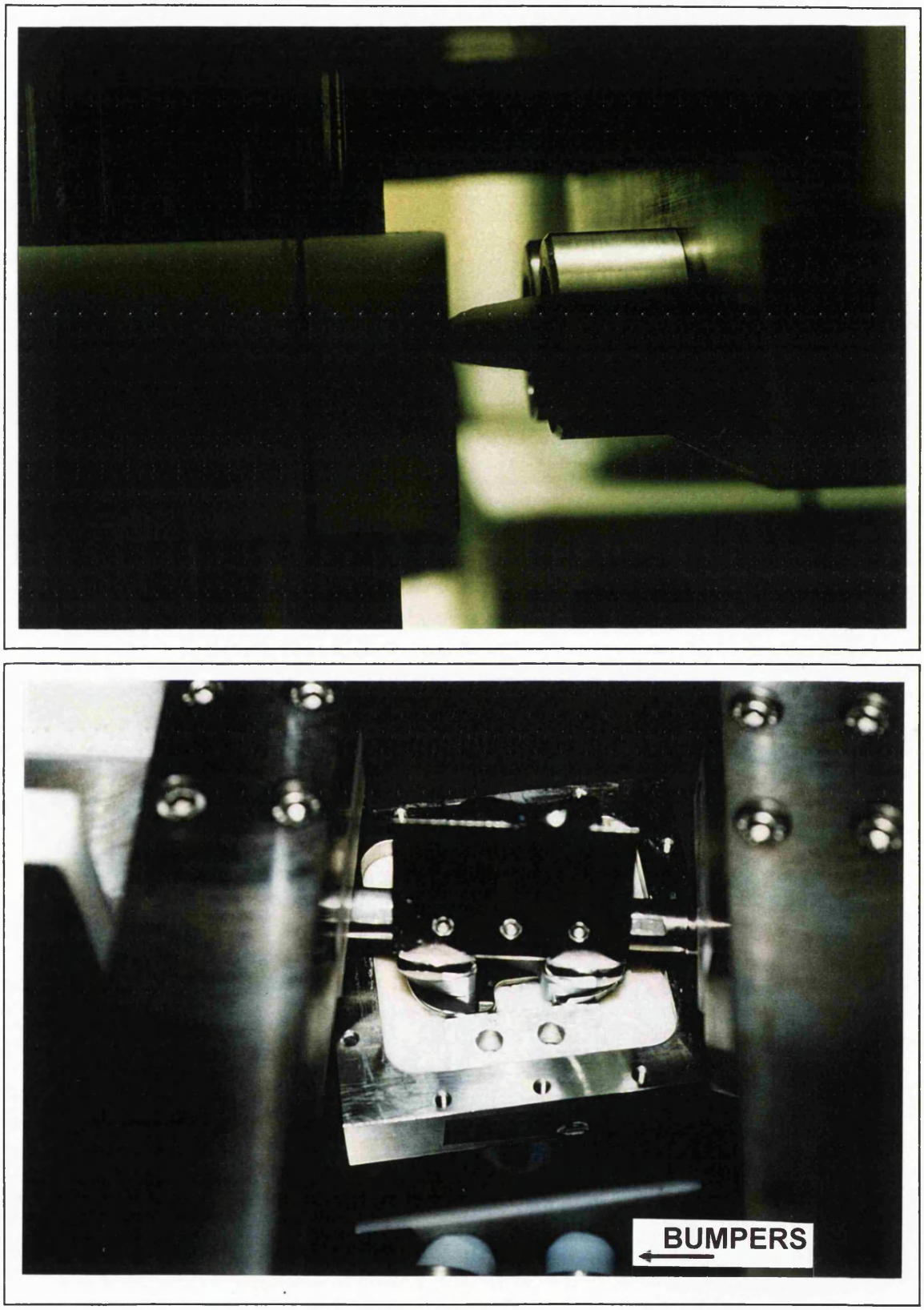

FIG. 2 a) One third strength bumpers used at the anterior of the tibial insert. b) Full strength bumpers used at the posterior of the tibial insert.

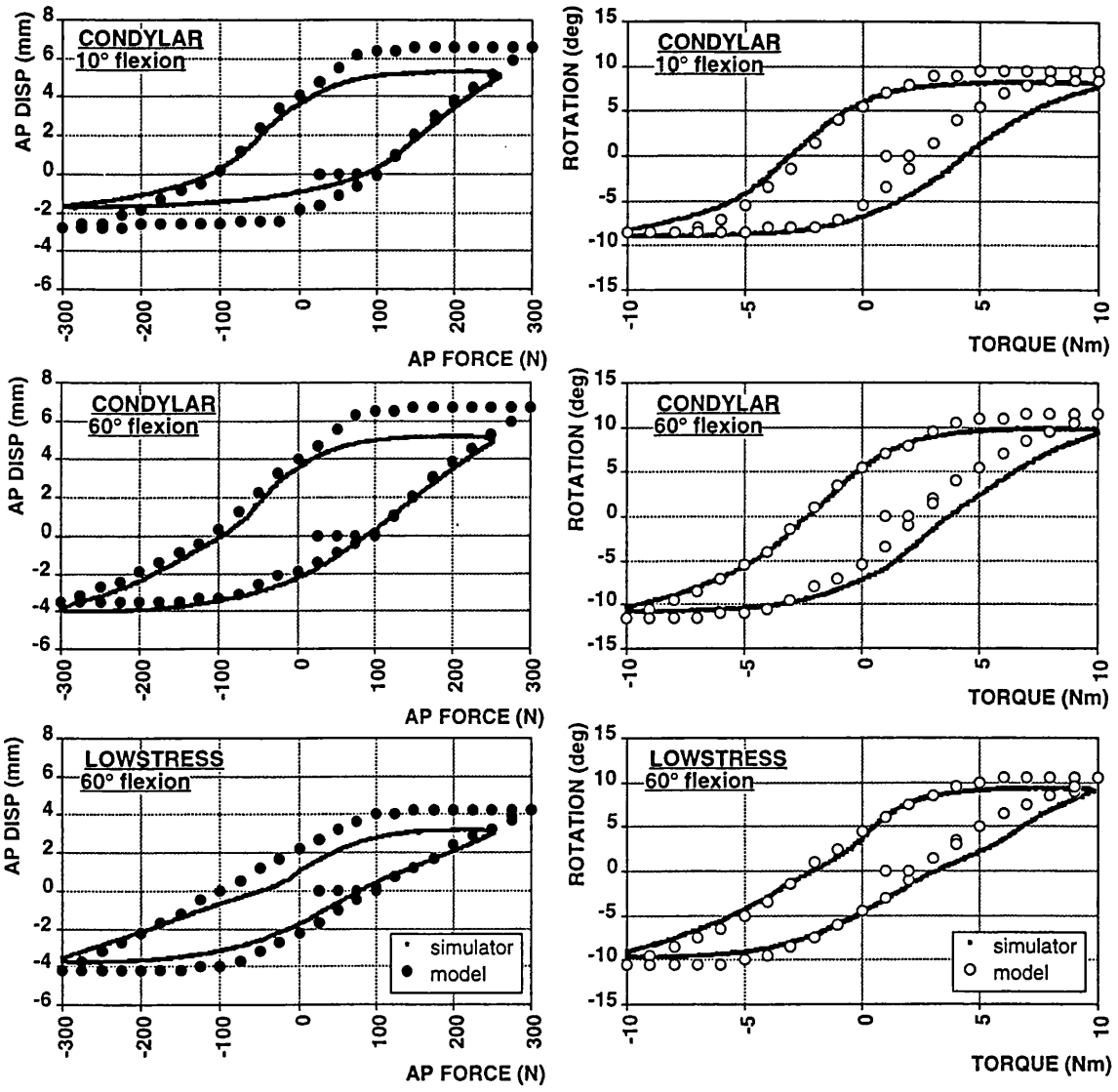

FIG. 3 Force-displacement and torque-rotation curves, comparing theoretical and experimental results. Positive displacement indicates anterior movement of the tibia. Full strength bumpers were used anteriorly and posteriorly.

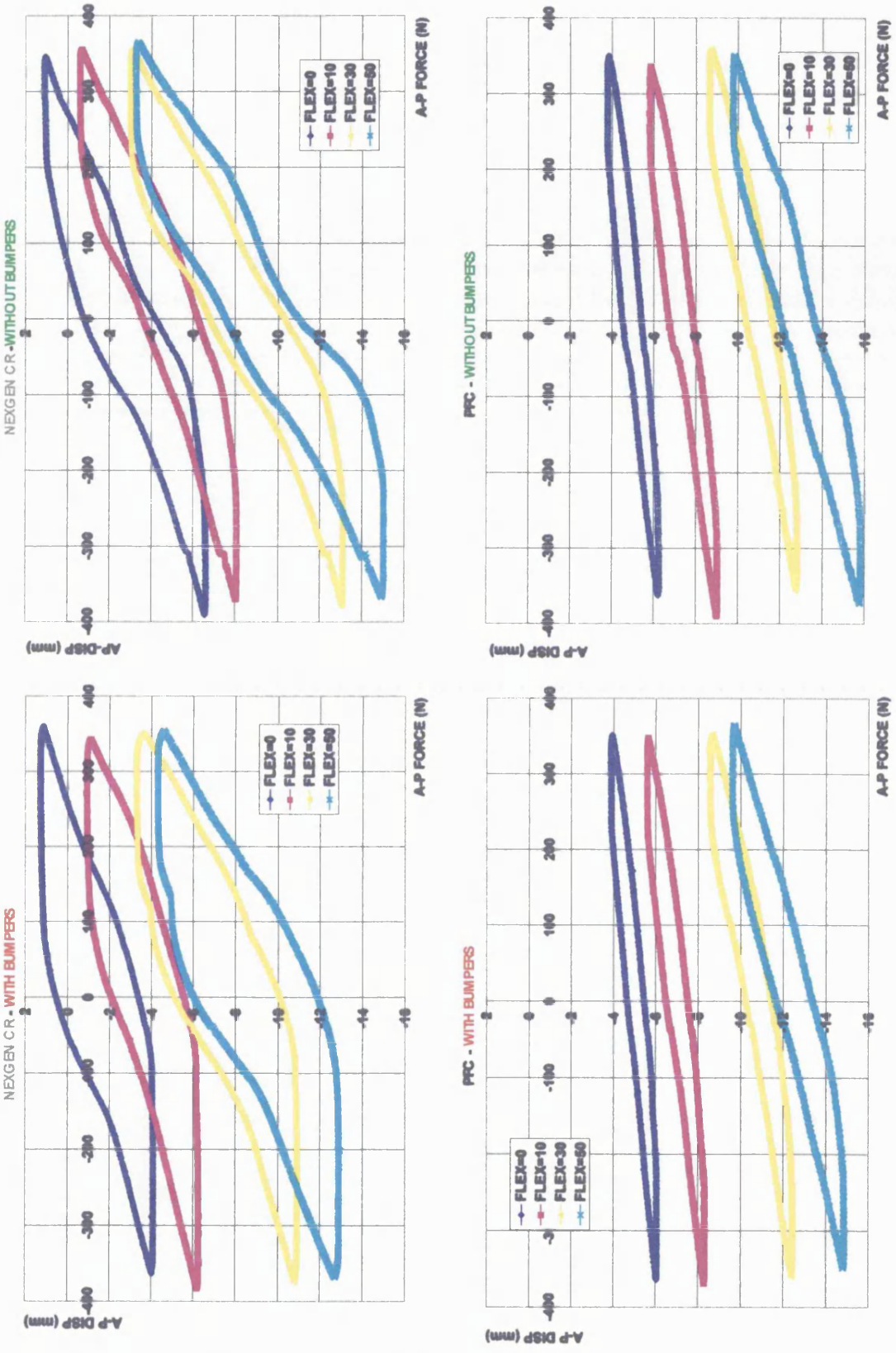

FIG.4 A-P force cycles were applied to the NEXGEN and PFC knees at different flexion angles, with and without a bumper system to represent soft tissue restraints with the ACL resected. The compression load was 1500N.

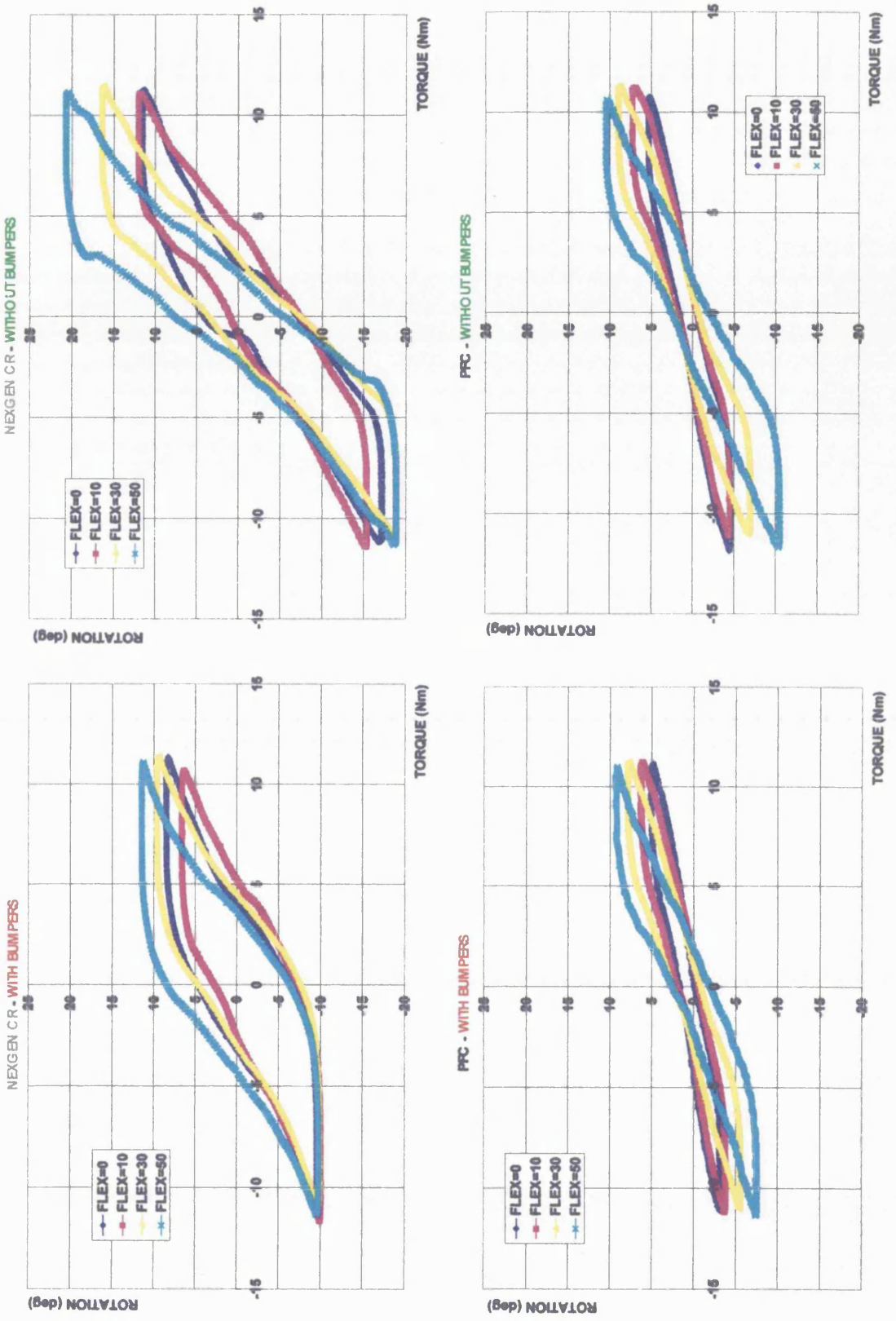

FIG.5 Int-ext force cycles were applied to the NEXGEN and PFC knees at different flexion angles, with and without a bumper system to represent soft tissue restraints with the ACL resected. The compression load was 1500N.

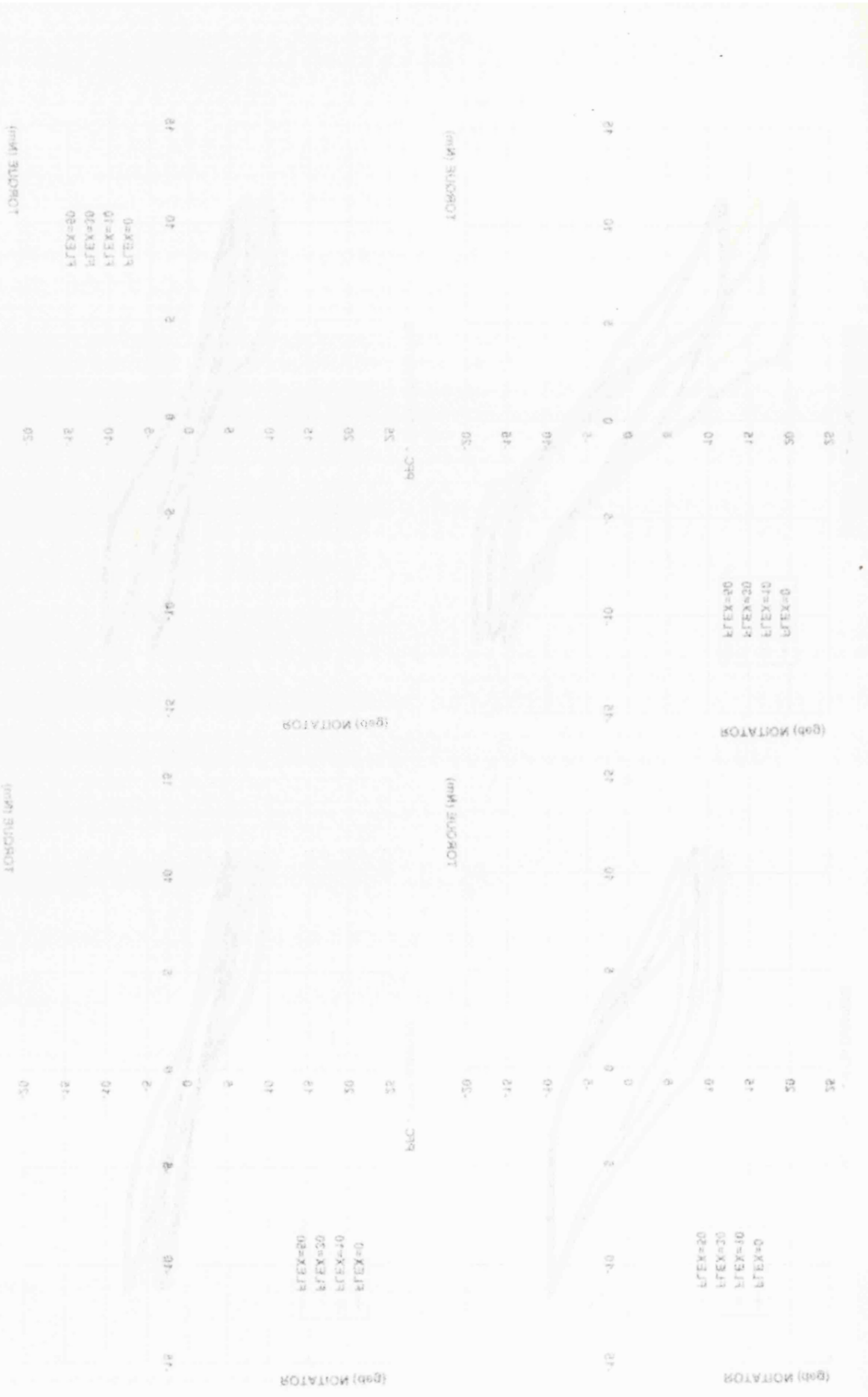

FIG.5 Int-ext force cycles were applied to the NEXGEN and PFC knees at different flexion angles, with and without a bumper system to represent soft tissue restraints with the ACL resected. The compression load was 1500N.

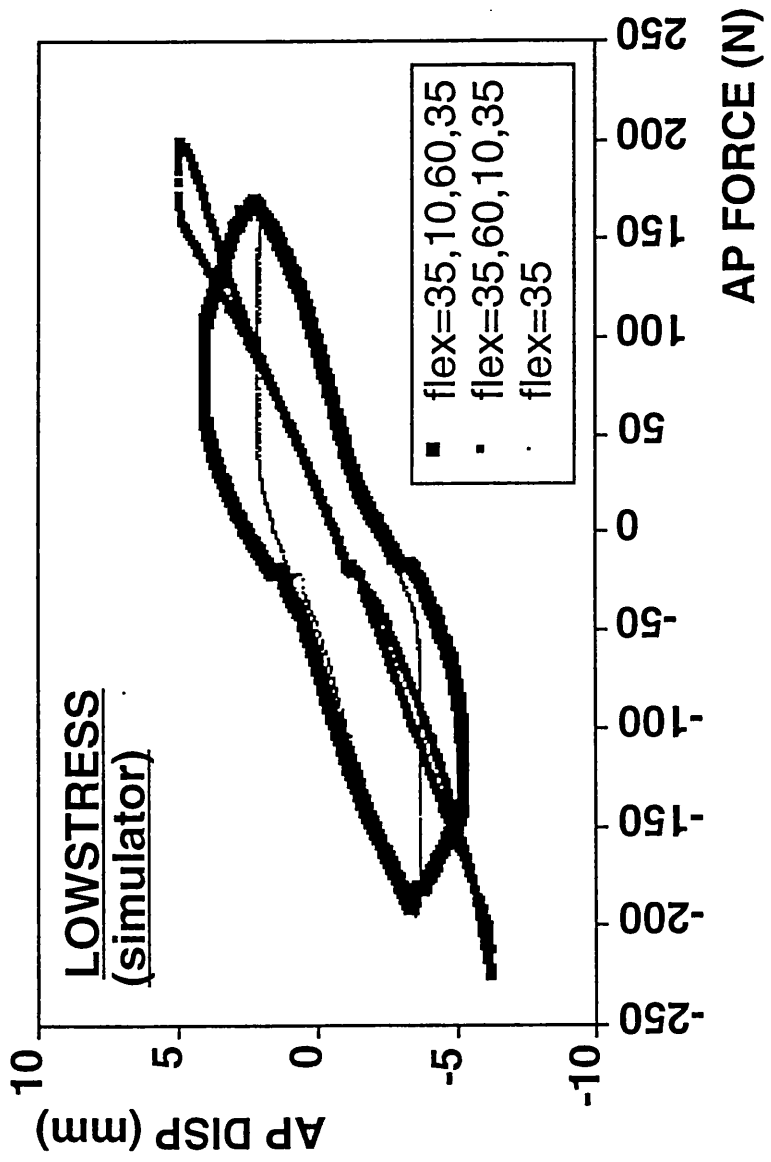

FIG. 6 Curves produced by the knee simulating machine for tests where anterior-posterior force and flexion were combined in different ways.

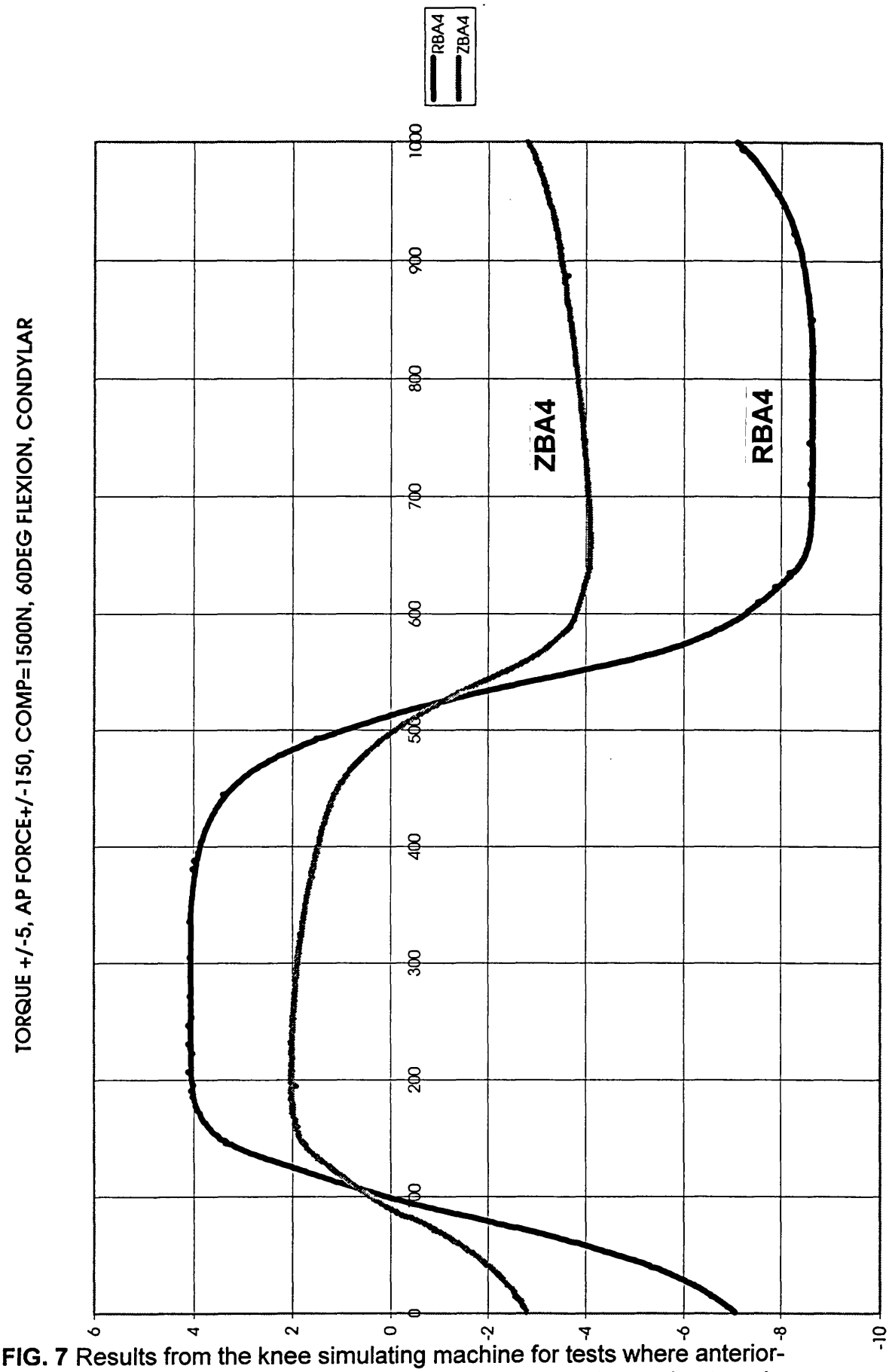

FIG. 7 Results from the knee simulating machine for tests where anterior-posterior force and torque were combined. RBA4 is the internal-external rotation, ZBA4 is the anterior-posterior displacement of the tibal insert.

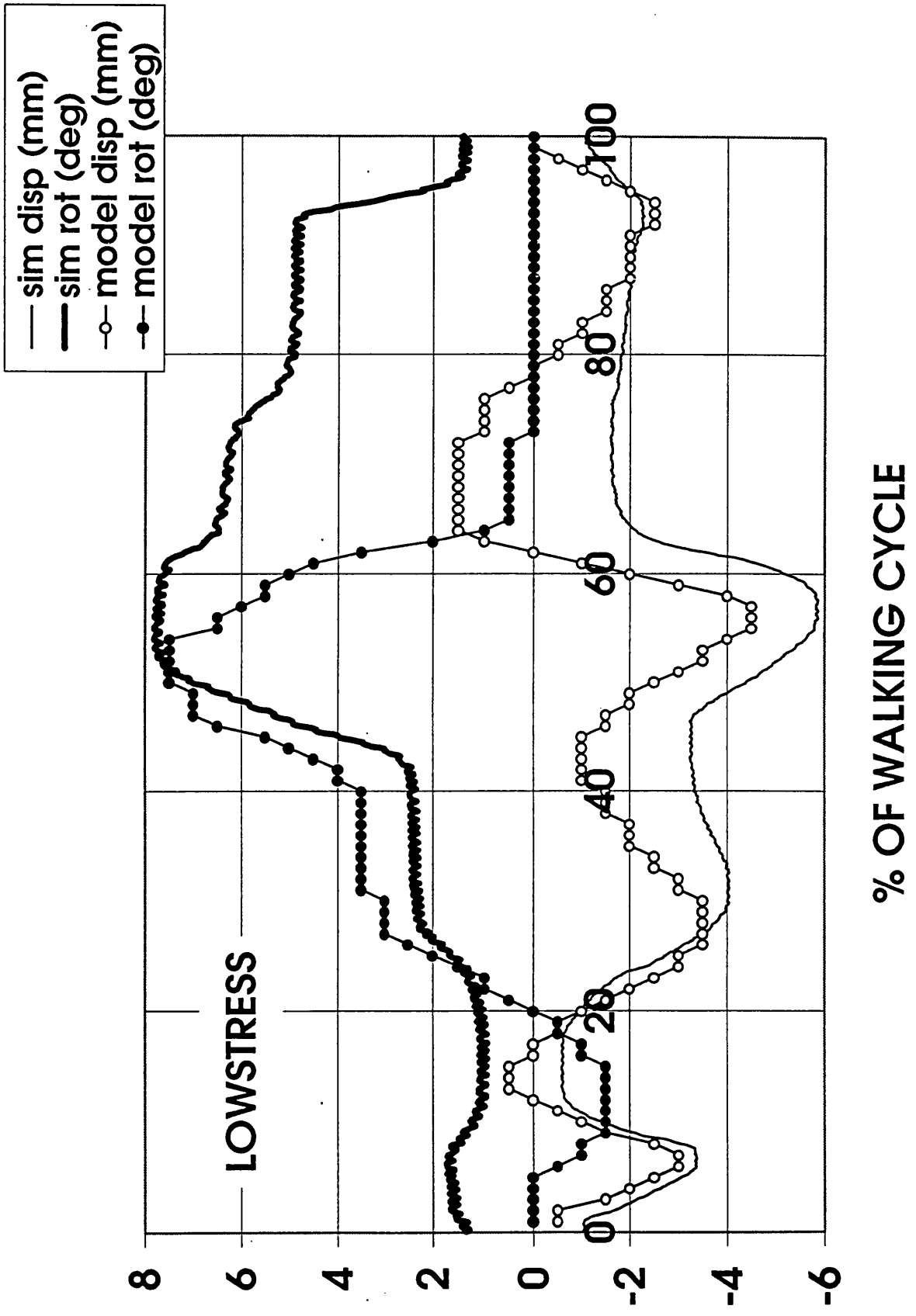

FIG.8 Comparing the predictions of the computer model for the output rotations and displacements during level walking with results from the knee simulating machine. Input cycles provided by J.P. Paul

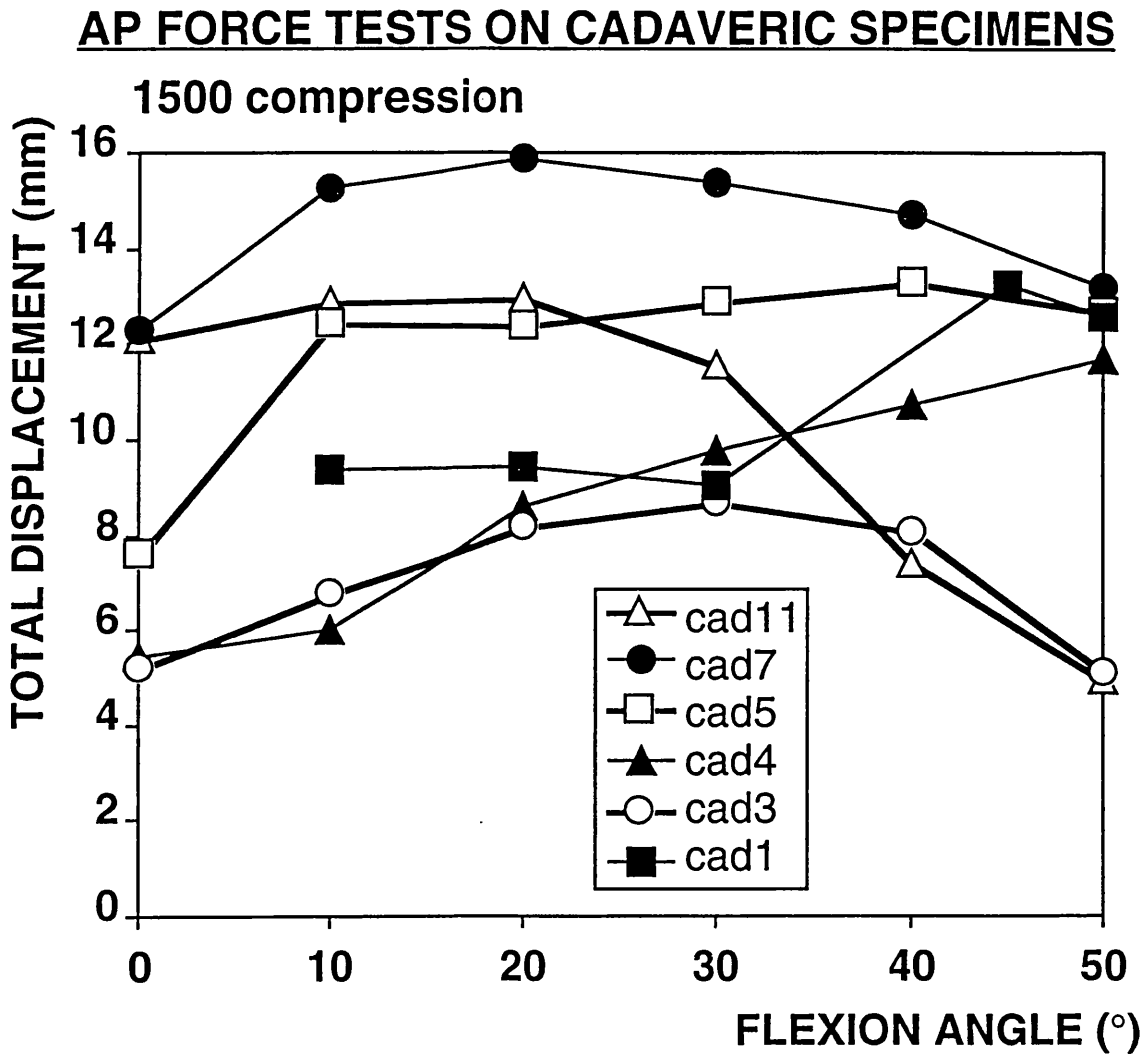

FIG. 9 Total anterior-posterior displacement plotted against flexion for six knee specimens.

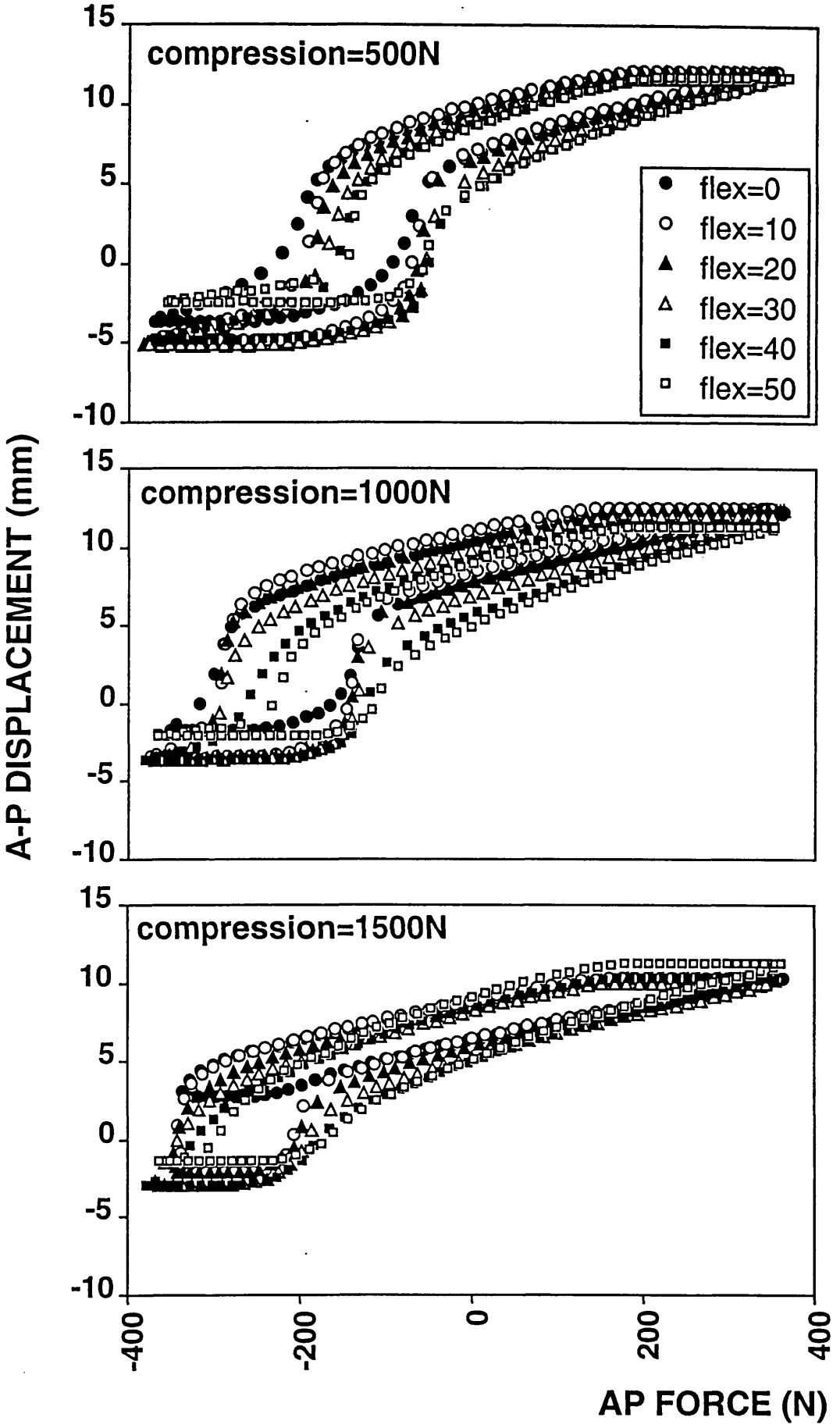

FIG. 10 Anterior-posterior displacement plotted against anterior-posterior force at 3 compressive forces for a typical knee specimen.

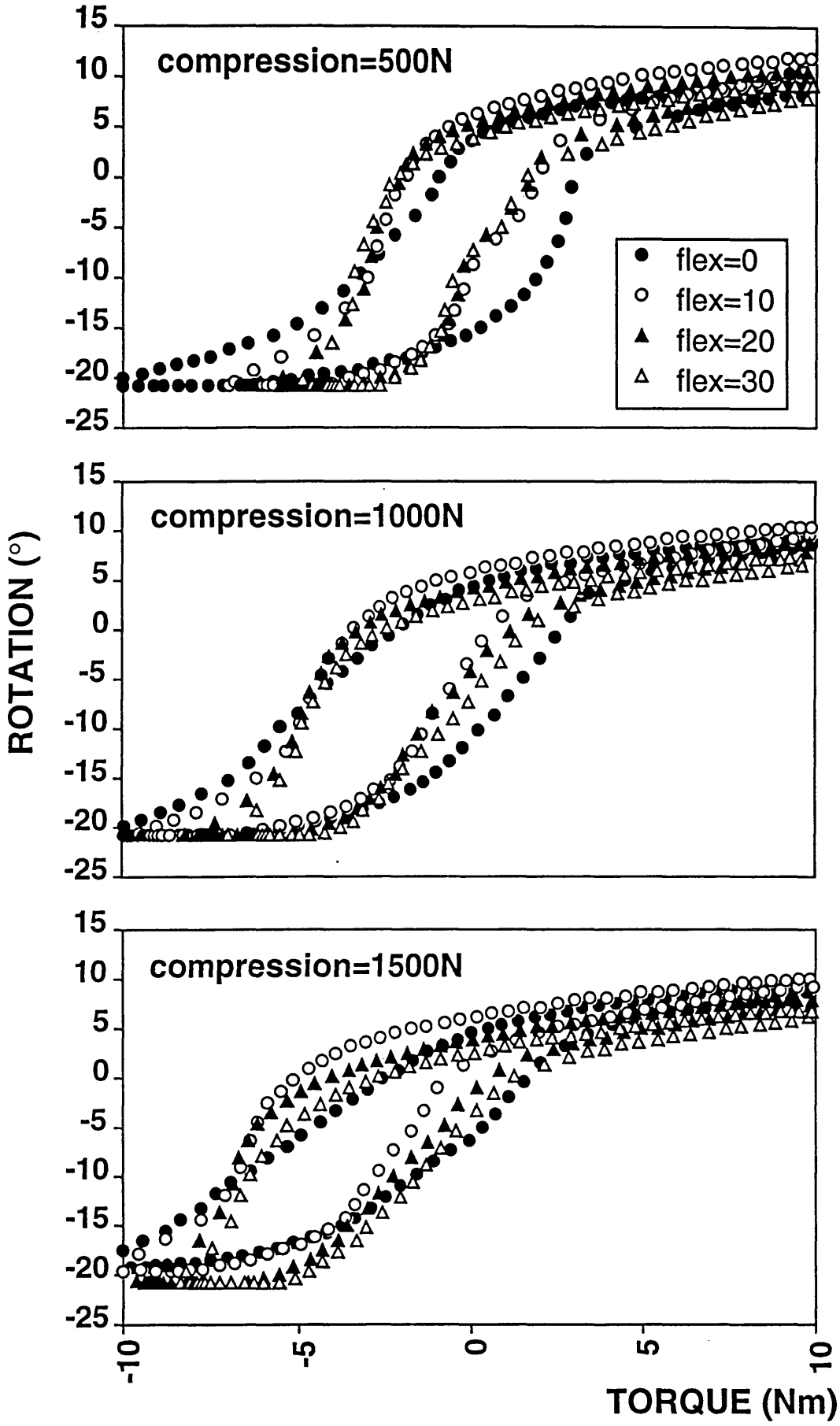

FIG. 11 Rotation plotted against torque at 3 compressive forces for a typical knee specimen.

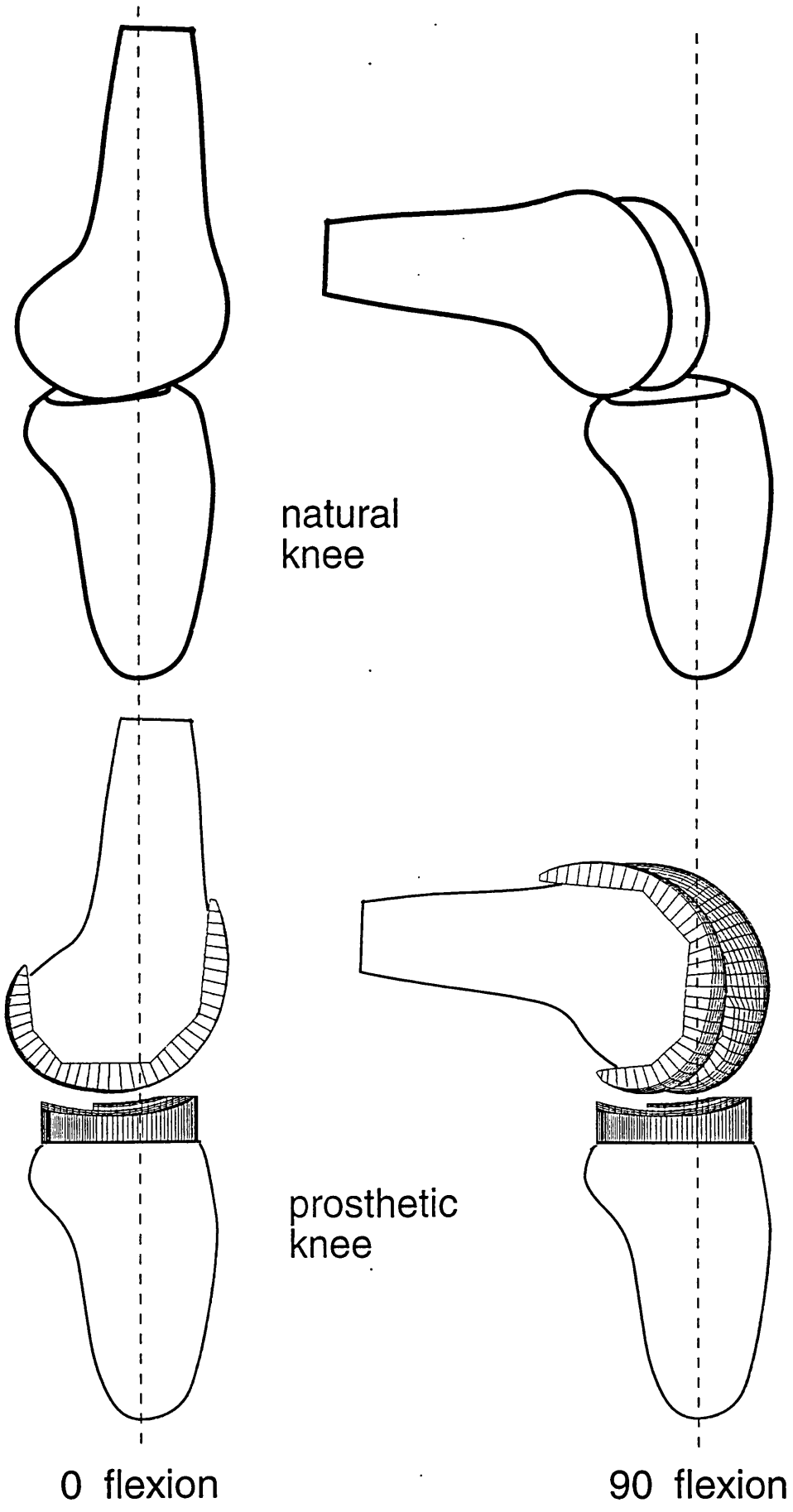

FIG. 12 Graphic showing the incompatibility of a TKR with normal knee motion and PCL tension, due to the preferred TKR position at the bottom of the tibial dish under the compressive forces acting during activities.

Chapter 6

DETERMINING THE VARIATION OF STRESSES IN THE TIBIAL INSERT DURING GAIT

6. DETERMINING THE VARIATION OF STRESSES IN THE TIBIAL INSERT DURING GAIT

6.1 INTRODUCTION

The magnitudes of the fluctuating stresses produced in the tibial insert during gait are functions of the bearing surface geometry and the forces applied. For elastoplastic solids in contact bearing situations, subsurface cracking leading to yield and crack propagation has been associated with combined compression and shear stress [Suh, 1986] and cyclic compressive stress [Pruitt et al, 1995]. For the polyethylene in tibial inserts, this crack initiation and propagation results in delamination wear.

The stresses could be altered by the increased modulus produced by oxidation [Bostrom et al, 1994] which would particularly elevate surface tensile stresses [Kurtz et al, 1994]. Nevertheless, retrieval studies show that when delamination occurs, subsurface cracking precedes surface cracking [Blunn et al, 1996; Blunn et al, 1992; Collier et al, 1991; Landy & Walker, 1988]. Bartel et al. [1986] noted that during gait, a point on the surface of the plastic may be subjected to the fatiguing effect of cyclic tensile and compressive stresses, suggesting that sliding is an important factor in delamination wear. Whereas, Wimmer and Andriacchi [1996] proposed that the forces produced during tractive rolling, governed by the static rather than the dynamic coefficient of friction, could contribute to subsurface damage.

The likelihood of a tibial insert to delaminate is commonly assessed by determining the contact stresses with the knee in a neutral position [Szivek et al, 1995], though deficiencies of experimental methods exist [Bristol et al, 1996; Stewart et al, 1995]. These methods do not take into account the effects of varying displacements and rotations between the femoral and tibial components with design. The hypothesis was that the stresses produced in tibial inserts during gait would vary significantly for different designs, not only because of their differing geometries but also because of variations in their laxities. The rigid body

analysis described in the Chapter 4 was used to determine these laxities and the successive orientations of the components during gait. Then finite element models were generated of the components in these orientations to determine stress histories for every element in tibial inserts of two commercially available knee designs.

6.2 METHODS AND MATERIALS

6.2.1 GENERATING THE FINITE ELEMENT MODELS

Computer programs were written to create parametrised finite element models (Fig.1) in ABAQUS version 5.4 (Hibbitt, Karlsson, and Sorensen, Inc., Pawtucket, RI). The femoral component bearing surface was modelled with 15740 rigid body elements and was meshed very finely in comparison to the tibial component to minimise errors due to misalignment of the contact nodes. The femoral component was constrained in all directions, except the vertical direction as it would be subjected to vertical compression load, stabilised by a spring with stiffness of 10N/mm. The interfacing surfaces of the femoral component and tibial insert were defined as frictionless contact surfaces.

The tibial insert model consisted of 4660 8-noded solid brick elements with an elastic modulus of 600MPa and a Poisson's ratio of 0.4. The thickness of each tibial insert was 6mm from the bottom of the tibial dish to the base of the insert. The insert was made up of 5 layers of elements, the three upper layers each having a height of 0.7mm to obtain more accurate results near the surface. The base nodes of the tibial insert were constrained in all directions to represent a fully bonded interface with the metal tibial tray.

Appropriate parameters (Fig.2) were input to the computer programs to create finite element models of two commercially available products, the Kinemax Condylar Lowstress (Design 1) and the Zimmer Nexgen Condylar Cruciate Retaining (Design 2). Design 1 had moderate conformity and constraint. In comparison, Design 2 had increased outer radii of both components and increased posterior sagittal tibial radius. The femoral sagittal radius was not

increased, but sagittal conformity was maintained by continuing the larger distal femoral radius more posteriorly before it transferred to the small posterior radius.

The angle in extension at which the posterior arc transferred to the distal arc was called the posterior-distal transition angle, PDTA. The bearing spacing BS was the distance between the centres of the arcs which defined the femoral condyles and tibial dishes in the frontal plane. TRI, TRO, FRI, FRO were the inner and outer tibal and femoral frontal radii respectively and TPS, TAS, FPS, FAS were the posterior and anterior tibial and femoral sagittal radii.

Design	BS	TRI	FRI	TRO	FRO	TPS	FPS	TAS	FAS	PDTA
1	48	40	30	40	30	56	20	56	48	-8
2	44	28	25	80	75	78.9	20M /22L	57	36.4M/ 56.9L	-15

6.2.2 TO INCLUDE THE EFFECTS OF OXIDATION AT THE SURFACE OF THE TIBIAL INSERT

The elastic modulus of the polyethylene tibial insert was varied to include the effects of surface and subsurface oxidation. Design 1 was positioned at 60deg flexion, with the femoral condyles seated at the bases of the tibial dishes, and loaded with 2000N compression. Four tests were carried out where the only variations were the material properties of the polyethylene :

1) all of the elements of the tibial insert were given an elastic modulus of 600MPa.

2) the top layer (surface to 0.7mm deep) of elements was given an elastic modulus of 1200MPa, the remaining elements had an elastic modulus of 600MPa.

3) the subsurface layer (0.7-1.4mm deep) of elements was given an elastic modulus of 1200MPa, the remaining elements had an elastic modulus of 600MPa.

4) the top and subsurface layer (surface to 1.4mm deep) of elements was given an elastic modulus of 1200MPa, the remaining elements had an elastic modulus of 600MPa.

The contact stresses for these four cases were compared.

6.2.3 TO PREDICT THE VARIATION OF STRESSES DURING GAIT

Computer software [Sathasivam & Walker, 1994] which generated meshes of points describing the surfaces of total condylar knee replacements was used to describe the two designs being analysed.

Force and motion data (Fig. 3) for normal subjects in level walking were obtained from Andriacchi et al [1995]. The data were calculated from ground-to-foot kinematic and e.m.g. data, using a model similar to that of Morrison [1969]. The force and flexion cycles were split into discrete intervals at every 1% of the level walking cycle up to 60% (the stance phase) for input to quasi-static rigid body analysis [Sathasivam & Walker, 1997].

The relative motion between the femoral and tibial components will be constrained by the design of the bearing surfaces and by the soft tissues surrounding the knee. To represent the latter, pairs of non-linear bumpers were positioned anteriorly and posteriorly to the tibial component in the rigid body model. The bumpers provided the restraint of a knee replacement with the anterior cruciate ligament resected and the posterior cruciate ligament retained. Bumper stiffnesses were calculated from experimental anterior-posterior and rotational data [Fukubayashi et al, 1982; Shoemaker & Markolf, 1985].

Femoral component orientations on the tibial insert were determined so that the input joint reaction, friction and soft tissue restraints reached a state of equilibrium. This was achieved by using an iterative method which examined multiple positions of the femoral component resulting in a pattern of contact points on the tibial surface. The model had been validated experimentally by a knee simulating machine [Sathasivam & Walker, 1997].

For each knee, at every 2% of the gait cycle, the femoral components, in separate finite element models for each interval, were orientated according to the results of the rigid body analyses. Soft tissue restraints, the friction, the anterior-posterior force and internal-external torque were not included in these models, as their effects had already been taken into account in the rigid body analysis. Gait compression was applied to the prosthetic components in their various orientations and the maximum contact stress for each position was recorded. In addition, values of the maximum and minimum principal stress histories were recorded for each polyethylene element. These values were used to calculate the maximum shear stress.

As the aim was to investigate stress histories for each element in the tibial insert as the stance phase of a gait cycle progessed, the same mesh was required for each analysis of the stance phase intervals. Therefore, the meshes could not be refined in the regions of contact, but tests were carried out to ensure that the elements were of adequate size (see Chapter 3).

6.2.4 MODIFYING THE BOUNDARY CONSTRAINTS ON THE FINITE ELEMENT MODEL OF THE FEMORAL COMPONENT

Varus-valgus moments had not been included in the cycles input to the rigid body analysis, but varus-valgus tilt correction had been included to make certain that two contact points were made. To satisfy the equilibrium equations, the resultant varus-valgus moment was set to zero. However, for some cases where the contact points predicted by the rigid body analysis were not in the centre of the contact patches produced by the finite element analysis, the pressure exerted onto the medial and lateral portions of the tibial insert sometimes seemed uneven. It was apparent that further varus-valgus tilt correction was required in the finite element analyses for these cases, which was not allowed by the boundary constraints. Two dimensional finite element analyses were run to determine the feasibility of including this extra degree of freedom in the three-dimensional models.

A flat plastic slab was modelled to represent the tibial insert, using 4-noded quadrilateral elements, and the frontal profile of the femoral condyles was modelled by two curves using 2-noded rigid elements. One curve was raised by 0.5mm to represent a femoral component in need of varus-valgus correction. First the femoral component was constrained as in the three-dimensional models so that it was not allowed to varus-valgus tilt, only being allowed to lower vertically onto the tibial insert. As before, a spring was used for stability while 1000N of vertical compression was applied to the femoral component. Having recreated the three-dimensional problem in two-dimensions, the problem could be analysed at much greater speed. To introduce varus-valgus correction to the finite element analysis, the boundary constraint which prevented the femoral component turning around the z-axis (running from posterior to anterior through the femoral component) was removed.

6.3 RESULTS

6.3.1 INCLUDING THE EFFECTS OF OXIDATION AT THE SURFACE OF THE TIBIAL INSERT

1) When all the elements were given an elastic modulus of 600MPa the maximum contact stress was 32.3MPa

2) When the top layer of elements was given an elastic modulus of 1200MPa the maximum contact stress was 34.1MPa.

3) When the subsurface layer of elements was given an elastic modulus of 1200MPa the maximum contact stress was 35.3MPa.

4) When the top and subsurface layer of elements was given an elastic modulus of 1200MPa the maximum contact stress was 38.4MPa.

6.3.2 PREDICTING THE STRESSES DURING GAIT

The contact patches and stresses for the two designs were very different. The maximum contact stresses plotted for the gait cycle (Fig.4) showed that the values for Design 2 were generally lower, almost half the values of Design 1 at some instances. However, at the beginning of the stance phase, the stresses for

Design 1 were lower because in extension it had greater sagittal conformity due to its tighter tibial sagittal radii. Design 2, on the other hand, had an especially large posterior sagittal tibial radius to accommodate the femoral frontal geometry, which was constructed from large arcs, when there was relative rotation. Therefore, in extension the contact patches for Design 1 were large and round, while the contact patches for Design 2 were narrow in the anterior-posterior direction but wide in the medial-lateral direction due to its conforming frontal geometry (Figs.5 at 1% of the gait cycle). Contact patches are plotted for a right knee.

The shapes of these contact patches varied as gait progressed (Figs.5). For Design 1, the area of the contact patches reduced as flexion of the femoral component transferred contact from the large distal arc to the small posterior arc. Meanwhile the patches for Design 2 were larger in comparison, as the femoral component still contacted the tibial component with its large distal arc. The contact patches for this design were especially large when relative external rotation of the femoral component occurred, the condyles bearing on the anterior sagittal tibial arc which was more conforming compared with the posterior arc. In fact in some cases the combination of this conforming anterior sagittal tibial arc and the tight frontal conformity of Design 2 produced double contact patches on the medial portion of the tibial insert.

The maximum principal stress and maximum shear stresses were recorded for each element, of each position during the gait cycle, of each design. Thus stress histories could be plotted for each element. In order to choose one element to be analysed for each design, the stresses in the elements of each design were averaged over the gait cycle and the results of the elements subjected to the highest average stress were plotted (Figs. 6). These elements were in different positions for the two designs.

6.3.3 REDUCING THE BOUNDARY CONSTRAINTS ON THE FINITE ELEMENT MODEL OF THE FEMORAL COMPONENT

Each finite element analysis of each of the 30 orientations during the gait cycle of the three-dimensional prosthetic components of a particular design took over

two hours (running on a Digital AlphaStation), depending on the sizes of the areas in contact. Investigations were made to determine the feasibility of removing one of the boundary constraints on the femoral component to allow varus-valgus tilt correction. The first two dimensional model, which was set up as a 'small displacement' analysis, recreated the scenario of a femoral component which had not been allowed to tilt in the varus-valgus direction. The solution converged after one time increment as friction was not included, and the stresses seen in the flat tibial insert were uneven as expected.

When the varus-valgus boundary constraint was removed from this model, the solution diverged. However, when the same analysis was set up as a 'large displacement' problem, the solution converged after 20 time increments, and even stresses were seen in the tibial insert under each femoral condyle even though one condyle was raised. For two-dimensional analyses, the difference in time between solving for one time increment and 20 was insignificant, however for three-dimensional analyses including the extra degree of freedom was unfeasible.

6.4 DISCUSSION

Generally, the likelihood of a tibial insert to delaminate has been determined by measuring contact stresses at a few angles of flexion. In reality, different designs exhibit varying anterior-posterior and rotational laxities at different stages of gait and the stresses fluctuate significantly as the contact areas change in shape depending on the orientations of the components. Nevertheless, excluding all relative motions of the components apart from flexion makes practical measurement of contact patches easier, because the femoral component can be held fixed in its flexed position and lowered onto the tibial insert, producing very neat contact patches.

The same test could be carried out if the femoral component was rotated and displaced with respect to the tibial insert. However uneven pressure would be exerted by each femoral condyle, unless the femoral component is allowed to tilt in the varus-valgus direction to cope with the different contact conditions that

each condyle will experience. If the femoral component is allowed to rotate in the varus-valgus direction, even contact would be achieved, but only after smearing the contact patches as it settled. With theoretical methods of generating contact patches, this smearing effect is not a problem, however including the extra degree of freedom does increase the time to solve a contact problem by several magnitudes.

This study attempted to solve the problem of calculating stresses for a sequence of realistic orientations of the femoral component on the tibial insert, with flexion, anterior-posterior displacement and internal-external rotations imposed, by using finite element analysis. The orientations were determined by rigid body analyses which took into account the geometry of the bearing surfaces, soft tissue restraints and frictional effects. An alternative method would have been to input the cycles of compression load, anterior-posterior force, internal external torque and flexion directly to a finite element model to obtain dynamically varying stresses. However, this would require the femoral component to be completely free to move without any boundary constraints, though it could be stabilised by springs, and the analyses would take an unreasonable amount of time. Instead, a quasi-static method was used in this study, where different prosthetic finite element models were generated for each discrete interval of the input cycles being analysed. Having determined the orientations of the components from the rigid body analysis, the components were simply compressed together under gait load.

There were limitations in the analysis which need to be considered. The input data for the forces, moments and flexion-extension angles, were based on calculations for normal subjects. There can be variations in these input cycles for a knee replacement patient, even depending upon the type of knee replacement [Andriacchi et al, 1995]. Furthermore, activities involving higher flexion angles such as stair-climbing were not considered, although they would produce higher stresses. The sequence of orientations of the femoral component on the tibial insert during the stance phase of walking was determined using a rigid body model. Although this model took the frictional forces and the soft tissue restraints

into account, it did not account for local changes in geometry due to the deformation of the polyethylene. Nevertheless, kinematic tests conducted by a knee simulating machine indicated that rigid body analyses predicted correct component orientations for a wide range of knee geometries.

The polyethylene was assumed to be linearly elastic. There is considerable uncertainty as to the most appropriate model for polyethylene in a condylar knee. Previous researchers have used a bilinear model with a reduced modulus above a critical yield stress [Bartel et al, 1986]. Other researchers have used a linear elastic model [Jin et al, 1995]. However, the situation is complicated by the increase in modulus in the surface or subsurface layers due to an oxidative process, a phenomenon which will depend on the sterilisation process, the subsequent treatment of the polyethylene, the shelf ageing, and the conditions within the patient [Blunn & Bell, 1996; Premnath et al, 1996]. The viscoelastic properties of the polyethylene will affect stresses [Anderson et al; 1995], although this may not be a major effect for the rapidly changing loading conditions of walking.

However, the stresses may not vary dramatically for changes in modulus at or below the surface. In analyses conducted for modulus variations of as high as 2:1, contact stress values changed by less than 20%, consistent with the data of Kurtz et al [1994]. When changes in material properties are imposed in finite element models, the density of the elements should be increased in the region where one material property transfers to the other, resulting in an increase in the number of elements in the tibial insert and longer solution times. As the aim was to compare stresses for different designs of bearing surfaces, rather than calculate accurate stresses based on realistic material properties, the increased value of the elastic modulus associated with oxidation of the tibial insert was not included in the analyses of the two designs with gait loads applied

Two features in the geometry of Design 2 appeared to produce low contact stresses. The relatively large, conforming radii in the frontal plane, producing a 'shallow' frontal appearance produced wide contact patches and the

larger distal femoral arc continued towards the posterior which contacted the polyethylene during flexion instead of the smaller posterior radius. Double contact patches were seen on the medial portion of the tibial insert in some instances during gait for this design. However, the rigid body analysis predicted the motion paths of the contact points, and hence the orientations of the prosthetic components in the finite element analyses, based on an assumption of one contact point for each femoral condyle. This would have resulted in inaccuracies in the orientations of the components in the finite element analyses. The geometry of Design 1 was moderately conforming in both planes, so in general the contact patches were small and rounded and the phenomenon of double contact occurring for one femoral condyle was not observed.

As the position of the maximum contact stress determined at each instance of the gait cycle varied, it was not apparent if a particular region of the polyethylene was likely to suffer damage. In any case, surface and subsurface cracking are caused by stresses around and under the contact area. For this reason, maximum principal and maximum shear stress histories were recorded and the fluctuating stresses of particular elements in each design could be plotted and compared. However, even though this study addressed the issue of the variability of stresses during gait for a particular design, the question still remained as to how this variability might render the tibial inserts of some knee replacements more prone to delamination wear compared to others.

Delamination wear is caused by a fatigue mechanism as it is a result of cyclic loading, not been observed during static loading. However, it is very difficult to reproduce delamination wear in the laboratory under accelerated wear conditions, though recent tests using oxidised polyethylene have been successful (Blunn & Bell, 1996). It is a well known fact that under cyclic loading a material can fail due to fatigue at much lower loads compared to when it is statically loaded, and relationships between the magnitude of the load and the number of cycles applied have been determined for various materials subjected to uniaxial cyclic loading. In this study, cyclic loading was also applied but the cycles were not uniform and the stress conditions within the polyethylene were

complex so it was difficult to determine if a particular region of the tibial insert was likely to delaminate.

In an attempt to accumulate the results for the two designs, the stresses were averaged over the gait cycle, to find the elements in each design subjected to the highest average stress. However, averaging was not a satisfactory way of recognising the elements most prone to fatigue because it disguised the fluctuations in the stresses rather than highlighting them. For example, for the maximum principal stress, values could fluctuate between negative and positive as the femoral condyles passed over the tibial insert. This is because at the edges of the contact patches the maximum principal stress is tensile, but in the region of contact it is compressive. An element which was permanently held in tension would score a higher average value compared to an element being alternately stretched and compressed.

There is some evidence from retrieval studies that there are certain characteristics in knee designs which either promote or resist wear, despite numerous other variables such as polyethylene quality and surgical technique. For example, the Kinematic-type design, which had low sagittal conformity and only moderate frontal conformity, suffered delamination after about ten years [Blunn et al, 1996]. The Miller-Galante, with low sagittal conformity but large almost fully conforming frontal radii, has shown some posterior wear [Lewis et al, 1994], but delamination has not been reported. The Total Condylar and Insall-Burstein designs have been reported to show extensive pitting but not delamination [Collier et al, 1991], except where there had apparently been excessive constraint, possibly due to misalignment [Blunn et al, 1996]. Annotated reports in recent years have upheld these observations.

The type of approach used in this study could be refined, based on more realistic polyethylene properties and the forces acting at the knee. A methodical analysis of possible geometries could be used to optimise the parameters describing the bearing surfaces to produce the required stresses. Even though more research is required to determine the roles of the magnitudes of the

stresses versus the fluctuations of the stresses when delamination of the polyethylene occurs, this study does suggest that commercially available designs could have very different durabilities.

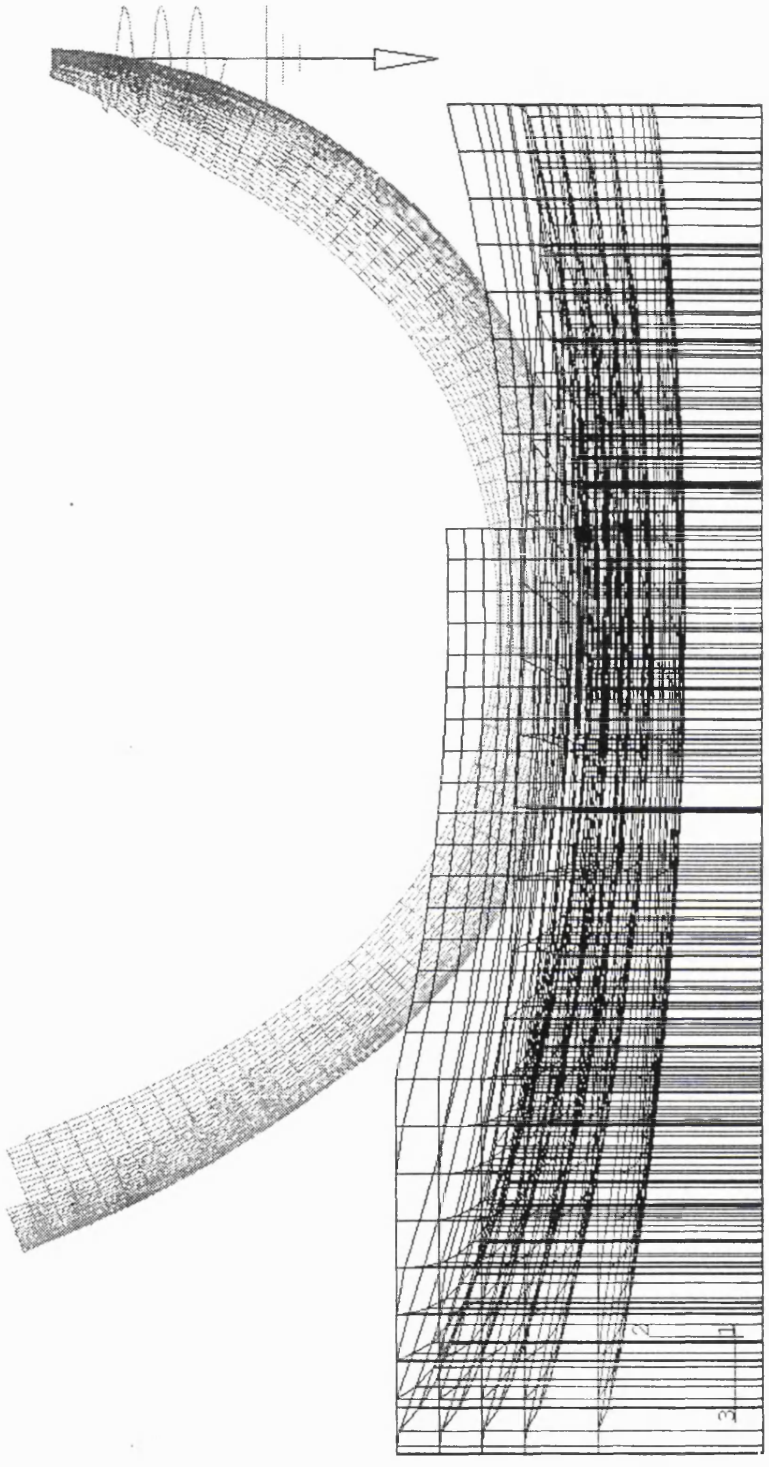

FIG.1 Finite element meshes of the femoral and tibial components of a knee replacement.

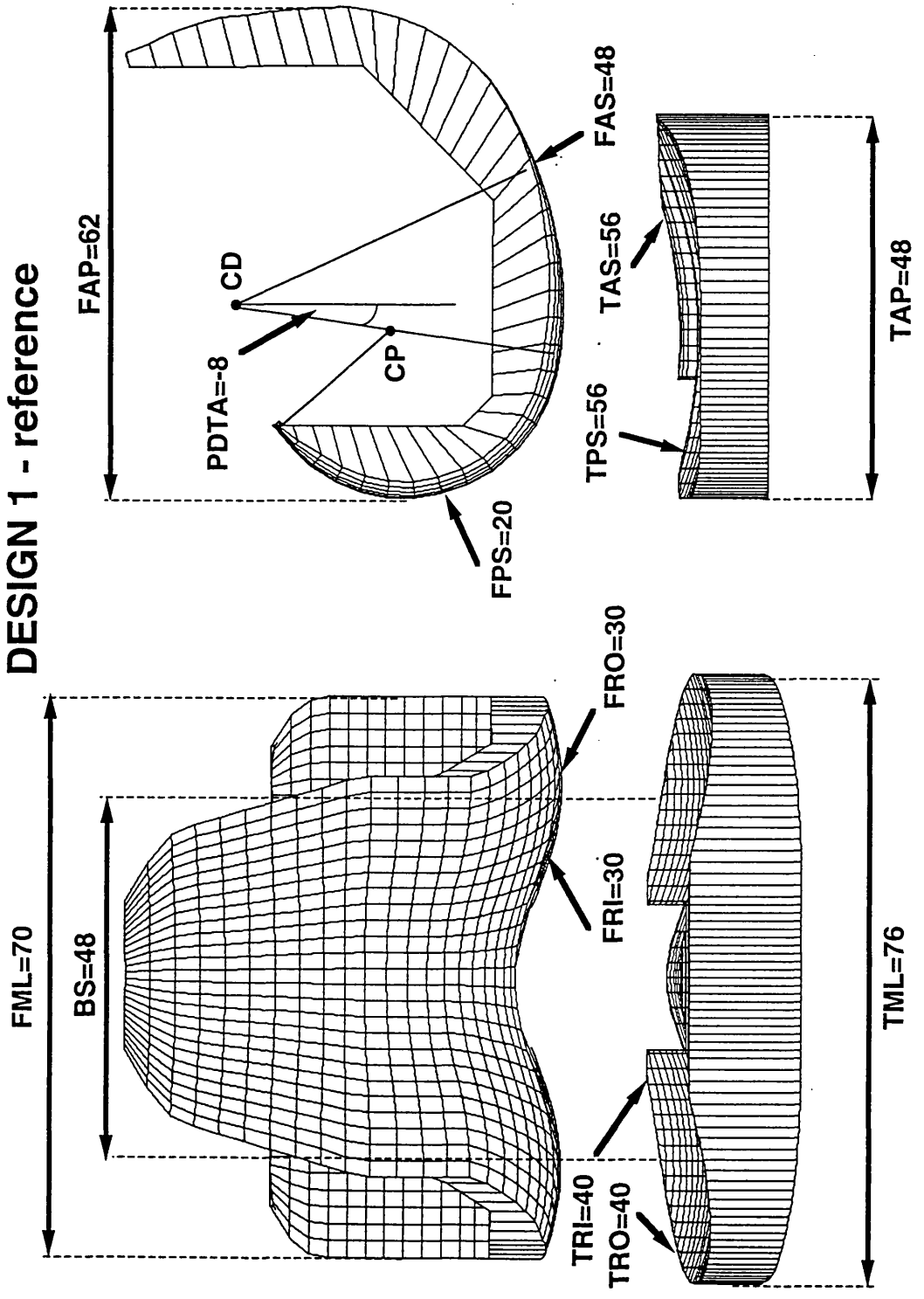

FIG.2 Defining the geometry of DESIGN 1.

Positive torque refers to internal torque applied to the femur relative to the tibia.
Positive shear force refers to force pushing the femur forward relative to the tibia.

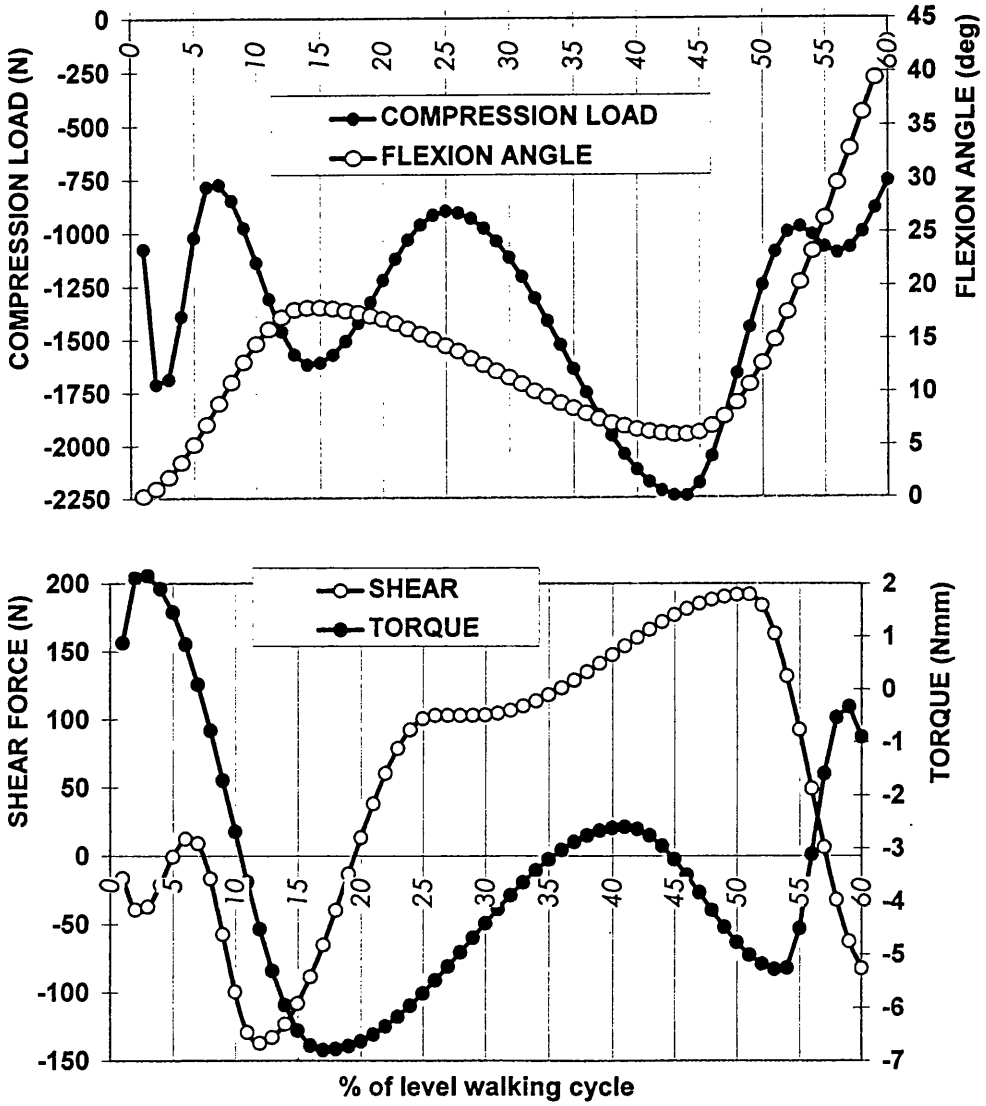

FIG.3 The input cycles of flexion, anterior-posterior force, internal-external torque and compression load obtained from T.P. Andriacchi.

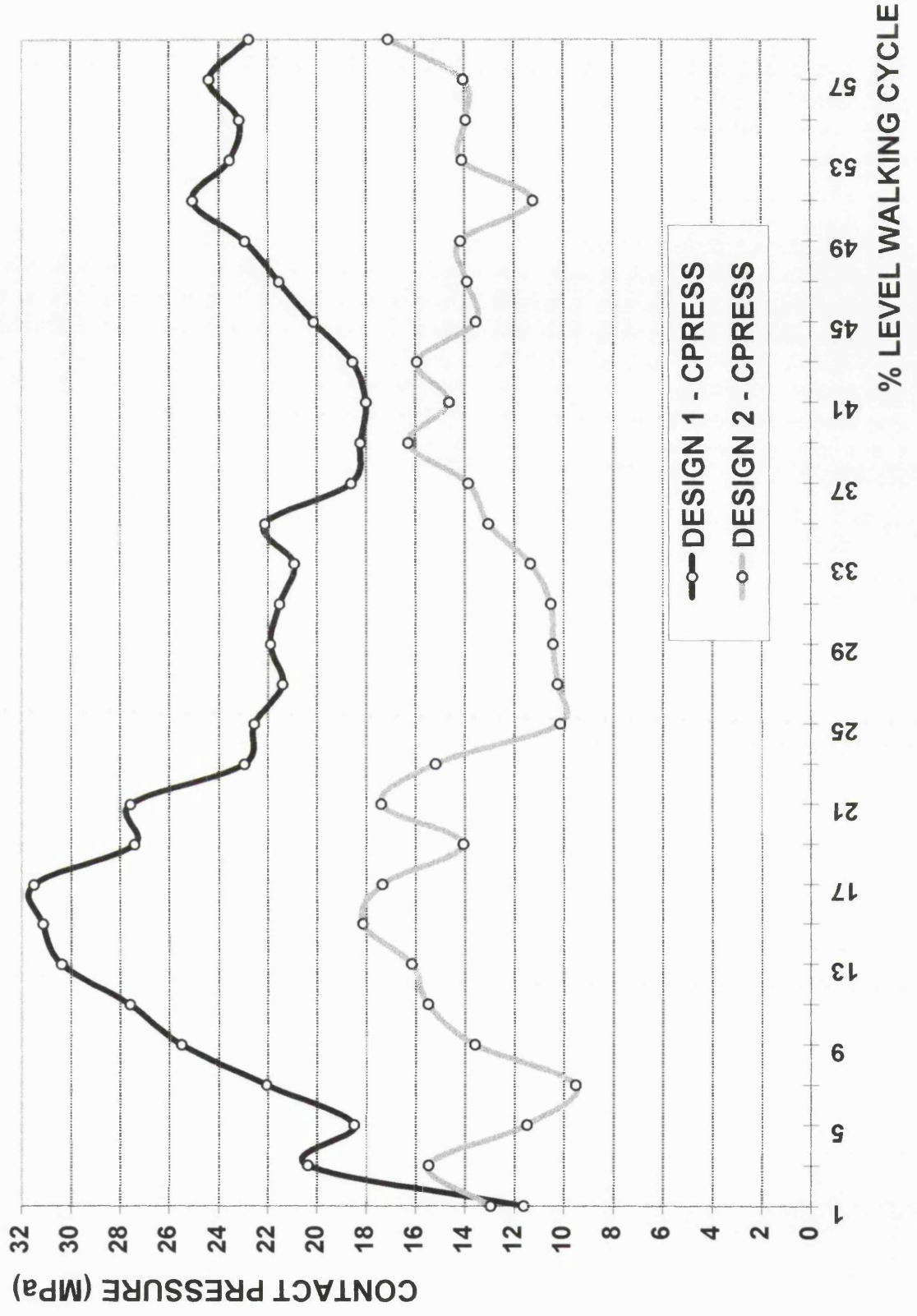

FIG. 4 Values of the maximum contact pressure on the tibial insert during the gait cycle for DESIGNS 1 and 2.

CONTACT PRESSURES AT 1% OF THE GAIT CYCLES

DESIGN 1 ABAQUS

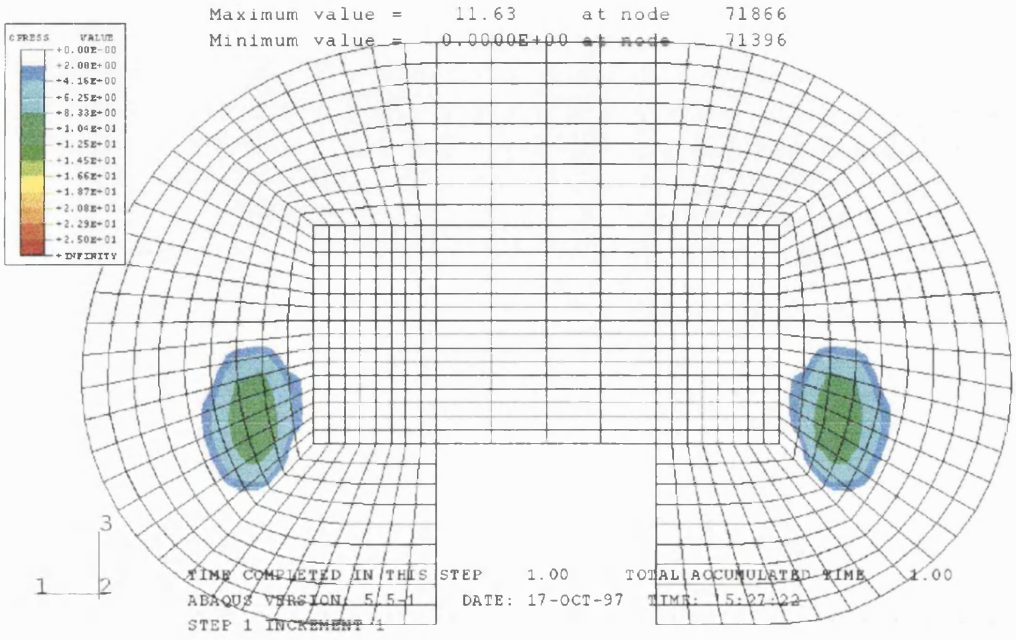

DESIGN 2 ABAQUS

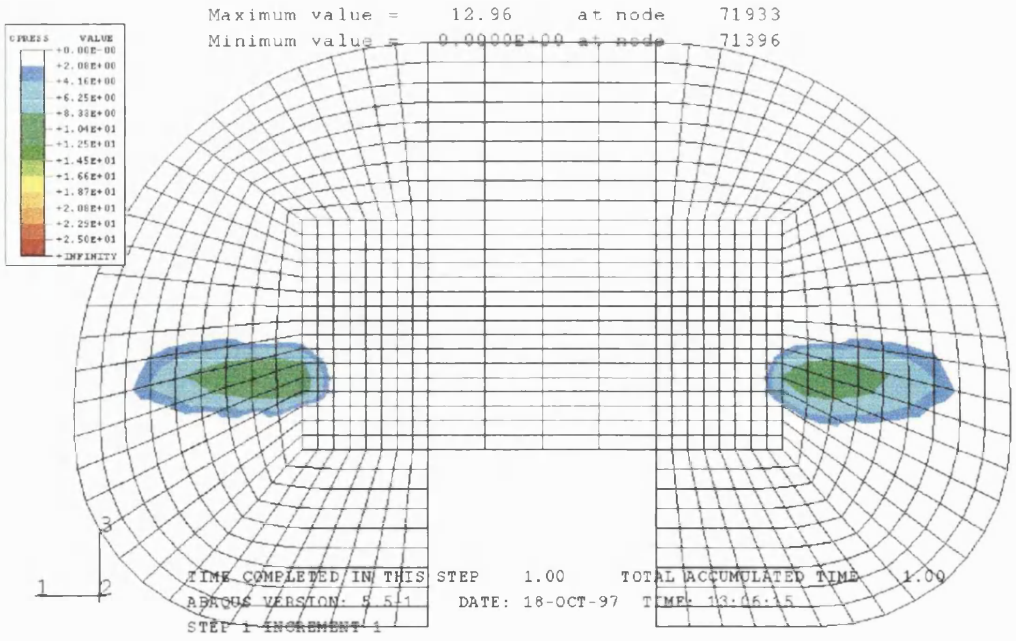

FIGS. 5 The varying shapes and locations of the contact areas for DESIGN 1 and DESIGN 2 druing gait.

CONTACT PRESSURES AT 5% OF THE GAIT CYCLES

DESIGN 1 ABAQUS

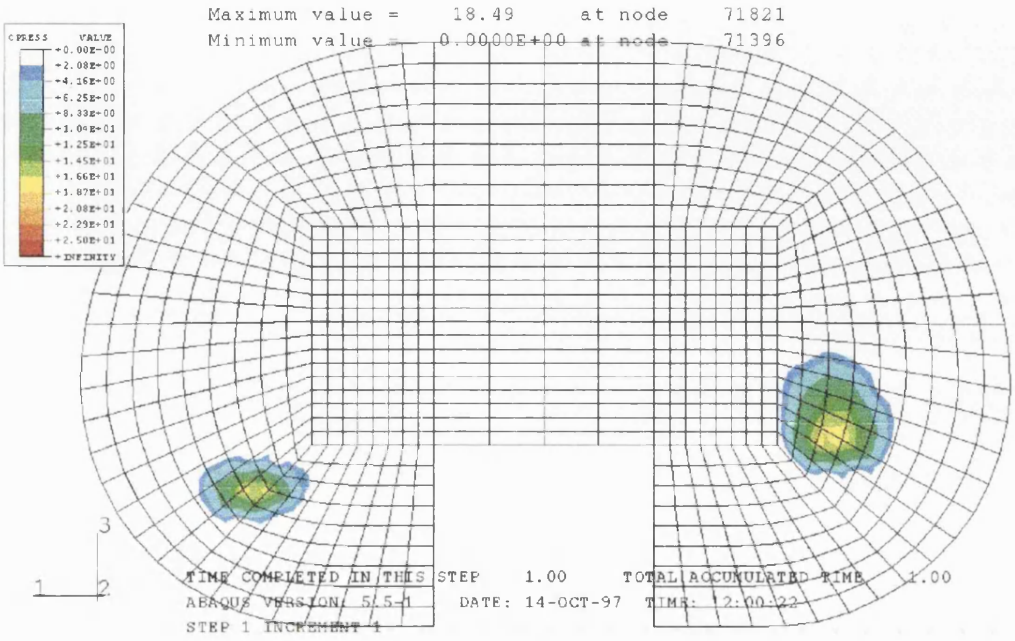

DESIGN 2 ABAQUS

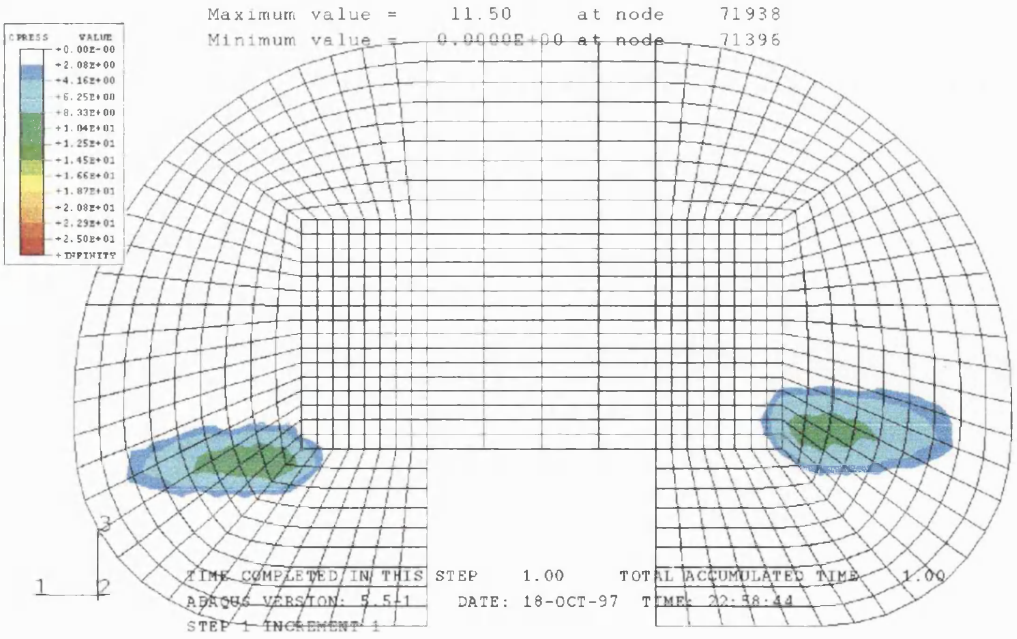

CONTACT PRESSURES AT 15% OF THE GAIT CYCLES

DESIGN 1 ABAQUS

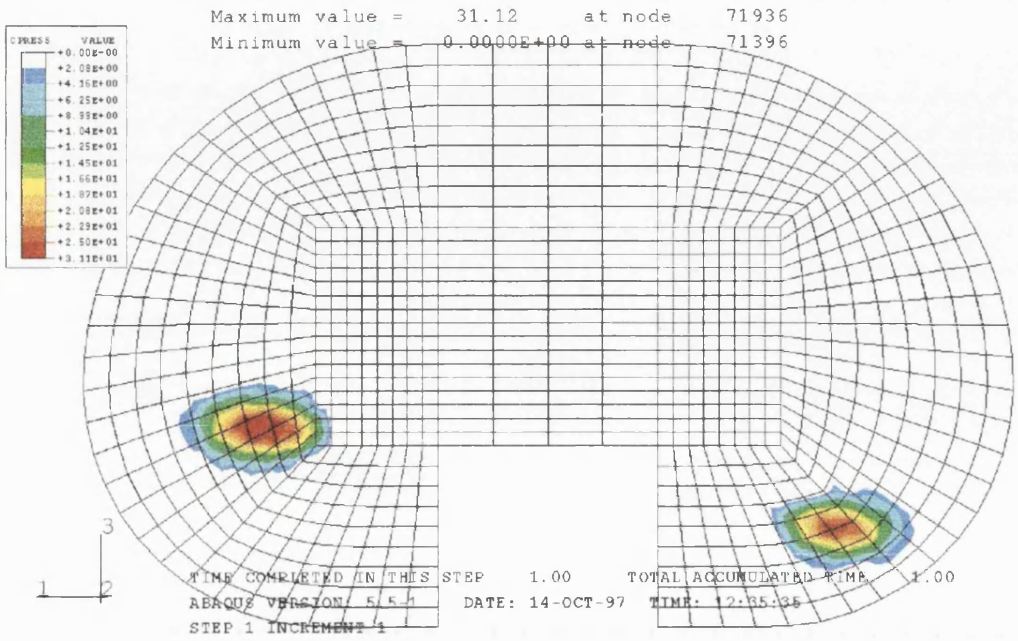

DESIGN 2 ABAQUS

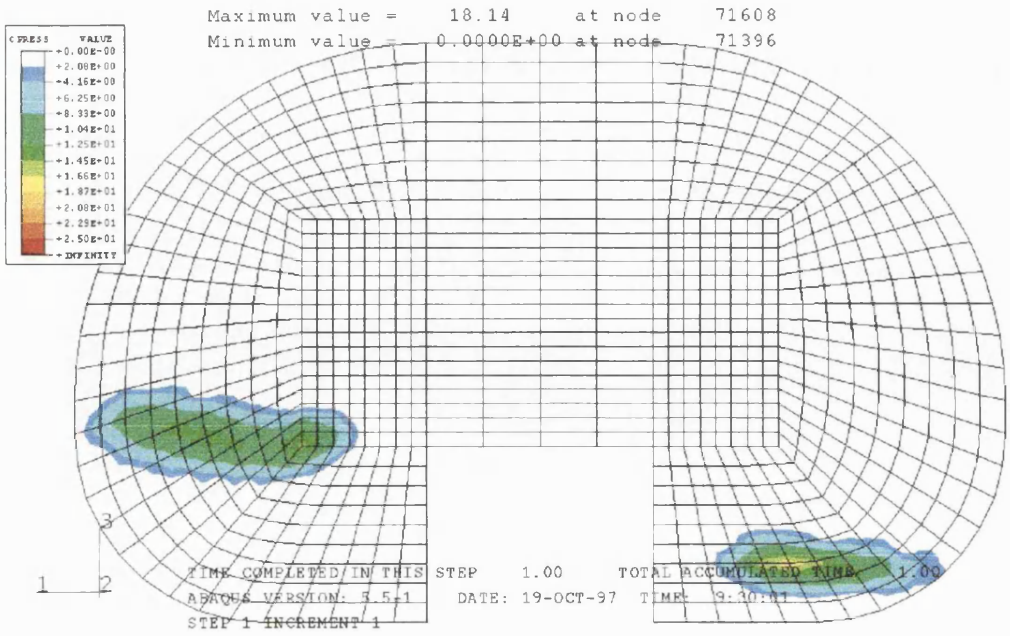

CONTACT PRESSURES AT 25% OF THE GAIT CYCLES

DESIGN 1 ABAQUS

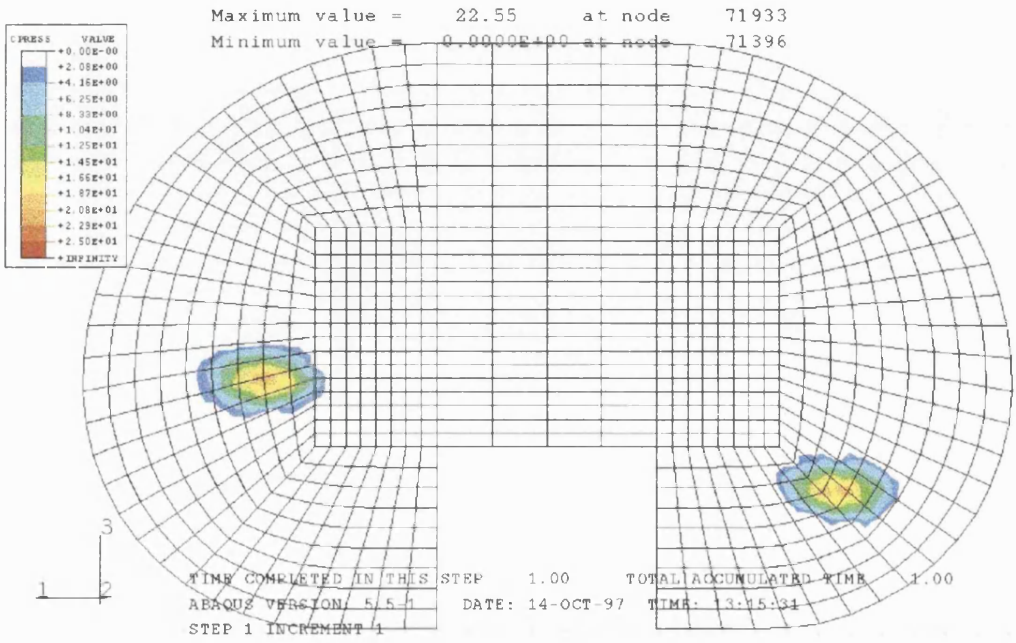

DESIGN 2 ABAQUS

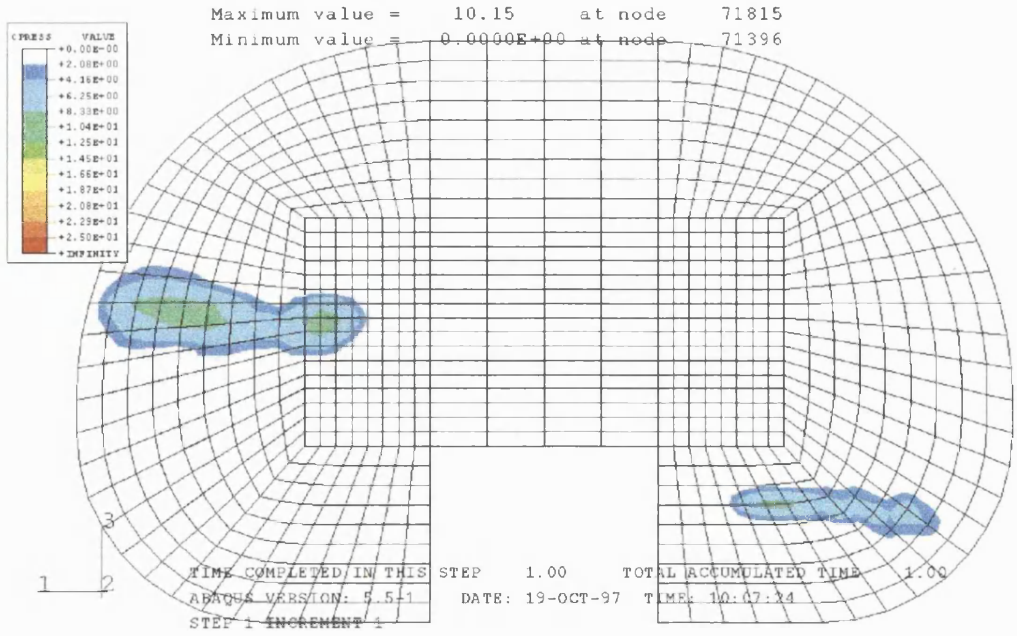

CONTACT PRESSURES AT 35% OF THE GAIT CYCLES

DESIGN 1 ABAQUS

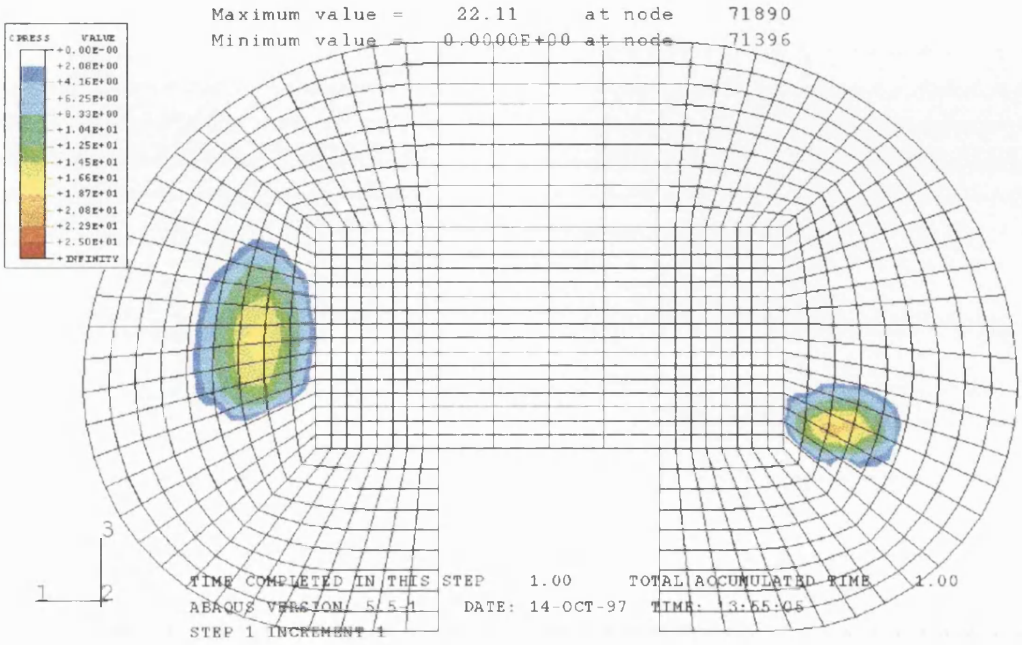

DESIGN 2 ABAQUS

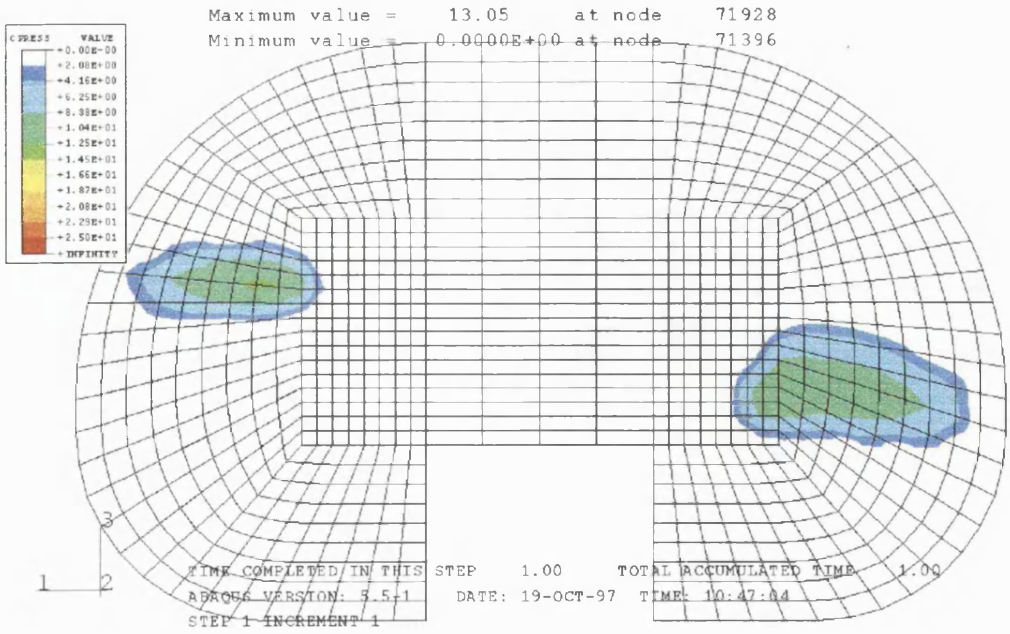

CONTACT PRESSURES AT 45% OF THE GAIT CYCLES

DESIGN 1 ABAQUS

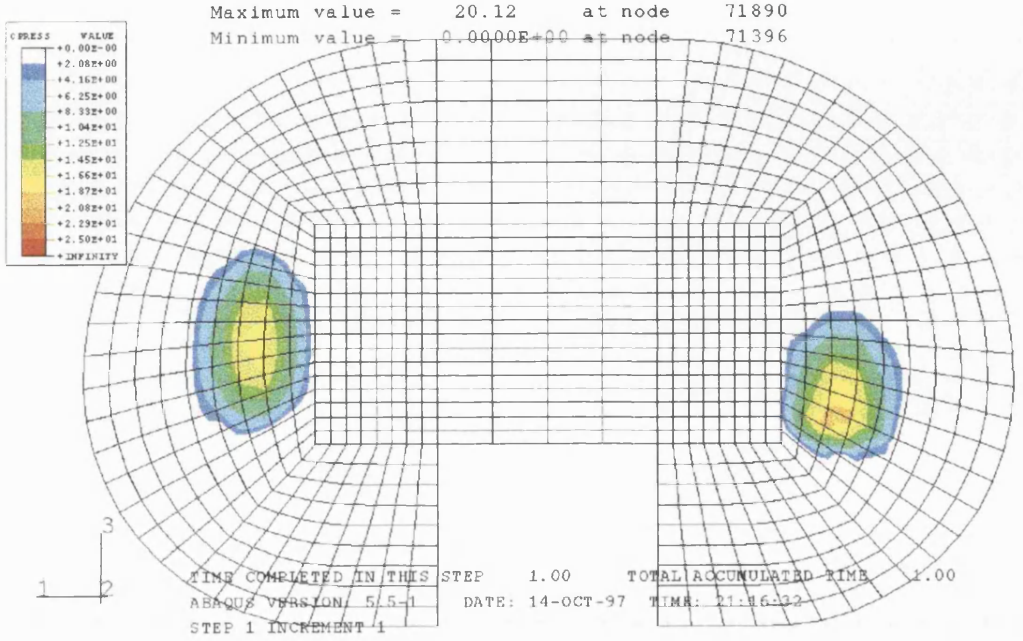

DESIGN 2 ABAQUS

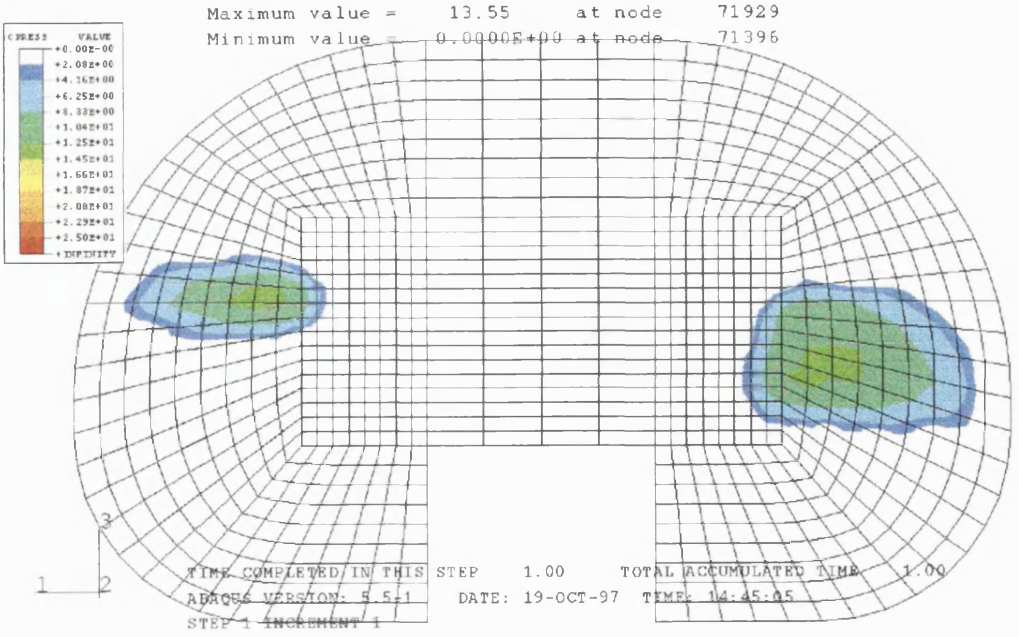

CONTACT PRESSURES AT 55% OF THE GAIT CYCLES

DESIGN 1 ABAQUS

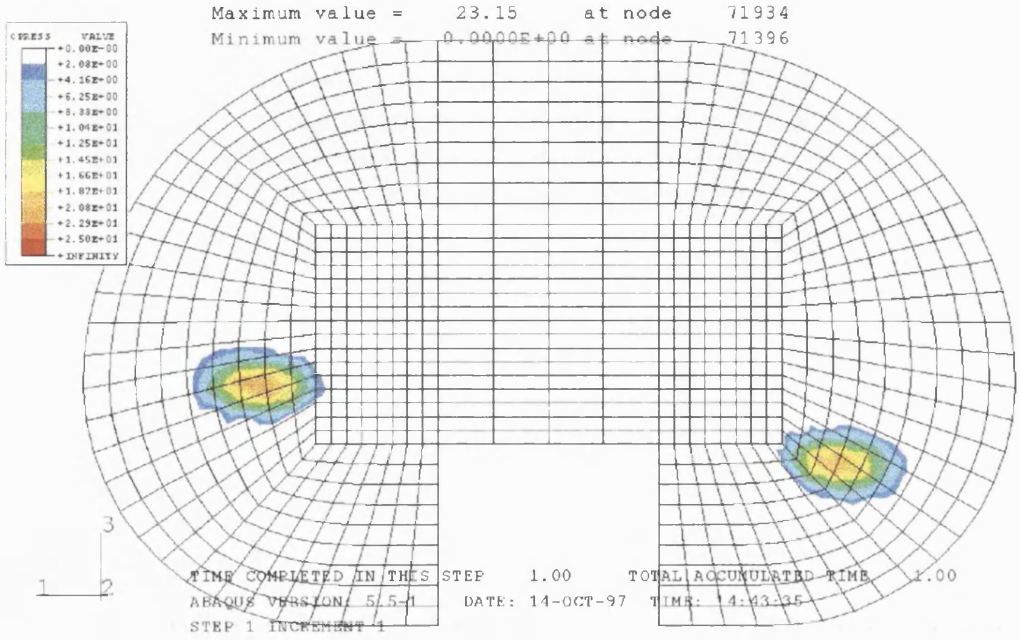

DESIGN 2 ABAQUS

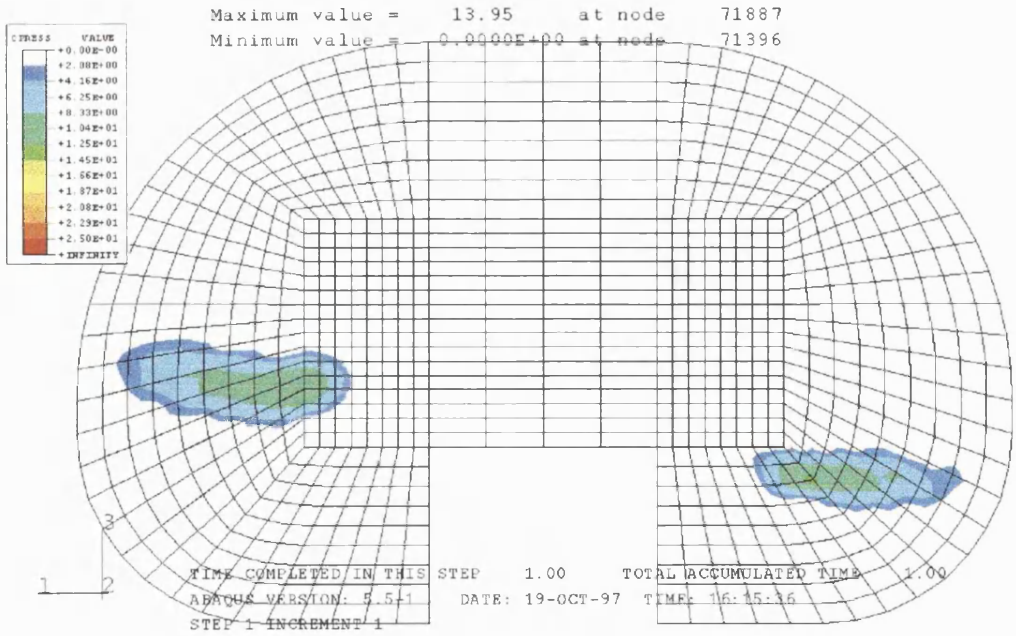

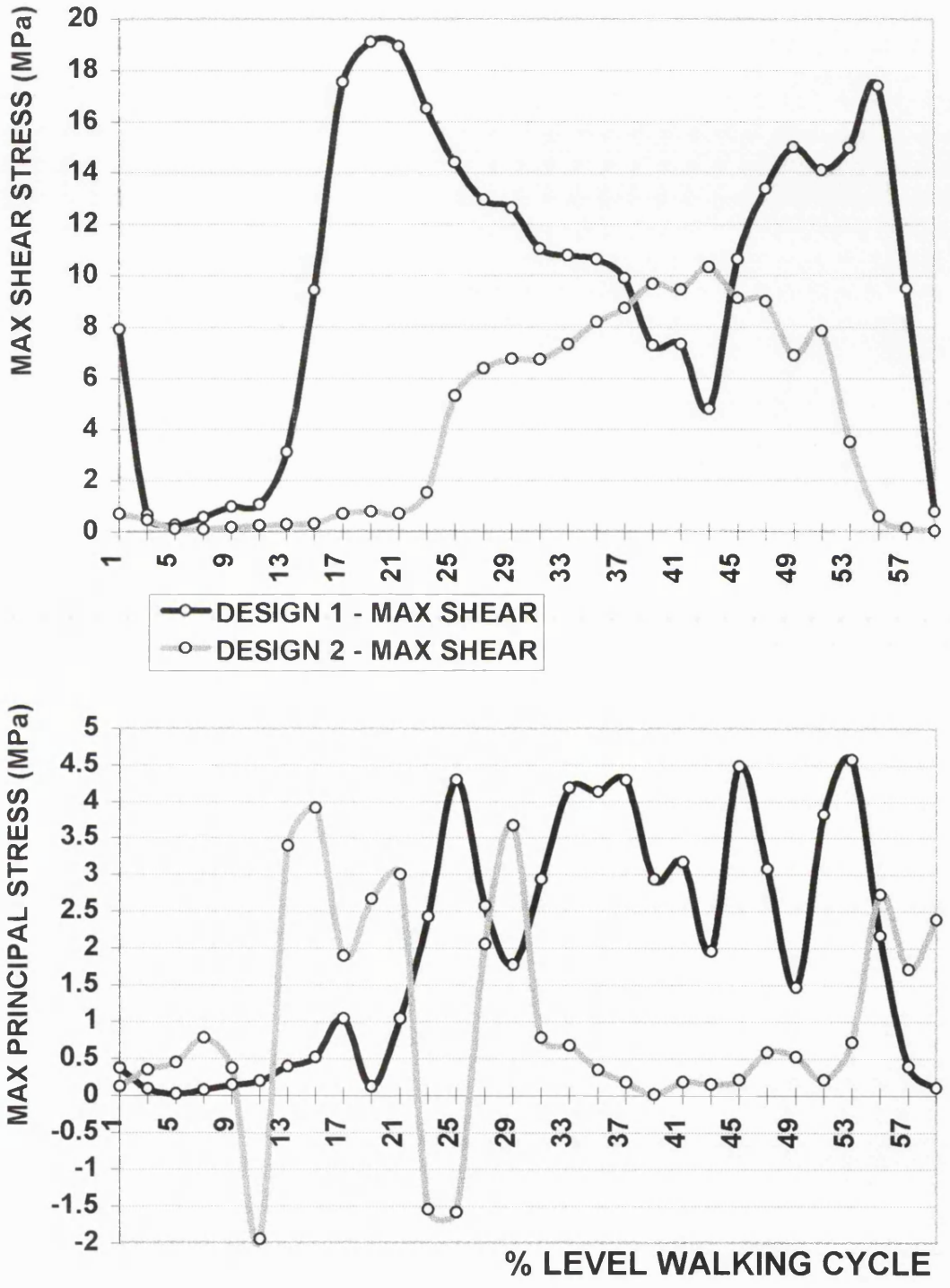

FIG. 6 The fluctuating maximum shear and maximum principal stresses for the elements of DESIGNS 1 and 2 which scored the highest average stresses.

Chapter 7

DAMAGE FUNCTIONS TO PREDICT DELAMINATION WEAR

7. DAMAGE FUNCTIONS TO PREDICT DELAMINATION WEAR

7.1 INTRODUCTION

The variety of total condylar knee replacements currently on the market suggests that there is still not a consensus amongst knee designers on the effects of geometry on wear and kinematics. As it is not necessary to reproduce the bearing surfaces of knee components anatomically, designs vary considerably (Fig. 1). Some have small frontal radii producing dished condyles whilst others have flat condyles due to their large frontal radii. Clearances vary so that there may be point, line or patch contacts. Some knees have the femoral sagittal distal arc swept so far back that the smaller posterior arc hardly contacts the polyethylene during walking, while for others the posterior arc contacts as soon as flexion begins.

It appears that there are two conflicting criteria for knee designs. They should resist abrasive and delamination wear as well as accommodate natural kinematics. The femoral-tibial surface geometry dictates both the magnitude of the stresses generated in the polyethylene tibial insert of total knee replacements and the sliding patterns on its surface during activity cycles. Therefore the conforming designs which produce low stresses in the polyethylene, may not allow the femoral and tibial components to move relative to each other in the same manner as the natural knee resulting in gait adaptation [Andriacchi et al, 1982]. In the natural knee, stability is provided by the ligaments and the joint capsule. On the other hand, in a resurfaced knee the laxity and stability is balanced by the dishing of the tibial insert and the ligaments that remain, the tibial insert dominating if it is very dished [Walker et al, 1996].

The aim of this study was to optimise a combination of four design parameters which vary to a large extent in the range of contemporary knee designs. This was achieved by using the techniques developed in the previous chapters. Ranges of the parameters were chosen, complete models of the bearing surfaces of 16 knees were generated, rigid body analyses were carried

out to determine the contact points and anterior-posterior and rotational laxities during the stance phase of level walking and finite element analysis was used to determine the variation of stresses as gait progressed.

In the previous chapter, it was noted that it was difficult to quantify the variation of stresses when comparing the commercially available designs because the tibial inserts of different knees were subjected to high stresses at various stages in the gait cycle in different regions of the polyethylene. In this chapter, damage functions were used to calculate the accumulated effects of the fluctuating maximum shear and maximum principal stresses so that the susceptibility of the polyethylene to subsurface and surface cracking could be determined. The optimal design would satisfy with least compromise both the requirements of natural kinematics and low stresses in the polyethylene.

7.2 METHODS & MATERIALS

The aim was to create a set of knee designs where there was variation in the size of the femoral frontal radii, the clearance between the femoral frontal radii and the tibial frontal radii, the size of the tibial sagittal radius and the size of the posterior-distal transition angle. This was the angle in extension at which the small posterior arc in the sagittal plane of the femoral component transferred to the larger distal arc. This was done by defining 16 knee designs assembled from four femoral components and four tibial components. Having defined a reference design, each new design varied from an existing one by just one parameter so that the effects of each parameter could be determined.

Four femoral components were defined (f1, f2, f3, f4) by parameters described in [Sathasivam & Walker, 1994]. The reference femoral component (f1) had a femoral frontal radius of 30mm and a posterior-distal transition angle of -8deg. Femoral components f2, f3, f4 were variations of f1 with the frontal radius varying to 70mm and the posterior-distal transition angle varying to -20deg. Each femoral component was mated with four different tibial components (t1, t2, t3, t4). Tibial component t1 was the reference tibial component, it had a sagittal radius of 80mm and its frontal radii were 10mm larger compared to its

mating femoral component. Tibial component t2 was the same as t1 except that the sagittal radius was closed to 56mm, t3 was the same as t1 except that the frontal clearance from the femoral component was closed to 2mm, t4 was closed in both the frontal and sagittal planes compared to t1. By varying the femoral and tibial component designs in this manner, 16 total knee replacements were defined. The reference knee was f1t1. The laxities and susceptibilities to delamination wear of the 16 designs were determined and compared using computer methods.

The values of the parameters for the different designs are listed in the following table where:

SAG RAD refers to the tibial sagittal radius.

FRO DIFF refers to the difference between the femoral and tibial frontal radii.

FEMFRO refers to the femoral frontal radius.

PDTA refers to the posterior-distal transition angle.

	SAG RAD=80, FRO DIFF=10	SAG RAD=56, FRO DIFF=10	SAG RAD=80, FRO DIFF=2	SAG RAD=56, FRO DIFF=2
FEMFRO=30, PDTA=-8	**f1t1**	**f1t2**	**f1t3**	**f1t4**
FEMFRO=30, PDTA=-20	**f2t1**	**f2t2**	**f2t3**	**f2t4**
FEMFRO=70, PDTA=-8	**f3t1**	**f3t2**	**f3t3**	**f3t4**
FEMFRO=70, PDTA=-20	**f4t1**	**f4t2**	**f4t3**	**f4t4**

Meshes were generated [Sathasivam & Walker, 1994] to describe the surface geometries of the 16 knees. Rigid body analyses [Sathasivam & Walker, 1997] were used to determine the total anterior-posterior and rotational laxities

and the contact points for the 16 knees during the stance phase of gait. The analysis included the effects of friction and the soft tissue restraints of a knee with the posterior cruciate ligament resected [Fukubayashi et al, 1982]. Cycles of the axial force, anterior-posterior shear force, torque, and flexion angle for the stance phase of level walking [Andriacchi et al, 1995] were divided into discrete time increments and input to the rigid body analysis. At each increment the orientations of tibial and femoral surface meshes which satisfied the equilibrium equations were determined. These positions were required in order to investigate the fluctuating nature of the stresses for the 16 designs.

Finite element models of the different designs were generated. The femoral component was surfaced with rigid elements and the tibial insert was filled with linear elastic elements with elastic modulus 600MPa. The tibial inserts of all of the designs had a thickness of 6mm from the base of the dish to the base of the insert, to represent the thinnest thickness currently used. For each successive femoral-tibial position determined by the rigid body analysis, finite element analysis was used to compress the prosthetic models together to determine the stresses in each element of the polyethylene insert. The elements approximated cubes of 2mm side, reducing to 0.7mm depth approaching the articulating surface. Hence a stress history of each element for the stance phase of level-walking was determined.

In the previous chapter, the fluctuating stresses for each element were averaged to accumulate the results over the gait cycle, in order to predict wear. It was stated that this was not the ideal method to use because the fluctuations in the stress were ignored. In uniaxial cyclic tests, it is general practice to plot S-N curves which show the number of cycles it takes to cause fatigue in a material at different levels of stress. In this study such a damage function which linked stress and number of cycles to the occurrence of fatigue was required, but the facts that the cycles of stress produced in each element were not uniform and the stress state in the polyethylene was complex caused complications. Therefore, damage functions were formulated for this special case.

The objective was to accumulate the results in each element over the stance phase because the movement of the knee causes different regions of the polyethylene in the tibial insert to be stressed at different times. The fluctuating stresses can promote crack initiation and propagation by a fatigue mechanism and researchers who have investigated fatigue crack growth describe an initial 'shear' mode of propagation followed by a 'tensile' mode [Liu, 1985]. Strain energy density has been used in the field of materials science to formulate multiaxial life prediction models [Ellyin, 1989]. This method involves computing the area within a hysteresis loop of stress against plastic strain in the material. However, plastic strain was not predicted by the model in this thesis as the polyethylene was assumed to be linear elastic, therefore stress-based formulae were considered to be more appropriate for the damage functions. The damage functions were based on the hypothesis that the number of cycles required to produce fatigue failure is a function of the magnitudes of the stress fluctuations and the levels of stress at which they occur. This hypothesis requires experimental validation which is currently in progress but beyond the scope of this thesis.

The first damage mode was subsurface cracking which is considered to be associated with cyclic shear stresses. To account for both the fluctuating stresses and the number of cycles in all of the polyethylene elements in the tibial insert, the damage function expressing the susceptibility to subsurface cracking was defined as:

Damage function S:

$$\sum_{i=1}^{i=N-1} \text{abs}(S_{i+1}-S_i) \times 0.5 \times (\text{abs}(S_{i+1}) + \text{abs}(S_i))$$

where S_1 to S_N are the values at successive turning points in the graph of maximum shear stress seen by each element against n discrete steps in one level walking cycle.

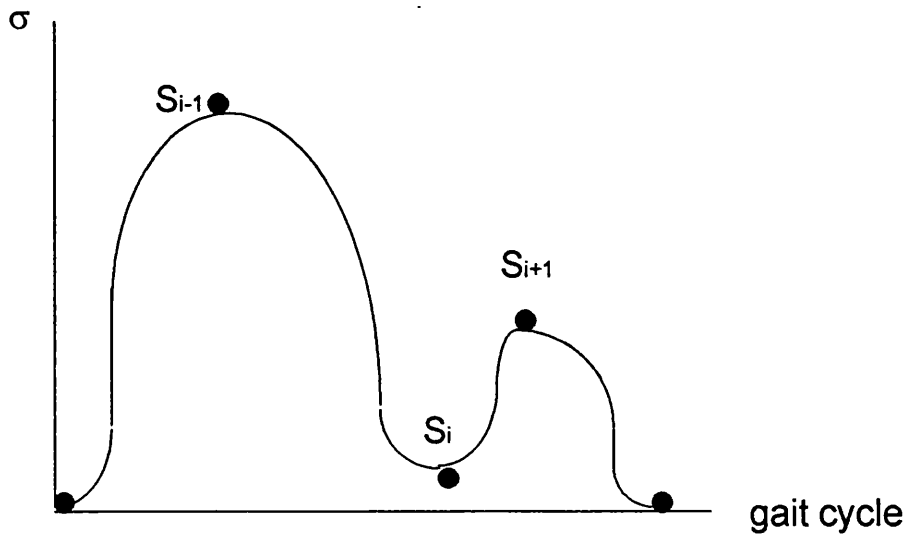

The second damage function was surface cracking which is considered to be related to tensile stresses and was applied to the surface elements only:

Damage function T:

$$\sum_{i=1}^{i=N-1} \text{abs}(T_{i+1}-T_i) \times 0.5 \times (\text{abs}(T_{i+1}) + \text{abs}(T_i))$$

where T_1 to T_N are the values at successive turning points in the graph of maximum principal stress seen by each element against n discrete steps in one level walking cycle. The first and last points of the stress histories of each element were considered as turning points.

Each damage function was applied to the stress history of each polyethylene element, and the highest value calculated for a particular design was called the damage score. This value could be used to compare the susceptibilities of different designs to wear. In addition finite element models of the tibial inserts were sectioned horizontally to show the different layers of elements. Each element was assigned a colour depending on its damage function value where an arbitrary value was chosen for the upper limit when scaling the 13 colours from zero. All the models were plotted according to the same colour scale so that they could be compared. These plots illustrated the

varying values of the damage function in the polyethylene and were called damage maps.

7.3 RESULTS

Fig.2 shows the total anterior-posterior and rotational laxities of the 16 designs for the stance phase of gait obtained from the rigid body analyses. The parameters which affected anterior-posterior laxity were the tibial sagittal radius and the posterior-distal transition angle. For knees with a posterior-distal transition angle of -8deg, designing a tibial sagittal radius of 80mm instead of 56mm increased the laxity by up to 2mm. For the knees with the larger transition angle, more relative displacement occurred due to the movement of the contact point during flexion. However, the bumpers representing the posterior cruciate ligament restricted this motion, so for these knees the size of the sagittal radius did not appear to affect the total anterior-posterior laxity. The rotational laxity was influenced by both femoral and tibial design. Increasing the tibial sagittal radius increased the rotational laxity of some knees by more than 4deg. Increasing the magnitude of the femoral posterior-distal transition angle reduced rotational laxity.

Fig. 3b shows the maximum shear damage scores of the 16 knees, larger values indicating the designs which would be more likely to suffer from subsurface cracking. The damage function values peaked at 0.7-1.4mm below the surface which can be seen in the damage maps (Flg.4) for the reference knee f1t1 compared with f1t4 and f4t4. Knee f1t4 had the reference femoral component but a tibial component which was more conforming sagitally and frontally compared to the reference tibial component. Its damage function values and damage score were lower compared to f1t1. Knee f4t4 also had a tibial component which was conforming in both planes but its damage function values were significantly lower than the other two knees because it had a different femoral geometry. Damage maps are plotted for right knees.

The reference knee f1t1 had small frontal radii, large clearances between the femoral and tibial frontal radii, large tibial sagittal radius and small distal-

posterior transition angle. The femoral geometry f1 was maintained for three other knee designs (f1t2, f1t3, f1t4) where the only variations were in the tibial geometry. Closing the tibial sagittal radius only for f1t2 increased the subsurface damage score by 7%, but reducing the frontal clearance between the femoral component and tibial insert only for f1t3 reduced the damage score by 45%. When both these modifications were applied to the reference knee to create f1t4, the damage score was similar to f1t3. This showed that for the tibial sagittal radii analysed, this parameter did not affect the damage scores significantly for the femoral component design f1.

Knees f2t1, f2t2, f2t3, f2t4 were similar to the f1 series, the only difference being the magnitude of the femoral posterior distal transition angle was increased to 20deg. Damage function values for f2 were lower compared to f1 when the difference between the femoral and tibial frontal radii was 10mm, the damage score for f2t1 was 11% lower than f1t1. Knees f3t1, f3t2, f3t3, f3t4 were similar to the f1 series, the only difference being the femoral frontal radius was increased to 70mm. Damage function values for f3 were lower compared to f1 and f2, the damage score for f3t1 was 35% lower than f1t1. Knees f4t1, f4t2, f4t3, f4t4 were similar to the f3 series, the only difference being the magnitude of the femoral posterior distal transition angle was increased to 20deg. Damage function values for f4 were similar to f3, with knee f4t4 obtaining the lowest damage score of the 16 knees analysed..

The results in Fig. 3b show that increasing the femoral frontal radius and reducing the frontal clearance between the femoral component and tibial insert had the effect of lowering the damage score. However, changing the femoral geometry alone had a dramatic effect. It appeared that femoral component f4 combined with tibial insert t1, which had a large sagittal radius and large frontal clearance, had a comparable damage score to the combination of f1 with t4, which had a small sagittal radius and small frontal clearance. Even though the former knee had larger clearances frontally and sagittally, its damage score was low due to its femoral design.

Fig. 3a shows the maximum principal stress damage scores of the 16 knees, larger values indicating the designs which would be more likely to suffer from surface cracking. These damage scores were only calculated for the top layer of elements. Both surface and subsurface damage functions predicted that reducing the sagittal tibial radius would not always reduce the damage scores.

The subsurface damage maps and anterior-posterior displacements and rotations during gait for all 16 designs can be seen in the Appendix.

7.4 DISCUSSION

Retrieval studies [Blunn et al, 1996; Collier et al, 1991; Landy & Walker, 1988; Rose et al, 1979; Wright & Bartel,1986] have shown that very conforming polyethylene tibial inserts of condylar total knee replacements suffer less from delamination wear compared to moderately-conforming designs. The only exception was the unconforming Marmor design which (due to being manufactured from high quality polyethylene) deformed becoming more conforming to the femoral component and did not delaminate [Blunn et al, 1992]. Therefore, it appears that to prevent delamination wear the bearing surfaces should be made as conforming as possible to reduce stresses to a minimum. However, the femoral and tibial bearing surfaces of condylar knees cannot be completely conforming because in order to function naturally they must allow adequate relative motion between the prosthetic components. This has led to the advent of mobile bearing designs where the tibial plastic is free to slide over the surface of the tibial tray making it possible to combine complete conformity of the bearing surfaces with natural laxity. However, abrasion of large contact areas between two pairs of interfaces may produce a large quantity of small polythene particles leading to different types of failure which are yet to be realised [Campbell et al, 1995].

A method of quantifying the susceptibility of tibial inserts to delamination wear was formulated using computer simulations of the motions of different knee designs during level walking. In order to optimise condylar knee designs it is necessary to reduce the fatiguing effects of the stresses which cause subsurface

and surface cracking in the polyethylene whilst maintaining a certain amount of clearance in the sagittal plane to allow the femoral component to roll-back in flexion and apply the correct tension to the posterior cruciate ligament as in the natural situation [Lafortune et al, 1992; Luger et al, 1997]. Clearance for rotational laxity was not such an issue in the frontal plane for the frontal clearances analysed in this study. For the rotation angles involved, the contact points tend to move anterior-posterior rather than medial-lateral as long as the frontal radius of the femoral component is smaller than the sagittal radius of the tibial component [Sathasivam & Walker, 1994].

Damage functions which accounted for the magnitude of stresses and the fatigue cycles during activity were applied to quantify the susceptibility of polyethylene tibial components to delamination wear. The damage functions did not take into account the direction of the maximum principal and maximum shear stresses or yielding and the build-up of residual stresses [Estupinan et al, 1996; Suh, 1986]. In cases where yielding would be significant, there would be some modification to the results presented here. For the maximum principal stress damage function (T), tension and compression were given the same emphasis but it could be argued that a damage function dominated by compression and influenced less by tension would not predict surface cracking.

The subsurface damage function was analogous to strain energy density. In the field of materials science, cracks have been observed to propagate when strain energy density is high. The maximum shear stress was chosen because it peaks in the subsurface region where cracks in retrievals initiate. Accounting for the sliding conditions at the surface and cyclic nature of the stresses affected the cumulative damage scores, having the effect of varying the magnitude of the stresses produced and distributing the stresses between different elements in the plastic.

The question remains as to whether a design where the femoral component articulates in a less conforming tibial insert or one where the femoral component articulates in a highly conforming tibial insert would be

morely likely to receive a high damage score. The answer is probably the former because of its high stresses. Even though the less conforming design has more relative displacement between the prosthetic components compared to the highly conforming design, it does not necessarily follow that there is less movement of the contact points. For a highly conforming design, relatively small displacements between the components can result in much greater movements of the contact points. Therefore, it is possible for the number of fluctuations in the stresses to be similar for both designs. Considering the conformity in the sagittal plane alone, the results showed that reducing the tibial sagittal radius reduced the damage scores slightly in some cases but increased them in others. Altering the tibial sagittal geometry did not have a dramatic effect on the damage scores because the frontal geometry rather than the sagittal geometry dictates the magnitude of the stresses, and the bumpers representing the posterior cruciate ligament played a significant role in determining the laxities of the knees.

The damage score was defined as the maximum value of a damage function for a particular design. It was a useful quantity because it summed up the likelihood of delamination to occur with just one number, so different designs could be compared easily (Fig.3). However, in reality delamination may be more likely to occur if a group of elements have relatively high damage function values rather than just one element having a particularly high value. For this reason, the damage maps were probably better predictors of delamination wear because the susceptibility to damage every element could be seen. In fact, if the upper limit of the color scale was chosen appropriately, based on the results of experimental tests, the damage maps might predict the volume of wear after a certain number of cycles for a particular design.

This study analysed 16 designs which were generated by systematically varying four parameters which vary over the range of contemporary knee designs. The effects of varying one parameter alone or in combination with others could be observed. Damage scores were reduced for knees with the larger femoral frontal radius. This could have been because increasing the

femoral frontal radius made the contact points travel greater distances over the plastic so that the elements were experiencing less cycles of fatigue. Alternatively, it could be that the stresses were lower because the relative radius of 70 on 72mm is larger than that of 30 on 32mm even though the clearances between these pairs of femoral and tibial frontal radii are the same. A combination of 30 on 30.4mm would produce the same relative radius as 70 on 72mm. However, such a small clearance would reduce the rotational laxity, would be difficult to manufacture accurately and would also be more susceptible to three-body wear as seen in retrievals by Landy and Walker [1988]. It should be noted however that the femoral frontal radius should not be increased to the degree of flat-on flat designs, because when varus-valgus moments are applied, the femoral component may edge-load onto the polyethylene, producing small contact areas [Collier et al, 1991] and therefore high stresses.

The posterior-distal transition angle determines the point when the small posterior arc of the femoral profile transfers to the relatively larger distal arc. If the magnitude of this angle is large the distal arc sweeps back further than for a smaller angle. Increasing the magnitude of this angle also reduced the stresses because the larger distal femoral arc contacted the polyethylene during most of the walking cycle producing lower stresses compared to designs with the smaller angle where the smaller posterior femoral arc came into play. When large frontal radius and large distal-posterior transition angles were combined the optimum stress conditions were obtained, especially if the tibial component had small clearances in both frontal and sagittal planes.

However, taking laxity into account a design with less sagittal conformity would be preferable [Walker, 1988; Walker et al, 1974]. Fig.5 shows the change in anterior-posterior and rotational laxities produced by changing the tibial sagittal radius of the knee with the least damage score to 80mm. The damage score of this modified design was 8% greater than that for the knee with the least damage score. However, it was predicted considerably less likely to delaminate compared to other knees with similar tibial geometries where the femoral geometry differed. A commercially available knee which is designed along the

same lines as this modified design is the NEXGEN cruciate retaining knee (Fig.6).

This study considered the damage scores of different knee designs when the forces and flexions of level walking were applied. However, other activities such as stair-climbing may involve higher stresses and greater laxities [Andriacchi et al, 1982; Jonsson & Karrholm, 1994]. It was concluded that even though contemporary condylar knee replacements exist in many forms and in general perform satisfactorily, to avoid delamination wear after decades of implantation, the surfaces can be designed to reduce the fatiguing effects of stresses in the polyethylene. This study showed that a combination of large femoral frontal radius, large posterior transition angle, close frontal conformity between the bearing surfaces and a large tibial sagittal radius, satisfy the apparently conflicting requirements of resistance to delamination wear and natural function in condylar total knee replacements.

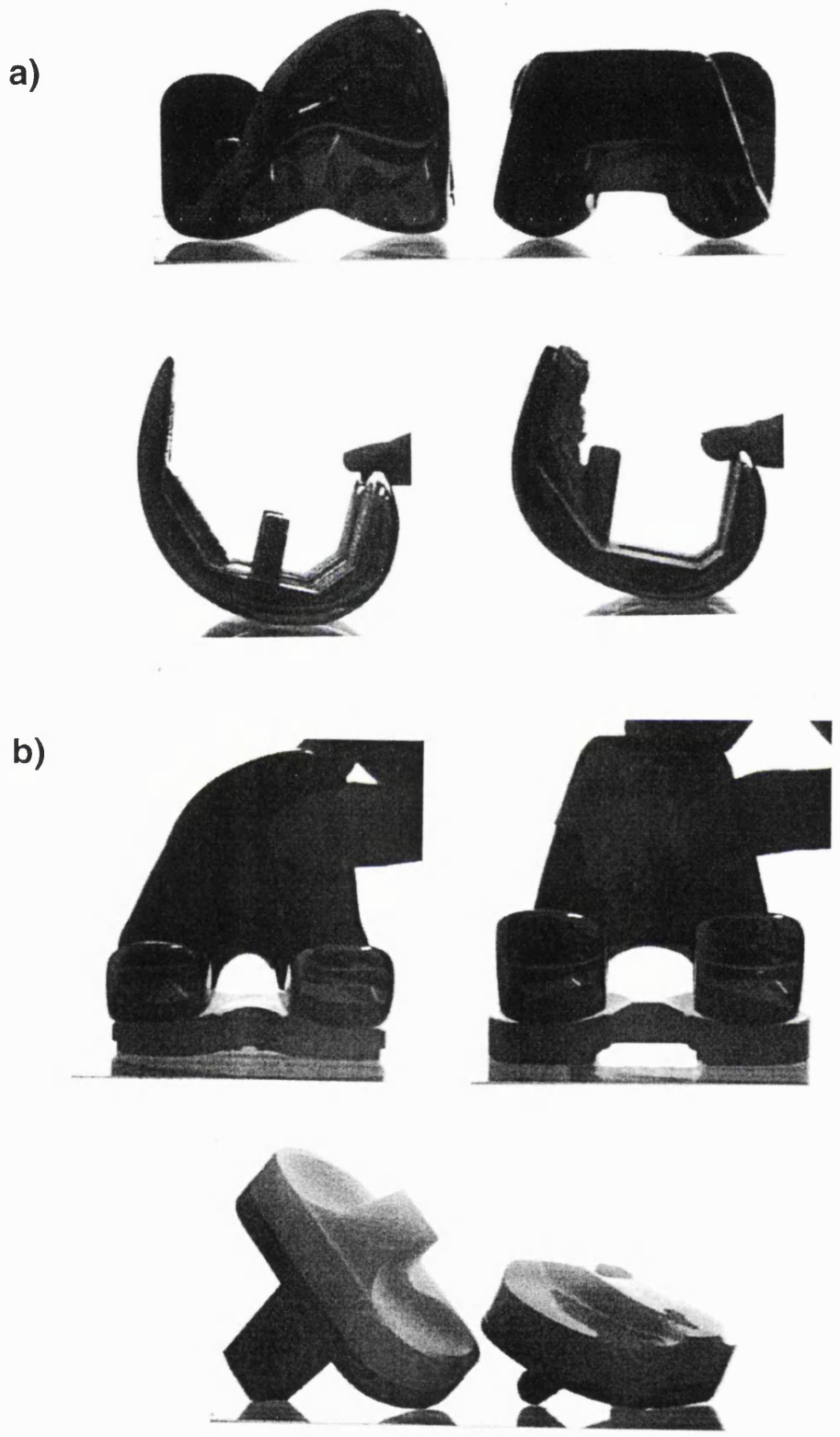

FIG.1 Variability in total knee replacement design : femoral outer frontal radius, femoral posterior-distal transition angle, clearance of the tibial insert from the femoral component and tibial sagittal radius.

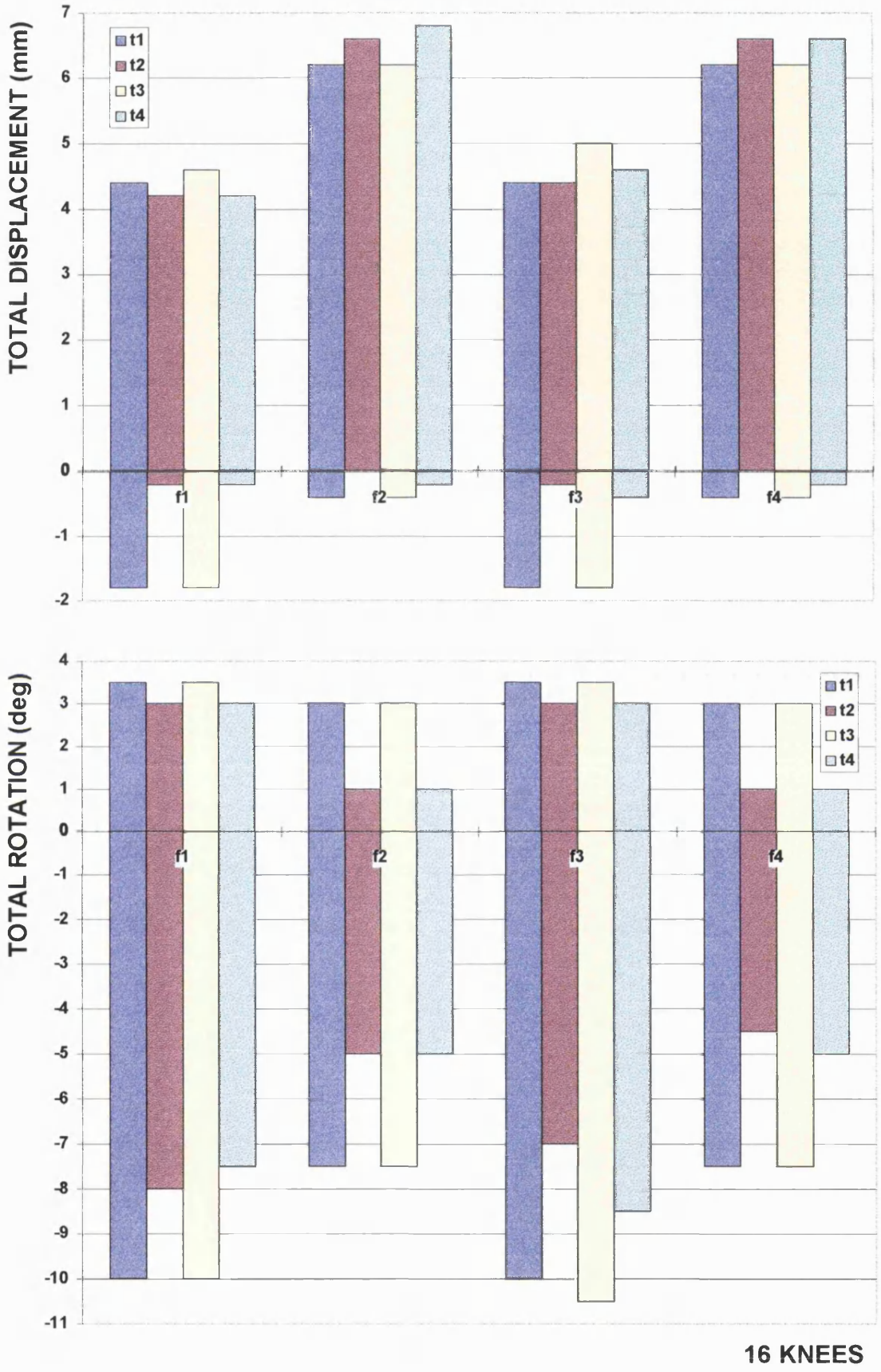

FIG. 2 The total anterior-posterior and rotational laxities of the 16 knees during the stance phase of gait.

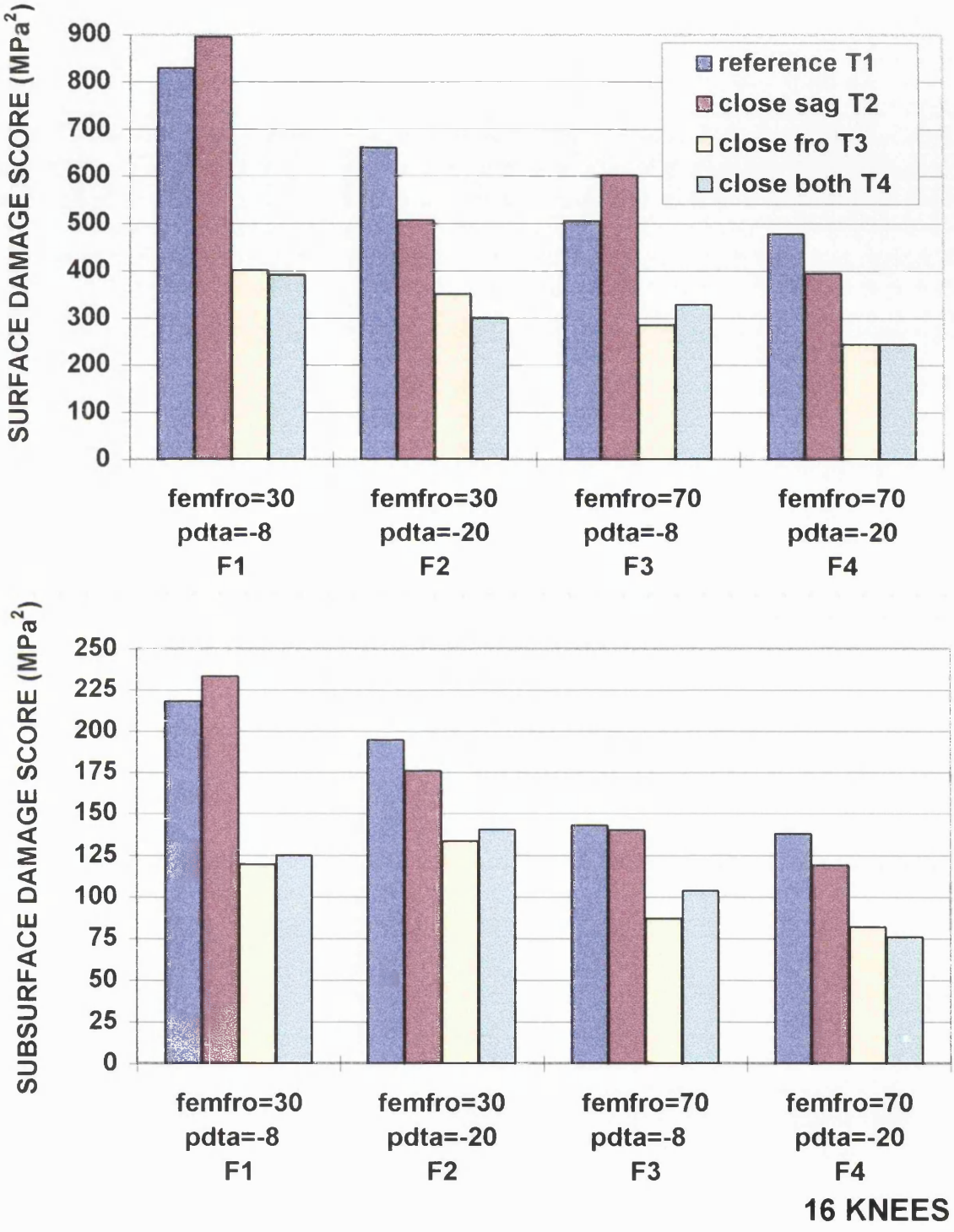

FIG.3 The damage scores accumulating a) the fluctuating maximum principal stresses b) the fluctuating maximum shear stresses for 16 knees during the stance phase of gait.

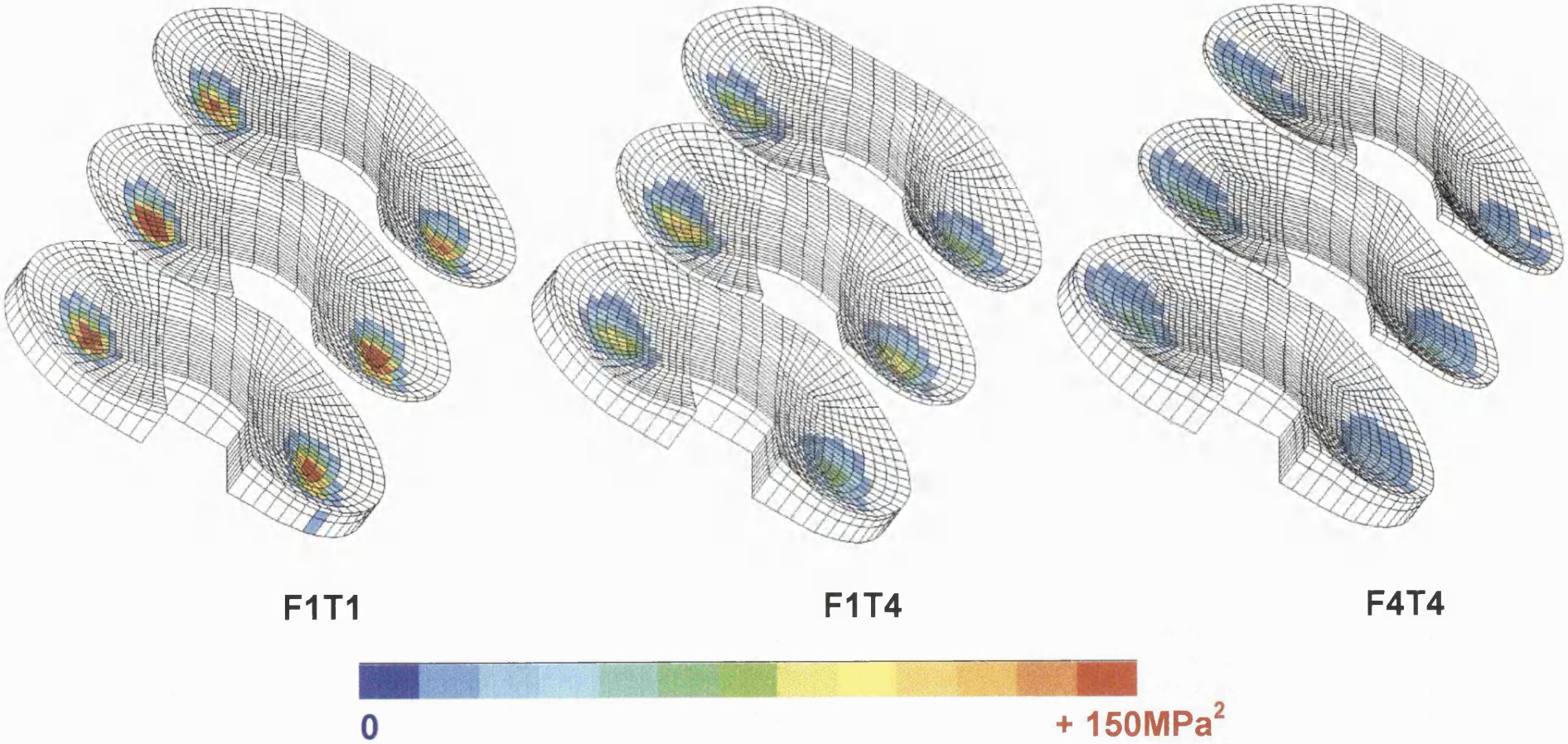

FIG. 4 Maximum shear stress damage function maps for 3 designs: F1T1, F1T4, F4T4

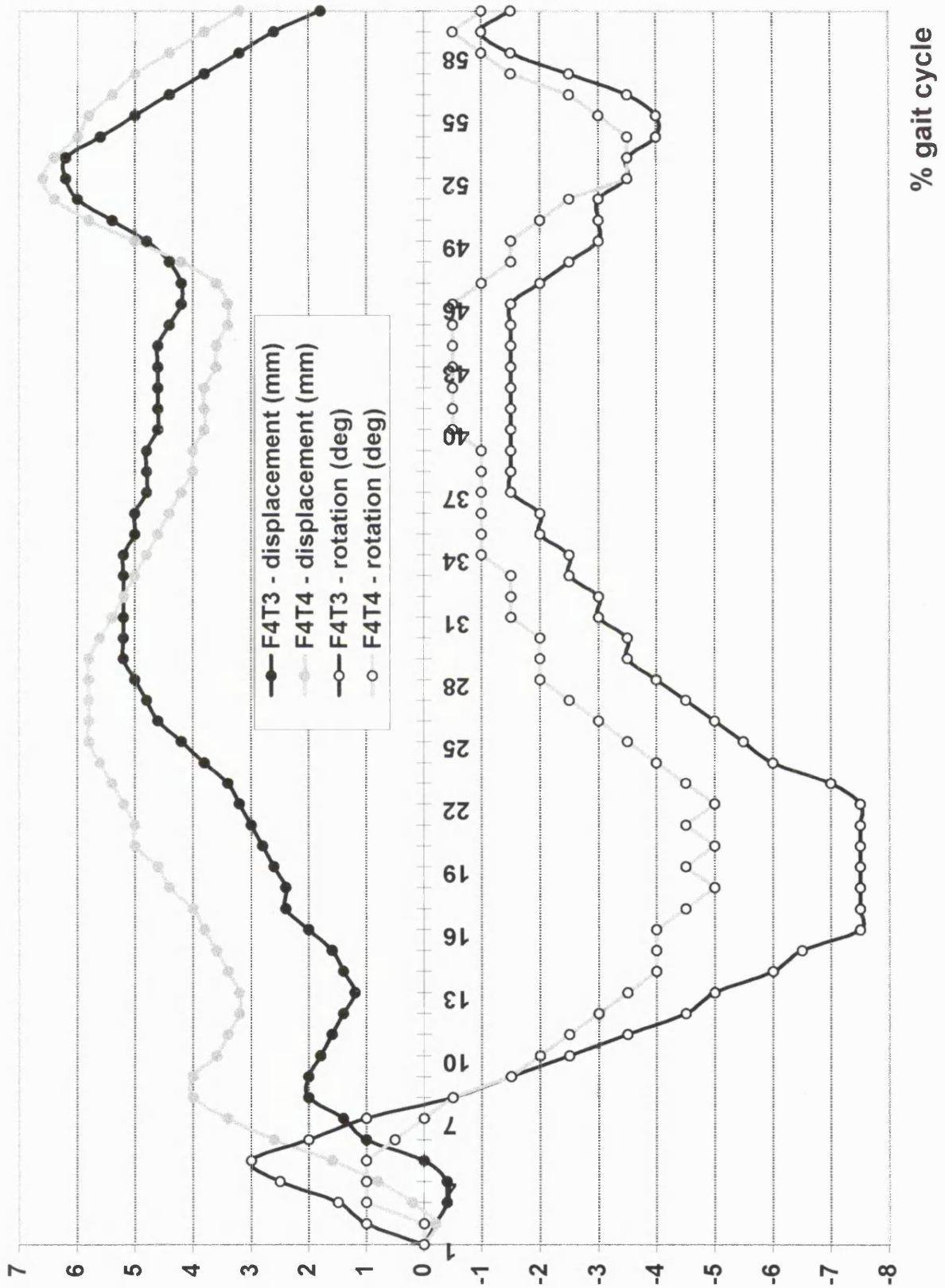

FIG.5 The anterior-posterior and rotational motions during the gait cycle of the knee with the least damage score (f4t4) and a knee (f4t3) with increased rotational laxity. Positive values mean that the femoral component moves forwards and rotates internally relative to the tibial component.

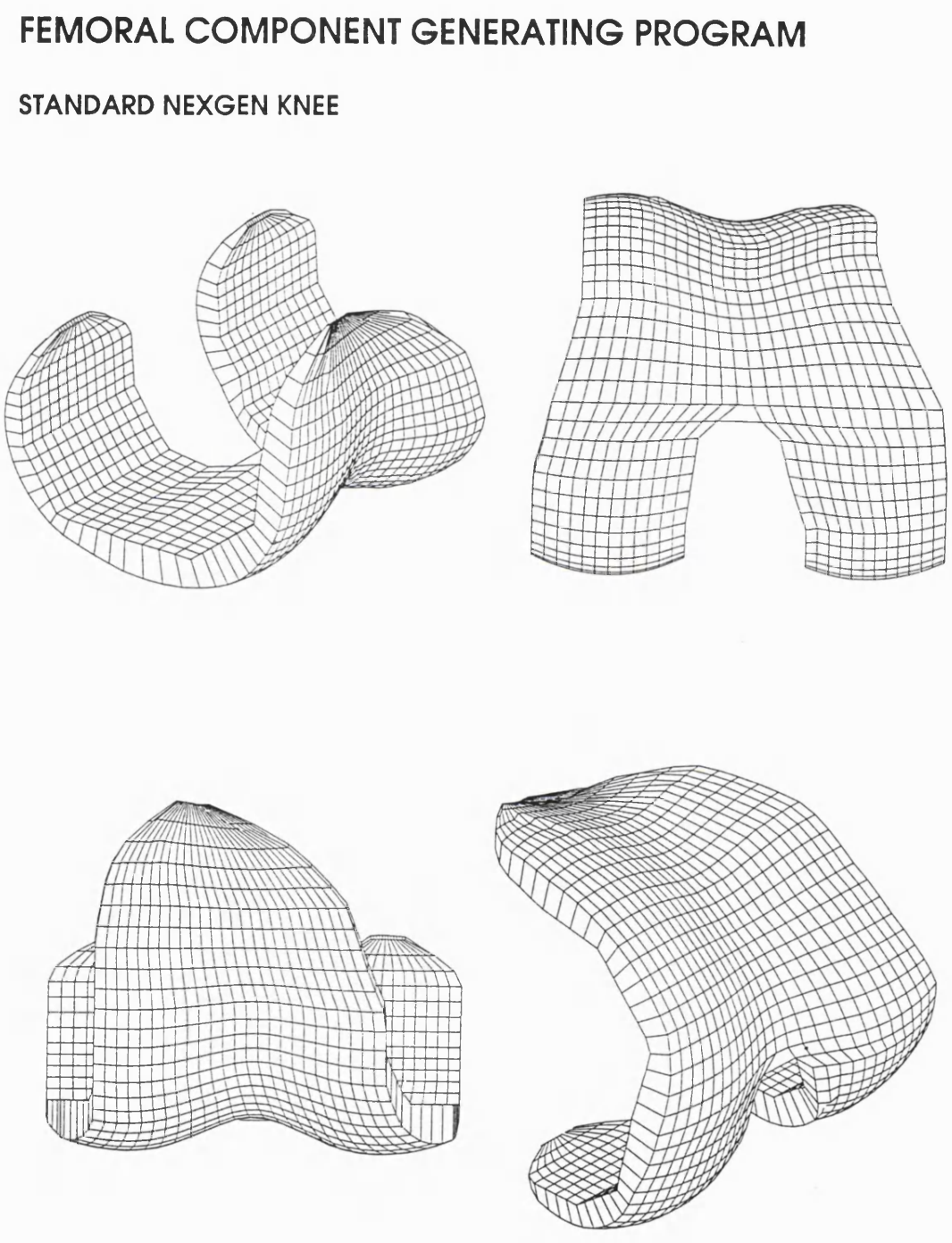

FIG.6 The NEXGEN cruciate retaining design.

Chapter 8

SUMMARY & CONCLUSIONS

8. SUMMARY & CONCLUSIONS

A total knee replacement is used to resurface the femur and tibia and usually the patella. This treatment is mainly used for bone degeneration caused by arthritis but can also be used to increase the stability of a knee where the soft tissues are in poor condition or the bone shapes are abnormal. Designs vary to suit different stability requirements, but the most commonly used form is called the condylar knee replacement where the femur is resurfaced with a double-convex cobalt-chrome layer and the tibia is resurfaced with a cobalt-chrome tray with double-concave dished ultra-high molecular weight polyethylene insert. These components require a minimal amount of bone removal and should reproduce natural relative motion between the femur and tibia. However, the longevity of these types of knee replacement is limited as the polyethylene suffers from delamination wear, where subsurface cracks join with surface cracks releasing large particles of polyethylene, causing catastrophic failure which requires revision surgery.

Delamination wear of polyethylene tibial inserts is a fatigue mechanism caused by fluctuating stresses produced as the femoral component articulates on the tibial insert. Previous researchers have theoretically and experimentally analysed the stresses produced in tibial inserts of different designs, however these studies cannot be used to predict delamination wear because they do not include the effects of fatigue. In order to achieve this the motion path of the knee needs to be considered, which will vary for different designs.

As follow-up studies of implants reaching their second decade revealed an increasing number of failures resulting from delamination wear, the trend in knee design was to make the bearing surfaces of the prosthetic components very conforming to produce low stresses. However, this has resulted in some designs being overconstrained, causing patients to adapt their gait, suggesting that ideally knees should be designed for both low stresses and natural function. Another problem with increasing the conformity of knee designs is that ideally

the conformity should be maintained when relative motions of the components occur, which is not often considered.

Various design criteria were examined in combination to find the ideal geometry for a condylar knee replacement. The criteria were the contact stresses on the polyethylene, femoral-tibial size interchangeability, patella lever arm, laxity and stability and the amount of bone resection required. The variables were the radii of curvature of the femoral and tibial bearing surfaces in the sagittal and frontal planes. Metal toroidal indentors were loaded onto dished surfaces of polyethylene covering a range of radii and the contact areas measured. Using elasticity equations, the apparent elastic modulus of polyethylene ranged from 400 to 600MPa for less conforming to closely conforming surfaces. Using a value of 600MPa, contact stresses were predicted for a complete spectrum of radii of curvature. Contact stresses and contact locations depended upon the combination of sagittal and frontal radii.

An influential variable was the sagittal curvature of the femoral component, notably the point of transition between the posterior curve of small radius and the distal curve of larger radius. This affected the patella lever arm, the stability, and the bone resection. The ability to interchange between femoral and tibial component sizes was primarily dependent upon the relative frontal radii. Finite element analysis was used to determine the stresses beneath the contact patches when different femoral-tibial sizes were interchanged. Based on these analyses the most suitable geometrical combinations overall were determined.

The criteria considered so far determined if the knee replacements were implantable, satisfying surgical requirements. However, prosthetic components designed accordingly would not necessarily function naturally or resist delamination wear. Therefore, when optimising the design of bearing surfaces, a primary set of criteria were employed to ensure that the components were implantable. This determined the ranges of suitable values for the different parameters. Within these ranges, a second set of criteria were applied, the

requirements of natural function and resistance to delamination of the tibial insert, to perform the final optimisation.

The analyses up to this point were carried out using a simplified model of the bearing surfaces constructed from convex and concave arcs, however for more detailed analyses and to compare different commercially available products, complete models of the surfaces were required. The design of condylar knee replacements was parametrised by defining dimensions commonly used in conventional engineering drawings as variables. Programs were written to generate surface meshes for rigid body analyses and solid models for finite element analyses. These programs could also be used to produce tool-paths for computer numerically controlled milling machines, and the manufacture of customised superstabilised total knee replacements for patients who could not be treated with off-the-shelf products was a useful application.

The programs were tested by carrying out finite element analyses to determine the effects of increasing the conformity of the tibial inserts to their mating femoral components. The relationship between conformity and magnitudes of the stresses produced in the tibial inserts was of particular interest. Analyses were carried out at different angles of flexion but these tests were not adequate for predicting stresses during gait as the other relative motions were not included. However, these tests were useful for understanding the stress conditions produced under dished metal on polyethylene interfaces, which was necessary when deciding which stresses were responsible for cracking in different regions of the tibial insert.

The rigid body analyses predicted the kinematics for a set of input forces and moments. The rigid body model included friction at the bearing surfaces and soft tissue restraint forces, including the effect of cruciate resection. The soft tissue restraints were necessary in order to compare knees of different conformities. For knees with high conformity between the bearing surfaces, the dishes of the tibial insert would provide most of the restraint, ensuring that the femur would not be subjected to unnaturally large relative displacements and rotations with respect to the tibia. Whereas for knees with low conformity,

restraint provided by the tibial dishes alone would not be sufficient. Predictions from the model were compared with data from a knee simulating machine. There was close agreement in the shapes of the curves and in the magnitudes of the displacements and rotations under most conditions. The model predicted major differences in kinematics when friction between metal and polyethylene was included, the differences being even greater at the friction levels associated with small embedded acrylic particles. Soft tissue restraint was shown to reduce the displacements and rotations for tibial surfaces of low constraint but for moderate to high constraint, the soft tissues affected the kinematics only slightly. When the model was used to predict the motions for different condylar geometries, widely different contact paths on the tibial surface were determined. This suggested that condylar geometries which appeared to be generally similar, could have important differences in kinematics, function and wear.

Contact area and contact stress studies to date have been carried out with the knees in neutral positions or with flexion included. However, during gait the prosthetic components are subjected to anterior-posterior displacements and internal-external rotations which vary the stresses and the shapes of the contact areas. Two commercially available designs of total knee replacements were studied using a combination of rigid body and finite element analyses to determine how bearing surface geometry would affect the contact areas and stresses on the surfaces of polyethylene tibial inserts during gait. There were significant differences between the shapes of the contact areas and the magnitudes of the stresses for these designs. However, it was difficult to compare their overall performances because peak contact stresses occurred at different instances during gait, in different regions of the polyethylene.

It became apparent that a method of quantifying the accumulated fluctuations of the stresses was required. Damage functions were formulated which quantified the fluctuations and average magnitudes of the stresses produced during the whole gait cycle. Therefore, for a particular knee design and a particular set of input cycles, a damage map could be generated to indicate the regions of the polyethylene which were most prone to fatigue.

Optimisation of the design of condylar knee bearing surfaces was required to ensure that knees designed with a high degree of conformity to produce low stresses in the polyethylene tibial insert would not be overconstrained. Studies were carried out to determine femoral and tibial bearing surface geometries which will induce the least destructive fatigue mechanisms in the polyethylene whilst conserving the laxity of the natural knee. Sixteen knee designs were generated by varying four parameters systematically to cover the range of contemporary knee designs. The parameters were the femoral frontal radius (30 or 70mm), the difference between the femoral and tibial frontal radii (2 or 10mm), the tibial sagittal radius (56 or 80mm) and the posterior-distal transition angle (-8 or -20 deg), which is the angle at which the small posterior arc of the sagittal profile transfers to the larger distal arc. Rigid body analyses determined the anterior-posterior and rotational laxities as well as the contact points during the stance phase of gait for the different designs. In addition a damage function which accumulated the fluctuating maximum shear stresses was used to predict the susceptibility to delamination wear of the polyethylene. Of the 16 designs, the knee with a frontal radius of 70mm, a difference in femoral and tibial frontal radii of 2mm, a tibial sagittal radius of 80mm and a posterior distal transition angle of -20deg was predicted to satisfy the conflicting needs of both natural kinematics and resistance to delamination wear.

The optimisation of the design of knee replacement bearing surfaces is not an easy task because apart from the geometry of the prosthetic components, the wear is affected by a number factors such as chemical reactions which occur in the environment of the knee, the variable quality of the polyethylene, the manufacturing method of the tibial inserts, the surgical technique used to implant the components, the condition of the soft tissues and the activity levels of the patients. However, the patterns of wear seen for different designs suggest that the geometry of the bearing surfaces must be one of the dominating factors. In the past, condylar knee replacement designers have introduced products to the market of various shapes and forms, but the varying levels of wear observed for

these implants suggested that there was a requirement for the design of condylar knee replacements to be optimised.

In 1986, Bartel et al wrote : 'The effects of the large compressive and tensile maximum principal stresses are compounded in the knee replacement because during articulation the contact area moves with respect to the tibial component'. However since then, the consequences of the mobile contact areas which change in shape during gait have not been investigated. The aim of this study was to show that the various designs of condylar knee replacements currently on the market have different durabilities. In addition, their susceptibility to delamination wear is a function of not only the geometry of the components but also their laxity, and measuring contact areas and stresses in the neutral position is not an adequate way of comparing different designs. Finally, delamination is a fatigue mechanism, so the manner in which the stresses fluctuate should be considered as well as the magnitude of the stresses. This study took all these factors into account.

Fig. 1 shows the maximum shear damage scores (calculated in the previous chapter) which compare the susceptibilities to subsurface cracking of 16 different knee designs. The maximum contact pressures produced when these designs were positioned in the neutral position and loaded with 1000N are also plotted, to represent the results of conventional testing methods. The ranking of the 16 knees using these two methods was very different. Using the damage functions, knees with large frontal radii and large posterior distal transition angle mated with unconforming tibial inserts were predicted to be less likely to wear compared to knees with small frontal radii and small posterior distal transition angles, even if they had conforming tibial inserts. Therefore the damage functions showed that it was possible to optimise for both criteria of natural function and resistance to delamination even though their needs seem to conflict. The contact pressures produced under static load for the 16 knees did not confirm this, but these results and those of other conventional tests only tell part of the story.

As with any other type of modelling, assumptions had to be made. In the rigid body analysis the motion was assumed to be quasi-static and force-controlled. The input forces were assumed to be those for a natural knee measured by gait analysis. The variations between the geometries, restraints and friction coefficients of the natural and prosthetic surfaces would suggest that the output displacements and rotations would vary, yet experiments have shown that muscles forces generated by the neuromuscular system can compensate for these differences to a certain extent. These effects were not taken into account.

The accuracy of the motion paths described by contact points on the tibial insert, predicted for different designs by rigid body analysis, reduced as the size of the contact areas increased. This had subsequent repercussions when finite element analysis was carried out. The restraints provided by the soft tissues were simplified to a bumper system where restraint remained constant with flexion, though experimental results carried out on cadaveric knees suggested that this was not the case. More realistic soft tissue restraints could be included in the computer model. The attachment points and stiffnesses of the ligaments could be obtained from cadaveric specimens. These attachment points could be input to the computer model and springs with the ligament stiffnesses could be inserted between the attachment points (Fig. 3). The advantage with this more realistic model would be that the soft tissue restraint would be influenced by the flexion angle. However, the cadaveric tests also illustrated the fact that soft tissue restraints are highly variable between different knees, questioning the use of even an averaged model of the soft tissue restraints

Separate damage functions were used to predict subsurface and surface cracking by summing the fluctuations and magnitudes of the maximum shear stress and the maximum principal stress respectively. The maximum principal stress damage function could have been improved by separating the compressive and tensile portions of the fluctuations, as polyethylene is weaker in tension than in compression. Both damage functions require validation, first with uniaxial tests carried out on fatigue test samples and ultimately with different

knee designs subjected to gait cycles in a knee simulating machine. However, as the input to the knee simulator and the computer knee model would be identical, this would only prove that the damage functions were correct for a given set of input forces. Ideally the damage maps should be compared with delaminated retrievals, however the other factors which affect wear may disguise the effects of varying the bearing surface geometry alone.

The polyethylene in the finite element models of the tibial inserts was assumed to be linear elastic with an elastic modulus of 600MPa. However, retrievals from patients (Fig.2) show signs of significant plastic deformation which cannot be predicted by the model in its current state. Plastic deformation of the tibial insert could be included by applying multiple cycles. During each cycle, the deformations and stresses of the polyethylene elements at discrete intervals of gait could be recorded. If the stresses of any elements were over the yield stress, then for the next cycle those elements would have new deformed shapes. If plasticity was included in the model an energy-based damage function such as strain energy density could be used instead of the stress-based damage functions.

In this thesis, a method was developed to compare the durabilities of different knee designs. For any given sets of input forces, soft tissue restraints and damage functions, the regions of the polyethylene most prone to fatigue failure can be predicted for any condylar knee design. The optimisation carried out in the previous chapter involved 16 knees where four geometrical parameters were varied. These parameters were the femoral frontal radius, the clearance of the tibial component from the femoral component in the frontal plane, the posterior-distal transition angle of the femoral component and the tibial sagittal radius. The values for the parameters chosen were at the extremes of the values currently used in knee replacement design. Lower values for the damage functions could be obtained by analysing more parameters and more values. The ultimate use for the damage functions would be to predict the volume of wear rather than the susceptibility to wear relative to a reference design. In order to do this experimental tests would have to be conducted to

determine the value of the damage functions at which cracking actually occurs, similar to determining S-N curves in the study of fatigue.

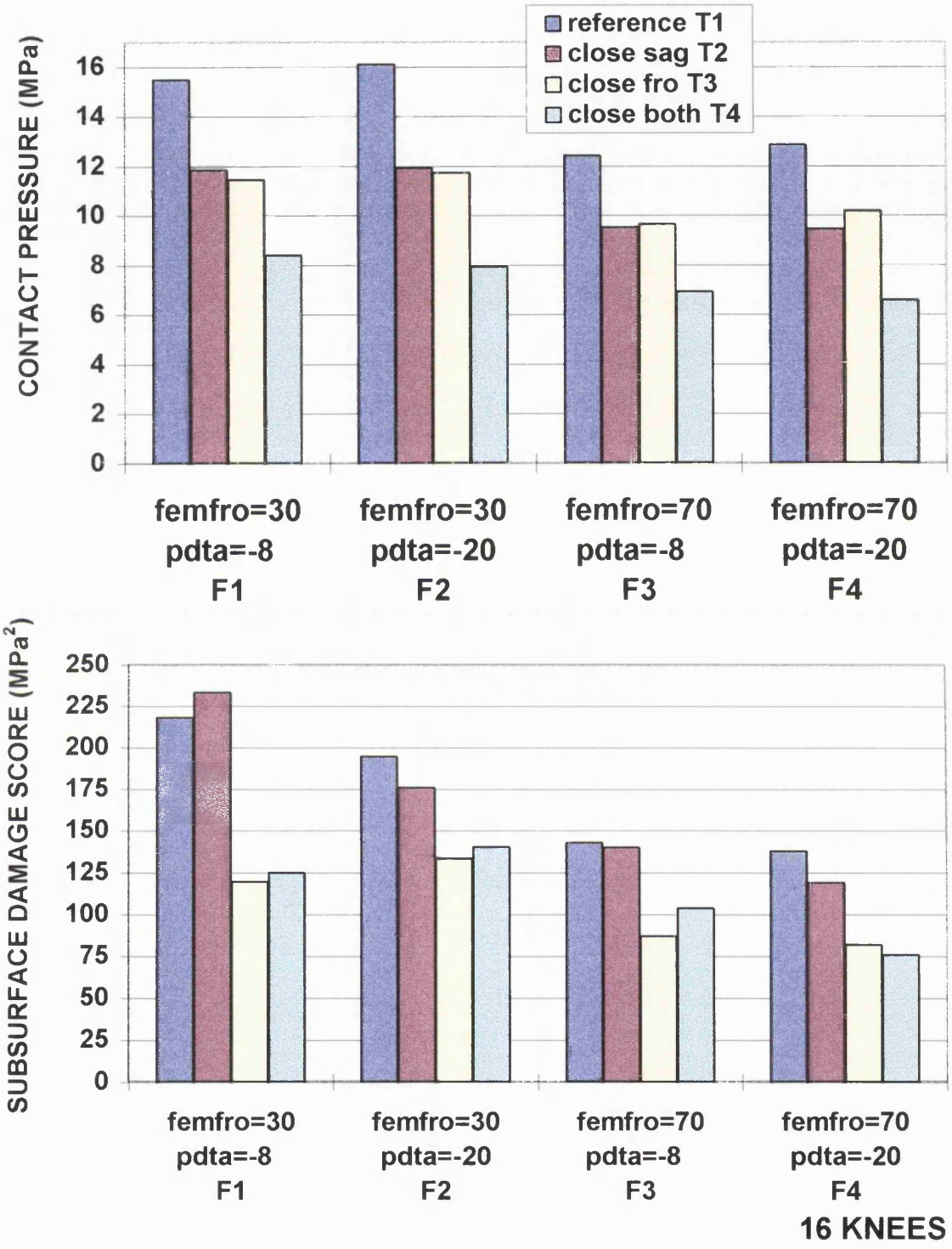

FIG.1 Using contact pressures versus subsurface damage scores to compare susceptibilities to delamination wear of tibial inserts in different knee designs.

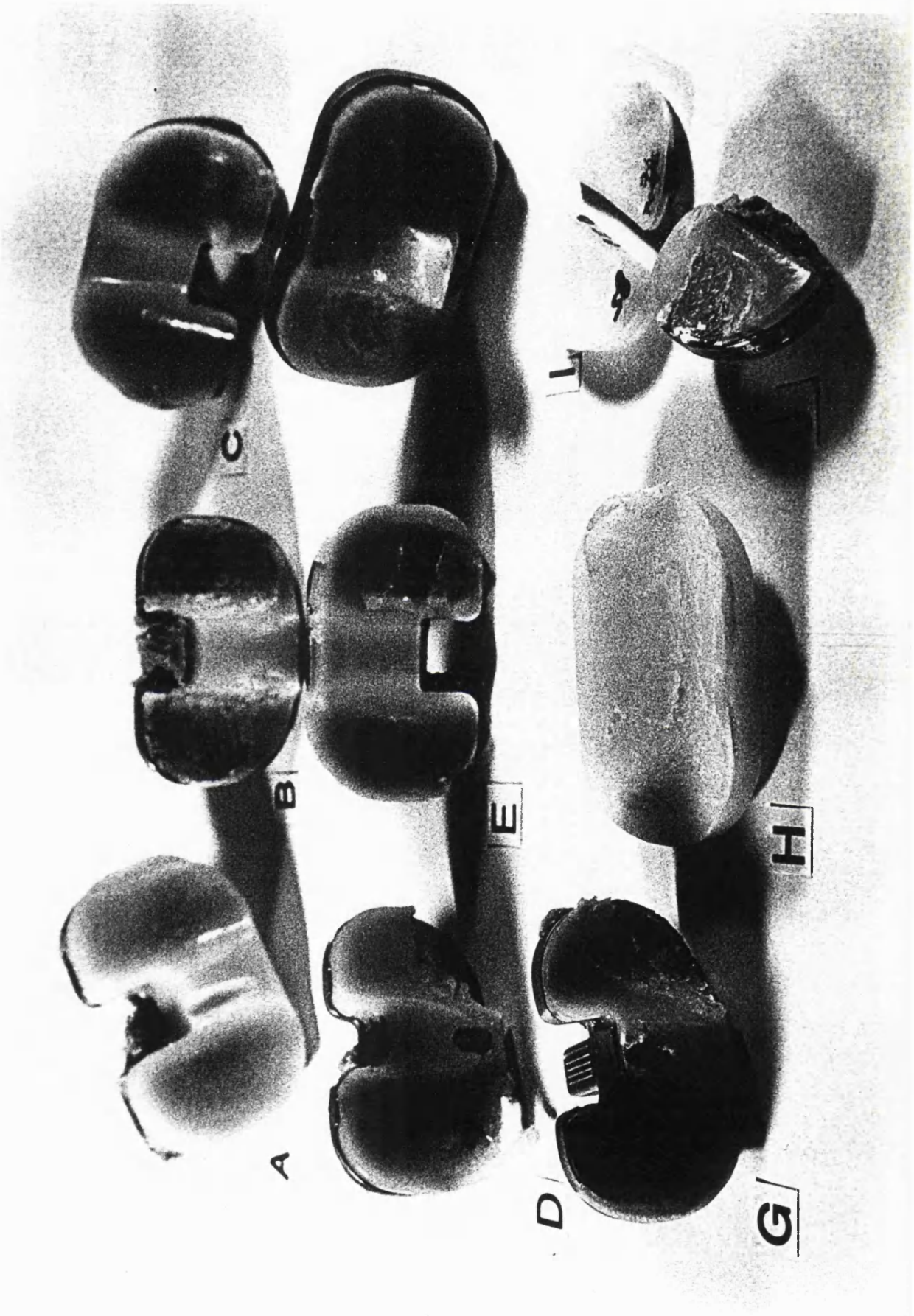

FIG.2 Retrieved tibial components collected by Dr. Gordon Blunn at the Centre for Biomedical Engineering.

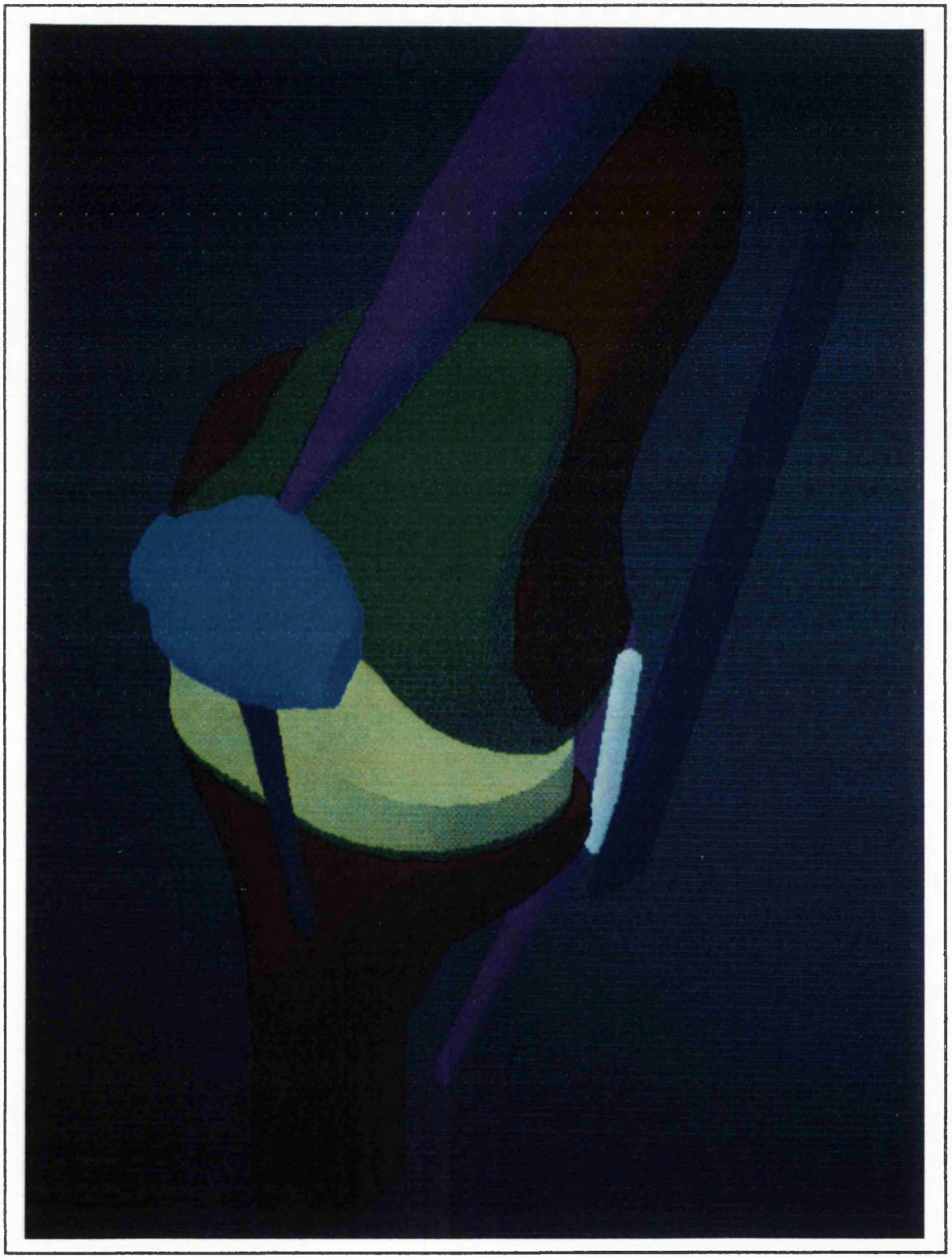

A computer model which includes realistic ligament restraints.

FIG.3

REFERENCES

1) Ahmed A.M.; Burke D.L.; Hyder A..: Force Analysis of the Patellar Mechanism. J. Orthop Res, 5, p.69, 1987

2) Ahmed, A.M.; Burke, D.L.: In Vitro Measurements of Static Pressure Distribution in Synovial Joints-Part1: Tibial Surface of the Knee. J. Biomech Engng, 105, p.216, 1983

3) Anderson, D.D.; Rullkoetter, P.J.; Hillberry, B.M. : Viscoelastic response of UHMWPE in finite element analysis of TKR components. Trans Orthop Res Soc, p.762, 1995

4) Andriacchi, T.P.; Galante, J.O. : Retention of the Posterior Cruciate in Total Knee Arthroplasty. J. Arthroplasty, 3, s13, 1988

5) Andriacchi, T.P.; Mikosz, R.P. : Musculoskeletal dynamics, locomotion and clinical applications. In Basic Orthopaedic Biomechanics. Mow VC, Hayes WC, eds. New York: Raven Press, p.51, 1991

6) Andriacchi, T.P.; Mikosz, R.P.; Hampton, S.J.; Galante J.O. : Model studies of the stiffness characteristics of the human knee joint. J. Biomechanics, 16, No.1, p.23, 1983

7) Andriacchi, T.P.; Yoder, D; Sum, J.: Gait Results as Input for the Durability Testing of Contemporary Total Knees on a New Simulating Machine (personal communication), February 1995

8) Andriacchi,T.P.; Galante, J.O.; Fermier, R.W. : The influence of total knee replacement design on walking and stairclimbing. J Bone Joint Surg [Am], 64-A, p.1328, 1982

9) Arima, J.; Martin, J.W.; White, S.E.; McCarthy; D.S.; Whiteside, L.A,. : Partial posterior cruciate ligament release and knee kinematics after total knee arthroplasty. Trans Orthop Res Soc, 19, p.87, 1994

10) Attenborough, C.G. :Total knee replacement using the stabilized gliding prosthesis. Ann. Royal College of Surgeons of England, 58, p.4, 1976.

11) Bartel,D.L.; Bicknell,V.L.; Ithaca,M.S.; Wright,T.M. : The Effect of Conformity, Thickness, and Material on Stresses in Ultra-High Molecular Weight Components for Total Joint Replacement. J.Bone Joint Surg, 68-A, No.7., p.1041, 1986

12) Berchuck, M.; Andriacchi, T.P.; Bach, B.R.; Reider, B. : Gait adaptations by patients who have a deficient anterior cruciate ligament. J Bone Joint Surg[Am], 72-A, p.871, 1990.

13) Blankevoort, L. ; Huiskes, R.; De Lange, A. : The envelope of passive knee joint motion. J. Biomechanics, 21 (9), p. 705, 1988

14) Blankevoort, L.; Huiskes, R.: Ligament-bone interaction in a three-dimensional model of the knee. J Biomech Engng, 113, p.263, 1991.

15) Blankevoort, L.; Kuiper, J.H.; Huiskes, R.; Grootenboer, H.J. : Articular contact in a three-dimensional model of the knee. J. Biomechanics, Vol.24, No.11, p.1019, 1991.

16) Blunn, G.W.; Bell C.J. : The effect of oxidation on the wear of untreated and stabilised UHMWPE. Trans Orthop Res Soc, p.482, 1996.

17) Blunn, G.W.; Joshi, A.; Lilley, P.A.; Engelbrecht,E.; Ryd, L.; Lidgren, L.; Hardinge, K.; Walker, P.S.: Polyethylene Wear in Unicondylar Knee Prostheses: 106 Retrieved Marmor, PCA and St. Georg Tibial Components Compared. Acta Orthop. Scand., 63(3), p.247, 1992

18) Blunn, G.W.; Joshi, A.B.; Minns R.J.; Lidgren L.; Lilley P.; Ryd L.; Engelbrecht E.; Walker P.S. : Wear in retrieved condylar knee replacement. J. Arthroplasty (In press, 1996)

19) Blunn, G.W.; Lilley, P.A.; Walker, P.S.: Variability of the wear of ultra high molecular weight polyethylene in simulated TKR. Trans Orthop Res Soc, 40, 1994.

20) Blunn, G.W.; Walker, P.S.; Joshi, A.; Hardinge, K.: The dominance of cyclic sliding in producing wear in total knee replacements. Clin. Orthop., 273, p253, 1991.

21) Booth RE, Gardner TA, Herschberger T, Sutton D. Computerised bisensor analysis of total knee arthroplasty. Presented at The Knee Society, New Orleans 19Feb 1994.

22) Bostrom, M.P.G.; Bennett, A.P.; Rimnac, C.M.; Wright, T.M. : Degradation in Polyethylene as a result of sterilization, shelf storage, and in vivo use. Trans Orthop Res Soc, p.288, 1994.

23) Bristol, R.E.; Fitzpatrick, D.C.; Brown, T.D.; Callaghan, J.J. : Non-uniformity of contact stress on polyethylene inserts in total knee arthroplasty. Clin. Biomech., Vol. 11, No.2, p.75, 1996.

24) Burstein, A.H. : Biomechanics of the Knee. In: Surgery of the Knee, Edited by.Insall JN, Churchill Livingstone, p.21, 1984.

25) Campbell, P.; Ma, S.; Yeom, B.; McKellop, H.; Schnalzried, T.P.; Amstutz, H.C. : Isolation of predominantly submicron-sized UHMWPE wear particles from periprosthetic tissues. J. Biomedical Mat Res, Vol. 29, p.127, 1995

26) Collier, J.P.; Mayor, M.B. McNamara, J.L. Surprenant, V.A.; Jensen, R.E.: Analysis of the failure of 122 polyethylene inserts from uncemented tibial knee components. Clin. Orthop., 273, p.232, 1991.

27) Crowninshield R.D.; Pope M.H.; Johnson R.J.: An analytical model of the knee. J. Biomechanics, 9, p.397, 1976

28) Draganich, L.F.; Andriacchi, T.P.; Andersson, G.B.J. : Interaction between intrinsic knee mechanics and the knee extensor mechanism. J. Orthop. Res., 5, p.539, 1987

29) Draganich, L.F.; Vahey, J.W. : An in vitro study of anterior cruciate ligament strain induced by quadriceps and hamstrings forces. J. Orthop. Res., 8, p.57, 1991.

30) Ellyin, F. : Cyclic Strain Energy Density as a Criterion for Multiaxial Fatigue Failure. Biaxial and Multiaxial Fatigue, EGF3 (edited by M.W. Brown and K.J. Miller). Mechanical Engineering Publications, London. p. 571, 1989.

31) Essinger, J. R.; Leyvraz, P.F.; Heegard, J.H.; Robertson, D.D. : A mathematical model for the evaluation of the behaviour during flexion of condylar-type knee prostheses. J. Biomechanics, Vol.22, No. 11/12, p.1229, 1989.

32) Estupinan, J.A.; Bartel, D.L.; Wright, T.M.: Surface Residual Tensile Stress After Cyclic Loading of UHMWPE by a Rigid Indenter. Trans Orthop Res Soc, p.48, 1996.

33) Fisher, J.; Dowson, D. : Tribology of total artificial joints. Proc Instn Mech Engrs, 205, p.73, 1991.

34) Freeman, M.A.R.; Railton, G.T. : Should the Posterior Cruciate Ligament be Retained or Resected in Condylar Nonmeniscal Knee Arthroplasty? The Case for Resection J. Arthroplasty, 3:S3-S12, 1988.

35) Freeman, M.A.R.; Swanson, S.A.V.; Todd, R.C. : Replacement of the knee with the Freeman-Swanson prosthesis. Total Knee Replacement CP16 published by Instn Mech Engrs , p.102, 1974.

36) Fukubayashi T.; Torzilli P.A.; Sherman M.F.; Warren R.F.: An in vitro biomechanical evaluation of anterior-posterior motion of the knee. J. Bone Jt. Surg., 64-A (2) p.258, 1982.

37) Gabriel S.M., Dennis D.A., Komistek R.D., Hoff W.A., Stiehl J.B. : In vivo TKA kinematics with consequences for system stresses and strains. Trans Orthop Res Soc, 21, 213-236, 1996.

38) Garg A. ; Walker P.S.: Prediction of total knee motion using a three-dimensional computer-graphics model. J. Biomechanics , 23 (1), p.45, 1990.

39) Gollehon D.L.; Torzilli P.A.; Warren R.F.: The role of the posterolateral and cruciate ligaments in the stability of the human knee. J. Bone Jt Surg [Am], 69-A, p.233, 1987

40) Goodfellow, J.; O'Connor, J. : The mechanics of the knee and prosthesis design. J Bone Joint Surg, 60-B, No. 3, p.358, 1978.

41) Goodfellow, J.W., Tibrewal, S.B., Sherman, M.A., O'Connor, J.J. :Unicompartmental Oxford Meniscal Knee Athroplasty. J. Arthroplasty, Vol.2, No.1, 1987.

42) Grood, E.S., Suntay, W.J. : A joint coordinate system for the clinical description of three-dimensional motions : application to the knee. J. Biomech Engng, Vol.105, p.136, 1983.

43) Gunsallus, K.L.; Bartel, D.L. : Stresses and Surface Damage in PCA and Total Condylar Polyethylene Components Trans Orthop Res Soc, 17, p.329, 1992.

44) Gunston, F. H. : Polycentric knee arthroplasty. J Bone Joint Surg 53B, p.272, 1971.

45) Hahn, D.L.; Mc Queen, D.A.; Pence, C.D. : Volumetric considerations for stress in irradiated UHMWPE for total joint replacement. Trans Orthop Res Soc, p.761, 1995.

46) Hsieh H-H, Walker PS. Stabilizing mechanisms of the loaded and unloaded knee joint. J Bone Joint Surg [Am], 58-A, p.87, 1976.

47) Huberti, H.H.; Hayes, W.C.; Stone, J.L.; Shybut, G.T. : Force Ratios in the Quadriceps Tendon and Ligamentum Patellae J. Orthop Res, 2, p.49, 1984.

48) Incavo, S.J.; Johnson, C.C.; Beynnon, B.D.; Howe, J.G. : Posterior cruciate ligament strain biomechanics in total knee arthroplasty. Clin. Orthop. Rel. Res. , 309, p.88, 1994.

49) Inman, V.T.; Ralston, H.J.; Todd, F. : Human Walking Williams and Wilkins, Baltimore, 1981

50) Insall, J.; Tria, A.J.; Scott, W.N. : The total condylar knee prosthesis : the first five years. Clin. Orthop. Rel. Res., 145, p.68, 1979.

51) Ishikawa, H.; Fujiki, H.; Yasuda, K. : Contact analysis of ultra-high molecular weight polyethylene articular plate in artificial knee joint during gait movement. J. Biomech Engng.,118, p.379, 1996.

52) Iverson B.F.; Sturup J.; Jacobsen K.; Anderson J.: Implications of muscular defence in testing for the anterior drawer sign in the knee. Am. J. Sports Medicine, 17 (3), p.409, 1989.

53) Jin, Z.M.; Dowson, D; Fisher, J : Contact pressure prediction in total knee replacements. Proc Instn Mech Engrs, 209, p.9, 1995.

54) Johnson, K.L. : Contact Mechanics. Camb. Univ. Press, 1985

55) Jonsson H, Karrholm J: Three-dimensional knee joint movements during a step-up: evaluation after anterior cruciate ligament rupture. J Orthop Res, 12, p.769, 1994.

56) Kurosawa, H.; Walker, P.S.; Abe, S.; Garg, A.; Hunter, T. : Geometry and motion of the knee for implant and orthotic design. J Biomechanics,18, p.487, 1985.

57) Kurtz, S.M.; Bartel, D.L.; Rimnac, C.M. : Post irradiation ageing and the stresses in UHMWPE components for total joint replacement. Trans Orthop Res Soc, p.584, 1994.

58) Lafortune, M.A.; Cavanagh P.R.; Sommer III, H.J.; Kalenak, A. : Three-dimensional kinematics of the human knee during walking. J. Biomechanics, Vol.25, No.4, p.347, 1992

59) Landy, M.M.; Walker, P.S. : Wear of Ultra-high-loecular-weight polyethylene componentsof 90 retrieved knee prostheses. J. Arthroplasty 3 (Supp) s73-s85, 1988

60) Lewallen, D.G.; Bryan, R.S.; Peterson, L.F.A. : Polycentric total knee arthroplasty. J Bone Joint Surg [Am], 66-A, No.8, p.1211, 1984.

61) Lewis, P; Rorabeck, C.H.; Bourne, R.B.; Devane, P : Posteromedial tibial polyethylene failure in total knee replacements. Clin. Orthop., 299, p.11, 1994.

62) Lilley, P.A.N. : An investigation of wear in lower limb endoprostheses. PhD Thesis, Faculty of Technology, Kingston University, 1994.

63) Liu, H.W. : Shear Fatigue Crack Growth : A Literature Survey. Fatigue Fract. Engng Mater. Struct. Vol.8, No.4, p.295, 1985.

64) Luger, E.; Sathasivam, S.; Walker, P.S. : Inherent differences in the laxity and stability between the intact knee and total knee replacements. The Knee No.4, pp.7-14, 1997.

65) Mahoney, O.M.; Noble, P.C.; Rhoads, D.D.; Alexander, J.W.; Tullos; H.S. : Posterior cruciate function following total knee arthroplasty. J. Arthroplasty, 9, p.569, 1994.

66) Markolf K.L.; Bargar W.L.; Shoemaker S.C.; Amstutz H.C.: The role of joint load in the knee stability. J. Bone Jt Surg, 63-A (4), p.570, 1981.

67) Markolf KL, Gorek JF, Kabo JM, Shapiro MS. Direct measurement of resultant forces in the anterior cruciate ligament. J Bone Jt Surg [Am], 72-A: p.557, 1990.

68) Mikosz R.P.; Andriacchi T.P.; Andersson G.B.J.: Model analysis of factors influencing the prediction of muscle forces at the knee. J. Orthop Res, 6, (2), p.205, 1988.

69) Mikosz, R.P.; Rosenberg, A.G.; Haberman T.M.: A comparison of postoperative function between patients with unicompartmental and total knee arthroplasties. Trans Orthop Res Soc, 15-18, 1993.

70) Mills O.S. and Hull M.L.: Apparatus to obtain rotational flexibility of the human knee under moment loads in vivo. J. Biomechanics, 24, p.351, 1991

71) Morrison JB. The mechanics of the knee joint in relation to normal walking. J Biomechanics, 3, p. 51, 1970.

72) Morrison, J.B. :Bioengineering analysis of force actions transmitted by the knee joint. Bio-Med. Engng. Vol. 3 (4), p.164, 1968.

73) Morrison, J.B. :The function of the knee joint in various activities. Bio-Med. Engng. Vol. 4 (12), p.573, 1969.

74) Mottershead, J.E.; Edwards P.D.; Whelan M.P.; English R.G. :Finite element analysis of a total knee replacement by using Gauss point contact constraints. Proc Instn Mech Engrs Vol 210, p.51, 1996.

75) Mow V.C.; Soslowsky L.J. : Ch.6, Friction, lubrication & wear of diarthrodial joints. in Basic Orthopaedic Biomechanics, ed. Mow V.C. & Hayes W.C., publ. Raven Press, New York, 1991.

76) Nahass, B.E.; Madson, M.M.; Walker, P.S. : Motion of the Knee after Condylar Resurfacing-An In Vivo Study J of Biomechanics, 24, p.1107, 1991.

77) O'Connor, J.J.; Goodfellow, J.W. : Theory and practice of meniscal knee replacement : designing against wear. Proc Instn Mech Engrs, 210, p.217, 1996.

78) Otis J.C; Gould J.D.: The effect of external load on torque production by knee extensors. J. Bone Jt Surg, 68-A, p.65, 1986

79) Paul, J.P. : Kinematics and kinetics of knee joint function. Personal communication, 1993

80) Piziali, R.L.; Rastegar, J.C.; Nagel, D.A. : Measurement of nonlinear, coupled stiffness characteristics of the human knee. J Biomechanics, 10, p.45, 1977.

81) Premnath, V; Harris, W.H.; Jasty, M; Merrill E.W. : Gamma sterilisation of UHMWPE articular implants : An analysis of the oxidation problem. Biomaterials Vol 17, p. 1741, 1996.

82) Pruitt, L; Koo, J; Rimnac, C.M.; Suresh, S; Wright, T.M. : Fatigue Crack Propagation Behavior of UHMWPE under Compressive Loading. J. Orthop. Res., 13, p.143, 1995.

83) Reeves, E.A.; Barton, D.C.; Fitzpatrick D.P.; Fisher J. : A time dependent analysis of cyclic strain accumulation in UHMWPE knee replacements. Trans Orthop Res Soc, p.792, 1997.

84) Reithmeier, E.; Plitz, W. : Theoretical and Numerical Approach to Optimal Positioning of the Patellar Surface Replacement in a Total Knee Endoprosthesis J. Biomechanics, 23, p.883, 1990.

85) Ritter MA, Faris PM, Keating EM. Posterior cruciate ligament balancing during total knee arthroplasty. J. Arthroplasty, 3, p.323, 1988.

86) Roark, R.J.; Young, W.C. : Formulas for Stress and Strain Fifth Edition, McGraw-Hill Book Company New York, 1975.

87) Rose, R.M.; Crugnola, A.; Ries, M.; Cimino, W.R.; Paul, I.; Radin, E.L. :On the Origins of High in Vivo Wear Rates in Polyethylene Components of Total Joint Prostheses. Clin. Orthop. Rel. Res.,145, p.277, 1979

88) Rose, R.M.; Goldfarb, H.V.; Ellis, E.; Crugnola, A.M. : On the Pressure Dependence of the Wear of Ultrahigh Molecular Weight Polyethylene. Wear, 92, p.99, 1983.

89) Rostoker, W; Galante, J.O. : Contact Pressure Dependence of Wear Rates of Ultra High Molecular Weight Polyethylene. J of Biomed Mat Res, 13, p.957, 1979.

90) Rovick, J.S.; Reuben, J.D.; Schrager, R.J.; Walker, P.S. : Relation between knee motion and ligament length patterns. Clin. Biomech. , 6, p.213, 1991.

91) Sathasivam S, Walker PS. A computer model with surface friction for the prediction of total knee kinematics. J. Biomechanics, Vol.30, No.2, p.177, 1997.

92) Sathasivam, S.; Walker, P.S. : Optimization of the Bearing Surface Geometry of Total Knees. J. Biomechanics, Vol.27, No.3, p.255, 1994.

93) Seedhom, B.B.; Longton, E.B.; Dowson, D.; Wright, V. : The Leeds knee. Total Knee Replacement CP16 published by Instn Mech Engrs , p.108, 1974.

94) Seedhom, B.B.; Longton, E.B.; Wright, V.; Dowson, D. : Dimensions of the knee. Ann. Rheum. Dis., 31, p.54, 1972.

95) Shoemaker, S.C.; Markolf, K.L. : Effects of joint load on the stiffness and laxity of ligament-deficient knees. J. Bone Jt Surg, Vol.67-A, p.136, 1985.

96) Skolnick, M.D.; Coventry, M.B.; Ilstrup, D.M. : Geometric total knee arthroplasty. J Bone Joint Surg [Am], 58-A, No.6, p.749, 1976.

97) Stein A.; Fleming B.; Pope M.H.; Howe J.G.: Total knee arthroplasty kinematics. An in vivo evaluation of four different designs. J. Arthroplasty, 3 S31-S36, 1988.

98) Stewart T.; Shaw, D.; Auger, D.D.; Stone, M.; Fisher, J. : Experimental and theoretical study of the contact mechanics of five total knee joint replacements. Proc Instn Mech Engrs, 209, p.225, 1995.

99) Suh, N.P. : Tribophysics. Ch.4, pp.114-122, publ. Prentice-Hall, New Jersey, 1986.

100) Szivek, J.A.; Cutignola, L.; Volz, R.G.: Tibiofemoral Contact Stress and Stress Distribution Evaluation of Total Knee Arthroplasties. J. Arthroplasty, Vol.10, No.4, p.480, 1995.

101) Taylor, S.J.; Walker, P.S.; Perry, J.; Cannon, S.R. : The forces of the distal femur and knee during different activities measured by telemetry. Trans Orthop Res Soc, p.259, 1997.

102) Thatcher, J.C.; Zhou, X.M.; Walker, P.S. : Inherent Laxity in Total Knee Prostheses J. Arthroplasty, 2, p.199, 1987.

103) Townley, C.O. : The anatomic total knee resurfacing arthroplasty. Clin. Orthop., 182, p.82, 1985.

104) Vergis, A.; Gillquist, J. : Comparison of knee translation during functional activity and static laxity testing in healthy and ACL deficient subjects. Trans Orthop Res Soc, p.350, 1997.

105) Walker P.S., Blunn GW, Broome DR, Perry J, Watkins A, Sathasivam S, Dewar M, Paul JP: The kinematic conditions required for valid comparison of wear of total knees in a simulating machine. Trans Orthop Res Soc, 1996

106) Walker P.S.; Amberek M.S.; Morris J.R.; Olanlokun K.; Cobb A.: A-P stability in partially conforming condylar knee replacements. Clin. Orthop., 310, p.87, 1995.

107) Walker PS, Blunn GW, Broome DR, Perry J, Watkins A, Sathasivam S, Dewar M, Paul JP. A knee simulating machine for performance evaluation of total knee replacements. J. Biomechanics, Vol. 30, No.1, p. 83, 1997.

108) Walker, P.S. : Bearing surface design in total knee replacement. Engng Med. 17, p.149, 1988

109) Walker, P.S. : Design of Knee Prostheses for Bone Loss and Instability. Total -Condylar Knee Arthroplasty. Edited by C.S. Ranawat, Springer-Verlag, New York, 1985

110) Walker, P.S.; Wang, C-J; Masse Y : Joint Laxity as a Criterion for the Design of Condylar Knee Prostheses. In Total Knee Replacement. Proc Instn Mech Engrs, 1974

111) Wang CJ, Walker PS. Rotary laxity of the human knee joint. J. Bone Jt Surg [Am], 56-A, p.161, 1974.

112) Warren J.S.; Olanlokun T.K.; Cobb A.G.; Walker P.S.; Iverson B.F.: Laxity and function in knee replacements. Clin. Orthop. Rel. Res. , 305, p.200, 1994.

113) Wascher DC, Markolf KL, Shapiro MS, Finerman GAM. Direct in vitro measurement of forces in the cruciate ligaments. J Bone Joint Surg [Am], 75-A, p.377, 1993.

114) Whelan, M.P.; Little, E.G. : A Theoretical and Photoelastic Contact Stress Analysis Relevant to Orthopaedic Knee Prostheses. Strain, p.61, 1992.

115) Wimmer M.A.; Andriacchi T.P. : Tractive rolling as a possible cause of wear in total knee replacement. Trans Orthp Res Soc,20, p.735, 1995

116) Wimmer, M.A.; Andriacchi, T.P.: Tractive Forces during Rolling Motion of the Knee: Implications for Wear in Total Knee Replacement. J. Biomechanics. In press. 1996.

117) Wismans, J.; Veldpaus, F.; Janssen, J. : A three-dimensional mathematical model of the knee-joint. J Biomechanics, Vol.13, p.677, 1980.

118) Wright, T.M.; Bartel, D. L. : The Problem of Surface Damage in Polyethylene Total Knee Components Clin. Orthop. Rel. Res., 205, p.67 , 1986.

119) Zavatsky, A.B.; O'Connor, J.J. : A model of human knee ligaments in the sagittal plane. Part 1 : response to passive flexion. Proc Instn Mech Engrs, 206, p125, 1992.

APPENDIX

MAXIMUM SHEAR DAMAGE MAP F1T1

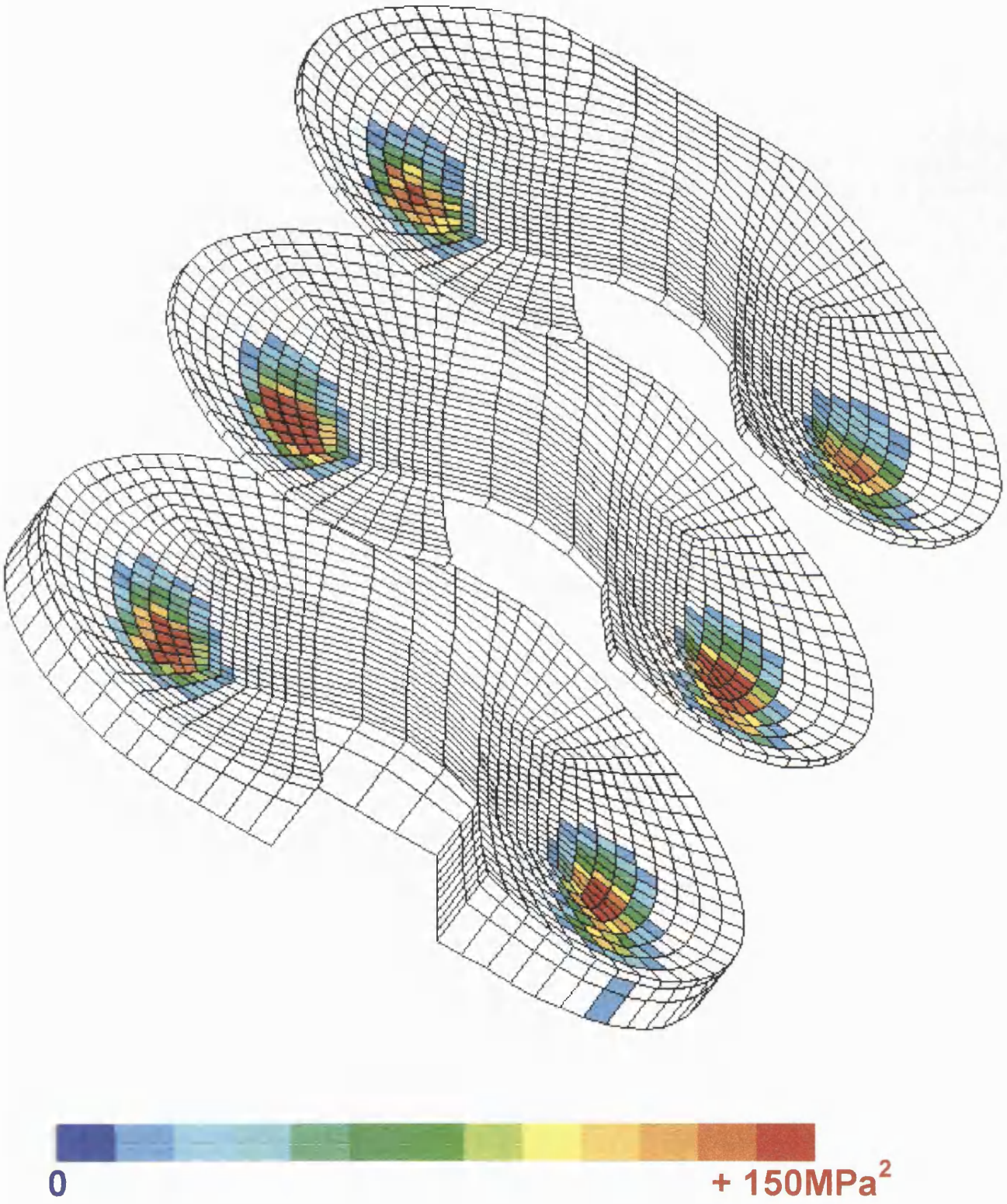

0 + 150MPa^2

MAXIMUM SHEAR DAMAGE MAP F1T2

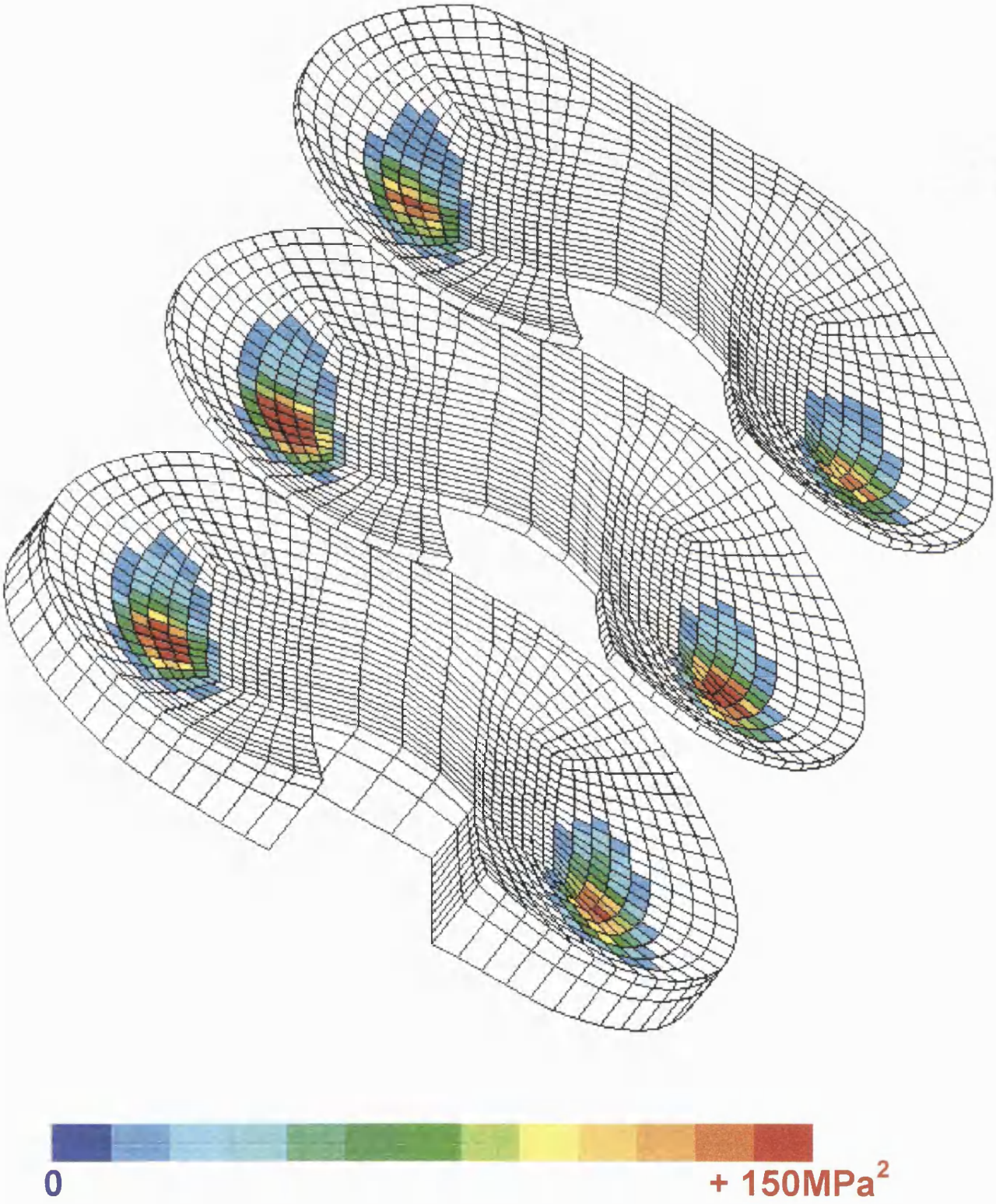

MAXIMUM SHEAR DAMAGE MAP F1T3

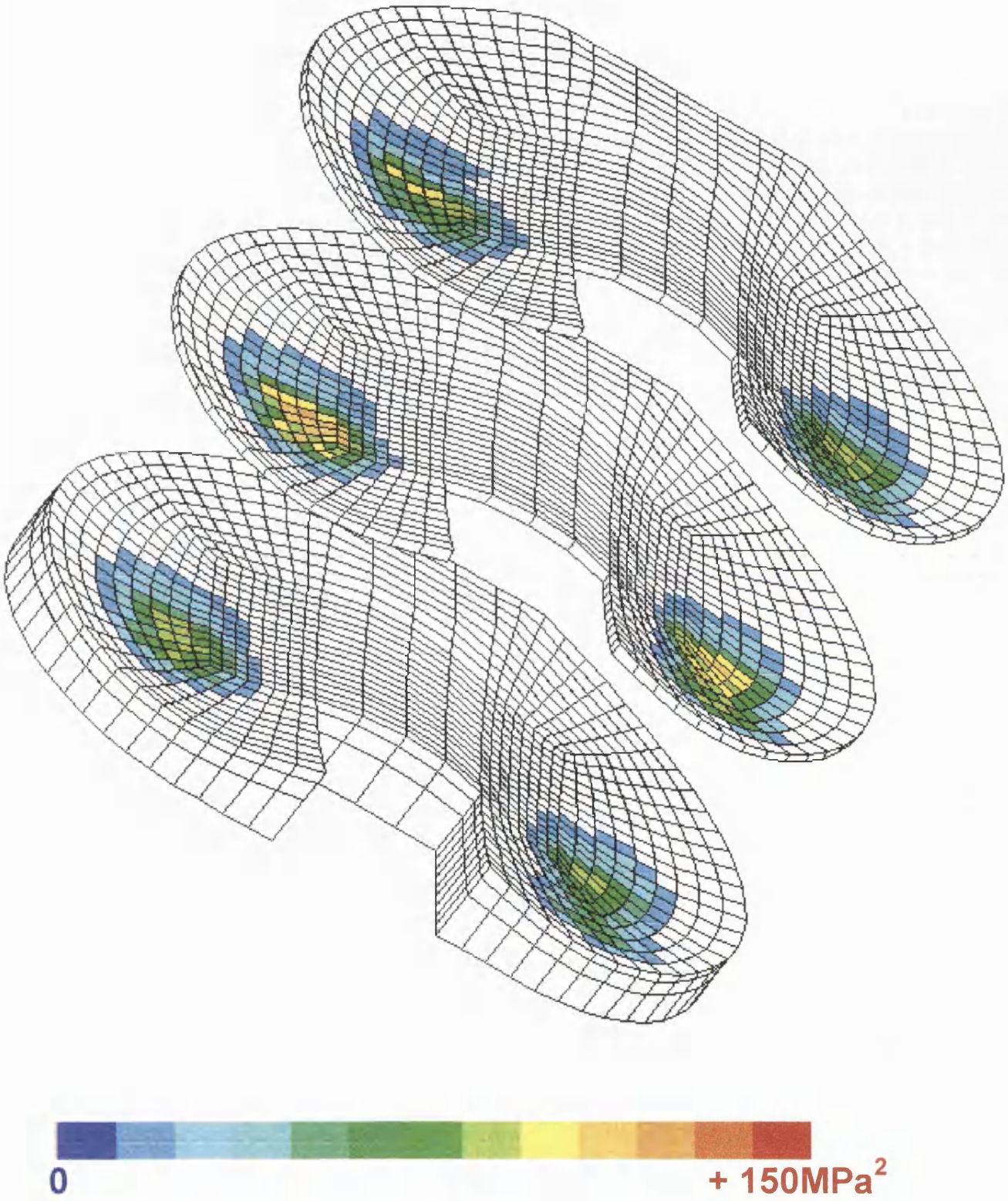

MAXIMUM SHEAR DAMAGE MAP F1T4

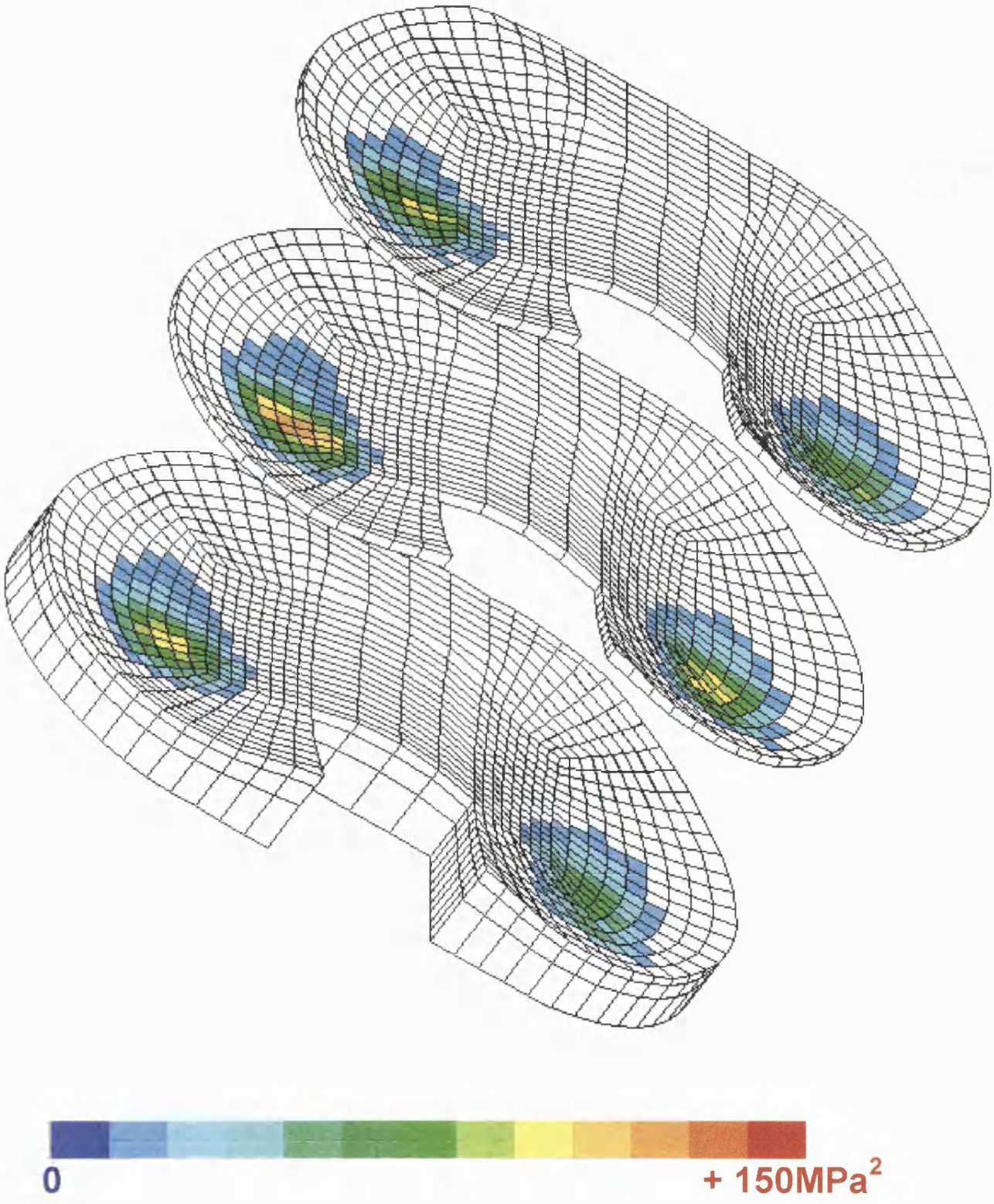

MAXIMUM SHEAR DAMAGE MAP F2T1

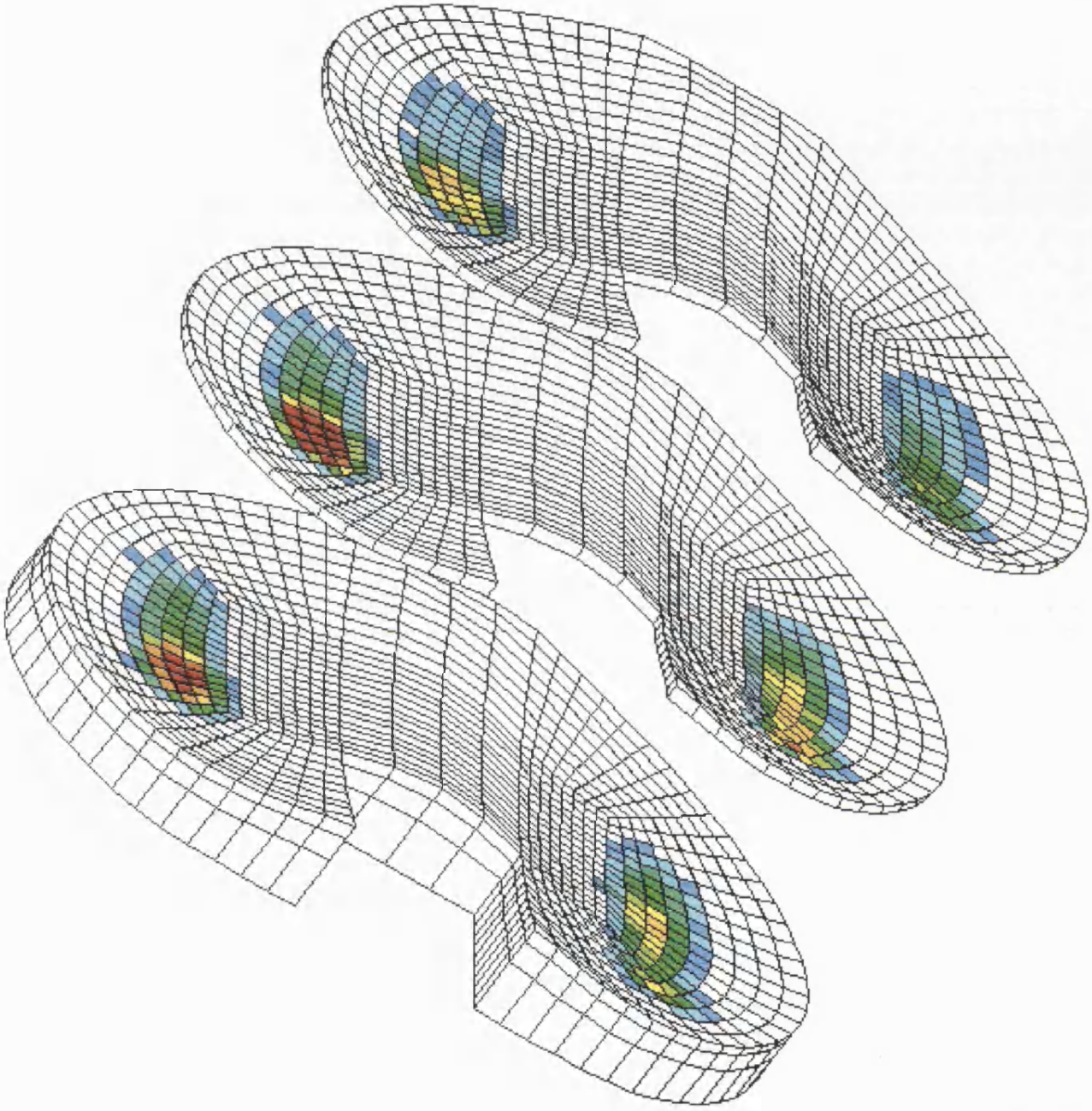

MAXIMUM SHEAR DAMAGE MAP F2T2

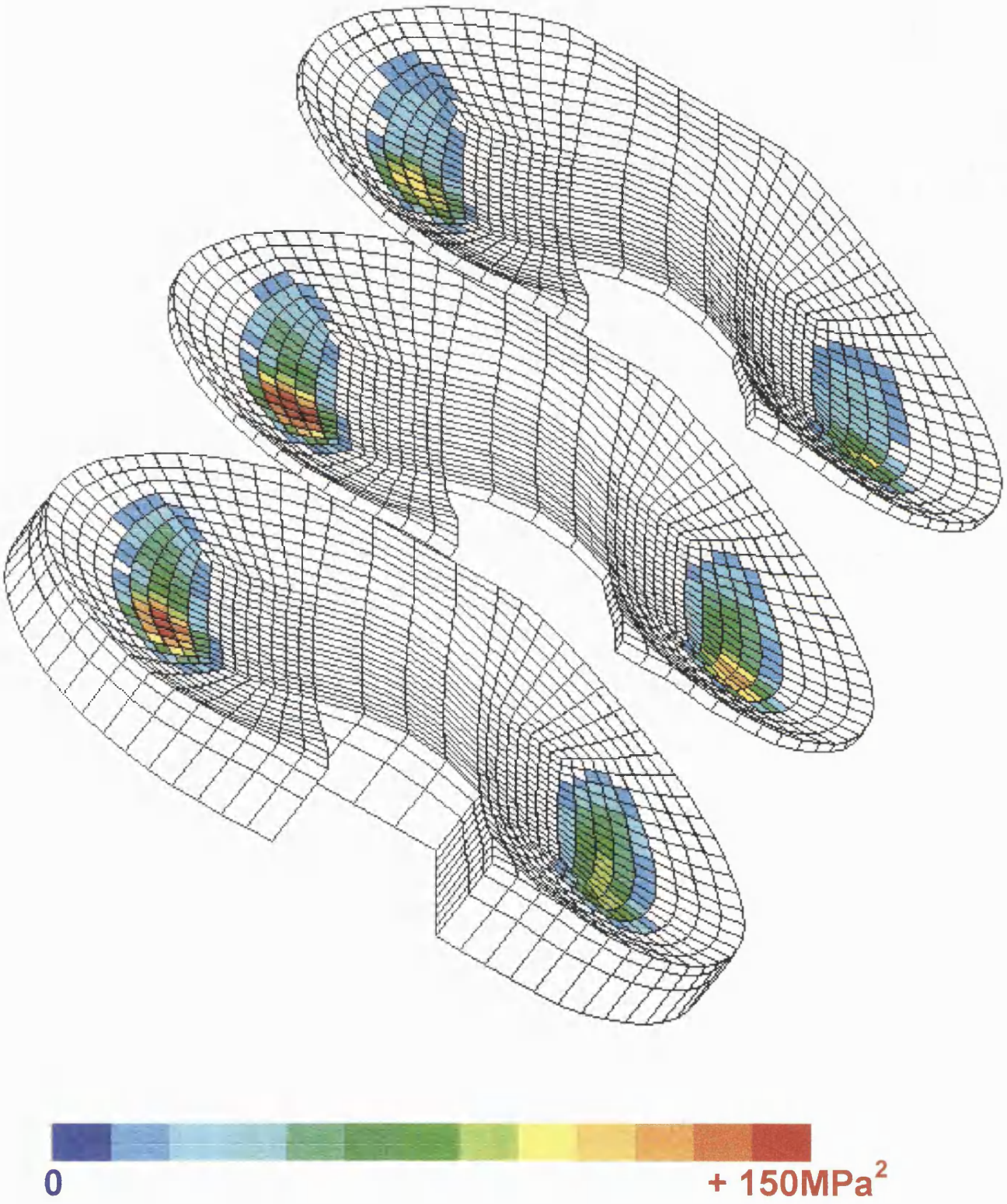

MAXIMUM SHEAR DAMAGE MAP F2T3

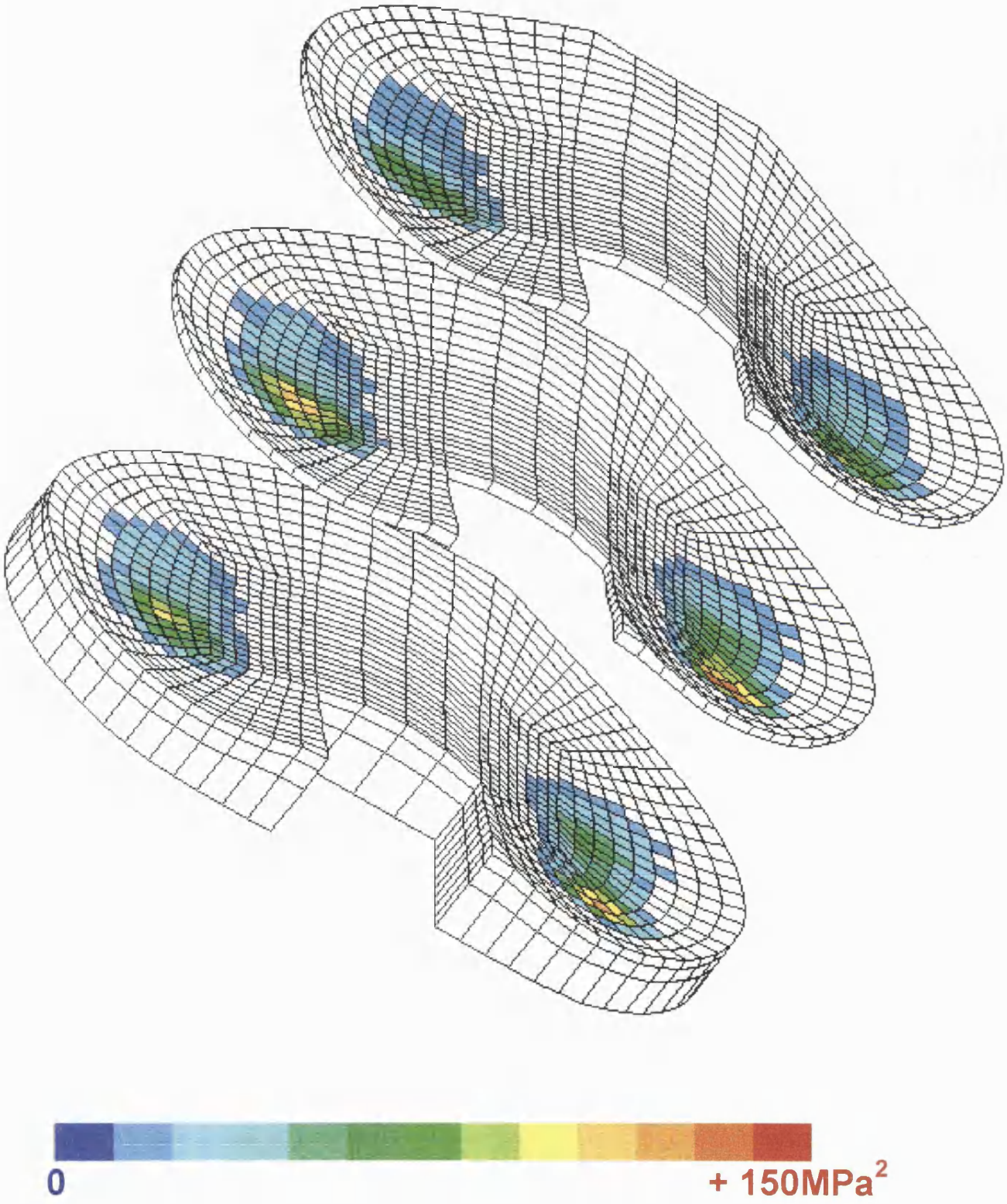

MAXIMUM SHEAR DAMAGE MAP F2T4

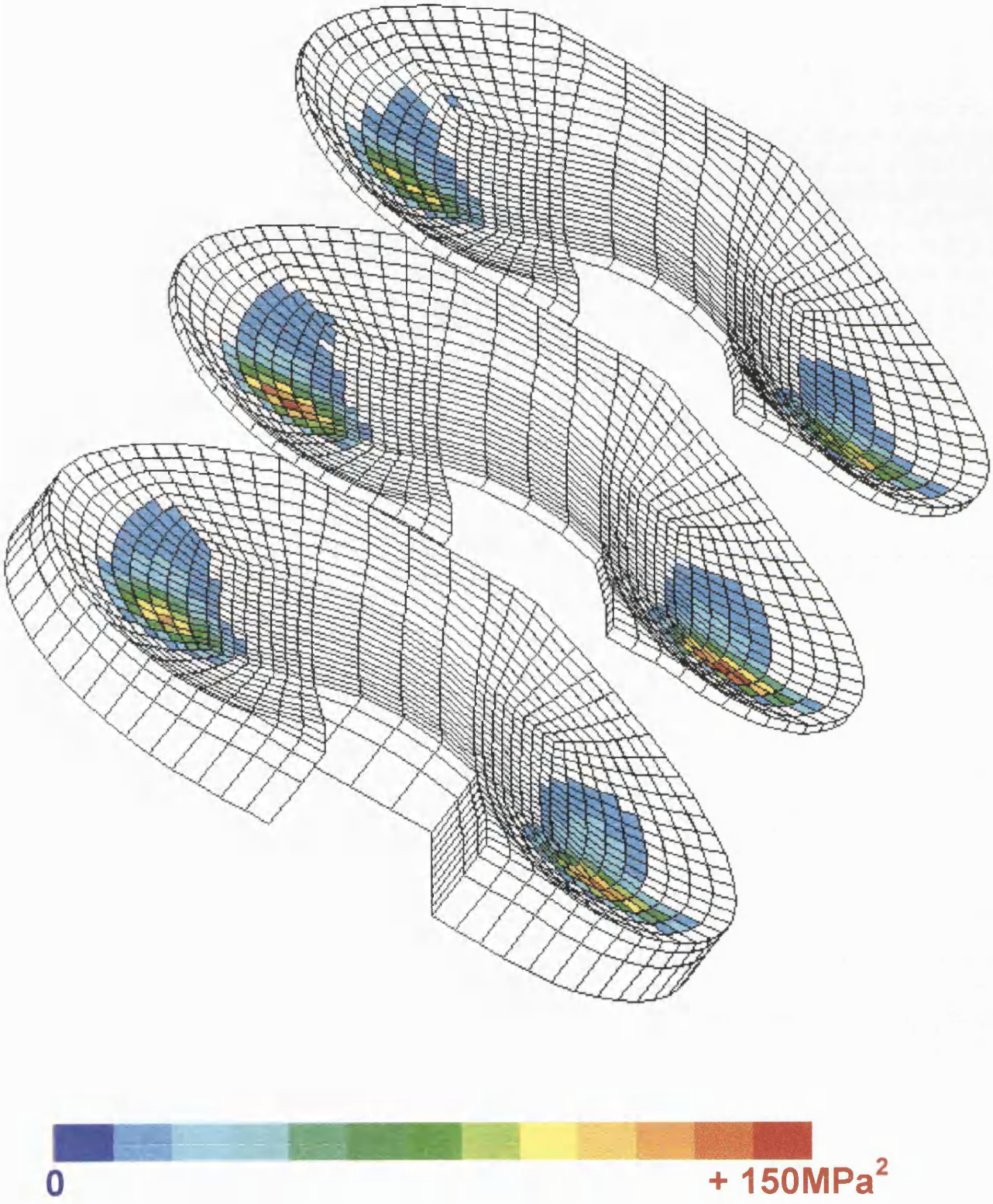

MAXIMUM SHEAR DAMAGE MAP F3T1

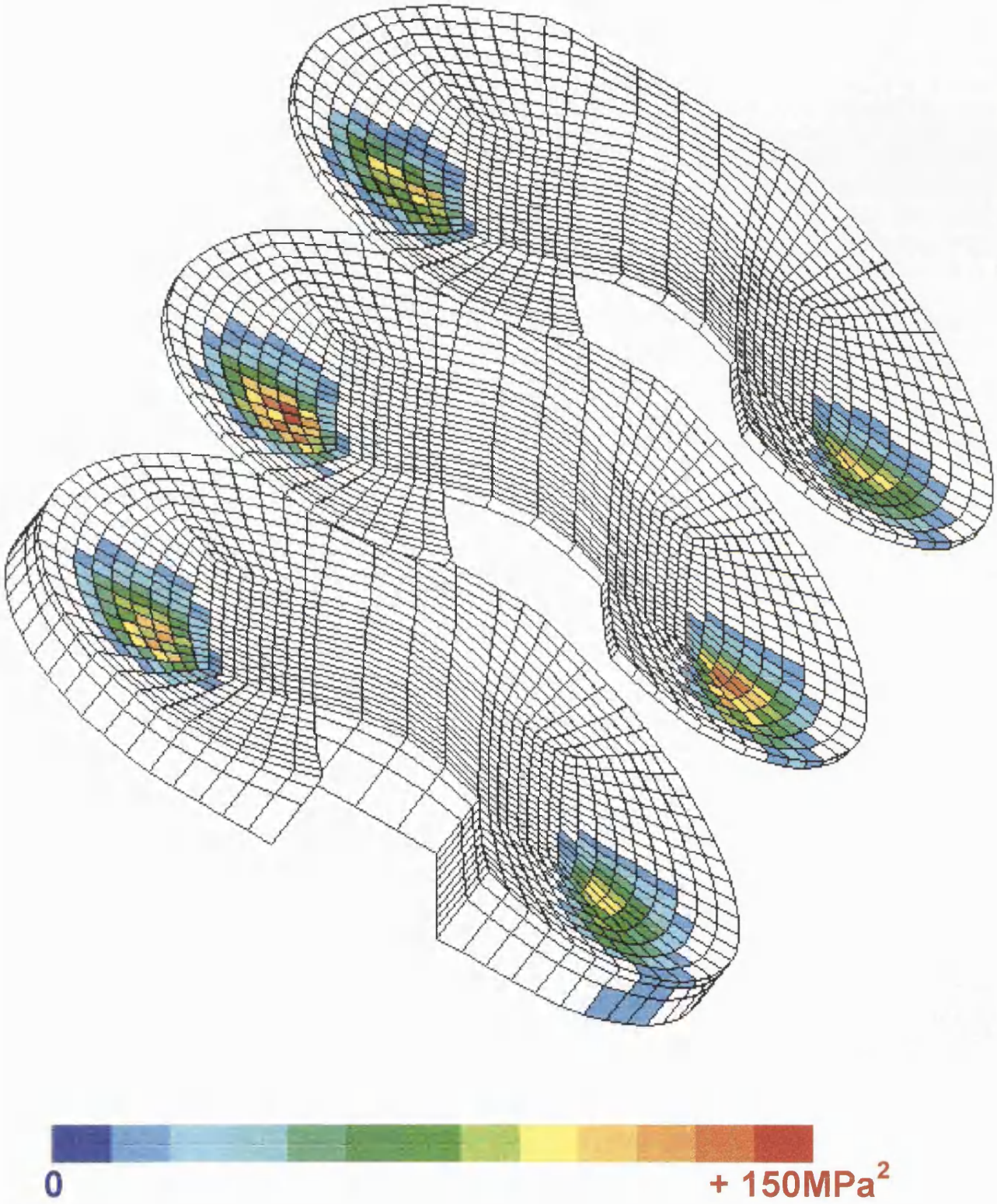

MAXIMUM SHEAR DAMAGE MAP F3T2

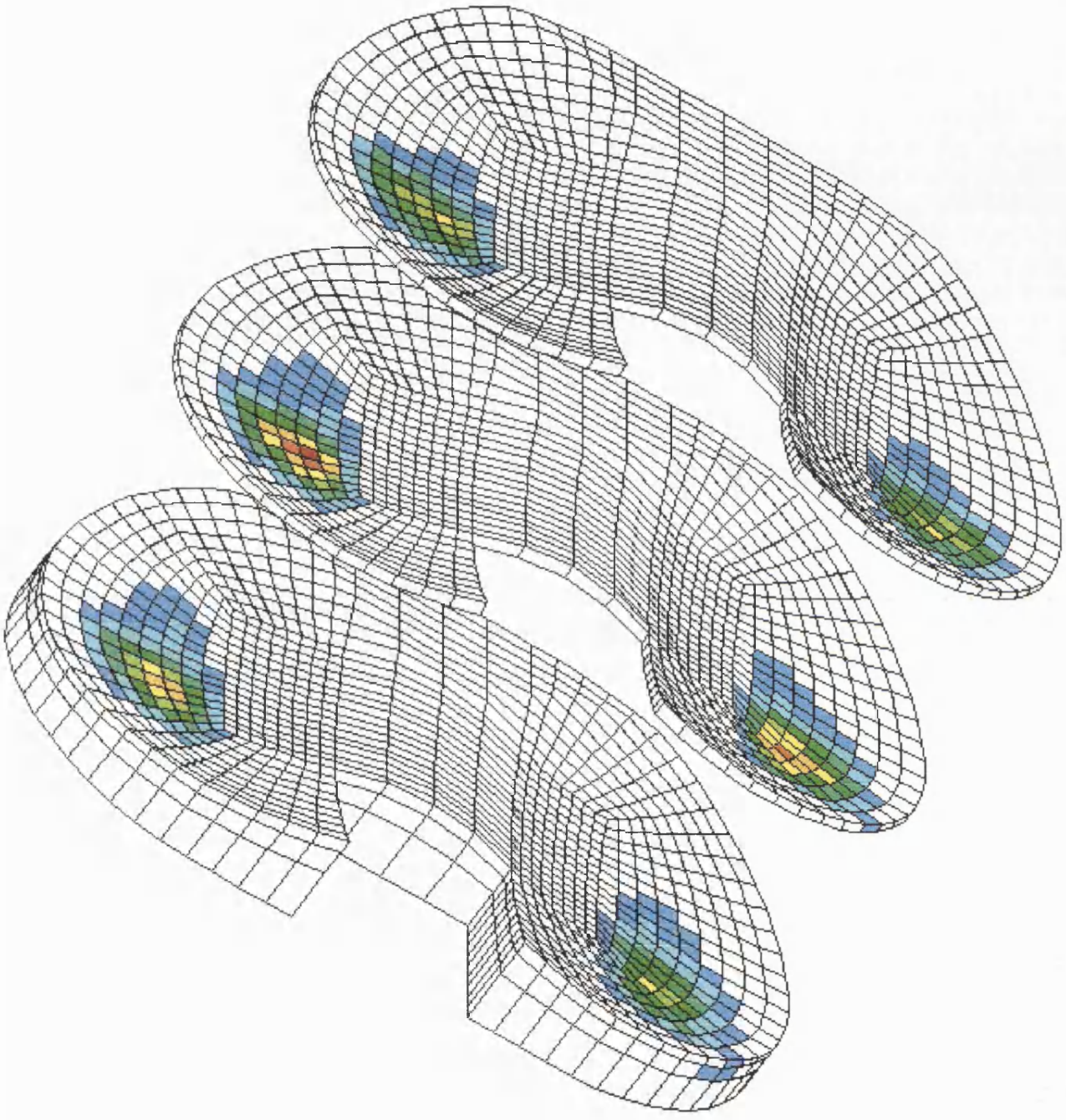

MAXIMUM SHEAR DAMAGE MAP

F3T3

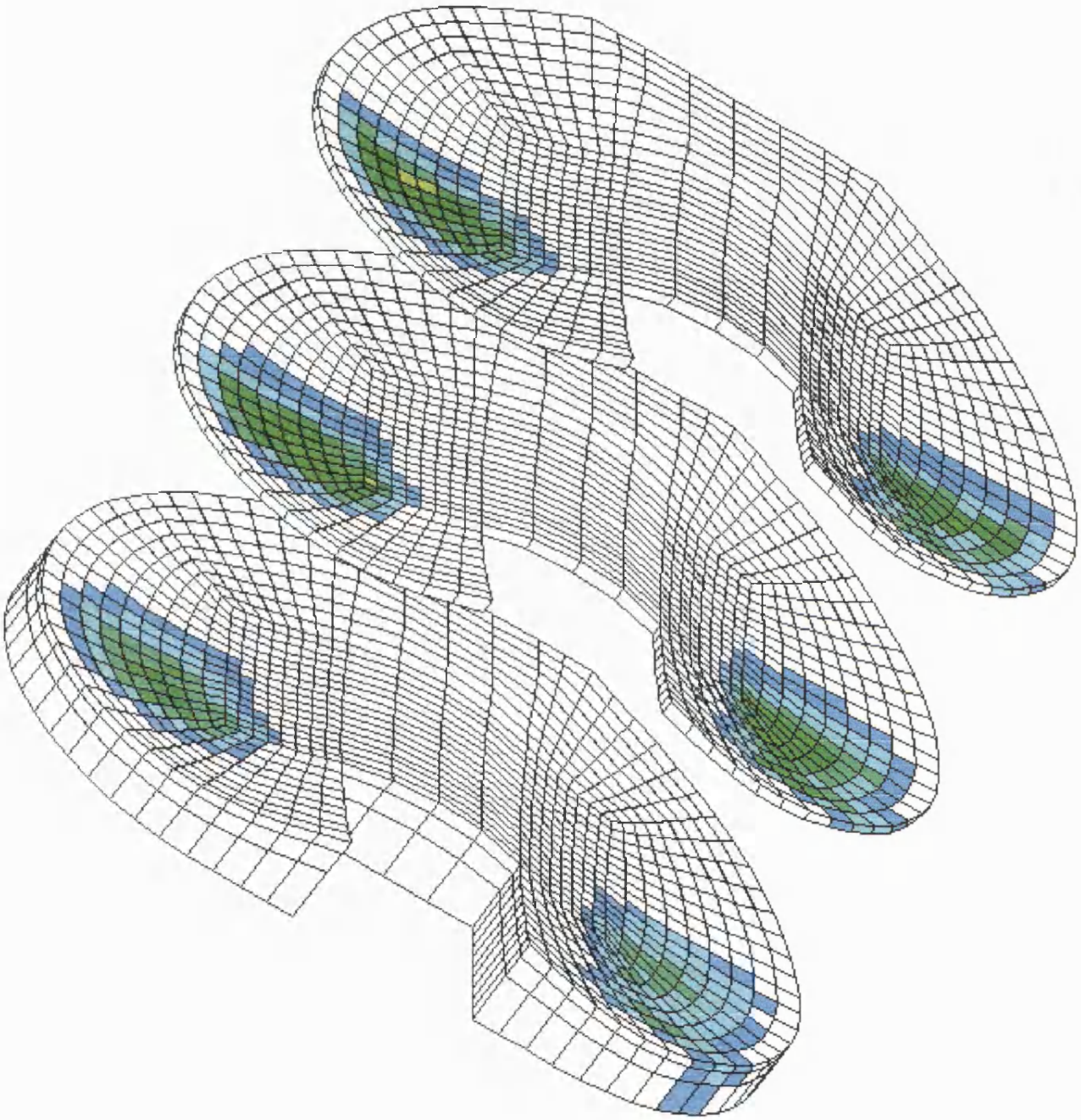

xi

MAXIMUM SHEAR DAMAGE MAP F3T4

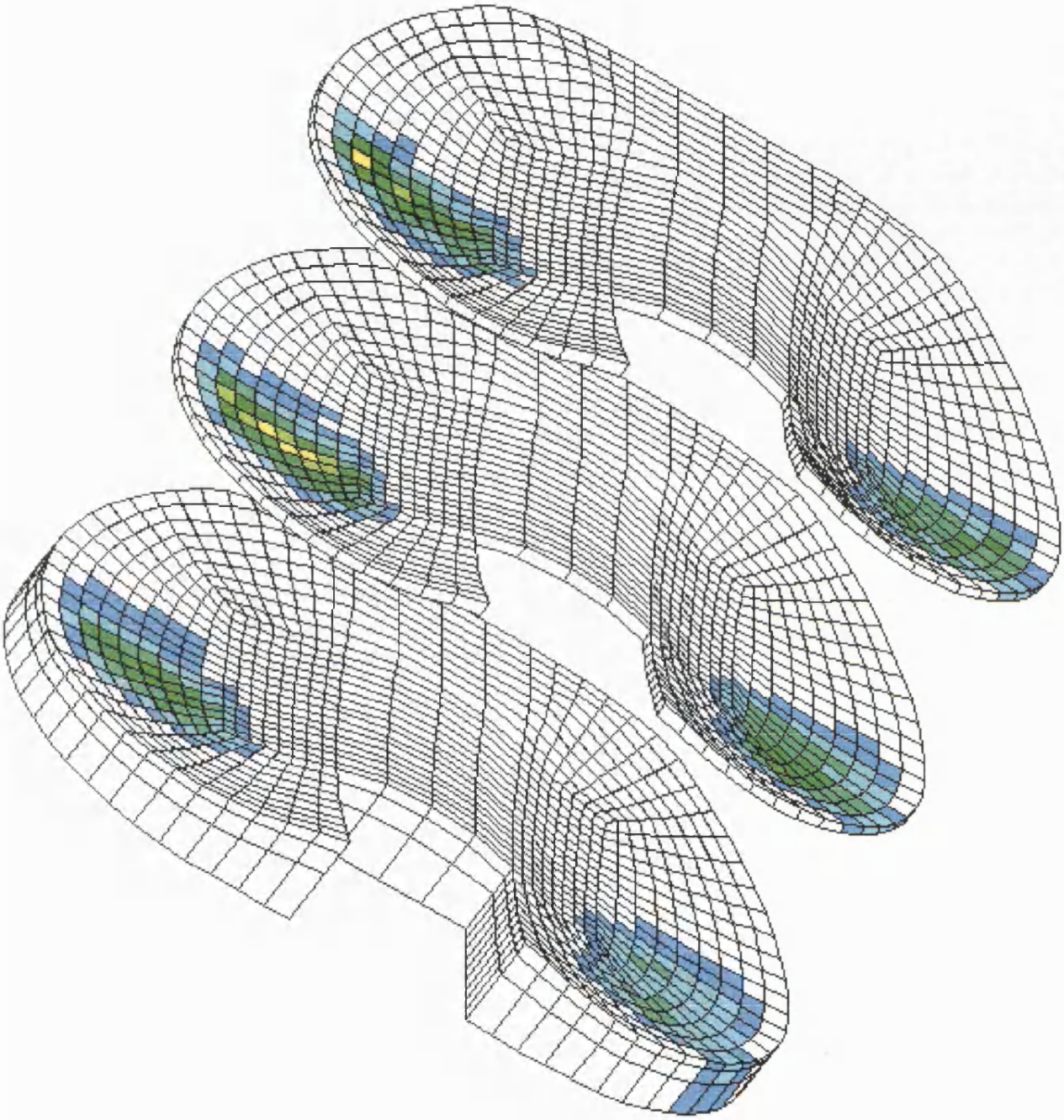

0 + 150MPa^2

MAXIMUM SHEAR DAMAGE MAP F4T1

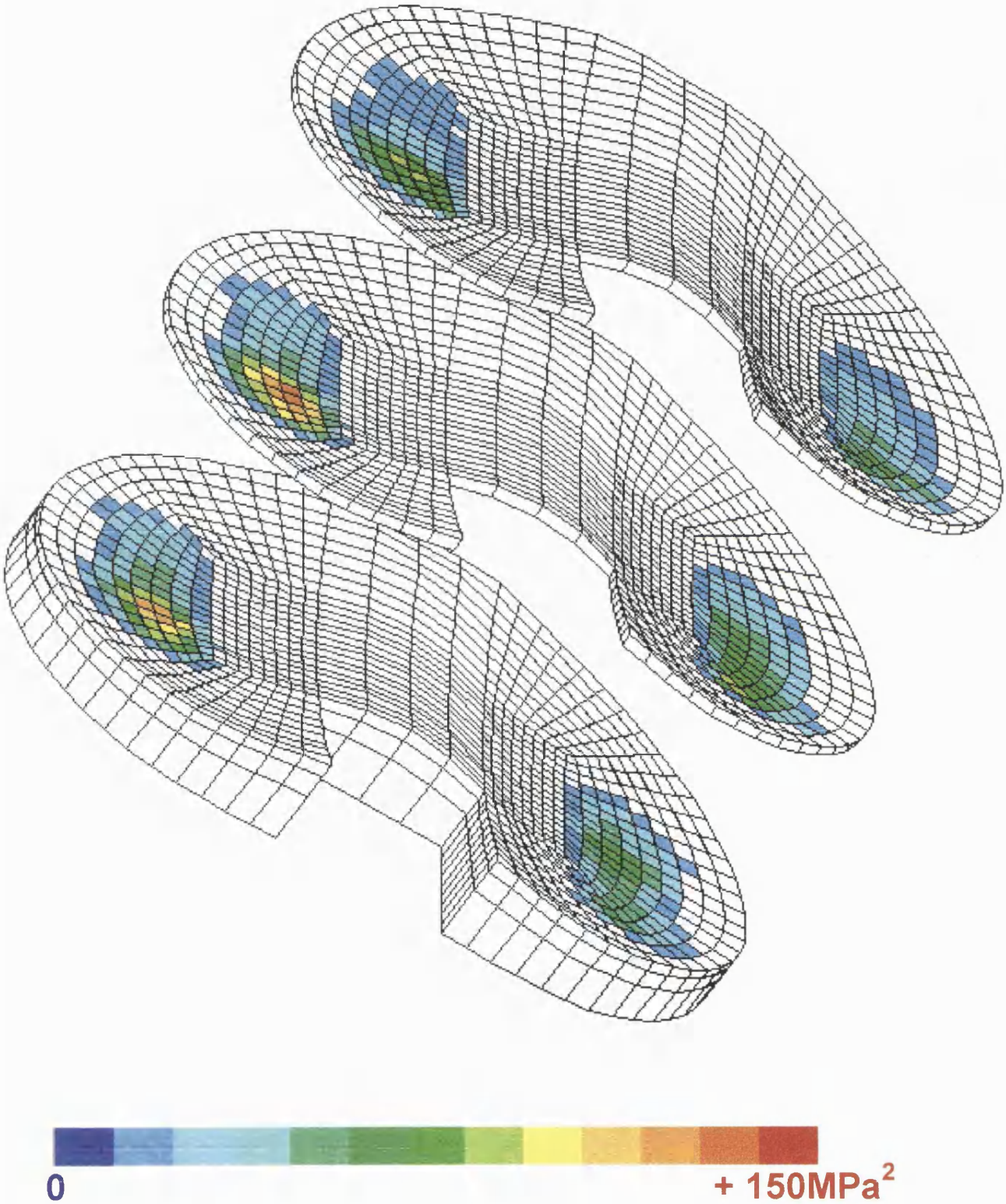

MAXIMUM SHEAR DAMAGE MAP F4T2

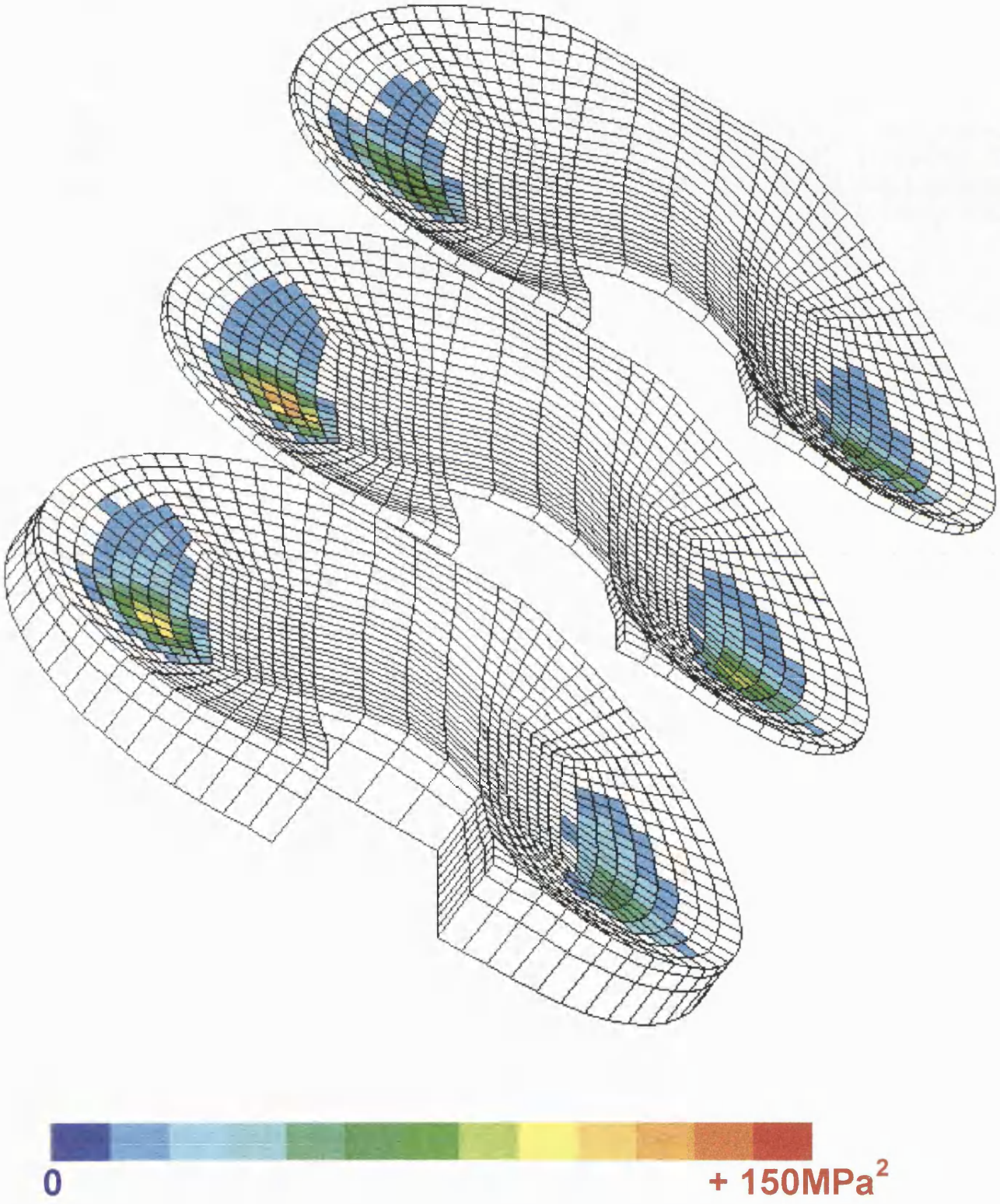

MAXIMUM SHEAR DAMAGE MAP F4T3

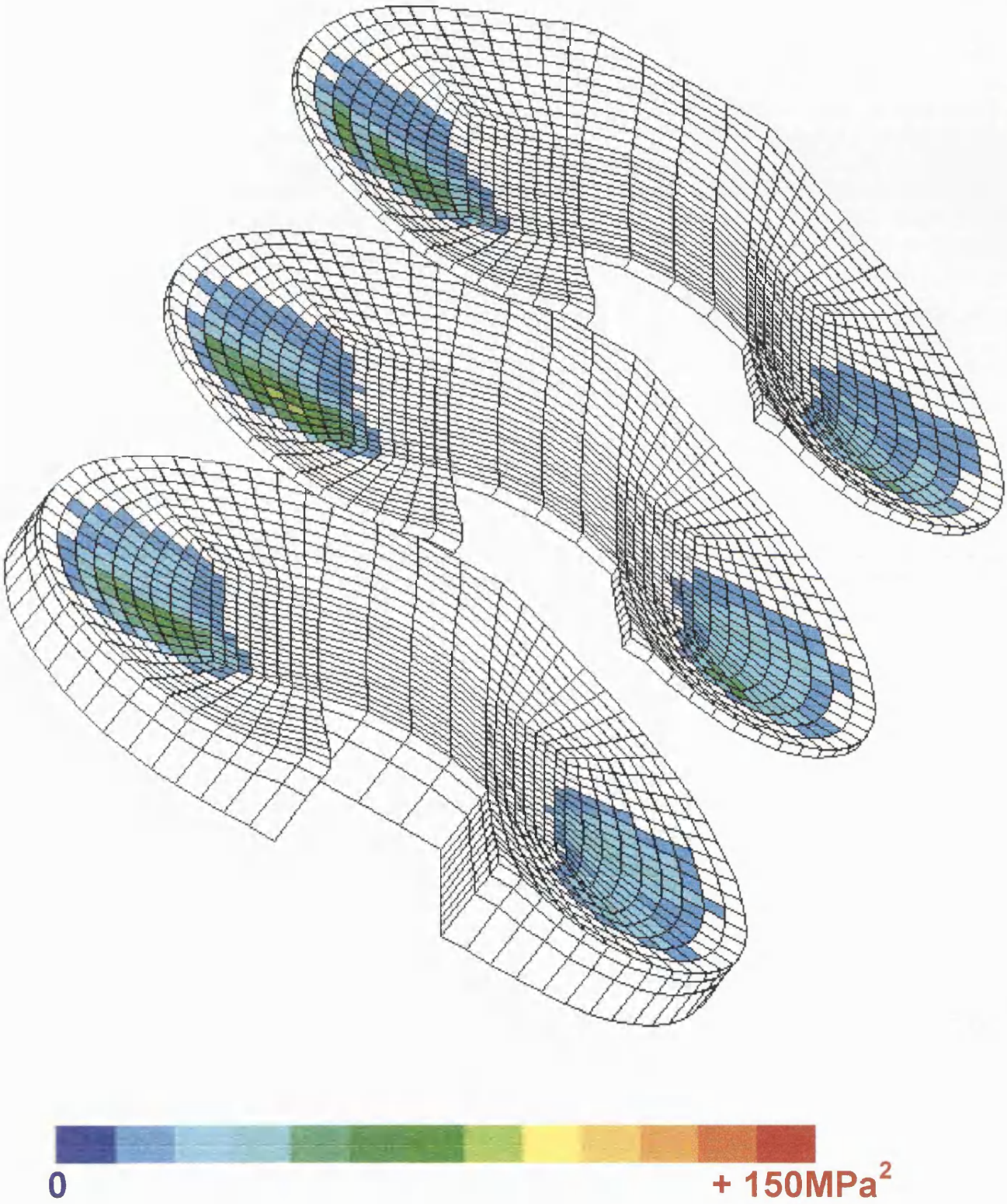

MAXIMUM SHEAR DAMAGE MAP F4T4

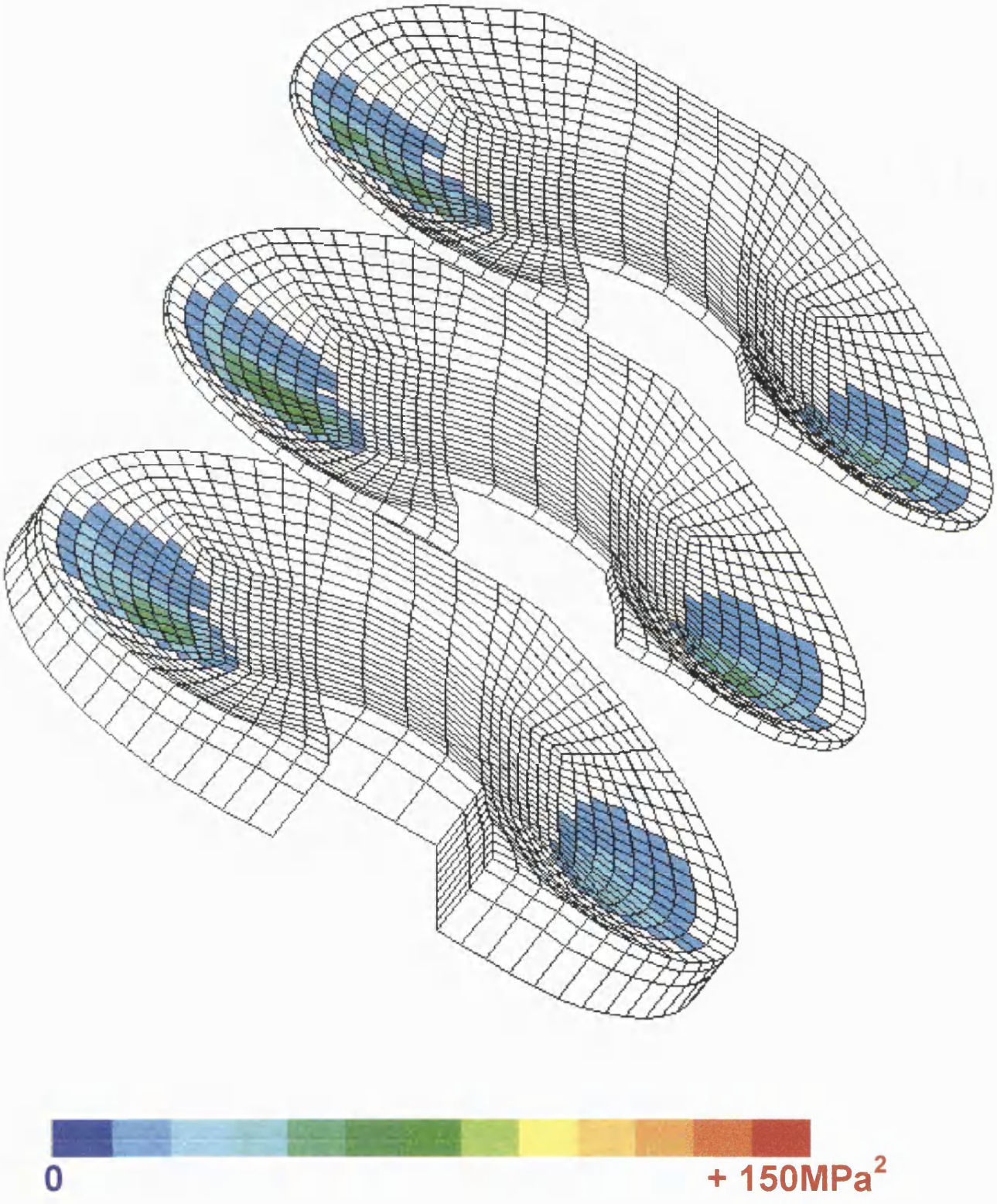

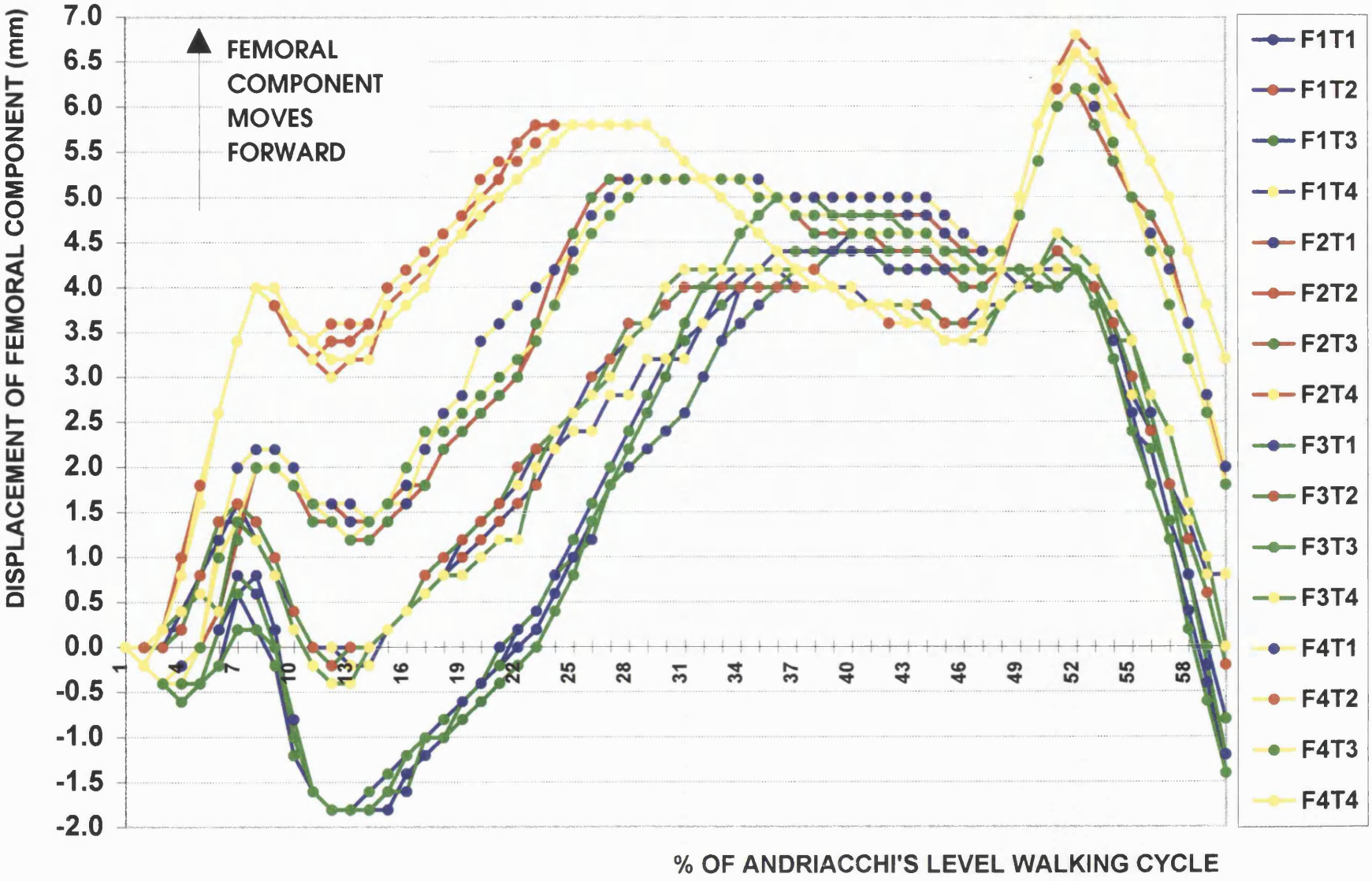
DISPLACEMENT OF FEMORAL COMPONENT (mm)
7.0
6.5
6.0
5.5
5.0
4.5
4.0
3.5
3.0
2.5
2.0
1.5
1.0
0.5
0.0
-0.5
-1.0
-1.5
-2.0
FEMORAL COMPONENT MOVES FORWARD
1
4
7
10
13
16
19
22
25
28
31
34
37
40
43
46
49
52
55
58
% OF ANDRIACCHI'S LEVEL WALKING CYCLE
F1T1
F1T2
F1T3
F1T4
F2T1
F2T2
F2T3
F2T4
F3T1
F3T2
F3T3
F3T4
F4T1
F4T2
F4T3
F4T4

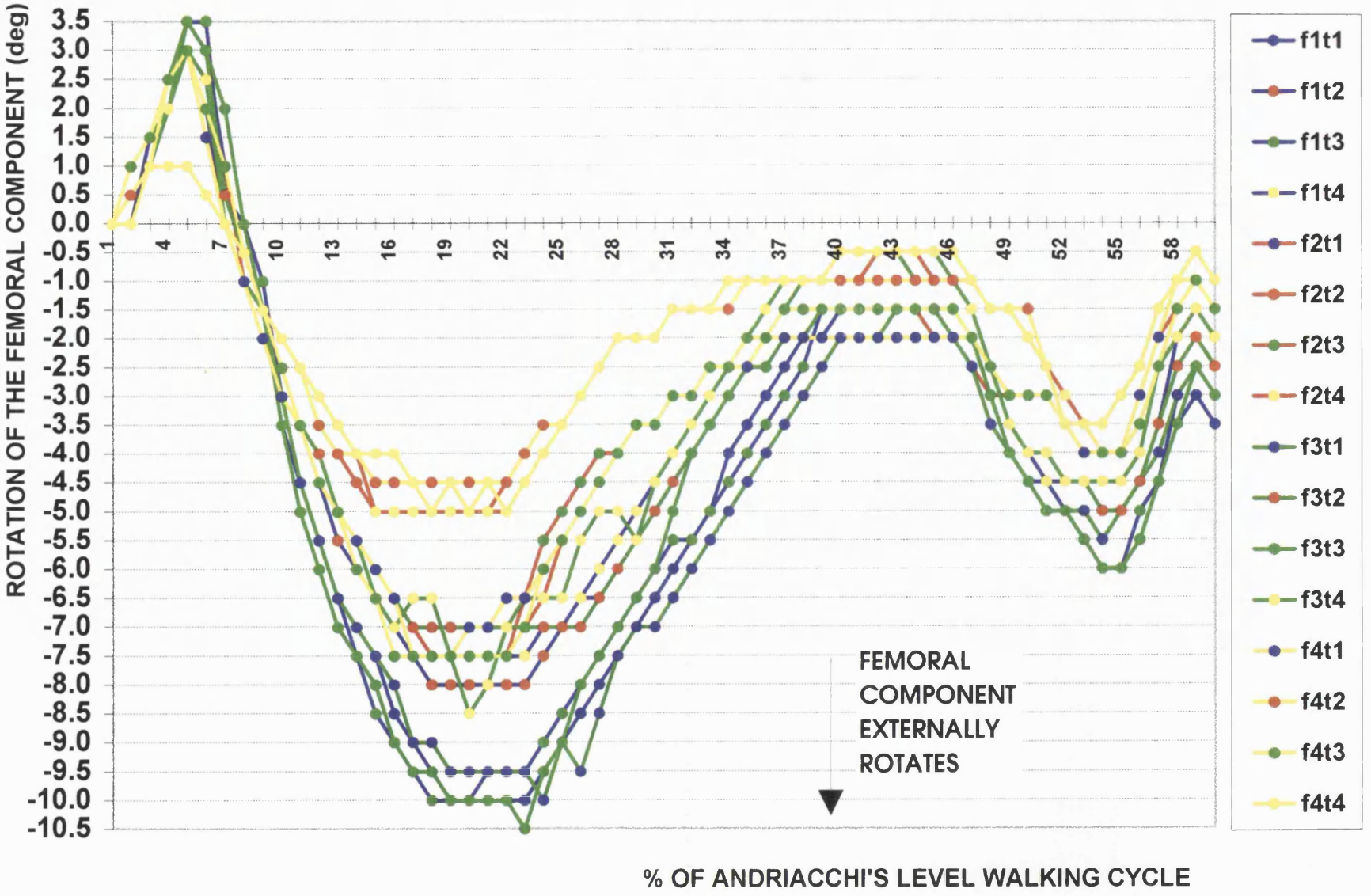
ROTATION OF THE FEMORAL COMPONENT (deg)
3.5
3.0
2.5
2.0
1.5
1.0
0.5
0.0
-0.5
-1.0
-1.5
-2.0
-2.5
-3.0
-3.5
-4.0
-4.5
-5.0
-5.5
-6.0
-6.5
-7.0
-7.5
-8.0
-8.5
-9.0
-9.5
-10.0
-10.5
1
4
7
10
13
16
19
22
25
28
31
34
37
40
43
46
49
52
55
58
FEMORAL COMPONENT EXTERNALLY ROTATES
% OF ANDRIACCHI'S LEVEL WALKING CYCLE
f1t1
f1t2
f1t3
f1t4
f2t1
f2t2
f2t3
f2t4
f3t1
f3t2
f3t3
f3t4
f4t1
f4t2
f4t3
f4t4

MOBILE BEARING KNEE STUDY

KNEE 1 - 0deg FLEXION
CONTACT PRESSURE

ABAQUS

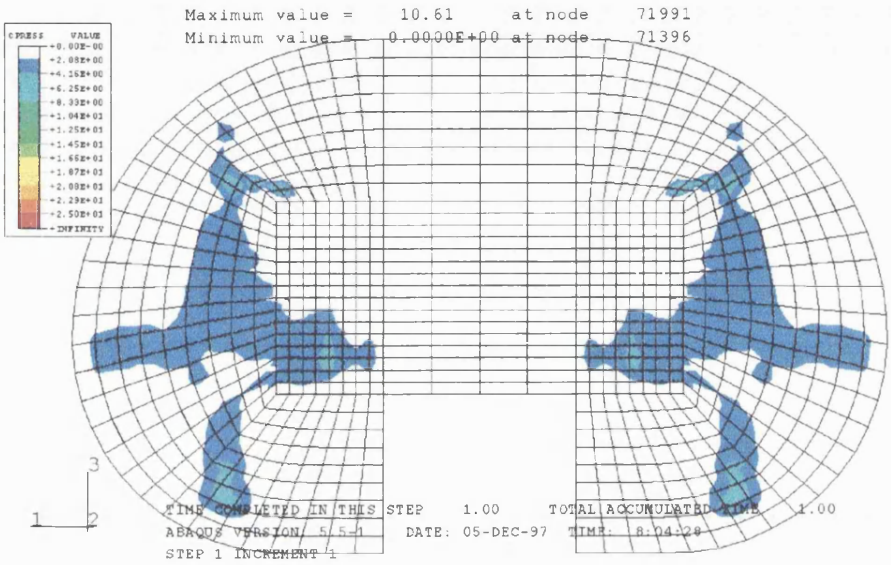

KNEE 1 - 60deg FLEXION
CONTACT PRESSURE

ABAQUS

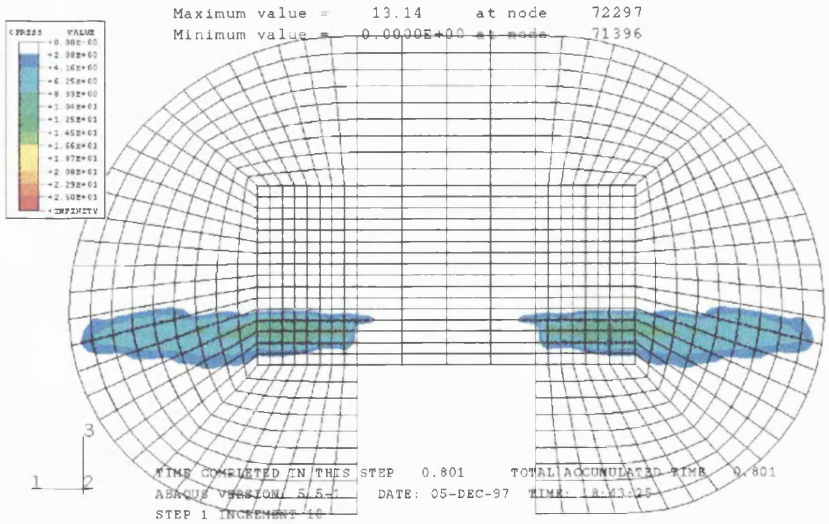

MOBILE BEARING KNEE STUDY

KNEE 2 - 0deg FLEXION
MAX SHEAR STRESS

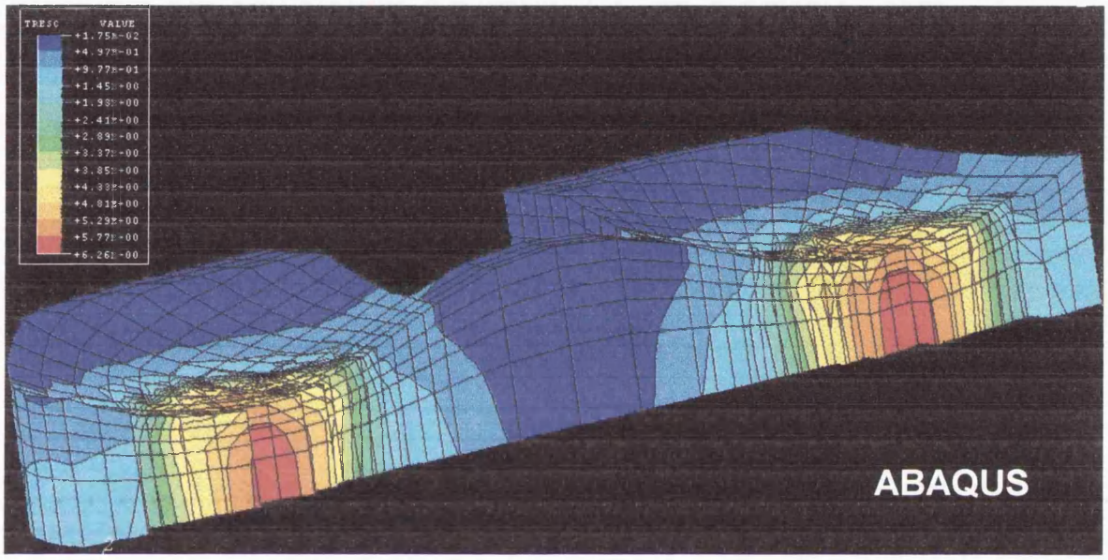

KNEE 2 - 0deg FLEXION
MAX PRINCIPAL STRESS